Ph.D. Thesis

Expanding the chemical space of enone-containing natural products: studies on ecdysteroid and protoflavone oxime derivatives

Máté Vágvölgyi

Szeged

2020

University of Szeged
Faculty of Pharmacy
Doctoral School of Pharmaceutical Sciences
Institute of Pharmacognosy

Ph.D. Thesis

Expanding the chemical space of enone-containing natural products: studies on ecdysteroid and protoflavone oxime derivatives

Máté Vágvölgyi

Supervisor
Attila Hunyadi, Ph.D.

Szeged, Hungary
2020

Table of contents

LIST OF PUBLICATIONS RELATED TO THE THESIS*

I. **Vágvölgyi M**, Martins A, Kulmány Á, Zupkó I, Gáti T, Simon A, Tóth G, Hunyadi A, Nitrogen-containing ecdysteroid derivatives vs. multi-drug resistance in cancer: Preparation and antitumor activity of oximes, oxime ethers and a lactam, *European Journal of Medicinal Chemistry* (2018) **144**; 730-739.

IF: **4.833** (2018) / Drug discovery, organic chemistry, pharmacology: **Q1**

II. Bogdán D, Haessner R, **Vágvölgyi M**, Passarella D, Hunyadi A, Tóth G, Stereochemistry and complete ^{1}H and ^{13}C NMR signal assignment of C-20-oxime derivatives of posterone 2,3-acetonide in solution state, *Magnetic Resonance in Chemistry*; (2018) **56**; 859–866.

IF: **1.731** (2018) / Chemistry (miscellaneous): **Q2**

III. Fumagalli G, Giorgi G, **Vágvölgyi M**, Colombo E, Christodoulou MS, Collico V, Prosperi D, Dosio F, Hunyadi A, Montopoli M, Hyeraci M, Silvani A, Lesma G, Dalla Via L, Passarella D, Heteronanoparticles by Self-Assembly of Ecdysteroid and Doxorubicin Conjugates To Overcome Cancer Resistance, *ACS Medicinal Chemistry Letters*; (2018) **9** 5; 468-471.

IF: **3.737** (2018) / Drug discovery, organic chemistry: **Q1**

IV. Ötvös SB, **Vágvölgyi M**, Girst G, Kuo C-Y, Wang H-C, Fülöp F, Hunyadi A, Synthesis of Nontoxic Protoflavone Derivatives through Selective Continuous-Flow Hydrogenation of the Flavonoid B-Ring, *ChemPlusChem* (2018) **83**; 72-76.

IF: **3.441** (2018) / Chemistry (miscellaneous): **Q1**

V. **Vágvölgyi M**, Girst G, Kúsz N, Ötvös SB, Fülöp F, Hohmann J, Devaux C, Chang F-R, Chen H, Chang L-K, Hunyadi A, Less cytotoxic protoflavones as antiviral agents: protoapigenone 1′-O-isopropyl ether shows improved selectivity against the Epstein-Barr virus lytic cycle, *International Journal of Molecular Sciences* (2019) **20** 24; 6269

IF: **4.183** (2018) / Organic Chemistry, Inorganic Chemistry, Medicine (misc.): **Q1**

*: Latin numerals of the corresponding publications related to the thesis will be referenced in this dissertation.

LIST OF ABBREVIATIONS

^{13}C NMR	Carbon nuclear magnetic resonance
1D	One-dimensional
^{1}H NMR	Proton nuclear magnetic resonance
20E	20-hydroxyecdysone
2D	Two-dimensional
anh.	Anhydrous
aq.	Aqueous
ATM	Ataxia telangiectasia mutated protein kinase
ATR	ATM and Rad3-related protein kinase
CCG	Chemical computing group
chk1 and 2	Checkpoint kinase 1 and 2
CI	Combination index
DAD	Diode array detector
DLS	Dynamic light scattering
DMAP	4-dimethylaminopyridine
DNA	Deoxyribonucleic acid
Dox	Doxorubicin
EBV	Epstein–Barr virus
EBV-EA	Epstein−Barr virus early antigen
EDC·HCl	1-ethyl-3-(3-dimethylaminopropyl)carbodiimide hydrochloride
ELSD	Evaporative light scattering detector
ESI	Electrospray ionization
GI	Grow inhibition
GI_{50}	Fifty percent grow inhibition inducing concentration
HESI	Heated electrospray ionization
HIV	Human immunodeficiency virus
H-NPs	Heteronanoparticles
HPLC	High-performance liquid chromatography
HR-MS	High-resolution mass spectroscopy
HSQC	Heteronuclear single quantum correlation
IC_{50}	Fifty percent inhibitory concentration
LC-MS	Liquid chromatography–mass spectrometry
LDL	Low-density lipoproteins
MDR	Multi-drug resistance
MeOH	Methanol
MOE	Molecular operating environment
MTT	3-(4,5-dimethylthiazol-2-yl)-2,5-diphenyltetrazolium bromide
NBS	N-bromosuccinimide
NPs	Nanoparticles

$Pd/BaSO_4$	Palladium on barium sulfate
Pd/C	Palladium on activated charcoal
PDA	Photodiode array
PdI	Polydispersity index
P-gp	P-glycoprotein
PIDA	(Diacetoxyiodo)benzene
PIFA	[Bis(trifluoroacetoxy)iodo]benzene
PMA	Phosphomolybdic acid
Py	Pyridine
QQQ	Triple quadrupole
ROESY	Rotating-frame overhauser effect spectroscopy
ROS	Reactive oxygen species
RP-HPLC	Reverse-phase high pressure liquid chromatography
RT	Room temperature
SAR	Structure-activity relationship
SB	Sodium butyrate
SPE	Solid-phase extraction
Sq	squalene
TEM	Transmission electron microscopy
THF	Tetrahydrofuran
TMS	Tetramethylsilane
TPA	12-O-tetradecanoyl-phorbol-13-acetate
TsCl	*p*-toluenesulfonyl chloride
UHPLC	Ultra-high pressure liquid chromatography
UV	Ultraviolet
XO	Xanthine oxidase
ζ-potential	Zeta potential

I. INTRODUCTION

I.1 Chemical and biological significance of oximes

I.1.1 The chemistry of oximes

Oximes represent a distinct group of organic compounds that belong to the family of imines. They can be described with the formula RR′C=NOH, where R is an organic side-chain (alkyl or aryl), and R′ may stand for hydrogen or another organic group so that the compound is an aldoxime or a ketoxime, respectively. Further, R′ can appear as an amine, and in that case, the moiety is an amidoxime [1,2]. As an overview, **Fig. 1** illustrates the chemical structures.

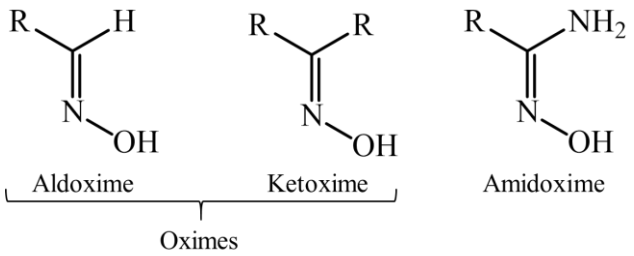

Figure 1. Chemical structures of oximes and amidoximes [3]. (R=alkyl, aryl)

The synthetic preparation of oximes from their corresponding parent compounds has been extensively studied and discussed in the literature [3,4]. Amidoximes are typically obtained from nitriles using hydroxylamine salt in water or alcohol [5–7]. Alternatively, hydrazide imides, thioamides, amidines [8], and, in some cases, imino ethers [9] can also be promising reactants for their preparation.

Similarly to amidoximes, the synthesis of ketoximes and aldoximes is typically achieved by using a hydroxylamine analog that, in this case, is reacted with an aldehyde or a ketone [10–12]. Following this preparative strategy, oxime or oxime ether analogs of various types of oxo-function possessing substrates may be conveniently obtained in typically good yields [13,14]. Besides, the nitrosation of aliphatic molecules [15] or the reduction of nitro compounds [16] can be alternatives for the preparation of ketoximes and aldoximes.

In some instances, oxime synthesis may be carried out under solvent-free conditions [17–19]. However, it is important to note that the wide-scale applicability of these procedures might be limited since most reports exclusively involve simple, liquid-state reactants that taken together, may question the procedures' extensibility towards solid-state, complex substrates.

Oximes are of great importance in the chemical industry and research. As for the former, the mass-scale production of ε-caprolactam represents an illustrative example. This derivative serves as a precursor in the preparation of nylon-6, and its synthesis commonly relies on the

acid-catalyzed Beckmann-rearrangement of cyclohexanone oxime. Importance of the oxime substrate may well be illustrated by the fact that, for example, in 2016, the world's caprolactam consumption had reached as much as ca. 5.5×10^6 t [20]. This example fits well to a broader perspective: oximes and their *O*-substituted analogs are attractive synthons in the preparation of various nitrogen-containing species, including amines, hydroxylamines, amino alcohols, nitriles, lactams and 3- to 7-membered ring nitrogen heterocycles [21–23]. Thus, in their intact form or as synthetic precursors, they indeed find their use among various fields of application.

It should be noted that oximes can occur in forms of geometric isomers where the stereochemical configuration can significantly influence a compound's chemical, physical, and biological properties [24,25]. Therefore, a remarkable scientific interest is appearing towards the development of regioselective synthetic procedures [26,27], and towards the employment of specific chromatographic techniques that can effectively separate the corresponding *E*/*Z*-isomers from their mixtures [28,29].

I.1.2 Natural occurrence and bioactivities of oximes

Despite the fact that synthetic analogs spectacularly outnumber them, many natural oximes also exist. In plants, oximes are predominantly derivatives of amino acids [30,31]. Most plant oximes and their typically *O*-methylated oxime ethers [32] possess relatively simple chemical structures, which usually reflect the structure of their precursor amino acids. Regarding their physiological role, it appears that they participate in both general and specialized plant metabolism, facilitating a set of biochemical processes influencing plant growth and development [30,33].

Besides plants, without attempting to be comprehensive, fungi [34], bacteria [35], marine sponges [36–38], and insects (e.g., millipedes (*Harpaphe haydeniana*)) [39] may also contain natural oxime derivatives. Moreover, even some mammals are known to be producing them. Interestingly, the sternal gland secretion of male koalas (*Phascolarctos cinereus*) contains volatile nitrile and oxime derivatives [40]. This oily gland plays a vital role in koalas' communication and is only produced by males that use it for scent marking on trees within their territorial range. Although the composition of the gland reflects versatile information, the specific relevance of individual oxime components has not yet been clarified in this regard [41].

Oximes are therefore widely present in the various Kingdoms of Nature, which might indicate a remarkable biological potential of this moiety. In this context, not surprisingly, synthetic oximes and oxime ethers are subjects of intensive research, and bioactive analogs are utilized for various purposes. Just to mention a few examples, synthetic oxime derivatives are

widely used in the agricultural sector as plant growth regulators [42], insecticides (e. g. Aldicarb) [43], herbicides [44], fungicides [45] or even anti-viral agents [46,47]. Besides, oximes are highly important for the health sector as well. Previously, derivatives such as pralidoxime [48], obidoxime, HI-6, or TMB-4 became well-known nerve agent antidotes available for clinical use [49,50]. Most recently, the first-in-class luso-inotropic steroid istaroxime has been granted Fast Track Designation by the FDA [51], and by the time of writing this Ph.D. thesis, it is undergoing a phase II clinical trial for the treatment of for acute decompensated heart failure with persistent hypotension [52]. Besides, there is much evidence on various oxime derivatives exerting e. g. antitumor [53], antioxidant [54], anti-inflammatory [55] or antibacterial [56] properties.

We have valuable examples available on the bioactivities of natural oximes too. Alkaloids derived from marine sponges (e. g. from species of the *Agelas* genus) are potent inhibitors of molecular fouling organisms [57]. Furthermore, derivatives from the corticioid fungi *Boreostereum vibrans*, including the first natural oxime esters isolated, were reported to exert pancreatic lipase inhibitory activity and to exhibit cytotoxicity against various human cancer cell lines with IC_{50} values comparable to that of cisplatin [58].

I.2 ECDYSTEROIDS

I.2.1 Chemistry and occurrence in nature

In this present Ph.D. research work, we selected our substrates for semi-synthetic transformations among the derivatives of two bioactive compound families containing an enone moiety in their structure, such as ecdysteroids and protoflavonoids. Among these, ecdysteroids represent a unique group of steroids, extensively studied for their versatile chemical and biological properties. Our research group has long been studying the chemistry and pharmacology of natural and semi-synthetic ecdysteroid derivatives [59–64].

Ecdysteroids are best known as hormones regulating the molting and metamorphosis of arthropods [65]. They were discovered rather late, in 1954, by german chemists Karlson and Butenandt, who successfully isolated α-ecdysone (now commonly referred to as ecdysone) from silkworm pupae [66]. Subsequently, the search for bioactive compounds in *Podocarpus nakaii* had led to the discovery of 3 novel analogs, ponasterone A, B, and C, which revealed the existence of the so-called phytoecdysteroids [67]. Subsequent intensive research on these compounds in the Plant Kingdom resulted in the discovery of a wide diversity of novel structures so that currently, 517 natural ecdysteroids are registered in the continuously updated online ecdysteroid database [68]. Research efforts had also revealed that certain derivatives could occur both in flora and fauna, and in general, plants appear to contain these compounds in

several orders of magnitude higher amounts than arthropods [69,70]. In this regard, the insect hormone 20-hydroxyecdysone (**1**; 20E; β-ecdysone) was found in the vast majority of ecdysteroid-containing plants, and it typically also dominates these plants' ecdysteroid composition. 20E is therefore by far the most abundant natural ecdysteroid [60] (**Figure 2**).

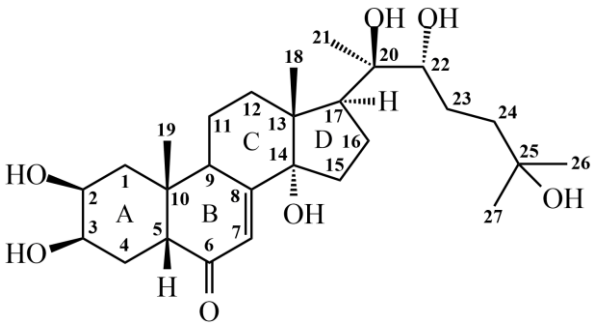

Figure 2. Chemical structure of 20E (**1**) with carbon atom numbering indicated.

Regarding structural properties, ecdysteroids are biosynthesized from cholesterol and thus, most derivatives possess a skeleton that contains 27-29 carbon atoms. Besides, C_{19}-C_{24} derivatives also exist (e.g., poststerone, rubrosterone), probably as products of sterol side-chain cleavage. A common structural feature of ecdysteroids is the 7-en-6-one chromophore moiety in the B-ring, responsible for their UV absorption with λ_{max} at ca. 243 nm in methanol. Most ecdysteroids are relatively hydrophilic compounds due to the 3-8 hydroxyl groups in their structure, predominantly at positions C-2β, C-3β, C-14α, C-20R, and C-22R. Each ecdysteroids contain β-orientated methyl groups at C-10 and C-13. Junctions of rings A and B are commonly cis, while junctions of C and D rings are generally *trans* [71].

I.2.2 Pharmacological effects and possible uses

Ecdysteroids exert strong hormonal effects on insects. However, their use as environmentally sound insecticides has not so far been successful, mostly due to their relatively high polarity that prevents absorption through the insect cuticle. Above their effect on insects, it is of interest that ecdysteroids also exert a number of bioactivities in mammals, including humans [72]. The effect of ecdysteroids in mammals greatly differs from that on insects. In mammals, that apparently lack a dedicated ecdysteroid receptor, these compounds display an almost negligible acute toxicity, and their effect is generally considered mild [73].

During this Ph.D. work, we focused on the preparation and investigation of potentially antitumor, chemo-sensitizing derivatives, therefore, after a brief summary of the most

fundamental bioactivities of these compounds, their antitumor effects and related structure-activity relationships will be presented more in detail (section I.2.3).

Anabolic effect. Ecdysteroids exert a non-hormonal anabolic activity, which has been compared by several authors to that of anabolic steroids. In this regard, certain phytoecdysteroids were shown to increase protein synthesis in skeletal muscle cells [74], and pure 20E treatment (5 mg/kg body weight) was demonstrated to enhance the muscle fiber size in either the normal and regenerating muscles of male Wistar rats [59,75]. All literature reports underline that ecdysteroids' are free from the adverse effects of androgenic steroids. Although there had been only a few human trials on low numbers of volunteers [73,76], this led to the blooming of an unregulated worldwide market of ecdysteroid-containing dietary supplements [73,77]. Considering that they indeed seem to influence sports performance [76], in 2019, the World Anti-Doping Agency (WADA) added ecdysteroid-containing substances to the 2020 list of monitored agents [78].

Adaptogenic effect. Extracts of certain ecdysteroid-containing plant species (*Tinospora cordifolia*, *Leuzea carthamoides*, *Achyranthes aspera*) are reported to exert adaptogenic activity, i.e., the ability to assist non-specific stress-response. These properties have long been recognized by various systems of traditional medicine wherein parts of these plants are used as ingredients to prepare medicinal consumables. Although the observations are typically associated with the plants' ecdysteroid-content, a proper scientific confirmation is still not available in this regard [79].

Antidiabetic activity. In traditional medicine, certain ecdysteroid-containing plant species (e. g. *Ajuga iva*) are processed to prepare antidiabetics from their extracts. Considering this, ecdysteroid content in these species were examined for their effects on the glucose metabolism of mammals. 20E (**1**) was found active from various aspects. On rodent *in vivo* models, pure 20E (**1**) could reduce hyperglycemia and could enhance glucose utilization by tissues [59,72]. Additionally, 20E (**1**) treatment was found to decrease gluconeogenesis and could induce the Akt2 phosphorylation of H4IIE cells. Furthermore, upon fed to high-fat diet mice, it could decrease the body weight gain and body fat mass of the animals [80].

Further bioactivities Beyond the highlighted features and the anticancer activities described in section I.2.3., ecdysteroids have been reported to exert various other bioactivities [59]. In this regard, their possible multi-purpose dermatological use seems particularly promising, considering the several patents on the use of ecdysteroid-containing formulations to prevent hair-loss or to stimulate cell defense mechanisms against UV-irradiation [81,82].

I.2.3 Anticancer activities

Since the discovery of ecdysteroids, numerous papers were published on their potential anticancer activities, although, more concordant data are only available since the 1990s [83]. During this decade, seven polyporusterone analogs were isolated from the fruit body of the fungus *Polyporus umbellatus* which showed dose-dependent, moderate to weak (IC_{50} ca. 30–100 μM) cytotoxicity on leukemia cells [84]. Furthermore, certain ecdysteroid derivatives (e. g., cyasterone) were found to have the potential to inhibit the Epstein−Barr virus early antigen induction (EBV-EA) by the tumor promoter [85]. However, the slowly unfolding picture of their possible antitumor effect was somewhat nuanced by the fact that muristerone A and ponasterone A showed anti-apoptotic effects on colon tumors [86].

Following these studies, our research group made a significant contribution to the field by discovering the potential of less polar ecdysteroids to sensitize cancer cells to chemotherapeutics (i.e., "chemo-sensitizing" activity) [87]. This activity of particularly ecdysteroid diacetonides was confirmed in combination with various chemotherapeutic agents, both on multi-drug resistant (MDR) and drug-susceptible cancer cells, with notably higher selectivity towards the former [88,89]. This MDR selectivity, i.e., potent sensitizing activity on ABCB1 transporter (P-glycoprotein; P-gp) over-expressing cell lines, is an interesting aspect of the bioactivity of these compounds because they were found only rather mild inhibitors of the efflux pump. Through the preparation and bioactivity testing of over a hundred derivatives, we have identified numerous structure-activity relationships (SARs); the most important are summarized in **Fig. 3**.

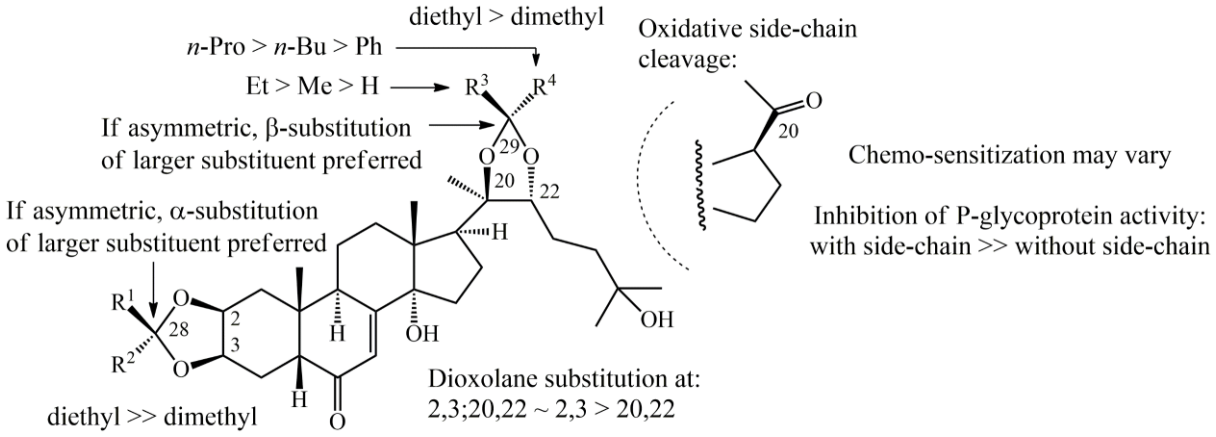

Figure 3. SARs of ecdysteroids' chemo-sensitization illustrated on a 20E 2,3;20,22-dioxolane analog [90].

Considering the characteristics displayed, the followings should be highlighted: 1) introduction of apolar substituents (e. g. acetonides) on the ecdysteroid diols, particularly on the 2,3-moiety, is required for chemo-sensitization [90], and 2) direct inhibitory effect on drug efflux by P-gp, that may be considered as a disadvantageous side-effect of these compounds, can be eliminated by the oxidative cleavage of the sterol side-chain [89].

Besides the above, the antitumor properties of an ecdysteroid may significantly be modified by introducing heteroatoms to its chemical backbone. In this regard, we observed notable differences in the pharmacological response of the parental 20E 2,3;20,22-diacetonide and its synthetically prepared difluorinated analog. Fluor-substitution at the C-14 and C-25 positions increased P-gp inhibition, as well as the strength of synergism with doxorubicin both on the P-gp-transfected MDR cell line and on its non-MDR counterpart [91].

In the context of the first two sections (I.1.1 and I.1.2) of the introduction, the carbonyl moiety/moieties at C-6 and, in some side-chain shortened derivatives, at C-20 of ecdysteroids allows simple semi-synthetic preparation of their oxime analogs. Previously, Galyautdinov et al. reported the synthesis of some ecdysteroid oximes; however, to the best of our knowledge, no pharmacological studies were so far performed on such derivatives [92].

I.3 Nano-formulation through self-assembling pro-drug conjugates

Very frequently, *in vitro* antitumor activity on cell cultures cannot be translated to *in vivo* efficacy. The reason is often related to pharmacokinetic limitations that may simply prevent the agent from reaching the site of action at a minimum required concentration. Nowadays, medicinal nanotechnology provides several solutions to overcome this obstacle, among which the synthesis of self-assembling drug conjugates represents a simple, yet efficient approach [93].

In the previous section, we have shown that the presence of the 2,3-acetonide function on an ecdysteroid is necessary for the antitumor effect; however, unfortunately, this moiety is one of the chemically most sensitive part of these molecules, especially in an acidic environment. Therefore, the idea of obtaining the self-assembling bioconjugates of an antitumor ecdysteroid can not only serve as a relevant targeting strategy to improve the *in vivo* pharmacokinetic properties of the drug but might contribute to the chemical stability of these molecules as well, e.g., by ensuring that the 2,3-acetonide pharmacophore remains intact in the intravenous matrix.

I.3.1 The theory of using self-assembling drug conjugates in anticancer treatment

In the course of this Ph.D. study, we utilized a variation of this technique that used squalene for nano-formulation to obtain the drug conjugates and, subsequently, the

corresponding self-assembled nanoparticles (NPs) of an antitumor ecdysteroid oxime. Therefore, in the current section, we aim to give a brief overview on the theoretical background of the methodology, while in section I.3.2, we will focus exclusively on the introduction of squalene-based bioconjugates.

The phrase "self-assembly" represents a spontaneously occurring process mediated by secondary intermolecular interactions (e. g., hydrophobic, van der Waals interactions) that results in the formation of an ordered nanostructure from molecular building blocks. Although numerous procedures exist to prepare self-assembled NPs, amphiphilicity of the substrates is usually a crucial factor that determines the chemical and pharmacological properties of the supramolecular products [93,94].

Self-assembling drug conjugates may be prepared through the covalent coupling of two functional units: a (chemo)therapeutic agent and a biocompatible lipid moiety that acts as the inducer of self-assembly. In some cases, the linkage of these molecular units through a so-called linker function may further improve the *in viv*o release of the drug [95]. In general, the related synthetic procedure consists of the formation of chemical bonds that are hydrolyzable in a biological environment (e. g., esters), while for this reason, NPs obtained from drug conjugates, once administered into the organism, will typically act as pro-drugs [96].

The drug delivery mechanism of NPs usually differs from that of molecular agents, and supramolecular structural attributes typically result in improved tumor-targeting properties for NPs in either a direct or indirect way (e. g., by taking advantage of the Enhanced Permeability and Retention or rather EPR effect [97]). Moreover, it is important to note that by the proper nano-formulation of the drug, we might have the ability to influence its physicochemical properties, including its chemical stability or solubility in a favorable way. Such parameters can be well predicted employing colloid chemical characterization, wherein the mean diameter and the surface charge are of decisive importance in the further fate of nano assemblies [98].

I.3.2 Self-assembling drug conjugates of squalene

Numerous self-assembly inducers exist that can form stable nanoparticles in serum without the need to use any additional surfactants. Among the substances available for the purpose, squalene is a subject of remarkable scientific interest [93]. This triterpene is mostly known as a precursor in the cholesterol biosynthesis, which as a natural lipid, occurs in a wide range of organisms, including that of humans [99,100].

The idea of using squalene as a self-assembly inducer relies on its biocompatibility and relative inertness that, altogether, make this compound an attractive synthon for the preparation

of bioconjugates. Although squalene is devoid of a proper anchor point for the chemical linkage of a drug, its terminal double-bond can be easily and regioselectively converted to a variety of functional groups that can later serve this purpose. In this regard, a typical synthetic procedure starts with the conversion of squalene to 1,1′,2-trisnorssqualene aldehyde that, as a key intermediate, can be further transformed into alcohol, amine or carboxylic acid, according to the task. The general overview of this preparative strategy is depicted in **Fig. 4** [99,101].

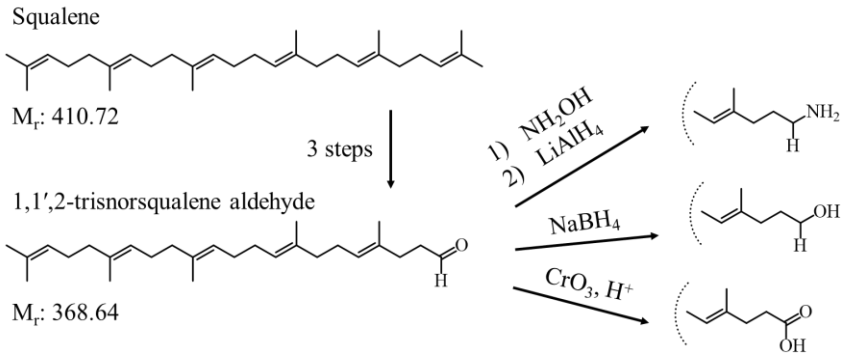

Figure 4. Schematic overview of the possible synthetic functionalization of squalene to obtain analogs possessing different terminal functional groups [99].

NPs of squalene bioconjugates can be conveniently prepared by nanoprecipitation in an aqueous medium. It was recently demonstrated that following intravenous administration, these particles do not remain intact in the bloodstream but get dissolved by lipoproteins, particularly low-density lipoproteins (LDL) in humans that will transport them, and this allows targeting cancer cells displaying high expression and activity of LDL receptors [102]. Although the method represents a relatively new platform for drug delivery, the technique's efficacy had already been successfully demonstrated with versatile bioactive molecules, including anticancer agents [103], antibiotics [104], and neuroprotective compounds [105].

I.4 PROTOFLAVONOIDS

I.4.1 Chemistry and occurrence in nature

In this Ph.D. study, besides ecdysteroids, the second substrate group of our investigation was the protoflavonoids. The chemical and biological diversity of these compounds have been previously reviewed by our research group [106].

Briefly, protoflavonoids represent a unique, naturally occurring group of flavonoids, possessing a non-aromatic B-ring and a hydroxyl moiety at C-1′. According to their widely accepted nomenclature, their trivial names are derived from the corresponding 4′-hydroxyflavones, wherein the addition of “proto-” prefix indicates the presence of the 4′-hydroxyl group, while the use of “-one” ending represents that the moiety is oxidized to an oxo

group. The protoflavone B-ring can appear in various forms; it may be a symmetric dienone *p*-quinol that may be partially or fully saturated, as illustrated by some examples of natural derivatives in **Fig. 5** [106].

Up to now, the natural occurrence of protoflavones was found almost exclusively in certain genera of ferns [107] though their 2,3-saturated structural analogs, such as protoflavanones, were found in other plants as well (*Piper carniconnectivum* [108], *Ongokea gore* [109]). Their biosynthesis was suggested to take place through the oxidation of 4′-hydroxyflavones. Subsequently, these already non-aromatic derivatives can be reduced to analogs with differently saturated B-rings whose 4′-oxo groups may also be reduced to a 4′-OH group [106].

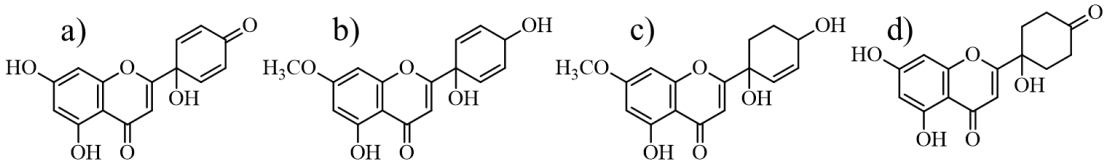

Figure 5. Selected examples of natural protoflavones with different levels of saturation in their B-ring. Trivial names of the compounds shown are a) protoapigenone, b) protogenkwanine, c) 5',6'-dihydroprotogenkwanin, d) tetrahydroprotoapigenone.

I.4.2 Bioactivities of protoflavonoids

Protoflavones are bioactive compounds, and many analogs are known for their potent anticancer effect that is currently by far their most deeply investigated pharmacological property. Numerous derivatives showed strong cytotoxicity on a wide range of cancer cell lines, while many can selectively kill certain types of resistant cancer cells that had been adapted to chemotherapeutics [110,111]. Up to now, the most extensively studied protoflavone is the oxidized analog of apigenin, protoapigenone (**Figure 5**, **a**). This compound was identified as a potent antitumor agent on various *in vitro* and *in vivo* tumor models [112–116]. Concerning the mechanism of action, there are several pharmacological pathways reported to be involved in the antitumor activity. It appears that the symmetric dienone *p*-quinol structure that is required for a potent antitumor action, allows these compounds to participate in redox reactions that induce oxidative stress within the cancer cells through the generation of reactive oxygen species (ROS) [117,118]. Additionally, protoapigenone interferes with crucial DNA-damage response mechanisms by inhibiting the ataxia-telangiectasia and Rad3-related protein (ATR)-dependent phosphorylation of checkpoint kinase 1, which confers this compound a chemo-sensitizing property towards DNA-damaging chemotherapeutics, such as cisplatin [119]. This mechanism is of high interest since ATR has become an emerging antitumor target, and several related clinical studies are

currently ongoing [120].

Besides the above, there are some pieces of evidence suggesting that the possible use of protoflavones might exceed their antitumor potential. In this regard, our group identified protoapigenone 1′-*O*-propargyl ether as the first non-planar flavonoid to express high inhibitory activity on xanthine oxidase (XO), the key enzyme in the development of gout [121]. Also, protoapigenone was shown to exert antiviral activity on Epstein-Barr virus by inhibiting the expression of lytic proteins, hence preventing the proliferation of the virus [122]. These suggest that the unique 3D structure of protoflavones among flavonoids, that is a direct consequence of the sp^3 configuration of C-2, may result in a versatile pharmacology of this compound class. However, any attempts to explore this are seriously limited by the potent cytotoxicity of the *p*-quinol dienone pharmacophore.

I.4.3 Synthetic preparation and SARs of protoflavonoids

Over the years, total- [123] and semi-synthetic [114] procedures were developed to obtain protoflavones as potent bioactive analogs of protoapigenone, and this enabled their preparation in large quantities and contributed to the exploration of their pharmacological properties, predominantly concerning their anticancer activities.

During the course of previous studies on protoflavonoids, it was found that, 1) the presence of a symmetric non-substituted dienone *p*-quinol in the B-ring is crucial for a strong cytotoxic effect [124], 2) the observed activity can be further increased through the introduction of a non-branching, alkyl side-chain of 3 or 4 carbon atoms at the 1′-OH or 3) significantly decreased through the addition of a branching (e. g. isopropyl) substituent at the same position [114]. It is important to note that the presence of 1'-OH alkyl substituents can significantly improve the chemical stability of the B-ring over that of the non-substituted *p*-quinol [114].

As discussed above, protoflavones may also exert bioactivities that are not related to cancer. Protoapigenone 1′-*O*-propargyl ether, a synthetic analog with potent XO-inhibitory activity, is a good example to this, even though this compound is also cytotoxic, therefore it would likely not be applicable as a therapeutic XO inhibitor. This justifies semi-synthetic strategies that point towards possibly decreased cytotoxicity. In this regard, the regioselective preparation of protoflavone oximes on the carbonyl group of their B-ring was an attractive strategy to obtain new, potentially bioactive compounds; prior to this Ph.D. study, no such derivatives have been reported.

II. OBJECTIVES

Oximes and their derivatives have remarkable significance both in chemistry and biology. Our scientific interest has recently turned towards the semi-synthetic preparation and investigation of such compounds from the derivatives of two, naturally occurring, bioactive compound groups, ecdysteroids and protoflavonoids. In this context, the primary aim of this Ph.D. study was to further extend the chemical diversity of these unique compound classes through the semi-synthetic preparation of new bioactive analogs, and to investigate the relevance of the oxime moiety in their chemical and pharmacological space. Therefore, we established the following objectives for this work.

ECDYSTEROIDS

1. Preparation of oxime derivatives from antitumor ecdysteroids. We aimed to transform 20E 2,3;20,22-diacetonide into its corresponding 6-oximes and oxime ethers, and subsequently to prepare lactam derivatives from the obtained oximes through Beckmann-rearrangement. Additionally, to further increase the chemical diversity of the products, we planned to subject a second substrate, poststerone 2,3-acetonide for oximation at its 20-carbonyl moiety.

2. The preparation of self-assembled NPs from an ecdysteroid oxime. We planned to select one of our synthetically obtained ecdysteroid derivatives possessing advantageous chemical and/or biological properties to prepare squalenoylated pro-drug nanoparticles.

3. Biological evaluation of the semi-synthetic ecdysteroids. The synthesized products were planned to be investigated for their *in vitro* anticancer properties in research collaborations.

PROTOFLAVONOIDS

4. Preparation of B-ring modified protoflavone derivatives including oximes. For the aim to extend the chemical–pharmacological space of protoflavones towards non-cytotoxic derivatives, we planned to prepare semi-synthetic analogs of protoapigenone. To achieve this, we aimed to perform the flow chemical hydrogenation or deuteration of the B-ring, and/or the preparation of 4′-oxime derivatives.

5. Biological evaluation of the synthetically obtained protoflavones. We aimed to study the pharmacological properties of the obtained protoflavones from various perspectives within the frameworks of scientific research co-operations. We planned to investigate the compounds' cytotoxic, ATR inhibitory and antiviral (anti-human immunodeficiency viral (anti-HIV) and anti-EBV) activities.

III. MATERIALS AND METHODS

Solvents and reagents were purchased from Sigma (Merck KGaA, Darmstadt, Germany) and were used without any further purification. The applied chromatographic instruments and columns are summarized in **Table 1**.

Table 1. Functional build-up of chromatographic instruments applied for different purposes during the course of this Ph.D. work.

Instrument	Functional units
Flash chromatograph (Teledyne ISCO, Lincoln, NE, USA; **preparative** purposes)	Combiflash Rf+ instrument equipped with diode array and evaporative light scattering detection (DAD-ELSD). We used it with commercially available prefilled "RediSep" columns.
HPLC instrument used for **analytical** purposes (Jasco, Hachioji, Tokyo, Japan)	A dual-pump Jasco HPLC instrument equipped with an "MD-2010 Plus" PDA detector. Columns: Phenomenex (Torrence, CA, USA) 250 x 4.6 mm 5 μm stationary phases (C18, C8)
HPLC instrument used for **semi-prep.** purposes (Agilent Inc., Santa Clara, CA, USA)	Agilent "1100 series" pump attached with a Jasco "UV-2070 Plus" single-wavelength UV detector. Columns: Phenomenex 250 x 10 mm 5 μm stationary phases (C18, C8)
HPLC instrument used for **preparative** purposes (Gilson Inc., Middleton , WI, USA)	Armen "Spot Prep II -250" preparative chromatographic system equipped with four individual solvent pumps and a dual-wavelength UV detector. Columns: Phenomenex 250 x 21.2 mm 5 μm stationary phases (C18, C8)

III.1 *ECDYSTEROIDS*

III.1.1 Source of natural ecdysteroids 1 and 2, later used as substrates in synthesis

III.1.1.1 Natural ecdysteroid 1 readily available from a commercial source

20-hydroxyecdysone (20E, **1**) was purchased from Shaanxi KingSci Biotechnology Co., Ltd (China) in a purity of 90%. By applying recrystallization from ethyl acetate – methanol (2:1, v/v), we afforded 20E (**1**) in an RP-HPLC purity of 97.8%.

III.1.1.2 Preparation of poststerone (2) via oxidative side-chain cleavage

An aliquot of 1 g of 20E (**1**) was dissolved in 80 ml of methanol. One molar equivalent of PIDA was added, and the solution was stirred for 45 minutes at RT. Following this, the reaction mixture was neutralized with 5% aq. $NaHCO_3$-solution and then, the solvent was evaporated under reduced pressure on a rotary evaporator. The products' dry residue was re-dissolved in methanol and silica gel (~6 g) was added to the solution. The solvent was

evaporated to prepare the sample for dry loading flash chromatographic separation that eventually yielded pure poststerone (**2**) (0.55 g, 72.9%; for details of chromatographic purification, see **Table 2**).

Table 2. List of chromatographic methods that were utilized for the purification of the prepared ecdysteroids and squalene analogs discussed in relation to this dissertation. "X g silica (plain) / C18" columns refer to commercially available "RediSep" (Teledyne ISCO, USA) flash chromatographic columns; "XB-C18": Kinetex 5 μm XB-C18 100A 250 x 21.2 mm HPLC column (Phenomenex Inc, USA); "XDB-C8": Agilent Eclipse Zorbax 5 μm XDB-C8 250 x 9.4 mm HPLC column (Agilent Technologies, USA). In each case, the yield refers to the isolated yield% of the pure (HPLC peak area% ≥ 95 at the λ_{max}, or at the PDA chromatogram recorded between 210-410 nm) compound. Numbers depicted as "*(x)*" indicate the corresponding step of the chromatographic purification. All solvent ratios refer to v/v.

cpd. x (yield)	column	flow rate	purification	detection
2 (72.9%)	80 g silica	60 ml/min	CH_2Cl_2 : CH_3OH 85:15 (40 min)	254 nm
3 (51%)	80 g silica	60 ml/min	CH_2Cl_2 : CH_3OH (A:B) 0→3% B (60 min)	254 nm
4 (71%)	80 g silica	60 ml/min	CH_2Cl_2 : CH_3OH (A:B) 0→3% B (60 min)	254 nm
5 (31%), **6** (38%)	XB-C18	15 ml/min	53% aq. CH_3CN	254 nm
7 (28.3%), **13** (43.3%)	4 g silica	18 ml/min	CH_2Cl_2 : CH_3OH (A: B) 45→100% B (35 min)	254 nm
8 (15.2%), **9** (2.8%), **14** (33.3%)	*(1)* 4 g silica *(2)* XDB-C8	*(1)* 18 ml/min *(2)* 3 ml/min	*(1)* CH_2Cl_2 : CH_3OH (A:B) 45→100% B (35 min) *(2)* 75% aq. CH_3CN	254 nm
10 (15.5%), **11** (1.6%), **15** (2%)	*(1)* 4 g silica *(2)* XDB-C8	*(1)* 18 ml/min *(2)* 3 ml/min	*(1)* CH_2Cl_2 : CH_3OH (A:B) 35→100% B (40 min) *(2)* 77% aq. CH_3CN	254 nm
12 (38.9%), **16** (8.3%), **17** (2.5%)	*(1)* 4 g silica *(2)* XDB-C8	*(1)* 18 ml/min *(2)* 3 ml/min	*(1)* CH_2Cl_2 : CH_3OH (A:B) 10→100% B (45 min); 100% B *(2)* 80% aq. CH_3CN	254 nm
18 (8%)	XB-C18	15 ml/min	75% aq. CH_3OH	254 nm
19 (69.7%)	XDB-C8	3 ml/min	35% aq. CH_3CN	243 nm
20 (12%)	30 g C18	35 ml/min	water : CH_3CN (A:B) 40→55% B (45 min)	254 nm
21a (71%)	80 g silica	60 ml/min	*n*-hexane : CH_2Cl_2 (A:B) 50% B	210 nm, 254 nm
22 (25%)	24 g silica	35 ml/min	*n*-hexane : EtOAc (A:B) 3.5→5% B (60 min)	210 nm, 254 nm
23 (62%) **24** (65%)	24 g silica	35 ml/min	*n*-hexane : EtOAc (A:B) 5→25% B (60 min)	210 nm, 254 nm
25 (73%) **26** (76%)	4 g silica	18 ml/min	*n*-hexane : EtOAc (A:B) 25% B	210 nm, 254 nm

III.1.2 Preparation of ecdysteroid acetonides 3 and 4 as starting materials for further transformations

Acetonide formation of ecdysteroids **1** and **2** was performed by dissolving 10 g of the corresponding substrate in acetone, in a concentration of 1 g/100 ml (1000 ml). To this solution, 10 g of phosphomolybdic acid was added, and the mixture was stirred or sonicated for 20 minutes at RT. Following this, the mixture was neutralized with 10% aq. $NaHCO_3$-solution and then, acetone was evaporated on a rotary evaporator. Products were extracted from their aqueous residue using ethyl acetate (3 x 100 ml), and the collected organic fractions were combined and dried over Na_2SO_4. The solution was then filtered, and the solvent was evaporated under reduced pressure. The obtained residue was subjected to flash chromatographic purification (see **Table 2**) that afforded 20E 2,3;20,22-diacetonide **3** (5.95 g, 51%), or poststerone 2,3-acetonide **4**, (7.88 g, 71%).

III.1.3 Preparation of oxime, oxime ether and lactam derivatives from ecdysteroid acetonides [I, II] [1]

III.1.3.1 Synthesis of 6-oxime derivatives 5-6 from 20E 2,3;20,22-diacetonide [I]

A 1 g aliquot of compound **3** (1.78 mmol) was dissolved in 10 ml of pyridine, and 1 g of hydroxylamine hydrochloride was added to the solution. The mixture was stirred at 70 °C for three days. Following this, pyridine was evaporated on a rotary evaporator, water (50 ml) was added to the dry residue, and extraction was carried out using ethyl acetate (3 x 50 ml). The collected organic fractions were combined and dried over Na_2SO_4. Subsequently, the solution was filtered and evaporated to dryness under reduced pressure. Purification of products was carried out by means of preparative RP-HPLC (see **Table 2**) to obtain ecdysteroid (6*E*)-oxime **5** (0.31 g, 31%) and (6*Z*)-oxime **6** (0.38 g, 38%) as pure, amorphous, white solids.

III.1.3.2 Synthesis of 6-oxime ether derivatives 7-17 from 20E 2,3;20,22-diacetonide [I]

A 200 mg aliquot of 20E 2,3;20,22-diacetonide (**3**, 0.35 mmol) was dissolved in 8 ml of pyridine and 200 mg of the alkoxyamine hydrochloride corresponding to the target oxime ether was added. The reaction was stirred at 70 °C for 24 hours, and subsequently, it was cooled to 0 °C and neutralized with a methanolic solution of KOH. After this, the solvent was evaporated on a rotary evaporator, water (50 ml) was added to the dry residue, and extraction was performed with ethyl acetate (3 x 50 ml). All organic fractions were combined, dried over Na_2SO_4, and filtered. Then, the solution was evaporated on a rotary evaporator, and the residue

[1] Reference to own publication related to the thesis

was subjected to flash chromatography to obtain oxime ether isomer mixtures, and subsequent semi-preparative RP-HPLC (see **Table 2**) to afford pure isomers **7-17**.

III.1.3.3 Synthesis of ecdysteroid lactam 18 from compound 5 [I]

A 150 mg aliquot of ecdysteroid oxime **5** (0.27 mmol) was dissolved in 10 ml of acetone. Then, 29 mg Na_2CO_3 (0.27 mmol, 1 equiv.) and 104.3 mg of *p*-toluenesulfonyl chloride (TsCl, 0.54 mmol, 2 equiv.) were added to the solution, and the mixture was stirred for 6 hours at RT. Following this, the solution was cooled to 0 °C, water (50 ml) was added under stirring, and extraction was performed using ethyl acetate (3 x 50 ml). The collected organic fractions were combined, dried over Na_2SO_4, and filtered. Then, the solvent was evaporated under reduced pressure, and the residue was purified by preparative RP-HPLC (see **Table 2**) to afford ecdysteroid lactam **18** (11 mg, 8%).

III.1.3.4 Synthesis of (20*E*)-oxime derivative 19 from poststerone 2,3-acetonide [II]

A 42.2 mg (0.10 mmol) aliquot of compound **4** was dissolved in 5 ml of pyridine. Then, 10.9 mg (0.16 mmol; 1.5 equiv.) of hydroxylamine hydrochloride was added, and the reaction was stirred for 25 minutes at RT. Subsequently, the mixture was cooled to 0 °C, and neutralized with an ethyl alcoholic solution of KOH (8.8 mg; 0.16 mmol). The solution was evaporated under reduced pressure, water (30 ml) was added to its dry residue, and the products were extracted with ethyl acetate (4 x 30 ml). The collected organic fractions were combined, dried over Na_2SO_4, and filtered. Then, the solution was evaporated to dryness on a rotary evaporator, and the residue was purified by preparative RP-HPLC (see **Table 2**) to afford poststerone 2,3-acetonide (20*E*)-oxime (**19**, 30.7 mg, 69.7%).

III.1.3.5 Synthesis of (20*E*/*Z*)-oxime ether isomeric mixture 20 from substrate 4 [II]

A 300 mg (0.745 mmol) aliquot of compound **4** was dissolved in 6 ml of freshly distilled pyridine. Methoxyamine hydrochloride (186.7 mg, 2.235 mmol, 3 equiv.) was added to the solution, which was then stirred at 70 °C for 5.5 hr. Following this, the reaction mixture was cooled to 0 °C, and it was neutralized by KOH (125.4 mg; 2.235 mmol) dissolved in 5 ml of anhydrous ethanol. Then, the solvent was evaporated under reduced pressure, water (40 ml) was added to the residue, and extraction was performed with ethyl acetate (4 × 40 ml). The organic fractions were combined, dried over Na_2SO_4, and filtered. The solution was evaporated under reduced pressure, and the residue was purified by flash chromatography (see **Table 2**) to afford a mixture of (*E*/*Z*)-isomers of 20-*O*-methyl oxime ether (**20**) in a combined yield of 12% (38.6 mg) at a 95:5 ratio (*E* and *Z*, respectively).

III.1.4 Investigation of self-assembled ecdysteroid nanoparticles of compound 19 [II, III]

III.1.4.1 Preparation of 1,1',2-tris-norsqualene alcohol 22 from squalene

Functionalization of squalene (**21**) to obtain 1,1′,2-tris-norsqualene alcohol (**22**) was carried out in 4 synthetic steps, as follows.

(1) An aliquot of 10 g of squalene (24.3 mmol) was dissolved in 70 ml of tetrahydrofuran (THF). Water (20 ml) was added dropwise under magnetic stirring to the solution, followed by a further 30 ml of THF. Subsequently, N-bromosuccinimide (NBS; 5.20 g, 29.2 mmol) was added to the solution in small portions, and the reaction mixture was stirred for 3 hours at RT. Following this, THF was evaporated on a rotary evaporator, and the aqueous residue was diluted with brine (35 ml) and extracted with ethyl acetate (5 x 50 ml). The combined solution of the organic fractions was dried over Na_2SO_4, filtered, and the solvent was evaporated under reduced pressure. The oily residue was purified by flash chromatography (see **Table 2**) to afford *2-hydroxy-3-bromosqualene* (**21a**) in a yield of 27% (3.34 g).

(2) To a solution of compound **21a** (3.34 g, 6.58 mmol) in methanol (120 ml), K_2CO_3 (1.82 g, 13.16 mmol; 2 equiv.) was added, and the reaction mixture was stirred for two hours at RT. Subsequently, the solvent was evaporated under reduced pressure, water (50 ml) was added to the oily residue, and the products were extracted with ethyl acetate (4 x 50 ml). The combined organic fractions were dried over Na_2SO_4, filtered, and the solvent was evaporated on a rotary evaporator to afford *2,3-oxidosqualene* (**21b**) in a yield of 97% (2.72 g) without further purification.

(3) To a solution of compound **21b** (2.72 g, 6.38 mmol) in dioxane (30 ml) an aqueous solution (20 ml) of H_5IO_6 (11.48 mmol; 1,8 equiv.) was added under stirring. The reaction mixture was stirred for two hours at RT. Subsequently, the solution was evaporated on a rotary evaporator, water (50 ml) was added to the oily residue, and the products were extracted with ethyl acetate (4 x 50 ml). The collected organic fractions were combined and dried over Na_2SO_4. Later, the solution was filtered, and the solvent was evaporated on a rotary evaporator that afforded *1,1',2-tris-norsqualene aldehyde* (**21c**) in a yield of 79% (1.94 g) without any further purification.

(4) To a solution of **21c** (1.94 g, 5 mmol) in methanol (100 ml), $NaBH_4$ (0.094 g, 2.5 mmol; 0.5 equiv.) was added in portions, and the reaction mixture was stirred for one hour at RT. Subsequently, HCl (1 M) was added to quench the unreacted $NaBH_4$. Following this, the solvent was evaporated under reduced pressure, water (200 ml) was added to the oily residue, and extraction was performed with ethyl acetate (3 x 50 ml). Then, the organic fractions were

combined and dried over Na_2SO_4. Subsequently, the sample was adsorbed on silica for dry loading flash chromatographic purification (see **Table 2**), which allowed the isolation of 1,1′,2-tris-norsqualene alcohol (**22**; 1.38 g, yield: 71 %) as a colorless oil.

III.1.4.2 Preparation of compounds 23 and 24 from substrate 22

A 500 mg aliquot of 1,1′,2-tris-norsqualene alcohol **22** (1.29 mmol) was dissolved in 10 ml of anhydrous dichloromethane. To this solution, 4-dimethylaminopyridine (DMAP; 110.32 mg, 0.90 mmol; 0.7 equiv.), EDC·HCl (296.75 mmol, 1.55 mmol.; 1.2 equiv.) and, depending on which linker was used, either sebacic or 4,4′-dithiodibutyric acid (2.58 mmol; 2 equiv.) were added. The reaction mixture was stirred for 6 hours under an argon atmosphere at RT. Subsequently, the solution was neutralized with 10% aq. $NaHCO_3$, brine (20 ml) was added to it, and the products were extracted with dichloromethane (4 x 30 ml). Following this, the organic fractions were combined, dried over Na_2SO_4, and filtered. Subsequently, the sample was adsorbed on silica gel (1-2 g) for dry loading flash chromatographic purification (see **Table 2**), which allowed the isolation of compound **23** (458.1 mg, 62%) or the disulfide-bridge containing compound **24** (510.6 mg, 65%).

III.1.4.3 Preparation of ecdysteroid-squalene conjugates 25 and 26 [II, III]

An aliquot of 34.2 mg (0.08 mmol) of poststerone 2,3-acetonide 20-oxime (**19**) was dissolved in 6 ml of anhydrous dichloromethane in a two-neck round-bottom flask. Depending on the linker, 1.5 equivalents of either compound **23** (70.2 mg, 0.12 mmol) or **24** (72.8 mg, 0.12 mmol) was added dropwise to the solution. Subsequently, DMAP (13.1 mg, 0.16 mmol, 2 equiv.) and EDC·HCl (39.3 mg, 0.20 mmol, 2.5 equivalents) were added to the mixture, which was then stirred for 2 hours under an argon atmosphere at RT. Following this, the solution was neutralized by 10% aq. $NaHCO_3$, brine (30 ml) was added to it, and extraction was carried out with dichloromethane (4 × 30 ml). The organic fractions were combined, dried over Na_2SO_4, filtered, and evaporated to dryness on a rotary evaporator. The oily residue was subjected to flash chromatographic purification (see **Table 2**) to afford ecdysteroid conjugate **25** (61.0 mg, 73%) or the disulfide-bridge containing conjugate **26** (66.1 mg, 76%), as colorless oils.

III.1.4.4 Preparation of self-assembled nanoparticles 25_{NP} and 26_{NP}, heteronanoparticles $25_{NP\text{-}DOX}$ and $26_{NP\text{-}DOX}$ and their characterization [III]

Nanoparticles (NPs) and heteronanoparticles (H-NPs) were prepared and characterized by the research group of *Prof. Daniele Passarella* (Department of Chemistry, University of Milan, Milan, Italy). Briefly, the following procedure was used.

In the cases of NPs, a 250 μg aliquot of ecdysteroid conjugate **25** or **26** was dissolved in 125 μl of THF (2 mg/ml), and under mild stirring (400 rpm), this solution was added dropwise within a one-minute period of time to a double volume of Milli-Q® (Merck KGaA, Germany) ultrapure water at RT. Finally, the organic solvent was evaporated at 30 °C under reduced pressure to obtain the corresponding aqueous nanosuspensions **25**$_{NP}$ and **26**$_{NP}$ in a final concentration of 1 mg/ml.

H-NPs were prepared by mixing a solution of ecdysteroid conjugate **25** or **26** (125 μL, 250 μg, 2 mg/ml) with squalene-functionalized doxorubicin solution (2 mg/ml) in THF in a 1:50 molar ratio of ecdysteroid conjugate/doxorubicin conjugate –to obtain a mixture in a final concentration of 2 mg/ml. Squalene-functionalized doxorubicin was previously prepared by the collaborating research group. The self-assembly process was performed as described above, to afford the aq. nanosuspensions of **25**$_{NP\text{-}DOX}$ or **26**$_{NP\text{-}DOX}$ at a final concentration of 1 mg/ml.

The average diameter and polydispersity index (PdI) of each nano assembly was determined by dynamic light scattering (DLS) technique on a Malvern ZS zetasizer (Malvern Panalytical Ltd., UK) instrument with disposable folded capillary. During the investigations, 100-150 μg/ml concentration aq. samples were diluted from the dispersions, which were then placed in the electrophoretic cell of the Malvern ZS zetasizer, to determine their zeta potential. Transmission electron microscopy (TEM) images were obtained at 25 °C, upon filtering the 1 mg/ml nanosuspensions through a 0.45 μm filter.

III.1.5 Procedures for the structure elucidation of obtained products [I, II]

^{1}H (950 or 500 MHz) and ^{13}C (239 or 125 MHz) NMR spectra of ecdysteroid and squalene derivatives were recorded at room temperature on a Bruker Avance-II or Avance-III spectrometer (Bruker Co., Billerica, MA, USA) equipped with cryo probeheads. The investigations were performed in research collaboration with *Prof. Dr. Gábor Tóth* (Department of Inorganic and Analytical Chemistry, Budapest University of Technology and Economics, Budapest, Hungary), *Dr. Dóra Bogdán* (Department of Organic Chemistry, Semmelweis University, Budapest, Hungary) and *Dr. Rainer Haessner* (Institute of Organic Chemistry and Biochemistry, Technical University of Munich, Garching, Germany) [I, II].

High-resolution mass spectrometry (HR-MS) analysis of the obtained products was carried out utilizing a Waters Acquity I-Class UHPLC system (Waters Co., USA) coupled with a Thermo Scientific Q Exactive Plus orbitrap mass spectrometer (Thermo Fisher Scientific Inc., USA) equipped with heated electrospray ionization (HESI) source. Each spectrum was recorded in positive ionization mode.

III.1.6 Biological evaluation of ecdysteroid derivatives

III.1.6.1 *In vitro* antiproliferative assays of compounds 7-18 [I]

The antiproliferative effects of compounds **7-18** were tested by MTT assay on human gynecological cancer cell lines in collaboration with *Prof. István Zupkó* (Institute of Pharmacodynamics and Biopharmacy, University of Szeged, Szeged, Hungary). Cell viability data were obtained on four human adherent cancer cell lines; MDA-MB-231, MCF-7 (breast cancers), HeLa (cervical adenocarcinoma) and SiHa (cervical carcinoma). Cisplatin was used as a positive control [I].

III.1.6.2 Rhodamine 123 accumulation assay of compounds 5-19 [I]

ABCB1 inhibitory activities of ecdysteroids **5-19** were studied *in vitro* in research cooperation with *Dr. Ana Martins* (Department of Medical Microbiology and Immunobiology, Faculty of Medicine, University of Szeged, Szeged, Hungary). Functional inhibition of efflux by the compounds was measured by the intracellular accumulation of rhodamine 123, a fluorescent dye that is an ABCB1 substrate. As a positive control, tariquidar was used [I].

III.1.6.3 Cytotoxicity assays of compounds 5-19 on murine lymphoma cell lines [I]

In vitro cytotoxic activity of ecdysteroid analogs **5-19** alone, or in combination with doxorubicin, were tested in research collaboration with *Dr. Ana Martins* (Department of Medical Microbiology and Immunobiology, University of Szeged, Szeged, Hungary). Two mouse lymphoma cell lines were used, a drug-susceptible mouse T-cell lymphoma (L5178) and its multi-drug-resistant counterpart ($L5178_{MDR}$) that had been transfected with pHa MDR1/A retrovirus to express the human ABCB1 transporter [125]. The checkerboard microplate method was used, and results were evaluated by the Chou-Talalay method [126], according to our previously published procedure [87]. When the ecdysteroids were studied in the presence of doxorubicin, the interactions were evaluated at each constant ratio of compound vs. chemotherapeutics (M/M), and combination index (CI) values were obtained for 50%, 75%, and 90% of growth inhibition [I].

III.1.6.4 Cytotoxicity assay of self-assembled ecdysteroid nanoparticles [III]

The *in vitro* antiproliferative activity of NPs $\mathbf{25_{NP}}$ and $\mathbf{26_{NP}}$, and doxorubicin-containing H-NPs $\mathbf{25_{NP\text{-}DOX}}$ and $\mathbf{26_{NP\text{-}DOX}}$ on $A2780_{ADR}$ cancer cells (doxorubicin-resistant human ovarian carcinoma) was investigated by the Trypan blue assay in research collaboration with the research group of *Prof. Daniele Passarella*. Results were expressed as GI_{50} (GI: grow inhibition) values, i.e., the concentration of the test agent inducing 50% reduction in cell number

compared with control cultures [III].

III.2. *PROTOFLAVONOIDS*

III.2.1 Preparation of protoapigenone analogs 28-34 as substrates of further semi-synthetic transformations

Apigenin (**27**) was purchased from Changsa Inner Natural Inc. (Hunan, China) in an RP-HPLC purity of 98% and was used as a starting material for semi-synthetic transformations. In a typical reaction, a 1 g aliquot of apigenin (3.70 mmol) was dissolved in a concentration of 1 mg/ml in a 9:1 (v/v) mixture of acetonitrile and either water or the alcohol to be coupled at C-1′. Two equivalents of PIFA (3.18 g, 7.40 mmol) were added to the solution, and the mixture was stirred at 80 °C for an hour. Following this, the solution was cooled down to RT, and the solvent was evaporated under reduced pressure on a rotary evaporator. The obtained residue was re-dissolved in acetone and subjected to flash chromatographic purification by our previously published methods [114] that afforded protoapigenone analogs **28-34** with the following yields: **28** (308.2 mg, 29.1%), **29** (381.1 mg, 34.3%), **30** (380.3 mg, 32.7%), **31** (370.5 mg, 30.5%), **32** (292.8 mg, 24.1%), **33** (445.9 mg, 35.2%), **34** (372.0 mg, 31.0%).

III.2.2 Preparation and functionalization of protoflavonoid analogs [IV, V]

III.2.2.1 Preparation of tetrahydroprotoapigenone analogs 35-40 through the flow chemical hydrogenation of the B ring [IV, V]

Selective saturation of the protoflavone B-ring was achieved relying on the utilization of ThalesNano's H-Cube (ThalesNano Inc., Budapest, Hungary) continuous flow hydrogenation system. Part of our device was a stainless-steel cartridge (internal dimensions: 50 mm × 4.6 mm), filled with 100 or 200 mg of 5% Pd/C catalyst, varied according to the amount of substrate desired to be converted. The column was inserted to an external thermostat (Jetstream 2 plus, Jasco, Japan) set to 25 °C. Solvent pumping was provided by a standard HPLC pump, that ensured a continuous flow rate of 1 ml/min in the presence of 40 bar backpressure.

In each reaction's case, a 1 mg/ml solution of the corresponding protoflavone substrate was prepared using HPLC grade ethyl acetate or methanol as solvents. For small-scale test reactions, 15 ml solutions were prepared. For the transformations, 20 ml substrate solutions were prepared, except for compounds **35** and **40**, which were synthesized from 360 ml solutions. To ensure synthetic reproducibility, the catalyst bed was washed with the solvent for 15 minutes between the reactions. Following synthesis, the collected solutions were evaporated on a rotary evaporator and samples were applied to preparative RP-HPLC (see **Table 3**) that

allowed the isolation of compounds **35-40** with the following yields: **35** (253.0 mg, 69.3%), **36** (5.1 mg, 25.2%), **37** (15.5 mg, 70.5%), **38** (6.1 mg, 30.1%), **39** (8.9 mg, 44%), **40** (209.4 mg, 57.5%).

III.2.2.2 Preparation of tetradeuteroprotoapigenone analogs 41-46 through the flow chemical deuteration of the B ring [V]

Deuteration of the protoapigenone B-ring was carried out utilizing the flow chemical conditions described for hydrogenation (for further details, see III.2.2.1 above), but for this purpose, as a catalyst, 400 mg of 5% $Pd/BaSO_4$ was applied, and the reservoir of the reactor was filled with high purity heavy water (D_2O). Following the transformations, each obtained sample was evaporated to dryness on a rotary evaporator and was subsequently purified with preparative RP-HPLC (see **Table 3**) that yielded deuterated protoapigenone analogs **41-46** as follows: **41** (12.6 mg, 63.1%), **42** (8.2 mg, 40.5%), **43** (12.1 mg, 60.6%), **44** (10.4 mg, 51.4%), **45** (11.3 mg, 55.8%), **46** (14.7 mg, 73.5%).

III.2.2.3 Preparation of protoapigenone 4'-oxime derivatives 47-52 [V]

A 150 mg aliquot of compound **32**, **33** or **34** was dissolved in a concentration of 2.5 mg/ml in HPLC grade methanol (60 ml). Three equivalents of hydroxylamine hydrochloride were added to the solution under stirring, and the mixture was stirred under reflux for 24 h at 70 °C. Following this, silica gel (3-5 g) was added to the reaction mixture, and compounds were adsorbed on its surface through solvent evaporation under reduced pressure. The acquired sample was subjected to flash chromatography to remove soluble and insoluble contaminants, and later, the products of the simplified sample were separated by means of preparative RP-HPLC (see **Table 3**) that allowed us the isolation of oxime racemates **47-52** with the following yields: **47** (41.7 mg, 24.3%), **48** (47.4 mg, 27.8%), **49** (43.1 mg, 25.1%), **50** (50.7 mg, 29.6%), **51** (56.6 mg, 33.2%), **52** (54.6 mg, 31.8%).

III.2.2.4 Preparation of tetrahydroprotoapigenone 4'-oxime derivatives 53-54 [V]

A 60 mg aliquot of tetrahydroprotoflavone substrate **35** or **40** was dissolved in a concentration of 2 mg/ml in HPLC grade methanol (30 ml). 4 equivalents of hydroxylamine hydrochloride were added to the solution under stirring, and the reaction was stirred under reflux for 3 h at 70 °C. Following this, methanol was evaporated under reduced pressure, brine (40 ml) was added to the solid residue, and extraction was carried out using ethyl acetate (3 x 40 ml). The collected organic fractions were dried over Na_2SO_4. Later, the drying agent was removed through filtration, and the solution was evaporated to dryness on a rotary evaporator.

The obtained sample was applied to preparative RP-HPLC (see **Table 3**) that afforded oxime racemate **53** (30.5 mg, 48.3%), or **54** (26.4 mg, 42.1%).

Table 3. List of chromatographic methods that were utilized for the purification of synthetically obtained protoflavonoid analogs discussed in relation to this dissertation. "X g silica" columns refer to commercially available "RediSep" (plain) silica (Teledyne ISCO, USA) flash chromatographic columns; "XB-C18" column: Kinetex 5 µm XB-C18 100A 250 x 21.2 mm HPLC Column (Phenomenex Inc, USA); "XDB-C8" column: Agilent Eclipse Zorbax 5 µm XDB-C8 250 x 9.4 mm HPLC Column (Agilent Technologies, USA); "Gemini C18" column: Phenomenex 5µm Gemini-XN C18 HPLC column 250 x 10 mm (Phenomenex Inc, USA). In each case, the yield refers to the isolated yield% of the pure (HPLC peak area% ≥ 95 at the λ_{max}, or at the PDA chromatogram recorded between 210-410 nm) compound. Numbers depicted as "*(x)*" indicate the corresponding step of the chromatographic purification.

cpd. x (yield)	column	flow rate	purification	detection
35 (69.3%)	XB-C18	15 ml/min	18% aq. CH_3CN	254 nm
36 (25.2%)	Gemini C18	3 ml/min	45% aq. CH_3CN	254 nm
37 (70.5%)	Gemini C18	3 ml/min	50% aq. CH_3CN	254 nm
38 (30.1%)	Gemini C18	3 ml/min	50% aq. CH_3CN	254 nm
39 (44.0%)	Gemini C18	3 ml/min	55% aq. CH_3CN	254 nm
40 (57.5%)	XB-C18	15 ml/min	55% aq. CH_3CN	254 nm
41 (63.1%)	Gemini C18	3 ml/min	18% aq. CH_3CN	254 nm
42 (40.5%)	Gemini C18	3 ml/min	45% aq. CH_3CN	254 nm
43 (60.6%)	Gemini C18	3 ml/min	55% aq. CH_3CN	254 nm
44 (51.4%)	Gemini C18	3 ml/min	50% aq. CH_3CN	254 nm
45 (55.8%)	Gemini C18	3 ml/min	55% aq. CH_3CN	254 nm
46 (73.5%)	Gemini C18	3 ml/min	61% aq. CH_3CN	254 nm
48 (27.8%) **51** (33.2%)	*(1)* 4 g silica *(2)* XDB-C8	*(1)* 18 ml/min *(2)* 3 ml/min	*(1)* *n*-hexane : EtOAc (A:B) 0→65% B (35 min) *(2)* 38% aq. CH_3CN	254 nm 300 nm
49 (25.1%) **52** (31.8%)	*(1)* 4 g silica *(2)* XDB-C8	*(1)* 18 ml/min *(2)* 3 ml/min	*(1)* *n*-hexane : EtOAc (A:B) 0→65% B (35 min) *(2)* 30% aq. CH_3CN	254 nm 300 nm
47 (24.3%) **50** (29.6%)	*(1)* 4 g silica *(2)* XDB-C8	*(1)* 18 ml/min *(2)* 3 ml/min	*(1)* *n*-hexane : EtOAc (A:B) 0→65% B (35 min) *(2)* 35% aq. CH_3CN	254 nm 300 nm
53 (48.3%)	XB-C18	15 ml/min	18% aq. CH_3OH	254 nm
54 (42.1%)	XB-C18	15 ml/min	40% aq. CH_3OH	254 nm

III.2.3 Procedures for the structure elucidation of obtained protoflavonoids [IV, V]

Mass spectra of the protoflavones were recorded on an Agilent 1100 LC-MS system (Agilent Technologies, Santa Clara, CA, USA) coupled with Thermo Q-Exactive Plus orbitrap analyzer (Thermo Fisher Scientific, Waltham, MA, USA) used in positive mode, or on an API 2000 triple quadrupole tandem mass spectrometer (AB SCIEX, Foster City, CA, USA) equipped with ESI source utilized in negative ionization mode.

^{1}H, ^{13}C, ^{13}C HSQC, and ^{13}C HMBC NMR spectra of the derivatives were recorded on a Bruker Avance DRX 400 MHz instrument or on a Bruker Avance NEO 500 MHz spectrometer (Bruker Co., Billerica, MA, USA) equipped with a Prodigy BBO 5 mm CryoProbe using TMS as an internal standard. In general, 5-10 mg of the corresponding protoflavone was dissolved in DMSO-*d6* and transferred to NMR tubes for spectra record. Data report and spectra analysis were carried out with MestReNova v6.0.2-5475 software (Mestrelab Research S.L., Santiago de Compostela, Spain). The NMR investigations were performed in research collaboration with *Dr. Norbert Kúsz* (University of Szeged, Institute of Pharmacognosy, Szeged, Hungary).

III.2.4 Biological evaluation of protoflavonoid derivatives [IV, V]

III.2.4.1 Antitumor assays of compounds 35 and 40 [IV]

Compounds **35** and **40** were tested for their *in vitro* cytotoxicity on MCF-7 (breast), HeLa (cervix), and SiHa (cervix) human adherent cancer cell lines. In this regard, different dilutions were prepared from the compounds, which were then analyzed using the checkerboard microplate method. The surviving cells were detected by the MTT method.

Furthermore, the analogs were tested for their potential to interfere with the ATR/ATM signaling pathways, whose inhibition would confer them chemo-sensitizing activity towards DNA-damaging chemotherapeutics. The investigation was carried out by pre-treating MCF-7 cells with or without 5, 10 or 20 μM of compounds for 30 min, and DNA damage was induced by exposing the cells to 1 μm of doxorubicin for 6 h. The detection of DNA damage response was achieved by Western blot assay, as previously described [113]. The studies were performed in research cooperation with *Dr. Ching-Ying Kuo* and *Dr. Hui-Chun Wang* (Graduate Institute of Natural Products, College of Pharmacy, Kaohsiung Medical University, Kaohsiung, Taiwan, R.O.C.) [IV].

III.2.4.2 Antiviral testing of protoflavonoids [V]

Antiretroviral assay against HIV. Derivatives **28**, **32-40** and **47-54** were tested against HIV-1 using a pseudotype virus assay (U373-CD4-CCR5 cells infected by pseudotyped virus) allowing only one cycle of viral replication and being more sensitive for compounds targeting the early steps of HIV replication, such as reverse transcription and integration. Drug cytotoxicity was evaluated by using the MTT assay. The measurements were performed in a scientific research collaboration with *Dr. Carole Seguin-Devaux* (Department of Infection and Immunity, Luxembourg Institute of Health, Luxemburg) [V].

Antiviral activity against EBV. Derivatives **28** and **32-54** were tested for their effects on the immunoblot assays of EBV Rta Protein. The concentration selected for wide-scale

screening was 0.25 μM, where protoapigenone (**28**) was previously found to exert a strong activity [122]. Additionally, we examined the cytotoxicity of the active analogs on P3HR1 cells. For the analysis, 96-well plates were used, and the compounds' cytotoxicity was determined by Cell Proliferation Kit I. The tests were performed in research collaboration with *Dr. Li-Kwan Chang* (Department of Biochemical Science and Technology, College of Life Science, National Taiwan University, Taipei City, Taiwan [V].

IV. RESULTS

IV.1 *ECDYSTEROIDS*

IV.1.1 Preparation of compounds 3 and 4 as substrates for further transformations

IV.1.1.1 Synthesis of poststerone (2) through the oxidative side-chain cleavage of 20E

Oxidative cleavage of the sterol side-chain of 20E (**1**) was achieved using hypervalent iodine reagent PIDA as previously reported by our research group [127].

Briefly, one equivalent of the reagent was added portion-wise to 20E dissolved in methanol, and this resulted in a total conversion of the substrate and highly selective cleavage of its sterol side-chain within 45 min of intensive stirring. Flash chromatographic purification resulted in the successful isolation of poststerone (**2**) in high yield (72.9%) (see **Table 2** of section III.1.1 for the chromatographic method, and **Scheme 1** for the transformation.).

IV.1.1.2. Acetonide formation of the vicinal diols of 20E (1) and poststerone (2)

We achieved the preparation of the 2,3-acetonide and 2,3;20,22-diacetonide analogs of poststerone (**2**) and 20E (**1**), respectively, following our previously described synthetic strategy [90]. Using phosphomolybdic acid as a catalyst in acetone resulted in the protection of the vicinal diols of the substrates (**Scheme 1**). The products were purified by flash chromatography that afforded 20E 2,3;20,22-diacetonide (**3**) in fair (5.95 g, 51%), and poststerone 2,3-acetonide (**4**) in good yield (7.88 g, 71%; for details of the chromatographic purification, see **Table 2**).

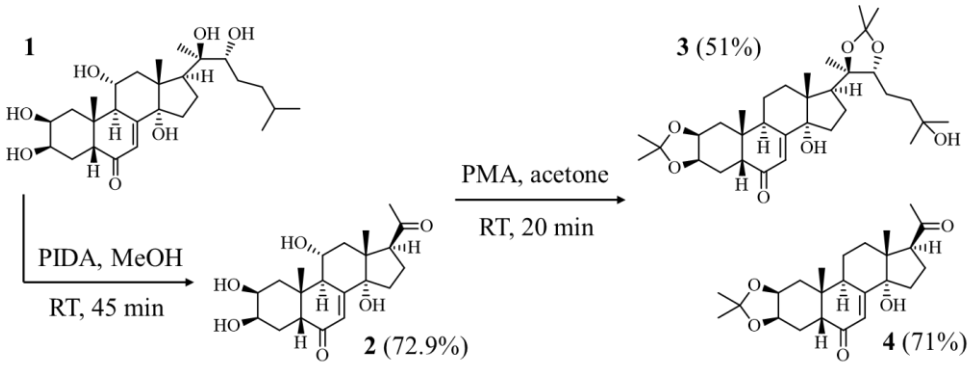

Scheme 1. Semi-synthesis of compounds **2-4** through the transformation of 20E (**1**).

IV.1.2 Synthesis and derivatization of oxime analogs from substrates 3 and 4

IV.1.2.1 Preparation of 6-oximes 5 and 6 from 20E 2,3;20,22-diacetonide (3) [I]

To obtain the 6-oxime analogs of 20E 2,3;20,22-diacetonide (**3**), we followed a previously published procedure [92]. Briefly, we reacted substrate **3** with hydroxylamine hydrochloride in pyridine that eventually afforded a pair of *E*/*Z*-isomeric oxime products, wherein the 14α-OH moiety was eliminated on both derivatives. As compared to the publication that provided the methodical basis of the synthesis [92], we succeeded in the separation of the corresponding oxime isomers by applying preparative RP-HPLC that yielded ecdysteroid (6*E*)-oxime **5** (0.31 g, 31%) and ecdysteroid (6*Z*)-oxime **6** (0.38 g, 38%) in pure form and in high purity (see **Table 2** of section III.1.1). **Scheme 2** depicts the transformation.

IV.1.2.2 Preparation of 6-oxime ethers 7-17 from 20E 2,3;20,22-diacetonide (3) [I]

We succeeded in the synthesis of the 6-oxime ether derivatives of ecdysteroid substrate **3**, by employing the appropriate alkoxyamine reagent in pyridine, depending on the oxime ether moiety desired at C-6. Following the transformations, we neutralized the reaction mixtures with methanolic solutions of KOH that allowed the preparation of both 14,15-anhydro- and intact ecdysteroid oxime ethers. This way, we obtained compounds **7-17**, a total of 11 ecdysteroid derivatives. Subsequently, we carried out the chromatographic purification of the products in two steps: at first, we used flash chromatography for fractionation, and this was followed by semi-preparative RP-HPLC (see **Table 2**) that allowed the isolation of each geometric isomer in pure form. **Scheme 2** shows the synthetic scheme.

IV.1.2.3 Beckmann-rearrangement of compound 5 to ecdysteroid lactam 18 [I]

Beckmann-rearrangement of ecdysteroid (6*E*)-oxime **5** was performed considering a previously published procedure [128]. In contrast to the 24 h reaction time reported in the publication, with the transformation's periodic TLC monitoring, we found that the use of TsCl in acetone, in the presence of Na_2CO_3, can effectively furnish the seven-membered lactam ring of the product, and succeeds with the total conversion of the substrate within only 6 hours.

In our publication related to the thesis [I], we employed liquid-liquid extraction for reaction work-up and purified the crude sample mixture by preparative RP-HPLC that afforded compound **18** (11 mg, 8%) in very low yield (see section III.1.3.3.). Here we report an update to our former work-up strategy: following the transformation process, the reaction solution needs to be evaporated to dryness, and after re-dissolving the solid residue in dichloromethane, it should be subjected to normal-phase solid-phase extraction (SPE) on silica previously pre-

conditioned with the solvent. Column washing with dichloromethane allows the selective elution of the apolar TsCl, while the dilution of the eluent with methanol in 10% (v/v), can elute the retained ecdysteroid product. By subjecting the pre-purified sample to preparative RP-HPLC (see **Table 2**), we can obtain compound **18** in a notably higher yield (23.2%) than before [I]. The reaction scheme is shown in **Scheme 3**.

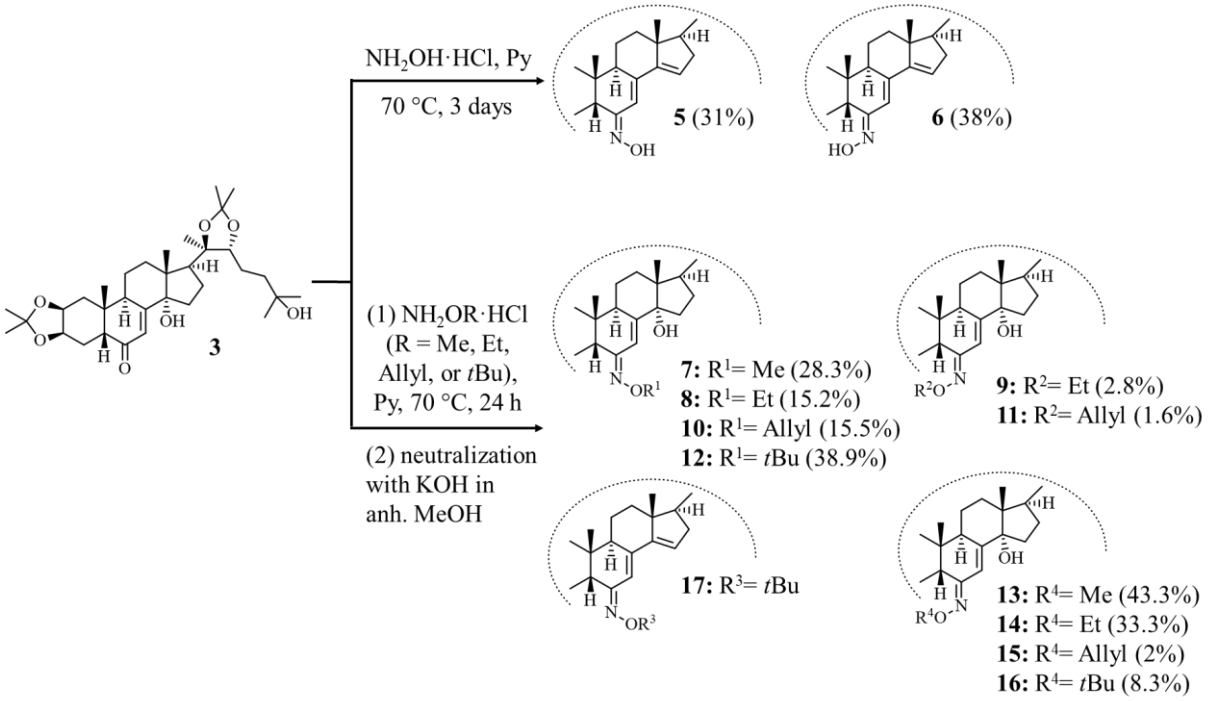

Scheme 2. Semi-synthesis of compounds **5-17** through the transformation of substrate **3**.

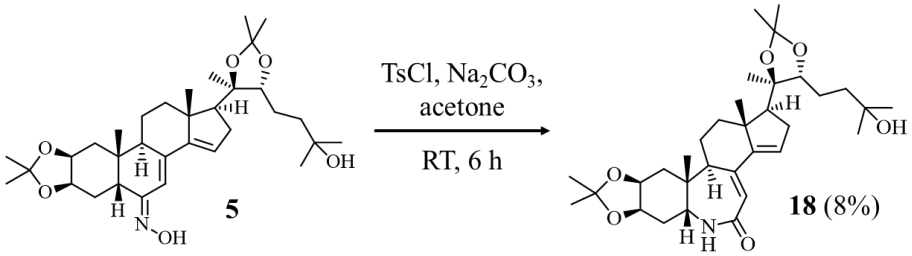

Scheme 3. Preparation of ecdysteroid lactam **18** through the transformation of (6*E*)-oxime **5**.

IV.1.2.4 Preparation of 20-oxime analogs of poststerone 2,3-acetonide (4) [II]

By employing hydroxylamine- or methoxyamine hydrochloride reagents to transform poststerone 2,3-acetonide (**4**) in pyridine, we achieved the preparation of its 20-oxime (**19**) and 20-*O*-methyl oxime ether (**20**) analogs, respectively. During this work, we found that our procedure was highly regioselective to afford 20-oxime analog **19** at ambient temperature. In contrast, we succeeded in effecting the transformation of the substrate to its 20-oxime ether analog **20** by applying heating and larger reactant amounts. Following transformations, we

performed neutralization on each reaction mixture with an ethanolic solution of KOH that allowed the convenient, decomposition-free work-up of the products. We purified compound **19** using semi-preparative RP-HPLC (see **Table 2**) that afforded the derivative in high yield (30.7 mg, 69.7%). Products of the oxime ether synthesis were separated by flash chromatography, which allowed us the isolation of a mixture of (*E*/*Z*)-isomeric 20-*O*-methyl oxime ethers (**20**) in a low combined yield (12 %, 38.6 mg). **Scheme 4** shows the reactions.

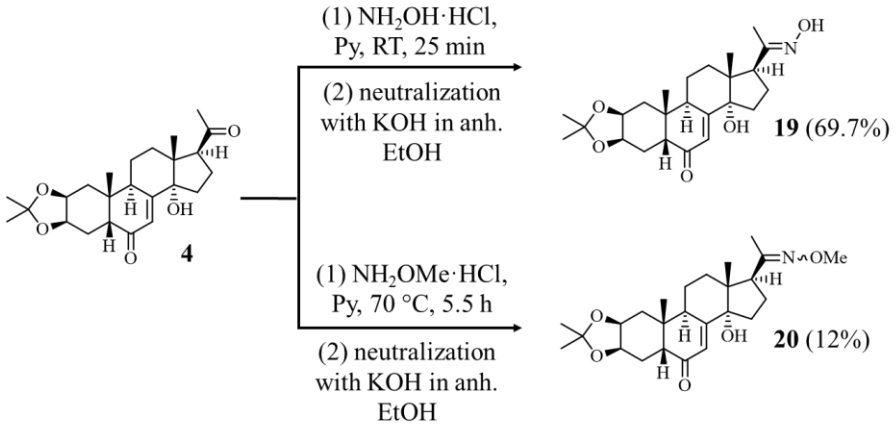

Scheme 4. Preparation of compounds **19-20** from poststerone 2,3-acetonide (**4**).

IV.1.3 Preparation of self-assembled nanoparticles from ecdysteroid oxime 19 [II, III]

IV.1.3.1 Preparation of compound 22 through the transformation of squalene (21)

Squalene (**21**) lacks a proper anchor point for the chemical linking, therefore it requires preliminary functionalization at its terminal double bond to serve the task. In this regard, we prepared our self-assembly inducing molecule, 1,1′,2-tris-norsqualene alcohol (**22**), considering previously published procedures [99,103].

Briefly, at first, we oxidized squalene (**21**) to 2-hydroxy-3-bromosqualene (**21a)** employing NBS in an aqueous-organic medium, and subsequently converted the molecule's terminal bromohydrin moiety to epoxide using K_2CO_3 as a base in the substrate's methanolic solution to afford 2,3-oxidosqualene (**21b**). Then, oxidative opening of the epoxide ring of 2,3-epoxysqualene was performed by aq. periodic acid in dioxane medium to afford 1,1′,2-tris-norsqualene aldehyde (**21c**). Eventually, we achieved the reduction of the aldehyde moiety of intermediate **21c** to alcohol using $NaBH_4$ in ethanol that resulted in the formation of 1,1′,2-tris-norsqualene alcohol (**22**). The product was purified by flash chromatography (see **Table 2**) and the pure compound was obtained in a yield of 71% (1.38 g). **Scheme 5** presents the synthetic process.

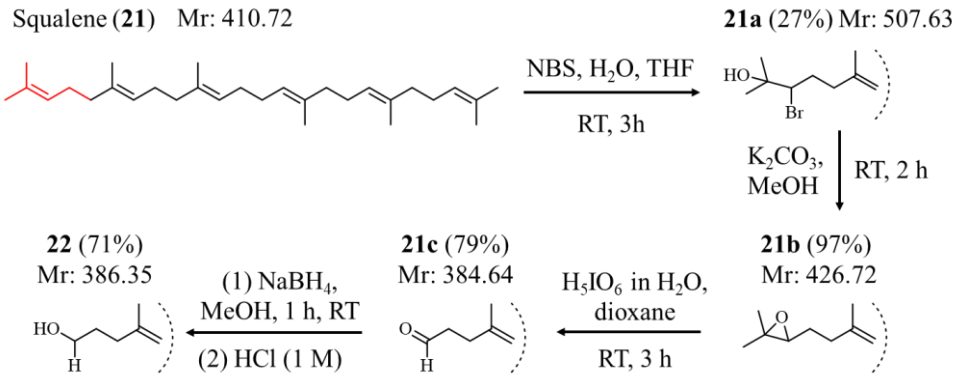

Scheme 5. Preparation of 1,1',2-tris-norsqualene alcohol (**22**) from squalene (**21**). Compounds **21a**-**21c** represent synthetic precursors.

IV.1.3.2 Condensation of compound 22 with chosen dicarboxylic acid linkers

We successfully reacted our self-assembly inducer compound **22** with two different dicarboxylic acids, sebacic acid or 4,4′-dithiodibutyric acid, intending to obtain monoester carboxylic acids that we can later link to a hydroxylated biomolecule through esterification.

We achieved the activation of the terminal carboxyl function of the acids with EDC hydrochloride in dry dichloromethane that, in the presence of DMAP catalyst, allowed the formation of the desired esters through condensation reactions with substrate **22**. Flash chromatographic purification on silica columns (see **Table 2**) afforded compound **23**, or the disulfide-bridge containing compound **24** as pure oils, in relatively good yields (compound **23**: 458.1 mg, 62%; compound **24:** 510.6 mg, 65%). **Scheme 6** shows the reactions.

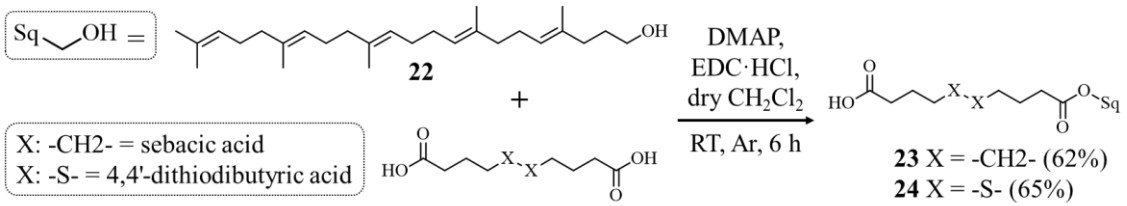

Scheme 6. Preparation of compounds **23** and **24** from substrate **22**.

IV.1.3.3 Synthesis of squalene-linked bioconjugates from compound 19 [II, III]

Poststerone 2,3-acetonide 20-oxime (**19**) was selected as a substrate for functionalization with the prepared self-assembly inducer squalene derivatives **23** and **24**. Condensation of the ecdysteroid with these was straightforward using similar reaction conditions for the esterification to those presented in section IV.3.2., and this resulted in the formation of squalene-coupled bioconjugates. In this regard, we found the conjugation process regioselective towards the hydroxyl group of the C-20 oxime moiety of compound **19**. By employing flash chromatographic purification (see **Table 2**), both derivatives were obtained in high yields

(conjugate **25**: 61.0 mg, 73%; conjugate **26**: 66.1 mg, 76%). Reactions are shown in **Scheme 7**.

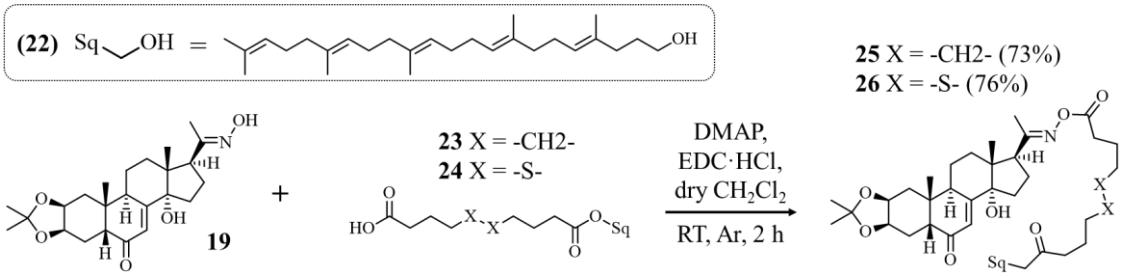

Scheme 7. Synthesis of conjugates **25** and **26** from their substrates.

Compounds **25** and **26** were further studied in collaboration with the group of *Dr. Daniele Passarella*, together with several further related compounds prepared by our collaborators. In the following sub-chapters, a brief description of these results is provided in context of the compounds prepared by our group.

IV.1.3.4 Preparation of self-assembled nanoparticles through nanoprecipitation [III]

Self-assembly of NPs was achieved by the nanoprecipitation approach, which relies on the prolonged, dropwise addition of the conjugates into ultrapure water under continuous stirring. Four different ecdysteroid-containing nanosuspensions were prepared from our compounds, two that contained only an ecdysteroid conjugate in their matrix (**25**$_{\mathbf{NP}}$ and **26**$_{\mathbf{NP}}$,), and two that contained heteronanoparticles (H-NPs) prepared from the 1:50 molar ratio mixture of an ecdysteroid conjugate and squalene-functionalized doxorubicin, respectively (**25**$_{\mathbf{NP\text{-}DOX}}$ and **26**$_{\mathbf{NP\text{-}DOX}}$).

IV.1.3.5 Colloid chemical characterization of nano assemblies [III]

Physical characterization of nanosuspensions was achieved by DLS and TEM techniques. Results of the DLS analysis are shown below, in **Table 4**.

Table 4. Characterization of nano assemblies **25**$_{\mathbf{NP}}$-**26**$_{\mathbf{NP}}$, and **25**$_{\mathbf{NP\text{-}DOX}}$-**26**$_{\mathbf{NP\text{-}DOX}}$ by dynamic light scattering. h.d., hydrodynamic diameter; PdI, polydispersity index; ζ-pot., ζ-potential.

NPs / H-NPs (#)	h.d. ± SD (nm)	PdI	ζ-pot. ± SD (mV)
25$_{\mathbf{NP}}$	366.3 ± 20.17	0.161 ± 0.032	−21.5 ± 4.55
26$_{\mathbf{NP}}$	221.8 ± 4.879	0.081 ± 0.088	−21.7 ± 1.50
25$_{\mathbf{NP\text{-}DOX}}$	187.7 ± 14.48	0.223 ± 0.069	−13.5 ± 9.65
26$_{\mathbf{NP\text{-}DOX}}$	298.7 ± 11.43	0.264 ± 0.014	−11.1 ± 3.48

DLS results confirmed the formation of nano assemblies in an aqueous medium. Nano

assemblies **25$_{NP}$** and **26$_{NP}$** were found monodisperse, exerting a polydispersity index (PdI) lower than the theoretical threshold of 0.2. In contrast, slightly higher values, though still close to the theoretical optimum, were recorded for H-NPS that also contained squalene-functionalized doxorubicin in their matrix. Besides, highly negative ζ-potential values (<−20.0 mV) were found for **25$_{NP}$** and **26$_{NP}$**, suggesting that the electrostatic repulsion between the NPs contributed to their stability in an aqueous medium. At the same time, nearly two-fold higher values were recorded for the corresponding H-NPs, indicating the slight possibility of particle aggregation on their long-term storage.

The nano assemblies were further characterized by TEM to investigate their morphology. **Figure 6** shows images recorded on **26$_{NP}$** and **26$_{NP\text{-}DOX}$**.

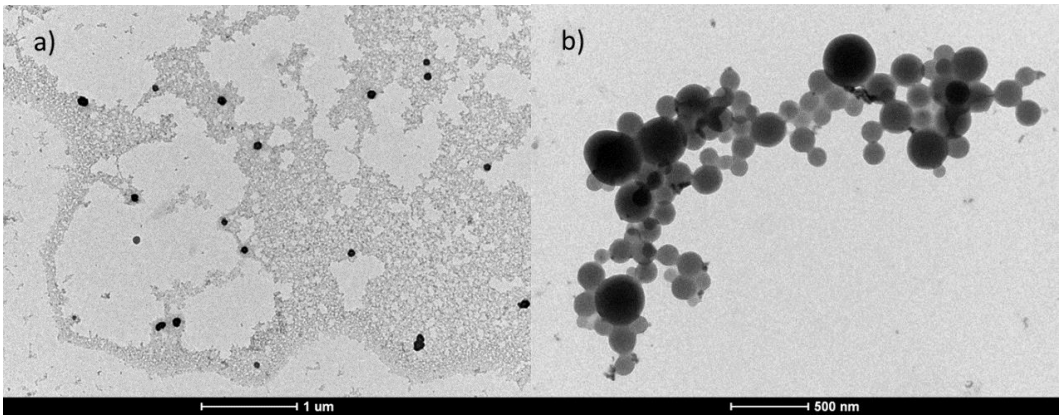

Figure 6. TEM analysis of **26$_{NP}$** (a, scale: 1 μm) and **26$_{NP\text{-}DOX}$** (b, scale: 500 nm).

The images suggested the formation of fluid, droplet-like structures. While for the sample of **26$_{NP}$** (**Figure 6**, a) the mean diameter of the particles was somewhat smaller, in the case of **26$_{NP\text{-}DOX}$** (**Figure 6**, b) it was in good agreement with the results of the DLS studies.

IV.1.4 Structure elucidation of the prepared compounds [I, II, III]

Compounds **1-4** and **21-24** were previously fully characterized, and 2-3 mg aliquots from them were readily available in our laboratory. These samples were utilized as pure reference materials during the large-scale synthetic preparation of novel batches [89,95,103]. Aliquots of derivatives **21-24** were provided for our use by the research group of *Dr. Daniele Passarella*.

Structure elucidation of derivatives **5-20** and **25-26** was performed by HR-MS, and 1D and 2D NMR techniques (see section III.1.5). The HR-MS analysis allowed the accurate determination of the molecular mass of products concerning the $[M+H]^+$ parental ion, which was systematically observed as the base peak of the mass spectra, predominantly accompanied by the presence of $[M+Na]^+$ or $[M+K]^+$ adducts. At the same time, HR-MS measurements

afforded experimental verification for the molecular formula of the compounds.

Chemical structures of the derivatives were determined by employing comprehensive 1D and 2D NMR methods. In general, modifications on the ecdysteroid skeleton were recognized by comparing the ^{1}H and ^{13}C chemical shifts of the products with those of the previously characterized starting materials. In the case of ecdysteroid oximes, the transformation of the carbonyl moiety to oxime resulted in a ca. 50 ppm diamagnetic shift of the corresponding carbon atom on the ^{13}C NMR spectra. For ecdysteroid 6-oximes, characteristical differences between the chemical shifts of the α-CH carbon atom in the *syn* and *anti*-position with respect to the oxime hydroxyl group could be used to determine the (*E*/*Z*)-configuration of the oxime moiety. This way, compounds **7-8**, **10**, **12** and **17** were unambiguously assigned as *E*-isomers, while compounds **9**, **11**, and **13-16** as *Z*-isomers. We determined the configuration of ecdysteroid 20-oxime **19** through the analysis of its 20-*O*-methylated oxime ether analogs that were available as a mixture of both isomers (**20**). Selective ROESY experiments revealed that compound **19** belongs to the *E*-series. We verified the success of the Beckmann-rearrangement of ecdysteroid (6*E*)-oxime **5** to compound **18** by considering a 13.1 ppm paramagnetic shift on δC-5 providing a proof that on the product, the nitrogen atom was coupled to C-5, and the appearance of the signal of C-6 at 170.6 ppm supported the formation of the lactam ring.

Structures of conjugates **25** and **26** were determined by correlating their chemical shift signals with those of compound **19,** while the appearance of five ═CH signals of substrates **23** or **24** in the ^{1}H (δ_H: 5.20–5.00 ppm) and ^{13}C (δ_C: 125.2–124.2 ppm) NMR spectra justified the connection of the lipophilic side-chain to the steroid. Thanks to our collaboration partners providing opportunity for 950 MHz NMR measurements, the complete ^{1}H and ^{13}C NMR signal assignment of both conjugates was achieved.

Among the synthesized products, derivatives **5**, **7-18**, **20** and **25-26**, a total of 15 compounds and a compound mixture (**20**) were new.

IV.1.5 Results of the bioactivity tests

IV.1.5.1. Antiproliferative activities against human gynecological cancer cell lines [I]

Compounds **5-18** were tested in collaboration for their antiproliferative effects on HeLa, SiHa, MDA-MB-231 and MCF7 human gynecological cancer cell lines. Briefly, the analogs exhibited weak to moderate activities against the tested cell lines with IC_{50} values in the range of ca. 8-30 μM or above, while the activity of the positive control cisplatin was exceeded by only one compound (**12**) on the HeLa and MDA-MB-231 models (IC_{50}=8.4 and 12.4 μM, respectively) [I].

IV.1.5.2. Cytotoxic activity, ABCB1-inhibition, and interaction with doxorubicin [I]

Compounds **5-19** were investigated for their cytotoxic activity and ability to interfere with the efflux function of the ABCB1 transporter on a murine lymphoma cell line pair, i.e., a drug-susceptible cell line (L5178) and its multi-drug-resistant counterpart ($L5178_{MDR}$) transfected to express the human ABCB1 transporter. **Table 5** shows the results of these bioassays.

Table 5. Cytotoxicity of compounds **3-19** on L5178 and $L5178_{MDR}$ cells, and functional inhibition of the ABCB1 transporter. Dox = doxorubicin; for the ABCB1 inhibition, *(+)* control: 100 nM of tariquidar (112.4% inhibition), *(-)* control: 2% DMSO (-0.07% inhibition).

Compound	Change in the B-ring of **3** [a]	14-OH or $\Delta^{14,15}$	IC_{50} (μM) [95% confidence intervals] [b]		ABCB1 inhibition (%)	
			L5178	$L5178_{MDR}$	2 μM	20 μM
3	-	14-OH	110.3 [77.50-157.1]	97.69 [71.07-134.3]	2.54	20.91
4 [89]	-	14-OH	>75	>75	0.08	0.64
5	*(E)*-oxime	$\Delta^{14,15}$	20.91 [17.68-24.74]	24.63 [19.82-30.63]	10.57	82.95
6	*(Z)*-oxime	$\Delta^{14,15}$	34.22 [28.21-41.51]	28.35 [21.97-36.58]	7.15	81.09
7	*(E)*; R=Me	14-OH	40.92 [35.66-46.97]	55.05 [41.53-72.98]	2.25	25.05
8	*(E)*; R=Et	14-OH	35.02 [25.35-48.38]	47.00 [31.14-70.93]	17.54	78.79
9	*(Z)*; R=Et	14-OH	37.26 [25.65-54.11]	42.16 [41.24-43.10]	18.96	75.03
10	*(E)*; R=Allyl	14-OH	31.48 [23.71-41.80]	51.91 [42.69-63.13]	20.98	89.39
11	*(Z)*; R=Allyl	14-OH	36.66 [28.32-47.44]	49.29 [43.07-56.40]	24.17	81.80
12	*(E)*; R=*t*-But	14-OH	28.06 [21.30-36.98]	29.12 [25.12-33.76]	38.75	112.4
13	*(Z)*; R=Me	$\Delta^{14,15}$	45.95 [36.97-57.11]	53.14 [43.54-64.86]	33.36	106.2
14	*(Z)*; R=Et	$\Delta^{14,15}$	53.20 [38.64-73.26]	58.94 [45.86-75.74]	56.41	107.7
15	*(Z)*; R=Allyl	$\Delta^{14,15}$	55.28 [46.21-66.13]	52.72 [39.97-65.53]	61.13	102.7
16	*(Z)*; R=*t*-But	$\Delta^{14,15}$	63.23 [58.57-68.26]	51.22 [39.13-67.04]	58.99	78.76
17	*(E)*; R=*t*-But	$\Delta^{14,15}$	63.84 [45.70-89.19]	65.44 [55.66-76.94]	67.46	93.95
18	δ-lactam	$\Delta^{14,15}$	63.42 [47.51-84.65]	72.35 [64.39-81.29]	1.16	4.27
19	-	14-OH	162.3 [82.41-319.7]	142.1 [77.47-260.5]	0.68	1.53
Dox	-	-	0.080 [0.053-0.12]	4.49 [3.43-5.89]	-	-

[a] *R groups refer to the alkyl substituents of ecdysteroid 6-oxime ethers **7-17***

[b] *IC_{50} values were calculated by the CompuSyn software as the median cytotoxic activities (Dm) from the control lanes on the checkerboard plates of the combination*

Although the tested compounds demonstrated weak to moderate cytotoxic effects on the mouse lymphoma cell line pair, all derivatives obtained through the transformation of 20E 2,3;20,22-diacetonide (**4)**, ecdysteroids **5-18**, respectively, were stronger than the parental compound. In contrast, we observed feeble cytotoxic effect for poststerone 2,3-acetonide 20-oxime (**19**); in this analog's case, the formation of the oxime moiety at C-20 could almost two-fold-decrease the cytotoxicity compared to its parental compound **4**.

Cytotoxic properties of the compounds were also tested in combination with doxorubicin, to which the MDR cells show efflux-mediated resistance, to study possible drug-drug interactions. Results of the combination assays are summarized in **Table 6**.

As it is displayed in the table, all tested compounds acted in synergism with doxorubicin, in other words, they exerted a chemo-sensitizing activity towards the cytotoxic effect of doxorubicin. The most promising compound we identified was the ecdysteroid lactam **18**,

which was slightly stronger than our previous lead (compound **3**) on both the MDR and the non-MDR cell lines. It is of further interest that this derivative, along with poststerone 2,3-acetonide 20-oxime (**19**), was found practically inactive as a functional inhibitor of the efflux transporter unlike compound **3** that was a weak inhibitor.

Table 6. Chemo-sensitizing activity of compounds **3** and **5-19** on the L5178 and $L5178_{MDR}$ cell lines towards doxorubicin at 50, 75 and 90% of growth inhibition (ED_{50}, ED_{75} and ED_{90}, respectively). CI: combination index; CI_{avg}: weighted average CI value; $CI_{avg} = (CI_{50} + 2CI_{75} + 3CI_{90})/6$. CI < 1, CI = 1, and CI > 1 represent synergism, additivity, and antagonism, respectively. Dm, m, and r represent antilog of the x-intercept, slope, and linear correlation coefficient of the median-effect plot, respectively.

Compound	Cell line	Drug ratio	CI at			Dm	m	r	CI_{avg}
			ED_{50}	ED_{75}	ED_{90}				
3 [91]	$L5178_{MDR}$	20.4 : 1	0.27	0.14	0.07	11.678	3.246	0.964	0.13
	L5178	163 : 1	0.67	0.55	0.46	11.236	2.103	0.942	0.53
5	$L5178_{MDR}$	15 : 1	0.26	0.16	0.12	4.454	6.638	1.000	0.16
	L5178	150 : 1	0.80	0.79	0.78	10.748	2.572	0.997	0.78
6	$L5178_{MDR}$	30 : 1	0.32	0.25	0.20	7.595	3.981	0.994	0.24
	L5178	150 : 1	0.98	0.76	0.61	16.049	3.239	0.986	0.72
7	$L5178_{MDR}$	15 : 1	0.17	0.16	0.16	6.605	3.721	0.978	0.16
	L5178	150 : 1	1.06	0.79	0.62	14.306	2.947	0.971	0.75
8	$L5178_{MDR}$	7.5 : 1	0.18	0.14	0.12	5.001	5.858	1.000	0.14
	L5178	37.5 : 1	0.55	0.58	0.60	8.598	2.495	0.972	0.59
9	$L5178_{MDR}$	3.75 : 1	0.27	0.16	0.13	3.030	3.329	0.993	0.16
	L5178	37.5 : 1	0.63	0.52	0.45	8.078	3.858	0.952	0.50
10	$L5178_{MDR}$	15 : 1	0.17	0.13	0.13	4.939	3.193	0.955	0.14
	L5178	150 :1	1.03	0.81	0.69	8.970	2.178	0.991	0.79
11	$L5178_{MDR}$	15 : 1	0.17	0.16	0.17	7.338	3.771	0.947	0.17
	L5178	75 : 1	0.70	0.83	1.03	8.202	1.722	0.956	0.91
12	$L5178_{MDR}$	7.5 : 1	0.30	0.20	0.17	3.928	4.610	1.000	0.20
	L5178	37.5 : 1	0.58	0.63	0.70	7.606	2.502	0.966	0.66
13	$L5178_{MDR}$	7.5 : 1	0.17	0.16	0.15	5.224	3.722	0.971	0.16
	L5178	37.5 : 1	0.77	0.47	0.31	8.165	3.044	0.982	0.44
14	$L5178_{MDR}$	7.5 : 1	0.21	0.14	0.11	6.133	4.890	0.992	0.14
	L5178	75 : 1	0.49	0.50	0.52	7.864	2.094	0.961	0.51
15	$L5178_{MDR}$	3.75 : 1	0.25	0.15	0.11	5.614	5.805	1.000	0.15
	L5178	37.5 : 1	0.46	0.47	0.47	8.295	2.882	0.981	0.47
16	$L5178_{MDR}$	7.5 : 1	0.34	0.26	0.23	8.365	3.378	0.939	0.26
	L5178	37.5 : 1	0.53	0.59	0.66	9.652	2.400	0.961	0.62
17	$L5178_{MDR}$	7.5 : 1	0.27	0.24	0.23	8.739	3.813	0.960	0.24
	L5178	37.5 : 1	1.16	0.85	0.64	7.199	3.273	0.977	0.80
18	$L5178_{MDR}$	15 : 1	0.20	0.12	0.09	6.419	4.953	0.970	0.12
	L5178	150 : 1	0.40	0.42	0.46	10.477	2.033	0.966	0.44
19	$L5178_{MDR}$	30 : 1	0.34	0.20	0.13	30.423	2.306	0.968	0.22
	L5178	300 : 1	0.56	0.45	0.40	84.393	1.665	0.995	0.47

IV.1.5.3 Antiproliferative effect of self-assembled ecdysteroid NPs on $A2780_{ADR}$ cells [III]

Ecdysteroid NPs and H-NPs **25_{NP}**, **26_{NP}**, **$25_{NP\text{-}DOX}$** and **$26_{NP\text{-}DOX}$** were tested for their potential to inhibit the cell growth of $A2780_{ADR}$ cells, a human ovarian carcinoma doxorubicin-resistant cell line. The results are shown in **Table 7**.

Table 7. Inhibitory activity of NPs and H-NPs of compounds **25** and **26** on the growth of $A2780_{ADR}$ cells. Dox-Sq: squalene-functionalized doxorubicin, GI: grow inhibition, GI_{50}: concentration of the test agent inducing 50% reduction in cell number compared with control cultures. Values are the mean ± SD of at least four independent experiments.

	$A2780_{ADR}$ cells (GI_{50}, μM)	
Compound (X)	**X_{NP}**	**$X_{NP\text{-}DOX}$**
25	19 ± 3	0.34 ± 0.08
26	39 ± 4	0.26 ± 0.03
Dox-Sq	1.17 ± 0.06	**----**

The results indicated remarkable differences between the cytotoxicity of the NPs and H-NPs of conjugates **25** and **26**. Accordingly, ecdysteroid NPs **25_{NP}** and **26_{NP}** exerted a measurable, yet low antiproliferative effect, while **$25_{NP\text{-}DOX}$** and **$26_{NP\text{-}DOX}$** displayed cytotoxicity in the sub-micromolar range, and presence of the ecdysteroid in these H-NPs resulted in a nearly four-time increase of activity as compared to that of squalene-coupled doxorubicin NPs.

IV.2 *PROTOFLAVONOIDS*

IV.2.1 Preparation of compounds 28-34 as substrates for further transformations

We achieved the oxidative dearomatization of the B-ring of apigenin (**26**) utilizing PIDA in acetonitrile medium in the presence of water or an appropriate alcohol according to the desired alkyl substituent to be coupled at C-1′. Under reflux, the reaction resulted in protoapigenone (**28**) or its 1′-*O*-alkyl ether analogs (**29-34**) in an hour. Purification of the derivatives was straightforward by flash chromatography, which afforded the pure products in typically fair yields. During the separation process, we used the chromatographic conditions similar to those described in our previous publication [114]. Compounds **28-34** served as intermediates for further transformations, therefore their synthesis is presented jointly with those in **Scheme 8**.

IV.2.2 Results of synthetic modifications on the protoapigenone B-ring

IV.2.2.1 Continuous-flow saturation of the B-ring of protoflavones 28-33 [IV, V]

We carried out the selective hydrogenation of the protoflavone B-ring of starting materials **28-33** employing a modified version of H-cube® continuous flow hydrogenation reactor. For this task, we developed a general synthetic procedure by performing a series of small-scale test reactions with compounds **28** and **33** to identify optimal synthetic conditions. **Figure 7** summarizes the results of this study.

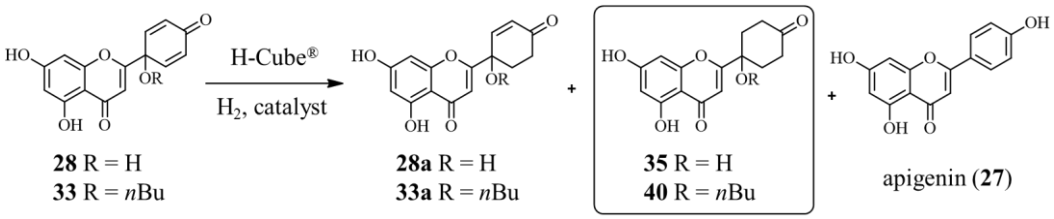

Entry	Starting material[a]	Catalyst	Solvent	*p* (bar)	*T* (°C)	Flow (ml/min)	Conv.[b] (%)	Selectivity[b] (%)		
								28a or **33a**	**35** or **40**	**27**
1	**33**	Lindlar catalyst	EtOAc	20	25	1	19	not detected		
2	**33**	Lindlar catalyst	EtOAc	40	25	1	43	0	88	12
3	**33**	Lindlar catalyst	EtOAc	80	25	1	99	0	92	8
4	**33**	Lindlar catalyst	EtOAc	80	25	1.5	38	0	not detected	
5	**33**	Lindlar catalyst	EtOAc	40	50	1	78	0	66	34
6	**33**	Lindlar catalyst	MeOH	80	25	1	97	0	81	19
7	**33**	5% Pd/C	EtOAc	20	25	1	71	0	82	18
8	**33**	5% Pd/C	EtOAc	40	25	1	100	0	84	16
9	**28**	5% Pd/C	EtOAc	40	25	1	99	traces	77	23
10	**28**	5% Pd/C	MeOH	40	25	1	99	traces	80	20

Figure 7. Results of the optimization of conditions for the continuous-flow hydrogenation of compounds **28** and **33**. [a]: $c_{starting\ material}$=1 mg/ml; [b]: Determined by ^{1}H NMR spectroscopic analysis of the crude product mixture.

We achieved our best results for the selective saturation of the B ring by employing 5% Pd/C catalyst, 1 ml/min sample solution flow rate, and 40 bar pressure at ambient temperature (**Figure 7**, entry 9 and 10). These conditions were then applied to prepare further B-ring reduced derivatives. The substrates were dissolved in ethyl acetate (compounds **29-33**) or methanol (compound **28**), considering their relative polarity. Following the transformations, we purified the products by preparative RP-HPLC to afford tetrahydroprotoapigenone derivatives **35-40** in fair yields (See **Table 3** for the details of chromatographic purification). In addition, we aimed to further increase the available number of interesting, potentially bioactive protoflavone derivatives by performing selective deuteration of the B-rings of substrates **28-33**. To this, we slightly modified the procedure employed during the hydrogenations, and by using 5% Pd/$BaSO_4$ catalyst, and ethyl acetate as a sample solvent, we successfully obtained the desired tetradeuteroprotoapigenone analogs **41-46** (**Scheme 8**). The compounds were purified by preparative RP-HPLC (see **Table 3**) to afford them in fair yields.

IV.2.2.2 Synthesis of protoflavone 4′-oxime derivatives [V]

We successfully transformed the 4′-keto group of protoapigenone analogs **32-34**, and tetrahydroprotoapigenone derivatives **35** and **40** to an oxime, by using hydroxylamine hydrochloride reagent in methanol. Each reaction was regioselective towards the 4′-keto group; however, in the cases of substrates **32-34**, the transformation was accompanied by the acid-catalyzed Michael-addition of the solvent at C-2′ that resulted in the saturation of one double bond on the *p*-quinol dienone. Product mixtures were successfully purified by flash

chromatography and preparative RP-HPLC (see **Table 3**) to afford the corresponding 2′-methoxy-2′3′-dihydroprotoapigenone 4′-oxime analogs **47-52**, or tetrahydroprotoapigenone 4′-oximes **53-54** as racemates, in low to moderate yields. Reactions are presented in **Scheme 8**.

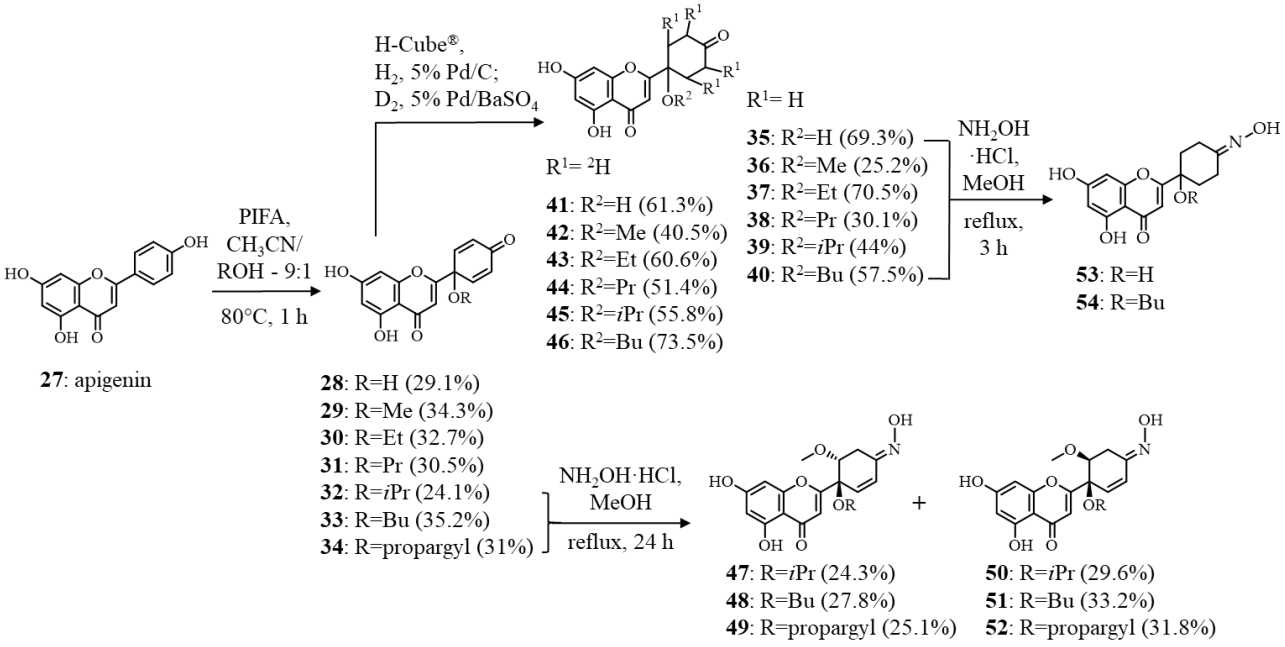

Scheme 8. Synthesis of tetrahydro-, tetradeutero- or 4′-oxime analogs of protoapigenone and its 1′-*O*-alkyl or propargyl ether derivatives. Oximes **47-54** were obtained as racemates; for simplicity only one enantiomer is shown.

IV.2.3 Structure elucidation of the prepared protoflavonoids [IV, V]

Protoflavonoid derivatives **28-34** were previously synthesized and fully characterized by our research group, therefore, their identification was straightforward in comparison with our readily available reference compounds.

Structure elucidation of products **35-54** was performed by means of HR-MS, MS, and 1D- and 2D-NMR spectroscopy (see section III.2.3). Molecular formula of derivatives **35** and **40** was confirmed by HR-MS [IV], and MS analysis of products **36-39** and **41-54** allowed the determination of their molecular mass with respect to the $[M-H]^-$ parental ion that was systematically observed as the base peak of the spectra [V].

Modifications in the protoflavonoid B ring were analyzed by comparing the ^{1}H and ^{13}C chemical shifts of the products **35-54** with those of the corresponding parent compounds (see **Scheme 8**). The synthesized *cis-trans* oxime isomers were assigned considering the characteristic coupling constant patterns observed between H-2′ and H-3′a or H-3′b. Structures were optimized by the MMFF94x force field in CCG-MOE, the H2′-C2′-C3′-H3′a, and H2′-C2′-C3′-H3′b dihedral angles were measured, and theoretical ^{1}H-^{1}H ^{3}J coupling constants were

calculated utilizing the Bothner-By equation [129]. The experimental coupling constants were in good agreement with the calculated ones allowing the assignation of compounds **47-49** as the 1′,2′-*trans*, and **50-52** as the 1′,2′-*cis* isomers. The orientation of the oxime moieties was determined by using compounds **53-54** as internal references; their C-3′ (*syn*) and C-5′ (*anti*) ^{13}C NMR chemical shifts appeared at ca. 18.8 and 26.2 ppm, respectively. The ^{13}C NMR signals of the 3′-CH_2 moieties of compounds **47-52** appeared within the range of 22.7–23.7 ppm, which suggested that the oxime is present in *E*-configuration in each of these compounds while we also considered the effect of the electron-rich neighbouring OCH_3 group.

Among the obtained protoflavonoid analogs, derivatives **36-54,** a total of 11 compounds and 8 racemates were new.

IV.2.4 Results of the bioactivity tests

IV.2.4.1. Cytotoxicity on cancer cell lines and inhibition of DNA-damage response [IV]

In vitro cytotoxic activity of compounds **35** and **40** were tested on MCF-7, HeLa, and SiHa human adherent cancer cell lines. As expected, selective saturation of the protoflavone B-ring resulted in a dramatic decrease in the compounds' cytotoxicity. Consequently, we could only determine an IC_{50} value for compound **40** on HeLa cells (55.12 ± 1.11 μM); in all other cases, the 50% inhibitory concentrations were systematically above 100 μM.

Besides, compounds **35** and **40** were also tested for their potential to inhibit the activation of DNA damage response through the ATR/ATM signaling pathways. While we found derivative **35** completely inactive inhibiting the phosphorylation of Chk1 and Chk2, its 1′-*O*-butyl ether **40** could exert measurable effect on Chk1, yet only at its highest tested dose (20 μM). To study the possible relevance of this finding, the compounds' chemo-sensitizing activity toward doxorubicin was tested by a series of combination studies, and neither protoflavonoid derivative was found to interact with this chemotherapeutic agent (data not presented).

IV.2.4.2 Antiviral activities of obtained protoflavonoid products [V]

Protoflavonoid products **28**, **32-40** and **47-54** were tested against HIV-1 by a pseudotype virus assay (see section III.2.4.2). Among these compounds, tetrahydroprotoapigenone (**35**) was able to inhibit viral infection by ca. 50% at a concentration of 100 μM, while no cytotoxicity was observed up to a concentration of 500 μM (data not presented).

Further, compounds **28** and **32-54** were tested for their activity against the EBV lytic cycle. To this, the expression of the EBV lytic protein Rta was studied in P3HR1 host cells. First screening was performed at a concentration of 0.25 μM, and three compounds (**32-34**) were found active. Then, dose-dependency of this activity was determined, as well as the

compounds' cytotoxicity on P3HR1 cells. Results are summarized in **Figure 8**.

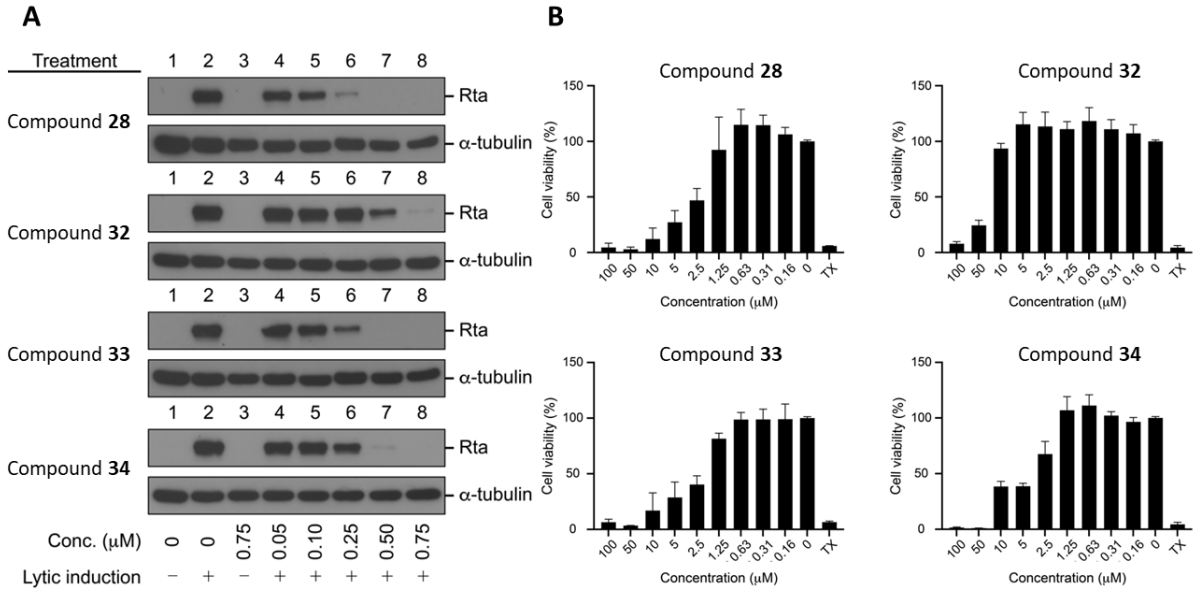

Figure 8. A) Inhibition of the expression of Epstein–Barr Virus (EBV) lytic protein Rta by protoapigenone (**28**) and its analogs **32-34**. P3HR1 cells were treated with the compounds at the time of lytic induction with SB and TPA. Cell lysates were harvested at 24 h after lytic induction. **B**) Cytotoxicity of the compounds on P3HR1 cells. Cells were cultured for 24 h in a medium containing protoapigenone (**28**) or compounds **32-34**. Cell viability was evaluated by the MTT assay. Cells treated with 1% Triton X-100 (TX) were used as a positive control.

Results of the anti-EBV activity testing (**Figure 16-A**) indicated the ability of all three compounds **32-34** to cause a reduction in the Rta levels at concentrations of 0.50, 0.25 and 0.50 μM, respectively. The calculated IC_{50} values for the positive control protoapigenone (**28**) and the tested protoflavonoids **32-34** were 0.127, 0.467, 0.208 and 0.285 μM, respectively.

Regarding the results of the cytotoxicity assays (**Figure 16-B**), compounds **33** and **34** were similarly active as protoapigenone (**28**), while the isopropyl ether derivative **32** was much weaker in this regard. Based on our results, selectivity of the anti-EBV vs cytotoxic effect of compounds **28** and **32-34**, expressed as a ratio of the corresponding IC_{50} values, were calculated as 30.1, 73.0, 9.80 and 17.3, respectively. Accordingly, we found a 73-times selectivity of antiviral over cytotoxic activity in the case of protoapigenone 1′-*O*-isopropyl ether (**32**), in contrast with the slightly stronger antiviral, yet much more cytotoxic protoapigenone (**28**).

V. DISCUSSION

V.1 ECDYSTEROIDS

V.1.1 Preparation and further derivatization of ecdysteroid oximes

Selection of ecdysteroid acetonide substrates. Since the discovery of certain

ecdysteroids' chemo-sensitizing activity, our research group performed several studies aiming to explore relevant SARs. We know that presence of acetonide groups on the ecdysteroid vicinal diols, particularly that of the 2,3-moiety is a prerequisite of a strong effect [87]. It is important to stress that, while acetonide is a widely used, popular protective group in organic chemistry, it is also a fully biocompatible building block for drug design. This is well demonstrated by the example of an approved drug, the corticosteroid triamcinolone acetonide that is not a pro-drug but acts in its intact form [130].

When we started to explore the chemical space of ecdysteroid oximes, 20E 2,3;20,22-diacetonide (**3**) was as a natural choice for transformation due to its potent chemo-sensitizing activity [87], and due to the abundance of its synthetic precursor 20E (**1**). We had kilogram-scale quantities of 20E as a high-purity (ca. 90% by HPLC) commercial product prepared from *Cyanotis arachnoidea* and marketed as a food supplement [131]. A second substrate we found particularly attractive for oximation was poststerone 2,3-acetonide (**4**): the key biosynthetic precursor of this compound is poststerone (**2**), which was identified as an *in vivo* metabolite of 20E (**1**) in mice after oral administration [132]. Poststerone (**2**) can also conveniently be prepared through semi-synthesis from 20E (**1**) by oxidative cleavage of the sterol chain in a yield of up to ca. 80% [64]. Poststerone (**2**) can simply be transformed to its 2,3-acetonide (**4**) that has similar chemo-sensitizing activity as 20E 2,3;20,22-diacetonide (**3**) but without interfering with the efflux function of P-gp [89]. Additionally, the C-20 carbonyl moiety of compound **4** was a promising target for oximation in our synthetic strategy to increase the number of interesting, potentially bioactive compounds for pharmacological testing.

Semi-synthesis of ecdysteroid 6-oxime and oxime ether analogs [I]. There is considerable scientific interest towards antitumor steroid oximes [133,134]. However, to the best of our knowledge, ecdysteroid oximes have not been studied previously for their bioactivities. Galyautdinov et al. reported the preparation of several ecdysteroid 6-oximes from 20E 2,3;20,22-diacetonide (**3**) through a variety of synthetic procedures that afforded derivatives retaining the 14-hydroxyl group, as well as 14,15-anhydro 6-oxime isomers [92]. Our synthetic approach confirmed their previous observations on the formation of these compounds, and highlighted regularity in the product patterns of ecdysteroid 6-oximation depending on the neutralization procedure applied. First, if the reaction's work-up process does not include a neutralization step, a mixture of 14,15-anhydro (*E*/*Z*)-isomeric oxime pairs are formed. Second, if neutralization is performed with alkali dissolved in anhydrous methanol, a 2-4 components mixture of both intact 14-hydroxy- and 14-OH-eliminated derivatives is formed. Third, if the neutralizing alkali is dissolved in anhydrous ethanol, a mixture of intact 14-hydroxy-(*E*/*Z*)-

oxime isomer pair can be obtained. It is worth noting that in our case, the relatively low isolated yield of the oxime and oxime ether products was not really a drawback, since the high structural diversity of the obtained compounds was coherent with our objectives to enhance chemical diversity towards potentially bioactive compounds instead of maximizing yields.

Beckmann-rearrangement of ecdysteroid (6*E*)-oxime 5. Previously, Shafikov et al. reported an in-depth study on the Beckmann-rearrangement of ecdysteroid 6-oximes [128]. Briefly, they found that this rearrangement of ecdysteroid oximes does not work through acid catalysis; instead, TsCl catalyst should be used in acetone in the presence of Na_2CO_3. It is essential to emphasize the importance of alkali; as mentioned above (see **Figure 3** of chapter II.3), the presence of the 2,3-acetonide is required for the strong antitumor activity, and, unfortunately, this moiety is highly acid-sensitive. Since under the applied reaction conditions the rearrangement process gives rise to hydrochloric acid, the use of alkali is particularly important in our case, to prevent the acid-promoted cleavage of the acetonide pharmacophore. Further, the Beckmann-rearrangement is known as a stereospecific reaction that involves the migration of the chemical group located in *anti-position* with respect to the oxime's hydroxyl. In case of (6*Z*)-oxime **6**, the corresponding group is C^7H with an sp^2-hybridized carbon atom whose migration is chemically disabled, and therefore this reaction does not produce the desired 7-membered lactam ring, but an ecdysteroid (6*Z*)-*O*-tosyloxime instead. Accordingly, we could perform the Beckmann-rearrangement solely of ecdysteroid (6*E*)-oxime **5**.

In our publication related to the thesis, we used liquid-liquid extraction for the reaction work-up [I]. Following this, we performed the RP-HPLC purification of the obtained ecdysteroid lactam derivative **18** that afforded the product in a very low, 8% yield (see section IV.1.2.3). In this Ph.D. dissertation, an update to this former work-up strategy is presented with the use of SPE instead of LLE. Due to its relatively low polarity, TsCl tends to remain in large quantities in the organic phase during LLE. Therefore, the sample's straightforward SPE fractionation on plain silica gel might represent a simple, yet effective work-up alternative that ensures the quantitative removal of unreacted reagent remains. This way, we can prevent the occurrence of rapid and undesired product decomposition related to the activity of the retained reagent, and subsequently isolate ecdysteroid lactam **18** in remarkably higher yields.

Semi-synthesis of ecdysteroid 20-oxime analogs. Previously, Savchenko et al. reported a procedure on the regioselective C-20 oximation of poststerone 2,3-acetonide (**4**) [135]. However, following the method described, we failed to obtain the desired 20-oxime product and instead, our attempt afforded a pair of isomeric dioximes. Consequently, we decided to perform the synthesis of the C-20 oxime (**19**) and methyl oxime ether (**20**) analogs of substrate **4** by

modifying the procedures we applied for the preparation of ecdysteroid 6-oxime and oxime ethers **5-17**. First, we performed small-scale test reactions to identify suitable synthetic conditions that could afford the products' synthesis with reasonable efficiency. As a result, we found different synthetic conditions optimal for the preparation of compounds **19** and **20**. This way, we achieved a complete conversion and the highly selective preparation of compound **19** in pyridine, upon stirring the reaction mixture for 25 minutes at RT. In contrast, when using the same reaction conditions for the synthesis of ecdysteroid oxime ether **20**, only traces of the target compound were formed. Thus, we decided to perform the transformation under heating and using higher reagent amounts. Results of our synthetic work-up method were in complete agreement with our previous observations since the 14-OH group was not eliminated in either of the products upon neutralizing their post-reaction mixture with an ethanolic solution of KOH.

V.1.2 Preparation of self-assembled ecdysteroid nanoparticles

To the best of our knowledge, self-assembling drug conjugates of ecdysteroids have not been prepared and studied before. Nano-formulation of these compounds may have several benefits. First, the acid sensitivity of the pharmacologically crucial 2,3-acetonide group is a weak point concerning the stability of these compounds, and this problem may be solved with such a formulation. Further, currently little is known about the *in vivo* efficacy and safety of ecdysteroid acetonides, and these properties may also be improved by this strategy [136]. Previously, Couvreur et al. described the concept of squalenoylation, which is based on the use of squalene (**21**) as a covalent partner in lipid-drug conjugates for drug delivery and targeting purposes [99] (for details, please see section I.4.2). Considering the simplicity, efficiency and flexibility of the method, in this Ph.D. study, we planned to initiate exploring the yet unknown chemical and pharmacological space of squalenoylated ecdysteroid bioconjugates and their corresponding self-assembled NPs.

Synthesis of squalenoylated ecdysteroid bioconjugates. Since ecdysteroids are relatively hydroxylated molecules, we found it reasonable to obtain their bioconjugates through esterification. To assure regioselectivity, this required the presence of possibly one single sterically accessible, reactive hydroxyl group on the antitumor ecdysteroid. Taking this into account, poststerone 2,3-acetonide 20-oxime (**19**) was a particularly attractive substrate for functionalization from multiple-aspects: *1)* similarly to its parent compound **4** (and ecdysteroid lactam **18**), the adjuvant antitumor effect of compound **19** was not accompanied by efflux pump inhibitory activity (see **Table 5** of section IV.1.5.2); and, *2)* the hydroxyl on the 20-oxime group of compound **19** appeared as free and easily accessible, in contrast with the 14α-OH and 25-

OH moieties of e.g., compounds **4** and **18**, respectively.

Considering the above, nano-formulation of compound **19** was performed in three major steps. First, squalene (**21**) was transformed to 1,1′,2-tris-norsqualene alcohol (**22**) in four synthetic steps according to the synthetic route previously described by Borelli et al. [95]. As mentioned in section I.4.1., the use of a well-chosen linker in bioconjugates may influence the *in vivo* fate of a drug. Previously, Borelli et al. reported the use of a linker bearing a disulfide bridge that could enhance the *in vitro* antitumor properties of squalenoylated paclitaxel NPs [95]. Considering this, the second major step of this work was to condensate 1,1′,2-tris-norsqualene alcohol (**22**) with two different types of dicarboxylic acid linkers, sebacic acid and its SS-bond-containing analog 4,4′-dithiodibutyric acid, to obtain monoesters **23** and **24**, respectively. Finally, in the third major step, poststerone 2,3-acetonide 20-oxime (**19**) was esterified by the monocarboxylic acids **23-24** to afford ecdysteroid conjugates **25** and **26**, respectively.

Preparation and characterization of ecdysteroid nanoparticles. Self-assembly of squalenoylated bioconjugates is typically obtained through nanoprecipitation in aqueous medium [93]. Fumagalli et al. previously demonstrated that NPs can be obtained by not only the self-assembly of a single bioconjugate but also from combined mixtures of drug conjugates that may consequently form heteronanoparticles (H-NPs). Accordingly, the concept of preparing H-NPs might be a promising approach to improve the pharmacological performance of either squalenoylated constituent in a task-oriented manner by adequately varying the ratio of the combined drugs [137]. Recognizing this, at this point of our study, batches from the ecdysteroid conjugates **25** and **26** were mixed with squalenoylated doxorubicin, which has been reported to have a better therapeutic index than free doxorubicin [103]. Therefore, self-assembly led to the formation of a total of four nano assemblies that were subsequently characterized by TEM and DLS techniques. TEM-images were recorded for the purposes to confirm the formation of NPs and to study their morphology. By employing DLS, two fundamental characteristics were studied: particle size distribution, which is a major determinant of biodistribution and retention of NPs in targeted tissues, and surface charge expressed as zeta potential, which influences the interaction of NPs with the environment [98]. At this point, however, it needs to be stressed that colloid chemical estimates of the biological efficacy of squalenoylated NPs might be of little *in vivo* relevance. This is because, once administered, these particles suffer a relatively fast disassembly by endogenous lipoproteins that will then transport the dismantled bioconjugates in the blood stream until taken up by the lipoprotein receptors of the target tissue [102].

V.1.3 *In vitro* antitumor activity of the ecdysteroid derivatives obtained

It was our hypothesis that the nitrogen-containing moieties of the newly prepared ecdysteroids may substantially influence their antitumor properties. Accordingly, we subjected derivatives **5-19** to related bioactivity testing.

Antiproliferative activities on human gynecological cancer cell lines. When analyzing SARs, we found that the orientation of the 6-oxime or oxime ether function had little if any impact on the observed antiproliferative activity, although the presence of a larger alkyl ether group on the oxime resulted in a noticeably stronger effect. Besides, on the MCF-7 cell line, a retained 14-αOH group was found favorable over the $\Delta^{14\text{-}15}$ olefin moiety, though the same conclusion could not be drawn from the results on other cell lines.

Cytotoxicity on murine lymphoma cell lines, and ABCB1-inhibition. Multi-drug resistance (MDR) is a major limitation to the chemotherapy of cancer [138]. Previously, we found that less polar ecdysteroid derivatives can strongly sensitize both MDR and drug-susceptible cancer cell lines to various chemotherapeutics [87,88]. Therefore, we subjected the synthesized ecdysteroid diacetonide derivatives **5-19** for related bioactivity testing. First, cytotoxicity of the compounds was tested on a susceptible/resistant murine lymphoma cell line pair. Then, the compounds were tested for their inhibitory activity on the ABCB1 efflux transporter, whose over-expression is the most frequent cause of the acquisition of an MDR phenotype in cancer [138]. Results of these assays (see **Table 5**) revealed several SARs. We found that, while each compound showed only weak to moderate cytotoxicity, the non-substituted 6-oxime derivatives **5** and **6** were stronger on both cell lines than the 6-oxime ethers (**7-17**) or the side-chain cleaved 20-oxime (**19**), and among the two isomers, the (6*E*)-oxime (**5**) was more potent. In this tendency, the only exception was compound **12** containing a *t*-butyl substituent and a retained 14-OH group; this compound exerted a cytotoxic effect comparable to that of the non-substituted oximes (**5-6**). Further, while derivatives with a retained 14-OH group were systematically more cytotoxic than those with a 14,15-anhydro moiety, the cytotoxic effect of the 20-oxime derivative **19** was ca. 2-3 times weaker than that of any of the B-ring modified analogs. Results of the rhodamine accumulation assay (see **Table 5**) indicated that only two compounds, the ecdysteroid lactam (**18**) and the side-chain cleaved 20-oxime (**19**) were inactive as functional efflux pump inhibitors at as much as 20 μM concentration. We consider this as a positive feature, since our main research interest concerns compounds that can sensitize MDR cancer cells without directly interfering with drug efflux. For other derivatives, we found that oxime, and particularly oxime ether formation significantly increased the ABCB1 inhibitory

activity. In this regard, for 6-oxime and oxime ether derivatives possessing the same type of D ring and oxime configuration, we found that the increase of C atom number in the C-6 substituent increased this activity. Further, while the orientation of the oxime moiety had no considerable influence on the ABCB1-inhibition, elimination of the 14-OH group could markedly increase this activity.

The compounds were subsequently tested for their chemo-sensitizing properties on the same murine lymphoma cell line pair towards the cytotoxicity of doxorubicin. Here, due to a large number of highly active compounds, SARs were concluded using our previously described "best ratio" approach that compared the compounds' chemo-sensitizing activities at their strongest effect observed on the checkerboard plates, instead of comparing activities at the same compound vs. doxorubicin ratio [87]. On the MDR cell line, we observed strong to very strong activities, according to the rating of Chou [126]. The length or nature of the oxime ethers' alkyl substituent had no apparent influence on the compounds' chemo-sensitizing property. Although we could observe a slight tendency for water eliminated derivatives possessing stronger activities than those with a retained 14-OH, this phenomenon was not unequivocal. Potent sensitizing activities were observed on the non-MDR cell line too; here, the formation of oxime moieties together with the elimination of the 14-OH group (**5** and **6**) decreased the strength of synergism with doxorubicin as compared to the parental compound **3**. In the case of the oxime ethers, derivatives with a 14,15-anhydro moiety were typically stronger chemo-sensitizers than their analogs with intact 14-OH groups, except compounds **12** and **17** with *t*-butyl substituents. Accordingly, we can hypothesize that a larger, bulky substituent might contribute to a decreased sensitizing property.

Nevertheless, taken all aspects together, the most promising compound we identified was the ecdysteroid lactam (**18**) due to its low intrinsic cytotoxicity, and strong ability to sensitize MDR and non-MDR cancer cells to doxorubicin without interfering with the efflux function of P-gp. Therefore, we suggest this compound as a promising novel lead for further studies.

Antitumor activity of self-assembled NPs. To the best of our knowledge, before our investigations, the adjuvant antitumor effect of ecdysteroids has not been studied in self-assembling nano-delivery systems. The most important finding of our study was that these compounds retain their chemo-sensitizing activities after such a formulation, and this was shown to contribute to the ability of their doxorubicin-containing H-NPs to overcome the drug resistance of $A2780_{ADR}$ cells. The obtained results may provide a promising basis for further investigations on the use of ecdysteroid acetonides in similar or other types of antitumor nanostructures, and such conjugates may provide a useful platform to overcome unfavorable

pharmacokinetic properties (such as acid sensitivity and poor water solubility) of these compounds. Additionally, the differences observed between the activity of the NPs underline the relevance of the linker entities in the intracellular penetration of the drug.

V.2 PROTOFLAVONOIDS

V.2.1 Semi-synthesis of protoflavonoid derivatives

Protoflavonoids are mostly recognized for their antitumor properties; however, evidence suggests that they may exert various bioactivities that point beyond their antitumor action [121,122]. In this Ph.D. work, we aimed to extend their chemical and pharmacological space towards less cytotoxic derivatives to initiate exploring their pharmacological potential in new directions.

We selected protoapigenone (**28**), and its 1′-*O*-alkyl analogs (**29-34**) as substrates of our studies; some of these derivatives have been previously reported to exert interesting, non-tumor-related bioactivities [121,122]. Since the key pharmacophore for the cytotoxicity of protoflavones is the symmetric dienone on the B-ring [124], we chose this moiety as the target of our semi-synthetic transformations to prepare less cytotoxic, yet potentially bioactive derivatives. In this context, we employed two different synthetic strategies: 1) the selective saturation of the protoflavone B-ring to obtain analogs possessing the rare, naturally occurring dihydro- and/or tetrahydroprotoflavone structural elements [139,140]; and/or 2) the substitution of the protoflavone 4′-oxo moiety with an oxime function. To the best of our knowledge, none of these transformations have been performed before our studies.

The first step of our preparative strategy (see **Scheme 8** of section IV.2.2.1) was the oxidative dearomatization of apigenin (**27**), which was carried out according to our previously published procedure using hypervalent iodine reagent PIFA in acetonitrile in the presence of water or alcohol [114]. Following a thorough chromatographic purification, we used the obtained products **28-34** as intermediates in subsequent synthetic transformations, while, from this set of derivatives, compound **32** was already a compound of interest for our bioactivity studies due to its very weak cytotoxicity when compared to the others [114].

Selective hydrogenation of the protoflavonoid B-ring. The selective hydrogenation of the protoflavonoid B-ring appeared as a significant synthetic challenge, since the process may be accompanied by numerous undesired side reactions such as the reduction of the carbonyl groups [141], the partial hydrogenation of the C- or even the A-ring, and the possible rearomatization of the B-ring [142]. Moreover, if hydrogenation is performed under traditional batch-based conditions, further difficulties should be taken into account, including the inconvenience of handling the explosive gas, inadequate control over the reaction conditions,

and the lack of sustainability and safety [143]. Considering that heterogeneous catalytic hydrogenations can provide notable benefits through the advantageous features of continuous processing [144], we set out to perform our planned transformations in a modified H-cube® continuous flow hydrogenation reactor. During operation, the device generated the hydrogen gas *in situ* by electrolytic decomposition of deionized water. The triphasic reaction took place in a stainless-steel cartridge that was previously filled with the hydrogenation catalyst and was subsequently placed in a thermostat to assure temperature control.

We selected two model substrates for method optimization: the protoflavone antitumor lead protoapigenone (**28**) and its less polar, 1′-*O*-butyl ether analog (**33**) that is more cytotoxic on certain cell lines and has improved chemical stability [114]. Considering previous results on the selective C-C double bond reduction of aromatic enones [141], our initial choice for the role of the catalyst fell on the Lindlar catalyst, and at first, we examined the applied pressure's influence on the transformation. At ambient temperature and a fixed flow rate, the total conversion of substrate **3** significantly increased as a function of the pressure (**Figure 7**, entries 1-3). Although we observed an almost complete conversion at 80 bar, the reaction's selectivity was decreased due to the rearomatization of the B-ring (**Fig. 7**, entry 3), leading to the formation of around 10% apigenin (27). Considering that rearomatization is known to be related to palladium-mediated hydrogenolysis at C-1′ [145], we attempted to suppress side-product formation by increasing the flow rate, thus reducing the residence time on the catalyst bed (**Fig. 7**, entry 4). Unfortunately, this attempt resulted in a significant decrease in conversion. Furthermore, the increase of the temperature was also disadvantageous, whereas it resulted in a decrease in the selectivity suppressing the formation of apigenin (**Fig. 7**, entry 5). Taken together, at this point, the reaction performed at 25 °C and 80 bar provided the complete and highly selective saturation (**Fig. 7**, entry 3) of the B ring of compound **3**; however, rapid deactivation of the catalyst prevented any synthetic scale-up. Considering this, we switched from Lindlar catalyst to 5% Pd/C, and after a couple of test reactions (**Fig. 7**, entries 7 and 8), we achieved total conversion and great chemoselectivity toward the formation of the desired tetrahydroprotoflavone product **40**. In this case, we observed no catalyst deactivation, and we could successfully up-scale the synthesis for preparative purposes. The method was compatible with other derivatives as well and afforded the convenient preparation of products **36-39** from their substrates. In the case of protoapigenone (**28**), due to the compound's poor solubility in ethyl acetate, the saturation was performed in methanol instead.

Selective deuteration of the protoflavonoid B-ring. Deuterium is of potential interest for drug discovery since it can considerably influence the bioactivity of a compound due to the

so-called isotope effect [146]. Considering this, we set out to perform the selective continuous flow deuteration of the B-rings of substrates **28-33**. We performed the reactions by slightly modifying the method used for the hydrogenations on the bases of previously published procedures [141,145]. Accordingly, we *in situ* generated the D_2 gas necessary for the transformations from high-purity D_2O with H-Cube®. Since activated charcoal might contain protic contaminations on its surface, we used barium sulfate as the catalyst carrier to ensure that no hydrogen-deuterium exchange occurs during the transformations. For the same reason, we performed the reactions strictly in an aprotic solvent, ethyl acetate. In every other aspect, we adopted the protocol employed during the hydrogenations.

Semi-synthesis of protoflavonoid 4′-oxime derivatives. It was among our primary aims in this Ph.D. work to prepare new protoflavonoid oxime derivatives. Since we intended to maximize chemical and pharmacological diversity for our research, we selected substrates with different B-ring saturation (**32-35** and **40**) and/or 1′-*O*-alkyl substituents for the preparation of their 4′-oxime analogs. Our preliminary test reactions showed that the oxime formation of protoflavones in the 4′-keto function is regioselective, and under the synthetic conditions used, it is not accompanied by the formation of 4-oxime or 4,4′-dioxime side product. However, other factors, such as solvent quality, had a crucial influence on the outcome of the transformations. Typically used solvents in oxime synthesis are ethanol, pyridine or acetonitrile, but none of these worked in our case. Eventually, we found methanol to be the most suitable for reacting protoflavones with hydroxylamine. The yields of the transformations greatly varied depending on the substrate's concentration, and, eventually, our best results were obtained at around 2-2.5 mg/ml concentrations. It is important to mention that while the transformations were straightforward for tetrahydroprotoapigenone analogs **35** and **40**, in the cases of compounds **32-34**, we observed the regioselective Michael-addition of the solvent at C-2′.

V.2.2 *In vitro* biological activity of the protoflavonoid derivatives obtained

Cytotoxicity on cancer cell lines, and inhibition of DNA-damage response. Protoflavonoids are known to be cytotoxic on a broad array of cancer cell lines [110], and certain analogs such as protoapigenone (**28**) exert chemo-sensitizing properties towards DNA-damaging chemotherapeutics due to their interference with the ATR/ATM signaling pathways [119]. Therefore, we subjected compounds **35** and **40**, B-ring saturated analogs of the antitumor leads protoapigenone (**28**) and its 1′-O-butyl ether derivative (**33**), respectively, to related bioactivity assays. The results clearly demonstrated that the selective saturation of the protoflavone B-ring could knock out these bioactivities of the derivatives that could potentially

confer them toxic side effects. Even though at the highest tested dose (20 μM) the 1′-*O*-butyl ether derivative **40** could significantly inhibit the ATR-dependent phosphorylation of Chk1, none of the tested analogs interacted with the *in vitro* cytotoxicity of doxorubicin.
Accordingly, our preparative flow chemical strategy allowed us not only to obtain the rare, naturally occurring tetrahydroprotoflavone moiety, but it also served as an effective tool to eliminate the cytotoxicity of protoflavones.

Antiviral activities. We hypothesized that protoflavones can exert specific antiviral properties based on two considerations. First, protoapigenone (**28**) was previously found to be active against the lytic cycle of EBV [122] at below-cytotoxic concentrations. Besides, protoflavones possess a 5-hydroxyflavone moiety, which is a known pharmacophore against HIV-integrase that may consequently confer them anti-HIV properties [147]. To the best of our knowledge, no previous studies on the antiviral activity of protoflavone derivatives have been performed, other than the above-mentioned study on EBV that was performed in collaboration with our group. Therefore, our less cytotoxic protoflavonoids, obtained from the oxidative de-aromatization of apigenin (compound **32**) and subsequent continuous-flow hydrogenation, deuteration, and/or 4′-oxime formation (compounds **35-54**), were subjected to related bioactivity testing.

The results of the anti-HIV assay revealed only one compound, tetrahydroprotoapigenone (**35**) exerting a significant anti-HIV activity. Though this activity was rather weak (50% inhibition of HIV-1 infection at 100 μM), it might still be of interest for further studies, whereas the derivative was not cytotoxic on the host cells at as high as 500 μM concentration.

Considering the results of the anti-EBV assays, protoapigenone 1′-*O*-isopropyl ether (**32**) was identified as a promising new lead for a possible design of protoflavone-inspired anti-EBV agents due to its 73-times selectivity of antiviral over cytotoxic activity, which exceeds protoapigenone's (**28**) selectivity by 2.4-times. As a first rational step to such a design, one may consider that protoapigenone 1′-*O*-butyl ether **33** showed an over two-fold stronger anti-EBV activity than compound **28**; therefore, it may be a relevant future strategy to study further analogs possessing a longer, branching substituent at position C-1′ (e.g. *i*-butyl or *i*-pentyl).

Concerning our new protoflavone oximes, even though they did not came out as hits in these first-line bioassays, they are considered to be tested in various further screening assays performed in our collaboration network. On the basis of the anti-EBV activity of compound **28**, we are also planning to develop a chemoselective strategy for the 4′-oximation of protoflavones that would leave the symmetric diene of the B-ring intact, to explore the pharmacological potential of derivatives whose cytotoxicity is abolished only by replacing the 4′-oxo group.

VI. SUMMARY

The aim of the present Ph.D. study was to further extend the chemical diversity of ecdysteroids and protoflavonoids towards novel derivatives, and to examine the pharmacological potential of introducing oxime function to the structure of these compounds. We can summarize our results as follows.

ECDYSTEROIDS

1. The preparation and further transformation of ecdysteroid oxime derivatives. A series of ecdysteroid oximes and oxime ethers were synthesized from two of our previous ecdysteroid antitumor leads, by reacting their available carbonyl functions with appropriate hydroxyl- or alkoxyamine derivatives. Further, one of the ecdysteroid 6-oximes was converted to a lactam through Beckmann-rearrangement. This way, a total of 16 nitrogen-containing ecdysteroid derivatives were prepared, including 14 new compounds.

2. The preparation of self-assembled NPs from an ecdysteroid oxime. Poststerone 2,3-acetonide 20-oxime **19** was selected for nano-formulation. The preparation of two different, novel squalenoylated bioconjugates (**25** and **26**) from the derivative was successfully achieved through a series of synthetic transformations. Following this, collaborative studies led to the successful preparation and characterization of four aqueous nano assemblies: two that contained NPs (**25**$_{\mathbf{NP}}$ or **26**$_{\mathbf{NP}}$), and two that contained H-NPs of an ecdysteroid conjugate and squalenoylated doxorubicin (**25**$_{\mathbf{NP}}$ or **26**$_{\mathbf{NP}}$) in their matrix.

3. Biological evaluation of the ecdysteroids obtained. Results on the *in vitro* antitumor activities of the synthesized ecdysteroid derivatives and ecdysteroid nano assemblies were achieved in research co-operations and could briefly be summarized as follows.

- Antiproliferative effects. Compounds **5-18** were tested on human gynecological cancer cell lines and moderate activities were observed, while compound **12** was stronger than the positive control cisplatin on HeLa and MDA-MB-231 cell lines.
- Functional inhibition of the ABCB1-mediated efflux transport. Compounds **5-19** were tested; several SARs were revealed, and two derivatives, the ecdysteroid lactam **18** and poststerone 2,3-acetonide 20-oxime **19** were inactive in this regard.
- Chemo-sensitizing activity in combination with doxorubicin. Compounds **5-19** were tested, and each of them could considerably sensitize both the MDR and the susceptible cancer cell line, with a noticeable selectivity towards the former. The lactam **18** was identified as our most interesting compound for further studies; its chemo-sensitizing activity exceeded that of our previous lead (compound **3**), while it did not inhibit the efflux function of P-gp.

- Inhibition of the growth of $A2780_{ADR}$ cells: ecdysteroid NPs and H-NPs were tested, and the chemo-sensitizing effect of squalenoylated ecdysteroid oxime **19** contributed to the ability of doxorubicin-containing H-NPs to overcome the drug resistance of the cancer cells with cytotoxic activity in the submicromolar range.

PROTOFLAVONOIDS

4. Preparation of B-ring modified protoflavone derivatives including oximes. With the aim of obtaining less cytotoxic protoflavones for bioactivity testing, synthetic modification of the B-ring was targeted. A total of 27 derivatives, including 19 new compounds, were successfully semi-synthesized from apigenin through oxidative de-aromatization and subsequent regioselective continuous-flow hydrogenation, deuteration, and/or 4′-oximation. The continuous-flow method that was developed allowed the first-time synthetic preparation of compounds containing the rare, naturally occurring tetrahydroprotoflavone moiety.

5. Biological evaluation of the protoflavones obtained. The following results on the bioactivity of the prepared protoflavone derivatives were achieved in research co-operations.

- Cytotoxic effects against cancer cell lines and DNA-damage response inhibitory activities. Tetrahydroprotoflavone derivatives **35** and **40** were tested; the reduction of the double bonds in the *p*-quinol B-ring of the derivatives resulted in a great decrease in the bioactivity of the compounds towards the tested properties. Accordingly, the employed synthetic strategy may serve as an effective tool to knock out these bioactivities of protoflavonoids that could potentially confer them toxic side effects.
- Antiretroviral activity. Compounds **28**, **32-40** and **47-54** were tested against HIV-1 on a pseudotype virus assay; among these compounds, tetrahydroprotoapigenone (**35**) was found to inhibit viral infection by ca. 50% at 100 μM that was more than 5-times below its cytotoxic concentration.
- Antiviral activity against EBV. Compounds **28** and **32-54** were tested; these studies revealed a 73-times selectivity of antiviral over cytotoxic activity in the case of protoapigenone 1′-*O*-isopropyl ether (**32**).

Altogether, a total of 47 semi-synthetic derivatives of natural enones were prepared during this work, including 16 new ecdysteroids and 19 new protoflavones. Moreover, bioactivity studies revealed a prospective novel lead compound in both major chemical directions, i.e., compound **18** (ecdysteroid; potent modulator of multi-drug resistance in cancer that does not inhibit P-gp) and compound **32** (protoflavone; potent antiviral agent against EBV that is more selective than its parent compound).

REFERENCES

(1) Eloy, F. The Chemistry of Amidoximes and Related Compounds. *Chem. Rev.* **1962**, *62* (2), 155–183.
(2) Fylaktakidou, K. Recent Developments in the Chemistry and in the Biological Applications of Amidoximes. *CPD* **2008**, *14* (10), 1001–1047.
(3) Sahyoun, T. Amidoximes and Oximes: Synthesis, Structure, and Their Key Role as NO Donors. *Molecules* **2019**, *24* (13), 2470.
(4) Porcheddu, A. Synthesis of Oximes and Hydroxamic Acids. In *The Chemistry of Hydroxylamines, Oximes and Hydroxamic Acids*; John Wiley & Sons, Ltd, 2008; pp 163–231.
(5) Sahyoun, T. Synthesis of Novel Mono and Bis Nitric Oxide Donors with High Cytocompatibility and Release Activity. *Bioorganic & Medicinal Chemistry Letters* **2018**, *28* (20), 3329–3332.
(6) Ovdiichuk, O. Efficient Synthesis of Nicotinic Acid Based Pseudopeptides Bearing an Amidoxime Function. *Synthesis* **2015**, *47* (15), 2285–2293.
(7) Vörös, A. Formation of Aromatic Amidoximes with Hydroxylamine Using Microreactor Technology. *Org. Process Res. Dev.* **2012**, *16* (11), 1717–1726.
(8) Nicolaides, D. N. The Chemistry of Amidoximes. In *Acid Derivatives: Vol. 2 (1992)*; John Wiley & Sons, Inc.: Chichester, UK, 1992; pp 875–966.
(9) Cashman, J. R. Blood Brain Barrier-Penetrating Oximes for Cholistenerases Reactivation. US9751831B2, September 5, 2017.
(10) Özyürek, M. Novel Oxime Based Flavanone, Naringin-Oxime: Synthesis, Characterization and Screening for Antioxidant Activity. *Chemico-Biological Interactions* **2014**, *212*, 40–46.
(11) Ouyang, G. Synthesis and Antiviral Activities of Pyrazole Derivatives Containing an Oxime Moiety. *J. Agric. Food Chem.* **2008**, *56* (21), 10160–10167.
(12) Luo, Y. Design, Synthesis, and Biological Evaluation of Chalcone Oxime Derivatives as Potential Immunosuppressive Agents. *Bioorganic & Medicinal Chemistry Letters* **2012**, *22* (9), 3039–3043.
(13) Perri, F. Naturally Occurring Sesquiterpene Lactones and Their Semi-Synthetic Derivatives Modulate PGE2 Levels by Decreasing COX2 Activity and Expression. *Heliyon* **2019**, *5* (3), e01366.
(14) Latif, A. D. Synthesis and In Vitro Antitumor Activity of Naringenin Oxime and Oxime Ether Derivatives. *IJMS* **2019**, *20* (9), 2184.
(15) Deng, H. Asymmetric Synthesis and Absolute Stereochemistry of a Labdane-Type Diterpenoid Isolated from the Rhizomes of Isodan Yuennanensis. *Org. Biomol. Chem.* **2016**, *14* (26), 6225–6230.
(16) Dighe, S. U. Metal-Free Oxidative Nitration of α-Carbon of Carbonyls Leads to One-Pot Synthesis of Thiohydroximic Acids from Acetophenones. *Org. Lett.* **2016**, *18* (17), 4190–4193.
(17) Guo, J.-J. TiO2/SO42–: An Efficient and Convenient Catalyst for Preparation of Aromatic Oximes. *Green Chem.* **2001**, *3* (4), 193–195.
(18) Hong, Z. Solvent-Free Mechanochemical Synthesis of Arylcyanomethylenequinone Oximes from Phenylacetonitriles and 4-Unsubstituted Nitroaromatic Compounds Using KF/Nano-γ-Al_2O_3 as Catalyst. *RSC Adv.* **2016**, *6* (16), 13581–13588.
(19) Sharghi, H. Solvent-Free and One-Step Beckmann Rearrangement of Ketones and Aldehydes by Zinc Oxide. *Synthesis* **2002**, *2002* (08), 1057–1060.
(20) Tinge, J. Caprolactam. In *Ullmann's Encyclopedia of Industrial Chemistry*; Wiley-VCH Verlag GmbH & Co. KGaA: Weinheim, Germany, 2018; pp 1–31.
(21) Bolotin, D. S. Metal-Involving Synthesis and Reactions of Oximes. *Chem. Rev.* **2017**, *117* (21), 13039–13122.
(22) Mirjafary, Z. Oxime Ethers as Versatile Precursors in Organic Synthesis: A Review. *RSC Adv.* **2015**, *5* (97), 79361–79384.
(23) Vessally, E. Oxime Ethers as Useful Synthons in the Synthesis of a Number of Key Medicinal Heteroaromatic Compounds. *J IRAN CHEM SOC* **2016**, *13* (7), 1235–1256.
(24) Burakevich, J. V. Phenylglyoxime. Separation, Characterization, and Structure of Three Isomers. *J. Org. Chem.* **1971**, *36* (1), 1–4.
(25) Heaney, F. The Influence of Oxime Stereochemistry in the Generation of Nitrones from ω-Alkenyloximes by Cyclization or 1,2-Prototropy. *J. Chem. Soc., Perkin Trans. 1* **1998**, No. 2, 341–350.
(26) Eshghi, H. REGIOSELECTIVE SYNTHESIS OF *E* -OXIMES CATALYZED BY FERRIC CHLORIDE UNDER SOLVENT-FREE CONDITIONS. *Organic Preparations and Procedures International* **2005**, *37* (6), 575–579.
(27) Chen, W. Selective Synthesis of E-Isomers of Aldoximes via a Domino Aza-Michael/Retro-Michael Reaction. *Chemical Papers* **2012**, *66* (4).
(28) Axelson, M. Separation and Configuration of Syn and Anti Isomers of Testosterone Oxime. *Analytical Letters* **1978**, *11* (3), 229–237.
(29) Johnson, W. M. P. Separation of Geometrical Isomers of Oxime O-Ethers by High-Performance Liquid Chromatography: Use of Extended Multiple Recycle on High-Efficiency Columns. *Journal of Chromatography A* **1984**, *291*, 449–452.
(30) Sørensen, M. Oximes: Unrecognized Chameleons in General and Specialized Plant Metabolism. *Molecular*

Plant **2018**, *11* (1), 95–117.
(31) Bak, S. Cyanogenic Glycosides: A Case Study for Evolution and Application of Cytochromes P450. *Phytochem Rev* **2006**, *5* (2–3), 309–329.
(32) Forslund, K. Biosynthesis of the Nitrile Glucosides Rhodiocyanoside A and D and the Cyanogenic Glucosides Lotaustralin and Linamarin in *Lotus Japonicus*. *Plant Physiol.* **2004**, *135* (1), 71–84.
(33) Mano, Y. The Pathway of Auxin Biosynthesis in Plants. *Journal of Experimental Botany* **2012**, *63* (8), 2853–2872.
(34) Castillo, M. A Heterocyclic Oxime from a Fungus with Anti-Juvenile Hormone Activity. *Archives of Insect Biochemistry and Physiology* **1998**, *37* (4), 287–294.
(35) Harper, D. B. The Bacterial Biogenesis of Isobutyraldoxime O-Methyl Ether, a Novel Volatile Secondary Metabolite. *Microbiology* **1982**, *128* (8), 1667–1678.
(36) Rodríguez, J. Isolation and Synthesis of the First Natural 6-Hydroximino 4-En-3-One- Steroids from the Sponges Cinachyrella Spp. *Tetrahedron Letters* **1997**, *38* (10), 1833–1836.
(37) Ortlepp, S. Antifouling Activity of Bromotyrosine-Derived Sponge Metabolites and Synthetic Analogues. *Mar Biotechnol* **2007**, *9* (6), 776–785.
(38) Hertiani, T. From Anti-Fouling to Biofilm Inhibition: New Cytotoxic Secondary Metabolites from Two Indonesian Agelas Sponges. *Bioorganic & Medicinal Chemistry* **2010**, *18* (3), 1297–1311.
(39) Duffey, S. S. Intermediates in the Biosynthesis of HCN and Benzaldehyde by a Polydesmid Millipede, Harpaphe Haydeniana (Wood). *Comparative Biochemistry and Physiology Part B: Comparative Biochemistry* **1974**, *47* (4), 753–766.
(40) Salamon, M. [No Title Found]. *Journal of Chemical Ecology* **1998**, *24* (10), 1659–1676.
(41) Tobey, J. R. Age and Seasonal Changes in the Semiochemicals of the Sternal Gland Secretions of Male Koalas (Phascolarctos Cinereus). *Aust. J. Zool.* **2009**, *57* (2), 111.
(42) Kirchner Juergen. Use Of Oxime Ether Derivatives For Bioregulation In Plants. AP 263 A, 0 10, 1993.
(43) Baron, R. L. A Carbamate Insecticide: A Case Study of Aldicarb. *Environmental Health Perspectives* **1994**, *102* (suppl 11), 23–27.
(44) Koo, S. J. Herbicidal Efficacy and Selectivity of Pyribenzoxim in Turfgrasses. *Weed Biol Manage* **2006**, *6* (2), 96–101.
(45) Drumm, J. E. Oxime Fungicides: Highly Active Broad-Spectrum Protectants. In *Synthesis and Chemistry of Agrochemicals IV*; American Chemical Society: Washington, DC, 1995; Vol. 584, pp 396–405.
(46) Wang, X. Synthesis and Antiviral Activities of Novel Penta-1,4-Diene-3-One Oxime Derivatives Bearing a Pyridine Moiety. *Chem. Pap.* **2017**, *71* (7), 1225–1233.
(47) Li, L. Synthesis and Antiviral, Insecticidal, and Fungicidal Activities of Gossypol Derivatives Containing Alkylimine, Oxime or Hydrazine Moiety. *Bioorganic & Medicinal Chemistry* **2016**, *24* (3), 474–483.
(48) Wilson, I. B. A Powerful Reactivator of Alkylphosphate-Inhibited Acetylcholinesterase. *Biochimica et Biophysica Acta* **1955**, *18*, 168–170.
(49) Jokanović, M. Pyridinium Oximes in the Treatment of Poisoning with Organophosphorus Compounds. In *Handbook of Toxicology of Chemical Warfare Agents*; Elsevier, 2015; pp 1057–1070.
(50) Dawson, R. M. Review of Oximes Available for Treatment of Nerve Agent Poisoning. *J. Appl. Toxicol.* **1994**, *14* (5), 317–331.
(51) Carbaugh, K. Islaroxime receives FDA Fast Track Designation https://fdahealthnews.com/stories/513136418-islaroxime-receives-fda-fast-track-designation (accessed Apr 25, 2020).
(52) The Safety and Efficacy of Istaroxime for Pre-Cardiogenic Shock - Full Text View - ClinicalTrials.gov https://clinicaltrials.gov/ct2/show/NCT04325035 (accessed Apr 25, 2020).
(53) Canário, C. Steroidal Oximes: Useful Compounds with Antitumor Activities. *CMC* **2017**, *24*.
(54) Özen, T. Screening and Evaluation of Antioxidant Activity of Some Amido-Carbonyl Oxime Derivatives and Their Radical Scavenging Activities. *Journal of Enzyme Inhibition and Medicinal Chemistry* **2009**, *24* (5), 1141–1147.
(55) Zeferino-Díaz, R. 22-Oxocholestane Oximes as Potential Anti-Inflammatory Drug Candidates. *European Journal of Medicinal Chemistry* **2019**, *168*, 78–86.
(56) Luo, Y. Synthesis and Antimicrobial Activities of Oximes Derived from O-Benzylhydroxylamine as FabH Inhibitors. *ChemMedChem* **2012**, *7* (9), 1587–1593.
(57) Shu-Hua Qi. Antifouling Compounds from Marine Invertebrates. *Marine Drugs* **2017**, *15* (9), 263.
(58) Chen, H. Novel Natural Oximes and Oxime Esters with a Vibralactone Backbone from the Basidiomycete *Boreostereum Vibrans*. *ChemistryOpen* **2016**, *5* (2), 142–149.
(59) Dinan, L. Dietary Phytoecdysteroids. In *Handbook of Dietary Phytochemicals*; Springer: Singapore, 2019; pp 1–54.
(60) Dinan, L. Phytoecdysteroids: Biological Aspects. *Phytochemistry* **2001**, *57* (3), 325–339.
(61) Thiem, B. Ecdysteroids: Production in Plant in Vitro Cultures. *Phytochem Rev* **2017**, *16* (4), 603–622.
(62) Hunyadi, A. Serratula Wolffii, as a Promising Source of Ecdysteroids. *Serratula wolffii, as a promising source of ecdysteroids* **2006**, No. PhD.
(63) Csábi, J. Preparation of Novel Bioactive Semi-Synthetic Ecdysteroid Derivatives. *Preparation of novel bioactive semi-synthetic ecdysteroid derivatives* **2017**, No. PhD.

(64) Issaadi Halima, M. *Preparation of bioactive oxidized ecdysteroid derivatives* **2019**, No. PhD.
(65) Dinan, L. On the Distribution of Phytoecdysteroids in Plants: *CMLS, Cell. Mol. Life Sci.* **2001**, *58* (8), 1121–1132.
(66) Butenandt, A. Über Die Isolierung Eines Metamorphose-Hormons Der Insekten in Kristallisierter Form. *Zeitschrift für Naturforschung B* **1954**, *9* (6), 389–391.
(67) Nakanishi, K. Insect Hormones. The Structure of Ponasterone A, Insect-Moulting Hormone from the Leaves of Podocarpus Nakaii Hay. *Chem. Commun. (London)* **1966**, No. 24, 915.
(68) Ecdybase (The Ecdysone Handbook) - a free online ecdysteroids database http://ecdybase.org/ (accessed Apr 26, 2020).
(69) Dinan, L. Effects and Applications of Arthropod Steroid Hormones (Ecdysteroids) in Mammals. *Journal of Endocrinology* **2006**, *191* (1), 1–8.
(70) Baltaev, U. A. [No Title Found]. *Chemistry of Natural Compounds* **2000**, *36* (6), 543–559.
(71) Lafont, R. Ecdysteroid Chemistry and Biochemistry. In *Insect Endocrinology*; Elsevier, 2012; pp 106–176.
(72) Lafont, R. Practical Uses for Ecdysteroids in Mammals Including Humans: And Update. *Journal of Insect Science* **2003**, *3* (1).
(73) Bathori, M. Phytoecdysteroids and Anabolic-Androgenic Steroids - Structure and Effects on Humans. *CMC* **2008**, *15* (1), 75–91.
(74) Gorelick-Feldman, J. Phytoecdysteroids Increase Protein Synthesis in Skeletal Muscle Cells. *J. Agric. Food Chem.* **2008**, *56* (10), 3532–3537.
(75) Tóth, N. 20-Hydroxyecdysone Increases Fiber Size in a Muscle-Specific Fashion in Rat. *Phytomedicine* **2008**, *15* (9), 691–698.
(76) Isenmann, E. Ecdysteroids as Non-Conventional Anabolic Agent: Performance Enhancement by Ecdysterone Supplementation in Humans. *Arch Toxicol* **2019**, *93* (7), 1807–1816.
(77) Parr, M. Ecdysteroids: A Novel Class of Anabolic Agents? *Biol Sport* **2015**, *32* (2), 169–173.
(78) WADA publishes 2020 List of Prohibited Substances and Methods (30 September 2019) https://www.wada-ama.org/en/media/news/2019-09/wada-publishes-2020-list-of-prohibited-substances-and-methods (accessed Dec 4, 2019).
(79) Laekeman, G. Phytoecdysteroids: Phytochemistry and Pharmacological Activity. In *Natural Products*; Springer Berlin Heidelberg: Berlin, Heidelberg, 2013; pp 3827–3849.
(80) Kizelsztein, P. 20-Hydroxyecdysone Decreases Weight and Hyperglycemia in a Diet-Induced Obesity Mice Model. *American Journal of Physiology-Endocrinology and Metabolism* **2009**, *296* (3), E433–E439.
(81) JP2005179367A - Use of ecdysteroid for preparing dermatological or cosmetological composition preventing hair loss - Google Patents https://patents.google.com/patent/JP2005179367A/en (accessed Dec 15, 2019).
(82) FR2893846A1 - Use of a composition containing ecdysteroid or its derivative, or vegetable/animal extracts to stimulate natural defenses of the cells against the consequences of their exposure to UV radiations - Google Patents https://patents.google.com/patent/FR2893843A1/en (accessed Dec 16, 2019).
(83) Lafont, R. Innovative and Future Applications for Ecdysteroids. In *Ecdysone: Structures and Functions*; Springer Netherlands: Dordrecht, 2009; pp 551–578.
(84) Ohsawa, T. Studies on Constituents of Fruit Body of Polyporus Umbellatus and Their Cytotoxic Activity. *Chem. Pharm. Bull.* **1992**, *40* (1), 143–147.
(85) Takasaki, M. Cancer Chemopreventive Agents (Antitumor-Promoters) from *Ajuga d Ecumbens*. *J. Nat. Prod.* **1999**, *62* (7), 972–975.
(86) Oehme, I. Agonists of an Ecdysone-Inducible Mammalian Expression System Inhibit Fas Ligand- and TRAIL-Induced Apoptosis in the Human Colon Carcinoma Cell Line RKO. *Cell Death Differ* **2006**, *13* (2), 189–201.
(87) Martins, A. Significant Activity of Ecdysteroids on the Resistance to Doxorubicin in Mammalian Cancer Cells Expressing the Human ABCB1 Transporter. *J. Med. Chem.* **2012**, *55* (11), 5034–5043.
(88) Martins, A. Ecdysteroids Sensitize MDR and Non-MDR Cancer Cell Lines to Doxorubicin, Paclitaxel, and Vincristine but Tend to Protect Them from Cisplatin. *BioMed Research International* **2015**, *2015*, 1–8.
(89) Hunyadi, A. Backstabbing P-Gp: Side-Chain Cleaved Ecdysteroid 2,3-Dioxolanes Hyper-Sensitize MDR Cancer Cells to Doxorubicin without Efflux Inhibition. *Molecules* **2017**, *22* (2), 199.
(90) Martins, A. Synthesis and Structure-Activity Relationships of Novel Ecdysteroid Dioxolanes as MDR Modulators in Cancer. *Molecules* **2013**, *18* (12), 15255–15275.
(91) Csábi, J. Synthesis and in Vitro Evaluation of the Antitumor Potential and Chemo-Sensitizing Activity of Fluorinated Ecdysteroid Derivatives. *Med. Chem. Commun.* **2016**, *7* (12), 2282–2289.
(92) Galyautdinov, I. V. Synthesis of 20-Hydroxyecdysone Oxime, Its Diacetonide, and Their 14,15-Anhydro Derivatives. *Russ J Org Chem* **2006**, *42* (9), 1333–1339.
(93) Fumagalli, G. Self-Assembly Drug Conjugates for Anticancer Treatment. *Drug Discovery Today* **2016**, *21* (8), 1321–1329.
(94) Wang, Y. Tuning the Amphiphilicity of Building Blocks: Controlled Self-Assembly and Disassembly for Functional Supramolecular Materials. *Adv. Mater.* **2009**, *21* (28), 2849–2864.
(95) Borrelli, S. New Class of Squalene-Based Releasable Nanoassemblies of Paclitaxel, Podophyllotoxin, Camptothecin and Epothilone A. *European Journal of Medicinal Chemistry* **2014**, *85*, 179–190.

(96) Cheetham, A. G. Self-Assembling Prodrugs. *Chem. Soc. Rev.* **2017**, *46* (21), 6638–6663.
(97) Greish, K. Enhanced Permeability and Retention (EPR) Effect for Anticancer Nanomedicine Drug Targeting. In *Cancer Nanotechnology*; Humana Press: Totowa, NJ, 2010; Vol. 624, pp 25–37.
(98) Cho, E. J. Nanoparticle Characterization: State of the Art, Challenges, and Emerging Technologies. *Mol. Pharmaceutics* **2013**, *10* (6), 2093–2110.
(99) Desmaële, D. Squalenoylation: A Generic Platform for Nanoparticular Drug Delivery. *Journal of Controlled Release* **2012**, *161* (2), 609–618.
(100) Reddy, L. H. Squalene: A Natural Triterpene for Use in Disease Management and Therapy. *Advanced Drug Delivery Reviews* **2009**, *61* (15), 1412–1426.
(101) Sen, S. E. Inhibition of Vertebrate Squalene Epoxidase by Extended and Truncated Analogs of Trisnorsqualene Alcohol. *J. Med. Chem.* **1990**, *33* (6), 1698–1701.
(102) Sobot, D. Conjugation of Squalene to Gemcitabine as Unique Approach Exploiting Endogenous Lipoproteins for Drug Delivery. *Nat Commun* **2017**, *8* (1), 15678.
(103) Maksimenko, A. A Unique Squalenoylated and Nonpegylated Doxorubicin Nanomedicine with Systemic Long-Circulating Properties and Anticancer Activity. *Proceedings of the National Academy of Sciences* **2014**, *111* (2), E217–E226.
(104) Sémiramoth, N. Self-Assembled Squalenoylated Penicillin Bioconjugates: An Original Approach for the Treatment of Intracellular Infections. *ACS Nano* **2012**, *6* (5), 3820–3831.
(105) Gaudin, A. Squalenoyl Adenosine Nanoparticles Provide Neuroprotection after Stroke and Spinal Cord Injury. *Nature Nanotech* **2014**, *9* (12), 1054–1062.
(106) Hunyadi, A. Protoflavones: A Class of Unusual Flavonoids as Promising Novel Anticancer Agents. *Phytochem Rev* **2014**, *13* (1), 69–77.
(107) Nikolic, N. A Characterization of Content, Composition and Antioxidant Capacity of Phenolic Compounds in Celery Roots. *Italian Journal of Food Science* **2011**, *23*, 214–219.
(108) Freitas, G. C. Cytotoxic Non-Aromatic B-Ring Flavanones from Piper Carniconnectivum C. DC. *Phytochemistry* **2014**, *97*, 81–87.
(109) Jerz, G. Cyclohexanoid Protoflavanones from the Stem-Bark and Roots of Ongokea Gore☆. *Phytochemistry* **2005**, *66* (14), 1698–1706.
(110) Dankó, B. Synthesis and SAR Study of Anticancer Protoflavone Derivatives: Investigation of Cytotoxicity and Interaction with ABCB1 and ABCG2 Multidrug Efflux Transporters. *ChemMedChem* **2017**, *12* (11), 850–859.
(111) Stanković, T. Lower Antioxidative Capacity of Multidrug-Resistant Cancer Cells Confers Collateral Sensitivity to Protoflavone Derivatives. *Cancer Chemother Pharmacol* **2015**, *76* (3), 555–565.
(112) Chang, H.-L. Protoapigenone, a Novel Flavonoid, Inhibits Ovarian Cancer Cell Growth in Vitro and in Vivo. *Cancer Letters* **2008**, *267* (1), 85–95.
(113) Chen, W.-Y. Protoapigenone, a Natural Derivative of Apigenin, Induces Mitogen-Activated Protein Kinase-Dependent Apoptosis in Human Breast Cancer Cells Associated with Induction of Oxidative Stress and Inhibition of Glutathione S-Transferase π. *Invest New Drugs* **2011**, *29* (6), 1347–1359.
(114) Hunyadi, A. Direct Semi-Synthesis of the Anticancer Lead-Drug Protoapigenone from Apigenin, and Synthesis of Further New Cytotoxic Protoflavone Derivatives. *PLoS ONE* **2011**, *6* (8), e23922.
(115) Chang, H.-L. Protoapigenone, a Novel Flavonoid, Induces Apoptosis in Human Prostate Cancer Cells through Activation of P38 Mitogen-Activated Protein Kinase and c-Jun NH_2 -Terminal Kinase 1/2. *J Pharmacol Exp Ther* **2008**, *325* (3), 841–849.
(116) Chiu, C.-C. Fern Plant–Derived Protoapigenone Leads to DNA Damage, Apoptosis, and G_2 /M Arrest in Lung Cancer Cell Line H1299. *DNA and Cell Biology* **2009**, *28* (10), 501–506.
(117) Chen, H.-M. A Novel Synthetic Protoapigenone Analogue, WYC02-9, Induces DNA Damage and Apoptosis in DU145 Prostate Cancer Cells through Generation of Reactive Oxygen Species. *Free Radical Biology and Medicine* **2011**, *50* (9), 1151–1162.
(118) Liu, H. DEDC, a New Flavonoid Induces Apoptosis via a ROS-Dependent Mechanism in Human Neuroblastoma SH-SY5Y Cells. *Toxicology in Vitro* **2012**, *26* (1), 16–23.
(119) Wang, H.-C. Inhibition of ATR-Dependent Signaling by Protoapigenone and Its Derivative Sensitizes Cancer Cells to Interstrand Cross-Link-Generating Agents In Vitro and In Vivo. *Molecular Cancer Therapeutics* **2012**, *11* (7), 1443–1453.
(120) Lecona, E. Targeting ATR in Cancer. *Nat Rev Cancer* **2018**, *18* (9), 586–595.
(121) Hunyadi, A. Discovery of the First Non-Planar Flavonoid That Can Strongly Inhibit Xanthine Oxidase: Protoapigenone 1′-O-Propargyl Ether. *Tetrahedron Letters* **2013**, *54* (48), 6529–6532.
(122) Tung, C.-P. Inhibition of the Epstein-Barr Virus Lytic Cycle by Protoapigenone. *Journal of General Virology* **2011**, *92* (8), 1760–1768.
(123) Lin, A.-S. First Total Synthesis of Protoapigenone and Its Analogues as Potent Cytotoxic Agents. *J. Med. Chem.* **2007**, *50* (16), 3921–3927.
(124) Lin, A.-S. New Cytotoxic Flavonoids from *Thelypteris torresiana*. *Planta med* **2005**, *71* (9), 867–870.
(125) Pastan, I. A Retrovirus Carrying an MDR1 CDNA Confers Multidrug Resistance and Polarized Expression of P-Glycoprotein in MDCK Cells. *Proceedings of the National Academy of Sciences* **1988**, *85* (12), 4486–

4490.
(126) Chou, T.-C. Theoretical Basis, Experimental Design, and Computerized Simulation of Synergism and Antagonism in Drug Combination Studies. *Pharmacol Rev* **2006**, *58* (3), 621–681.
(127) Issaadi, H. M. Side-Chain Cleaved Phytoecdysteroid Metabolites as Activators of Protein Kinase B. *Bioorganic Chemistry* **2019**, *82*, 405–413.
(128) Shafikov, R. V. 20-Hydroxyecdysone Oximes and Their Rearrangement into Lactams. *Russ J Org Chem* **2009**, *45* (10), 1456–1463.
(129) Bothner-By, A. A. Geminal and Vicinal Proton-Proton Coupling Constants in Organic Compounds. In *Advances in Magnetic and Optical Resonance*; Elsevier, 1965; Vol. 1, pp 195–316.
(130) Derendorf, H. Pharmacokinetics of Triamcinolone Acetonide After Intravenous, Oral, and Inhaled Administration. *The Journal of Clinical Pharmacology* **1995**, *35* (3), 302–305.
(131) Hunyadi, A. Ecdysteroid-Containing Food Supplements from Cyanotis Arachnoidea on the European Market: Evidence for Spinach Product Counterfeiting. *Sci Rep* **2016**, *6* (1), 37322.
(132) Kumpun, S. The Metabolism of 20-Hydroxyecdysone in Mice: Relevance to Pharmacological Effects and Gene Switch Applications of Ecdysteroids. *The Journal of Steroid Biochemistry and Molecular Biology* **2011**, *126* (1–2), 1–9.
(133) Berényi, Á. Synthesis and Investigation of the Anticancer Effects of Estrone-16-Oxime Ethers in Vitro. *Steroids* **2013**, *78* (1), 69–78.
(134) Martínez-Pascual, R. Novel Synthesis of Steroidal Oximes and Lactams and Their Biological Evaluation as Antiproliferative Agents. *Steroids* **2017**, *122*, 24–33.
(135) Savchenko, R. G. Synthesis of Novel α-Aminoecdysteroids via Regio- and Stereoselective Oximation/Hydrogenation of 20-Hydroxyecdysone Derivatives. *Can. J. Chem.* **2017**, *95* (2), 130–133.
(136) Li, Z. Cancer Drug Delivery in the Nano Era: An Overview and Perspectives. *Oncology Reports* **2017**, *38* (2), 611–624.
(137) Fumagalli, G. Heteronanoparticles by Self-Assembly of Doxorubicin and Cyclopamine Conjugates. *ACS Med. Chem. Lett.* **2017**, *8* (9), 953–957.
(138) Robey, R. W. Revisiting the Role of ABC Transporters in Multidrug-Resistant Cancer. *Nat Rev Cancer* **2018**, *18* (7), 452–464.
(139) Fang, W. Flavonoids from the Aerial Parts of *Macrothelypteris Torresiana*. *Natural Product Research* **2011**, *25* (1), 36–39.
(140) Tang, Y. A New Flavonoid from Macrothelypteris Torresiana. *Chem Nat Compd* **2010**, *46* (2), 209–211.
(141) Hsieh, C.-T. Highly Selective Continuous-Flow Synthesis of Potentially Bioactive Deuterated Chalcone Derivatives. *ChemPlusChem* **2015**, *80* (5), 859–864.
(142) Endo, K. Biogenesis-like Transformation of Salidroside to Rengyol and Its Related Cyclohexyletanoids Of. *Tetrahedron* **1989**, *45* (12), 3673–3682.
(143) Irfan, M. Heterogeneous Catalytic Hydrogenation Reactions in Continuous-Flow Reactors. *ChemSusChem* **2011**, *4* (3), 300–316.
(144) Mándity, I. M. Strategic Application of Residence-Time Control in Continuous-Flow Reactors. *ChemistryOpen* **2015**, *4* (3), 212–223.
(145) Ötvös, S. B. Highly Selective Deuteration of Pharmaceutically Relevant Nitrogen-Containing Heterocycles: A Flow Chemistry Approach. *Mol Divers* **2011**, *15* (3), 605–611.
(146) Gant, T. G. Using Deuterium in Drug Discovery: Leaving the Label in the Drug. *J. Med. Chem.* **2014**, *57* (9), 3595–3611.
(147) Li, B.-W. Design and Discovery of Flavonoid-Based HIV-1 Integrase Inhibitors Targeting Both the Active Site and the Interaction with LEDGF/P75. *Bioorganic & Medicinal Chemistry* **2014**, *22* (12), 3146–3158.

ACKNOWLEDGMENTS

Firstly, I would like to express my sincere gratitude to my supervisor, *Dr. Attila Hunyadi,* for the continuous mentoring of my Ph.D. studies and for guiding and helping me through the challenges of my post-graduate work. His inspirational and creative personality stood as an example of how to grow and improve as a researcher.

Secondly, I am thankful to *Prof. Dr. Judit Hohmann*, director of the Institute of Pharmacognosy, University of Szeged, for following my Ph.D. work with continuous interest and support, and for providing me the possibility to study at the institute.

I want to thank the work of all co-authors who contributed to the born of our joint publications representing the building blocks of this dissertation. I am especially grateful to *Prof. Dr. Gábor Tóth*, *Dr. Dóra Bogdán*, *Dr. Tamás Gáti*, *Dr. Rainer Haessner* and *Dr. Norbert Kúsz* for the NMR investigations and to *Mr. Attila Csorba* for the assistance provided in the HR-MS measurements.

On this page, I would like to express my gratitude to *Dr. Daniele Passarella* and *Dr. Lucia Tamborini,* senior researchers of the University of Milan (Italy), for allowing me to join and work in their research group within the frameworks of scientific exchange programs. Their scientific expertise allowed me to further expand my knowledge in the field of chemistry.

Further, I would like to express my sincere thanks to *Dr. Ana Martins* and the colleagues of *Dr. Daniele Passarella* for the bioactivity testing of ecdysteroid derivatives obtained during my Ph.D. work. For the pharmacological evaluation of protoflavonoid derivatives, I would like to thank the work of *Dr. Li-Kwan Chang*, *Dr. Carole Seguin-Devaux*, *Prof. Dr. Fang-Rong Chang* and all their research group members as well.

I would like to warmly thank the support and help of all my colleagues in our laboratory. Among them, I wish to address my special gratitude to our technician, *Ibolya Hevérné Herke*, whose outstanding routine and knowledge in the field of separation techniques had been of considerable help in my everyday laboratory work.

Besides the people mentioned, I wish to thank all members of the Institute of Pharmacognosy for the friendly and supportive atmosphere provided during these years.

Eventually, I address my special gratitude to the members of my family, and most importantly, to my father, whose wise and experienced words were of great value throughout my Ph.D. studies.

This Ph. D. work was supported by the National Research, Development and Innovation Office, Hungary (NKFIH; K119770 and K109293).

APPENDIX

Related articles

I.

European Journal of Medicinal Chemistry 144 (2018) 730–739

Contents lists available at ScienceDirect

European Journal of Medicinal Chemistry

journal homepage: http://www.elsevier.com/locate/ejmech

Research paper

Nitrogen-containing ecdysteroid derivatives vs. multi-drug resistance in cancer: Preparation and antitumor activity of oximes, oxime ethers and a lactam

Máté Vágvölgyi [a], Ana Martins [b, 1], Ágnes Kulmány [c], István Zupkó [c], Tamás Gáti [d], András Simon [e], Gábor Tóth [e], Attila Hunyadi [a, f, *]

[a] Institute of Pharmacognosy, Faculty of Pharmacy, University of Szeged, Szeged, Hungary
[b] Department of Medical Microbiology and Immunobiology, Faculty of Medicine, University of Szeged, Szeged, Hungary
[c] Institute of Pharmacodynamics and Biopharmacy, Faculty of Pharmacy, University of Szeged, Szeged, Hungary
[d] Servier Research Institute of Medicinal Chemistry (SRIMC), Budapest, Hungary
[e] NMR group, Department of Inorganic and Analytical Chemistry, University of Technology and Economics, Budapest, Hungary
[f] Interdisciplinary Centre for Natural Products, University of Szeged, Szeged, Hungary

ARTICLE INFO

Article history:
Received 27 October 2017
Received in revised form
8 December 2017
Accepted 9 December 2017
Available online 12 December 2017

Keywords:
Ecdysterone
Semi-synthesis
Beckmann-rearrangement
Chemotherapy
Adjuvant
ABCB1 transporter
P-glycoprotein
Efflux pump inhibitor

ABSTRACT

Multidrug resistance is a widespread problem among various diseases and cancer is no exception. We had previously described the chemo-sensitizing activity of ecdysteroid derivatives with low polarity on drug susceptible and multi-drug resistant (MDR) cancer cells. We have also shown that these molecules have a marked selectivity towards the MDR cells. Recent studies on the oximation of various steroid derivatives indicated remarkable increase in their antitumor activity, but there is no related bioactivity data on ecdysteroid oximes. In our present study, 13 novel ecdysteroid derivatives (oximes, oxime ethers and a lactam) and one known compound were synthesized from 20-hydroxyecdysone 2,3;20,22-diacetonide and fully characterized by comprehensive NMR techniques revealing their complete ^{1}H and ^{13}C signal assignments. The compounds exerted moderate to strong *in vitro* antiproliferative activity on HeLa, SiHa, MCF-7 and MDA-MB-231 cell lines. Oxime and particularly oxime ether formation strongly increased their inhibitory activity on the efflux of rhodamine 123 by P-glycoprotein (P-gp), while the new ecdysteroid lactam did not interfere with the efflux function. All compounds exerted potent chemo-sensitizing activity towards doxorubicin on a mouse lymphoma cell line and on its MDR counterpart, and, on the latter, the lactam was found the most active. Because of its MDR-selective chemo-sensitizing activity with no functional effect on P-gp, this lactam is of high potential interest as a new lead for further antitumor studies.

1. Introduction

Synthetic modification of steroidal compounds remains a promising strategy in the hunt for novel drug candidates since even minor changes in the substitution pattern of their chemical backbone may significantly modify specific bioactivities. Certain steroidal oximes and oxime ethers were shown to have antioxidant [1], antimicrobial [1], antineoplastic [2] or neuromuscular blocking [3] activities.

Currently, the antitumor activity of steroid oximes is by far the most deeply investigated and has recently attracted great scientific attention. For example, oximes and lactams of cholest-4-en-6-one were tested on two human cancer cell lines and were shown to have very high, tumor selective anticancer activity on HeLa cells [4]. Another study on the structure-activity relationships (SAR) of hydroxyiminosteroids bearing the oxime group on the steroid A and/or B ring showed that a C-6 oxime function is preferential over a 6-keto group concerning *in vitro* cytotoxic activity of these type of compounds [5]. In a follow-up study on the same compounds, the importance of 3- and 6-hydroxy functions was highlighted [6].

* Corresponding author. Institute of Pharmacognosy, Faculty of Pharmacy, University of Szeged, Eötvös u. 6, H-6720 Szeged, Hungary.
E-mail address: hunyadi.a@pharm.u-szeged.hu (A. Hunyadi).
[1] Current address: Synthetic Systems Biology Unit, Institute of Biochemistry, Biological Research Centre, Temesvári krt. 62, H-6726 Szeged, Hungary.

https://doi.org/10.1016/j.ejmech.2017.12.032
0223-5234/

Furthermore, a set of *in vitro* experiments on 63 novel estrone 16-oximes and oxime ethers revealed two oximes as promising antiproliferative agents with selectivity towards HeLa cells; the compounds modulated cell cycle and induced apoptosis through caspase-3 [7]. In a most recent study, a series of steroidal oximes and lactams were described to possess significant *in vitro* antiproliferative activity, and a 6,23-dioxime derivative, obtained from diosgenin acetate, was identified to be the most effective [8]. Several further recent reports can be found in the literature where well-defined mechanistic changes could also be connected to the increase in the antiproliferative activity observed after introducing an oxime moiety into an oxo-compound. For example, a number of α,β-unsaturated, cyclohexanone-based oximes showed greatly increased activity as compared to their parental oxo-compounds against $BRAF^{V600E}$ (the most common mutation in the v-raf murine sarcoma viral oncogenes homolog B1, involved in carcinogenesis and cancer agressiveness) and/or epidermal growth factor receptor TK kinases (involved in cell proliferation, evasion of apoptosis and invasive capacity) [9], or focal adhesion kinase (FAK; involved in stimulating metastasis and tumor progression) [10]. These reports suggest that the preparation of oxime derivatives from ketosteroids, and particularly from those with an α,β-enone moiety, should be a reasonable strategy to extend the chemical space towards new, potentially antitumor compounds.

Ecdysteroids are α,β-unsaturated 6-ketosteroids that occur in a wide range of plant species; as analogs of the insect molting hormone ecdysone, these compounds possess several biological functions in the flora and the fauna [11,12]. Since the isolation of the most abundant ecdysteroid 20-hydroxyecdysone (20E), these compounds were reported to also exert various, beneficial bioactivities in mammals [13,14,15,16]. Additionally, our group revealed that relatively apolar ecdysteroids can strongly sensitize cancer cells to chemotherapeutics (i.e. “chemo-sensitizing” activity), and suggested 20-hydroxyecdysone 2,3;20,22-diacetonide (**1**) as a promising anticancer lead compound [17]. Interestingly, this sensitization towards various chemotherapeutics could be observed both on multi-drug resistant (MDR) and drug susceptible cancer cell lines [18]. After several further studies, exploring this particular anticancer activity of ecdysteroids, we now know that 1) apolar substituents on the 2,3-diol moiety are more important than those at positions 20 and 22 [19], and 2) an oxidative side-chain cleavage knocks out the inhibitory activity on the efflux function of the ABCB1 transporter (P-glycoprotein; P-gp) while maintaining MDR selective sensitizing activity towards doxorubicin [20]. Regarding semi-synthetic modifications accompanied by the inclusion of heteroatoms, a difluorinated derivative of 20E 2,3;20,22-diacetonide was found to be a stronger P-gp inhibitor than its parental molecule (compound **1**), while, surprisingly, MDR selectivity of the difluorinated compound was lower: it sensitized a P-gp expressing MDR cell line to doxorubicin similarly to its parental compound **1**, and a stronger effect than that of **1** was observed on a non-MDR cell line [21]. The chemical structures of 20E and compound 1 are shown in Fig. 1.

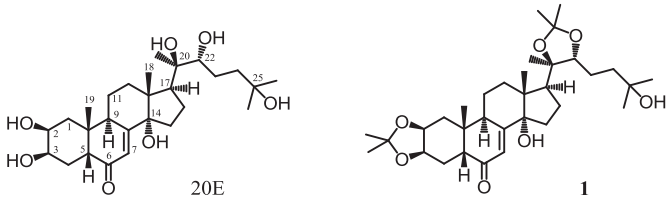

Fig. 1. Chemical structures of 20-hydroxyecdysone (20E) and 20-hydroxyecdysone 2,3;20,22-diacetonide (**1**).

Galyautdinov et al. have previously reported the successful preparation of several (*E*/*Z*)-isomeric ecdysteroid 6-oxime and some lactam derivatives [22]. Considering the above mentioned antitumor potential of steroidal oximes and the fact that no studies are available on the bioactivity of ecdysteroid oximes or lactams, the aim of the present work was to prepare a series of such compounds, and study their *in vitro* antitumor potential with a focus on their chemo-sensitizing activity.

2. Results and discussions

2.1. Chemistry

20-hydroxyecdysone 2,3; 20.22-diacetonide **1** and its 6-oxime and lactam derivatives were synthesized following previously published procedures [22,23]. Briefly, compound **1** was reacted with hydroxylamine or, aiming to prepare new oxime ethers, an alkoxylamine in pyridine at 70 °C. A total of 14 nitrogen-containing derivatives were prepared this way (Scheme 1).

Following each reaction, neutralization with KOH dissolved in anhydrous methanol was utilized with the aim of obtaining several different, structurally diverse and potentially bioactive products, including mixtures of 14,15-anhydro- and intact oxime derivatives: the oximes **2** and **3**, and oxime ethers with different 6-*O*-alkyl substituents **5**–**15**, respectively, were obtained through this method. Our results confirm previous observations that ecdysteroid 6-oximation can result in 3 different types of product mixtures depending on the neutralization procedure [22]: a mixture of 14,15-anhydro (*E*/*Z*)-isomeric oxime pairs form if the reaction does not include a neutralization step; a 2–4 components mixture of both intact and 14OH-eliminated derivatives is obtained if alkali dissolved in anhydrous methanol is added; and a mixture of intact (*E*/*Z*)-isomeric oxime pair with retained 14-OH groups is obtained if the neutralizing alkali is dissolved in anhydrous ethanol.

A second transformation involving the Beckmann-rearrangement of the (6*E*)-oxime compound **2** was performed utilizing *p*-toluenesulfonyl chloride (TsCl) in acetone in the presence of sodium carbonate to obtain a new ecdysteroid derivative, compound **4**, with a seven-membered lactam ring (Scheme 2). As expected, the (6*Z*)-oxime compound did not form the corresponding lactam but a tosylate was obtained (not presented, for more details see also reference [23]).

2.2. Structure elucidation

We have recently reported the structure elucidation and complete ^{1}H and ^{13}C signal assignment of a series of dioxolane derivatives of 20-hydroxyecdysone [19,20,21,24]. Here we discuss the complete ^{1}H and ^{13}C signal assignment of the corresponding 6-oxime and 6-oxime ether derivatives.

The structure and NMR signals of the products were assigned by comprehensive one- and two-dimensional NMR methods, such as ^{1}H, ^{13}C, DEPTQ, gradient-selected COSY, edited HSQC, HMBC, ROESY (**R**otating frame **O**verhauser **E**nchancement **S**pectroscopy) spectra and 1D-selective variants thereof. It is worth mentioning that due to the molecular mass (500–700 Da) the signal/noise value of the selective ROE experiments strongly exceeds that of the selective NOEs.

To facilitate the comparison of NMR signals of structurally analogous hydrogen and carbon atoms of the starting compound **1** with those of the 6-oxime **2**, and of its Beckmann rearranged product **4** and 6-oxime-ether derivatives **5**–**15**, we applied the usual steroid numbering, and for the central atoms of the 2,3;20,22-diacetonide moieties C-28 and C-29, respectively. The ^{13}C chemical shifts of compounds **1**, **2** and **4**–**15** in methanol-d_4 are compiled in

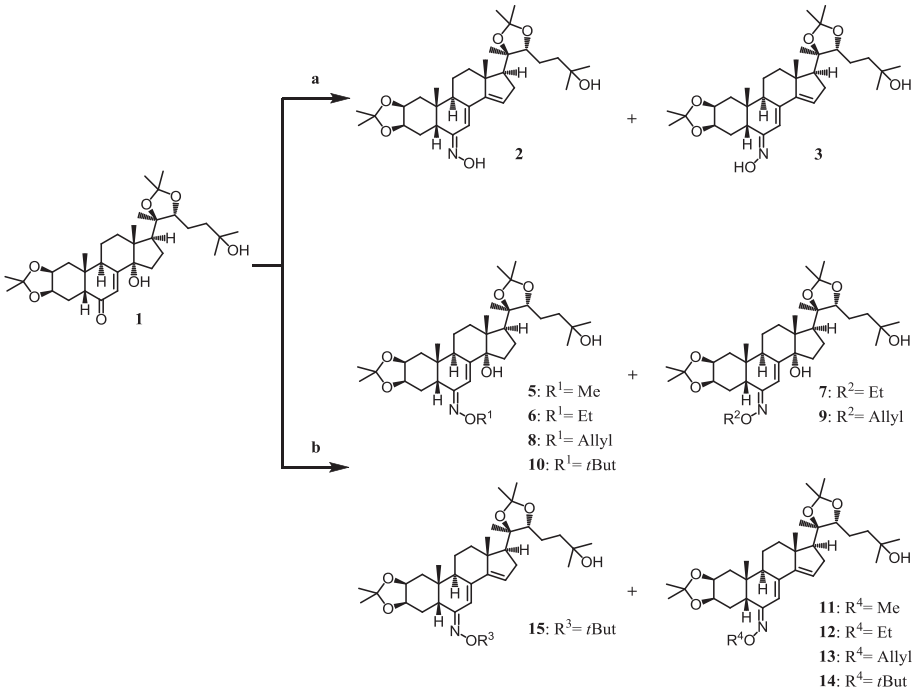

Scheme 1. Synthesis of oxime and oxime ether derivatives of 20-hydroxyecdysone 2,3;20,22-diacetonide.
Reagents and conditions: a) pyridine, $NH_2OH \cdot HCl$, 70 °C, 3 days; b) pyridine, $NH_2OR \cdot HCl$ (R = Me, Et, Allyl, or *t*But), 70 °C, 24 h; work-up with KOH in anhydrous MeOH.

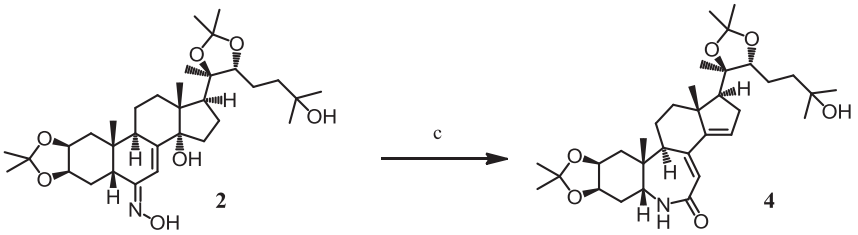

Scheme 2. Beckmann rearrangement of ecdysteroid (6*E*)-oxime **2** into lactam **4**.
Reagents and conditions: c) acetone, *p*-toluenesulfonyl chloride (TsCl, 2 equiv of oxime **2**), Na_2CO_3 (1 equiv of oxime **2**), RT, 6 h.

Table 1. The characteristic ^{1}H data of compounds with a $\Delta^{14,15}$ C=CH ethylene moiety **2**, **4** and **11**–**15** are summarized in Table 2, whereas that of the HO-C(14) derivatives **5**–**10** are shown in Table 3.

It is well known that oximation of ketones is accompanied with characteristic changes of several ^{13}C and ^{1}H chemical shifts. Successful conversion of a C=O group to C=N-OH results of ca. 50 ppm diamagnetic shift of the corresponding carbon atom, whereas the chemical shift of α-CH carbon atom in the *syn* position with respect to the oxime hydroxyl group exhibits ~14 ppm, in the *anti* position ~9 ppm diamagnetic shift. The significant (Δδ *syn-anti*) parameters on C-5 and =C-7 signals successfully can be utilized for the assignment of (*Z*/*E*) isomers. Galyautdinov et al. reported some NMR data on 20-hydroxyecdysone oxime [22], including compound **3** (*Z* isomer), but they failed on isolating the isomeric compound **2** with *Z* configuration. In addition they have taken the NMR measurements in solvents with rather different anisotropic nature (e.g. pyridine-d_5, methanol-d_4) and so in some cases the solvation effect was comparable with the Δδ *syn-anti* parameters. To avoid this ambiguity, we have performed our NMR experiments exclusively in methanol-d_4.

On the basis of our data, all of the oxime derivatives in Table 1 with δC-5 ~ 38.6 and δC-7 ~ 117.5 ppm values, respectively, are *Z* isomers, while δC-5 ~ 43.8 and δC-7 ~ 111.0 ppm values assign the *E* isomers. It is worth noting that the less different δC-4 (~30/27 ppm) and δC-6 (~157/161 ppm) values also reflect on the *E* or *Z* isomers, respectively.

In case of compounds **2** and **4**, and the 6-oxime-ether derivatives **11**–**15** the DEPTQ and HSQC measurements revealed only seven methylene groups, one less than in the parent compound **1**, and simultaneously distinctive chemical shift changes appeared at δC-14: 85.4 → C= ~142 ppm and $\delta H_2\underline{C}$-15: 31.8 → H$\underline{C}$= ~124 ppm, respectively, indicating the emergence of an $\Delta^{14,15}$ C=CH ethylene moiety. All this means that in these compounds (**2**, **11**–**15**), simultaneously with the oximation, dehydration by the elimination of the 14-OH group also took place. The presence of the 14-OH substituent in compounds **5**–**10** appears straightforward, considering of the chemical shift of C-14 (δC-14–85 ppm) confirmed by the HMBC cross-peak H_3-18/C-14. Success of the Beckmann rearrangement of ecdysteroid (6*E*)-oxime **2** into lactam **4** could be expected from the E configuration of the parent oxime. Indeed, the significant (13.1 ppm) paramagnetic shift on δC-5 proves that in **4** the nitrogen atom coupled to C-5, the appearance of the signal at 170.6 ppm supports the formation of the lactam ring.

Thanks to the comprehensive one- and two-dimensional NMR techniques utilized in the structure elucidation process, a complete ^{1}H signal assignment could be achieved for all compounds. The

Table 1
^{13}C chemical shifts of compounds **2**, **4**–**15** as compared to that of their parental compound **1** (20-hydroxyecdysone 2,3; 20,22-diacetonide) [21]; in methanol-d_4.

No.	1	2	4[a]	5	6	7	8	9	10	11	12	13	14	15
1	39.0	39.5	43.2	39.7	39.7	39.4	39.7	39.4	39.8	39.1	39.1	39.1	39.3	39.5
2	73.7	73.4	73.2	73.6	73.6	73.6	73.6	73.6	73.7	73.4	73.5	73.5	73.6	73.6
3	73.3	74.0	75.5	74.0	74.0	73.9	74.0	73.8	74.2	73.7	73.8	73.8	74.0	74.1
4	27.9	30.3	30.9	30.0	30.0	27.0	29.9	27.0	30.0	27.3	27.2	27.2	27.3	30.4
5	52.7	43.5	56.6	43.8	43.8	38.6	43.8	38.7	44.0	38.4	38.5	38.6	38.2	43.7
6	205.8	157.0	170.6	157.2	156.9	160.3	157.4	160.7	155.7	160.8	160.6	161.0	159.4	155.8
7	122.0	110.0	119.9	110.7	110.9	117.5	110.8	117.3	111.3	117.0	117.2	117.0	118.3	110.8
8	167.1	151.5	151.6	154.1	153.8	150.7	154.1	151.0	152.3	151.0	151.1	151.1	151.3	151.6
9	35.9	40.2	45.9	35.5	35.5	34.4	35.5	34.4	35.7	39.1	39.2	39.2	39.2	40.2
10	38.9	38.0	40.7	37.8	37.7	37.0	37.7	37.0	37.6	37.1	37.1	37.1	37.0	37.9
11	21.8	21.9	25.4	21.5	21.5	21.5	21.5	21.5	21.5	21.8	21.8	21.9	21.9	21.9
12	32.5	41.3	42.4	32.6	32.6	32.5	32.6	32.5	32.6	41.1	41.1	41.1	41.2	41.3
13	48.7	49.0	50.2	49.0	48.6	48.3	48.6	48.3	48.6	48.6	48.6	48.7	48.6	48.7
14	85.4	144.3	154.4	85.9	85.9	85.7	85.9	85.7	86.0	142.4	142.1	142.4	140.6	143.8
15	31.8	125.3	125.6	32.0	32.0	32.1	32.0	32.1	32.0	124.4	124.3	124.4	123.6	125.0
16	22.6	32.4	32.6	22.6	22.6	22.7	22.6	22.6	22.6	32.3	32.3	32.4	32.3	32.4
17	50.6	59.0	59.3	50.6	50.6	50.7	50.6	50.7	50.6	58.9	58.9	59.0	59.0	59.1
18	17.8	19.7	19.6	18.0	18.0	18.0	18.0	18.0	18.1	19.6	19.6	19.6	19.6	19.7
19	24.2	23.9	18.1	24.3	24.3	24.3	24.3	24.3	24.3	24.1	24.0	24.1	24.1	24.9
20	86.0	84.9	84.7	86.0	86.0	86.1	86.0	86.1	86.0	84.9	84.9	85.0	85.0	84.9
21	22.8	22.0	21.9	22.7	22.7	22.7	22.7	22.7	22.7	22.0	22.0	22.0	22.0	22.0
22	83.5	83.1	83.1	83.4	83.4	83.4	83.4	83.4	83.4	83.2	83.2	83.2	83.2	83.2
23	24.9	24.8	24.8	24.8	24.8	24.8	24.8	24.8	24.8	24.8	24.8	24.9	24.9	24.9
24	42.4	42.1	42.1	42.3	42.3	42.4	42.3	42.4	42.3	42.1	42.1	42.1	42.1	42.7
25	71.3	71.2	71.2	71.2	71.2	71.2	71.2	71.2	71.2	71.1	71.2	71.2	71.2	71.2
26	29.1	29.0	29.1	29.1	29.1	29.1	29.1	29.1	29.1	29.1	29.0	29.0	29.0	29.0
27	29.0	29.7	29.6	29.6	29.6	29.6	29.6	29.5	29.6	29.7	29.7	29.7	29.7	29.7
28	109.6		109.5	109.4	109.3	109.3	109.3	109.3	109.3	109.3	109.3	109.3	109.2	109.4
28Meα	26.8		26.6	26.8	26.8	26.8	26.8	26.8	26.9	26.8	26.7	26.7	26.7	26.8
28Meβ	29.0		28.9	29.0	29.0	29.0	29.0	29.0	29.0	29.1	29.0	29.0	29.0	29.0
29	108.2		108.0	108.1	108.0	108.1	108.0	108.1	108.0	108.0	108.0	108.1	108.0	108.1
29Meα	29.5		29.3	29.5	29.5	29.5	29.5	29.4	29.5	29.4	29.4	29.4	29.4	29.4
29Meβ	27.3		27.3	27.3	27.3	27.3	27.4	27.3	27.3	27.3	27.3	27.2	28.0	27.3
1′				61.8	70.1	70.4	75.5	75.7	78.9	62.2	70.5	75.8	79.3	
2′					15.0	15.2	135.9	136.0	28.0		15.2	135.9	28.0	
3′							117.6	117.5				117.6		

[a] To facilitate the comparison of NMR data of the Beckman product **4** and the parental oxime ethers we applied the steroid atomic numbering also for compound **4**.

characteristic ^{1}H NMR data of the 14,15-anhydro derivatives **2**, **4** and **11**–**15** are summarized in Table 2, whereas that of the other compounds **5**–**10** in Table 3. The main difference between the two sets of data is that in Table 2, besides H-7, a second olefinic signal appears for H-15 (~δ5.80 dd) instead of the H_2-16 hydrogen signals.

The retained *cis* junction of the A/B rings in each compound was obvious by considering the strong H_3-19/Hβ-5 ROESY response, whereas the assignment of the α/β position of the diastereotopic methylene hydrogens of the skeleton were revealed by the one-dimensional selective ROESY measurements irradiating e.g. the H_3-18, H_3-19 and H-5 atoms in combination with the observed proton-proton coupling pattern.

Considering the data of Tables 2 and 3 it is clear that the values of δH-5 and δH-7 chemical shifts allow the easy and unequivocal differentiation between the *E* and *Z* isomers. In case of the 14,15-anhydro derivatives **2** and **11**–**15**, the H-5 signals resonate around 2.25 ppm in the *E* and at 3.15 ppm in the *Z* isomers, and the δH-7 chemical shifts appear at 6.76 ppm in the *E* and at 6.16 ppm in *Z* isomers. Similar trend was observed for the compounds in Table 3, the chemical shift of H-5 in the *anti* position with respect to the oxime hydroxyl group exhibits ~2.23 ppm, while in the *Z* isomer it is ~3.18 ppm. The corresponding values for H-7 are 6.45 and 5.88 ppm, respectively.

To facilitate the comparison between the NMR data of *Z* and *E* isomeric pairs, the stereo-structures with atomic numbering (in red) of compounds **7** (upper) and **6** (lower) are shown in Fig. 2. Blue numbers refer to ^{1}H chemical shifts; black numbers give the δ ^{13}C values.

2.3. Biology

Antiproliferative activity of compounds **4**–**15** was tested on a panel of gynecological cancer cell lines, including cervical (HeLa, SiHa) and breast cancer cell lines (MDA-MB-231, MCF7); the results are presented in Table 4.

Although most of the ecdysteroid analogs displayed moderate activities against the tested cell lines, the *t*-butyl substituted compound **10** was stronger than the positive control cisplatin on the HeLa and MDA-MB-231 cell lines. In our previous study, the antiproliferative IC_{50} values of compound **1** were 106.1 and 75.1 μM on the MDA-MB-231 and MCF7 cell lines, respectively [21], showing that the inclusion of certain oxime ether functions can increase this activity by nearly an order of magnitude. While the orientation of the oxime ether had no obvious effect on the activity, a larger alkyl group led to a stronger antiproliferative action. It appears to be clear that the retained 14-OH function is favorable over the $\Delta^{14,15}$ moiety in this regard on the MCF-7 cell line (compounds **7** vs. **12**, **9** vs. **13**, and **10** vs. **15**), while such a conclusion cannot be drawn on the other cell lines.

Compounds **2**–**15** were also tested for their cytotoxic activity on a murine lymphoma cell line pair, including L5178 and its multidrug resistant counterpart transfected to express the human ABCB1 transporter, $L5178_{MDR}$. Following this, the compounds were tested for their potential to inhibit the ABCB1 efflux transporter through measuring the intracellular accumulation of rhodamine 123 by flow cytometry. Degree of inhibition (%) values were calculated by means of the rhodamine 123 accumulation of the ABCB1 transfected $L5178_{MDR}$ cells (i.e. 0% inhibition) and that of the

Table 2
^{1}H chemical shift, multiplicities and coupling constants of compounds **2**, **4**, **11**–**15** in methanol-d_4.

No.		2	*J* (Hz)	4[a]	*J* (Hz)	11	*J* (Hz)[b]	12	13	14	15
1	α	1.98	dd; 14.0, 6.5	2.19	dd; 14.0, 6.8	1.95	dd; 13.9, 6.3	1.94	1.95	1.92	1.98
	β	1.25		1.30		1.26		1.28	1.28	1.29	1.25
2		4.19	ddd; 11.0, 6.5, 4.5	4.25	ddd; 12.0, 6.8, 5.0	4.18	ddd; 10.8, 6.3, 4.5	4.19	4.19	4.19	4.19
3		4.26	td; 4.5, 1.7	4.39	dt; 5.0, 3.0	4.24	td; 4.5, 1.2	4.25	4.25	4.24	4.27
4	α	1.77		1.29		1.60		1.60	1.61	1.57	1.77
	β	1.97		2.06		2.10		2.11	2.14	2.11	1.95
5		2.25	dd; 12.1, 4.2	3.30	dd; 10.2, 6.5	3.14	dd; 12.8, 4.6	3.15	3.19	3.15	2.26
7		6.81	d; 2.7	5.94	d; 2.6	6.14	d; 2.6	6.16	6.16	6.20	6.70
9		2.27		2.37	ddd; 11.5, 3.6, 2.6	2.31		2.31	2.31	2.29	2.24
11	α	1.65		1.88		1.63		1.63	1.62	1.61	1.64
	β	1.72		1.74		1.68		1.68	1.67	1.67	1.71
12	α	1.53		1.60		1.50		1.50	1.50	1.50	1.52
	β	2.23		2.21		2.22	dt; 12.7, 3.0	2.22	2.22	2.22	2.22
15		5.86	dd; 3.5, 2.0	5.74	dd; 3.5, 1.9	5.81	dd; 3.3, 2.1	5.81	5.81	5.79	5.82
16	α	2.33		2.33		2.32		2.32	2.31	2.31	2.32
	β	2.60		2.58		2.58		2.58	2.58	2.58	2.59
17		2.04	dd; 10.7, 7.7	2.11	dd; 10.7, 7.8	2.02	dd; 10.8, 7.7	2.02	2.02	2.01	2.03
18		1.06		1.06		1.05		1.05	1.05	1.05	1.05
19		0.83		0.96		0.84		0.84	0.85	0.84	0.81
21		1.22		1.21		1.22		1.22	1.22	1.22	1.22
22		3.76		3.75		3.76		3.76	3.76	3.77	3.76
23	a	1.53		1.53		1.53		1.53	1.53	1.53	1.54
	b	1.53		1.53		1.53		1.53	1.53	1.53	1.54
24	a	1.48		1.48		1.48		1.48	1.48	1.48	1.48
	b	1.72		1.72		1.72		1.72	1.72	1.72	1.72
26		1.20		1.20		1.19		1.19	1.19	1.19	1.19
27		1.21		1.21		1.21		1.20	1.20	1.21	1.21
28Meα		1.30		1.30		1.31		1.31	1.31	1.32	1.32
28Meβ		1.47		1.46		1.49		1.49	1.49	1.50	1.49
29Meα		1.40		1.40		1.40		1.40	1.40	1.40	1.40
29Meβ		1.30		1.30		1.30		1.30	1.30	1.30	1.31
1′						3.86		4.11	4.56	–	–
2′								1.27	6.00	1.29	1.29
3′	*Z*								5.19		
	E								5.29		

[a] To facilitate the comparison of NMR data of the Beckman product **4** and the parental oximethers, we applied the steroid atomic numbering also for **4**.
[b] Because the stereostucture of the steroid frame is nearly identical within compounds **11**–**15,** we described the *J* coupling contents only for **11**.

L5178 cells (i.e. 100% inhibition); results are presented in Table 5.

While the compounds also exerted weak to moderate cytotoxic activities on the mouse lymphoma cell line pair, all of them were more potent than their parental compound **1**. No cross resistance was observed to any of them on the ABCB1 over-expressing MDR cells. The oximes **2** and **3** showed the strongest activity on either cell lines with IC_{50} values ca. 4–5 times below that of compound **1**, and the *E*-oxime (**2**) was more cytotoxic than the *Z*-oxime (**3**). The oxime ethers typically exerted weaker cytotoxic activities than the non-substituted oximes, with the exception of compound **10** where a bulky *t*-butyl substituent and a retained 14-OH group were present. When comparing corresponding analogs with a retained 14-OH group or a $\Delta^{14,15}$ moiety, there appeared to be a clear tendency for the former structural element to be associated with a stronger cytotoxic activity on the mouse lymphoma cells, similarly to the case of MCF-7 cells (see above).

Evaluation of the results obtained from the rhodamine accumulation assay reveals that the lactam derivative (**4**) is the only one among the compounds that was completely inactive in this regard at as much as 20 μM concentration. For the other compounds, several structure-activity relationships could be observed. The oxime formation markedly increased the ABCB1 inhibitory activity, and this was particularly true for oxime ethers. The orientation of the oxime group had little if any influence on the ABCB1 inhibition (compound **2** vs. **3**, **6** vs. **7**, **8** vs. **9**, and **14** vs. **15**), while the 14-OH elimination, forming a $\Delta^{14,15}$ double bond in the ecdysteroid D-ring, clearly increased this activity (compound **7** vs. **12**, **9** vs. **13**, and **10** vs. **15**). When comparing the activity of oximes and oxime ethers between analogs containing the same type of D-ring and orientation of oxime but different substituents on the latter, the following order of bioactivity could be concluded: H < Me < Et < Allyl ≤ *t*-But.

The compounds were also tested for their ability to sensitize the susceptible/resistant mouse lymphoma cell line pair towards the cytotoxic activity of doxorubicin. Since each compound showed a measurable cytotoxic activity on both cell lines when applied alone, combination indices could be determined through the checkerboard microplate method similarly to our previous related studies [17,19]. Table 6 shows the strongest activity observed for each compound on the L5178 and $L5178_{MDR}$ cell lines; further details and results at other compound:doxorubicin ratios are available in supporting information Table S1.

All tested derivatives showed strong synergism ($0.1 < CI_{avg} < 0.3$) [25] with doxorubicin on the P-gp expressing $L5178_{MDR}$ cells, similarly to their parental compound (**1**). As it was previously reported by us, chemo-sensitizing activity of ecdysteroids has little if any correlation to their (most typically weak) inhibitory effect on the efflux function of P-gp [20]. This was clearly confirmed in the present study as well: even though for example compounds **11**–**15** are much stronger P-gp inhibitors than their parental compound **1**, no difference can be observed in the strength of synergism with the P-gp substrate doxorubicin on the MDR cell line. Most interestingly, among all derivatives obtained, the ecdysteroid lactam **4** was found to express the strongest chemosensitization on the MDR cells, while being the only one to show no interference with P-gp function. Accordingly, this compound has a further advantage over the diacetonide of 20E, namely that it would likely be free from the potential adverse effects and unwanted drug-drug interactions

Table 3
^{1}H chemical shifts, multiplicities and coupling constants of compounds **5**–**10** in methanol-d_4.

No.		5	*J* (Hz)[a]	6	7	8	9	10
1	α	1.98		1.98	1.94	1.98	1.95	1.98
	β	1.22		1.23	1.24	1.23	1.24	1.23
2		4.21	ddd; 10.5, 6.7, 5.1	4.21	4.21	4.22	4.21	4.22
3		4.28		4.28	4.26	4.28	4.27	4.28
4	α	1.93		1.93	1.73	1.93	1.74	1.92
	β	1.93		1.93	2.06	1.93	2.08	1.92
5		2.22	dd; 12.2, 5.5	2.23	3.16	2.24	3.19	2.26
7		6.44	d; 2.7	6.47	5.88	6.49	5.88	6.47
9		2.72	ddd; 11.8, 6.9, 2.7	2.71	2.72	2.72	2.73	2.70
11	α	1.65		1.65	1.65	1.64	1.63	1.64
	β	1.59		1.58	1.58	1.59	1.58	1.59
12	α	2.03	td; 12.0, 5.5	2.04	2.04	2.04	2.04	2.03
	β	1.80	dm; 12.0	1.81	1.80	1.81	1.80	1.80
15	α	1.61		1.62	1.63	1.62	1.63	1.62
	β	1.96		1.97	1.94	1.97	1.94	1.96
16	α	1.85		1.85	1.85	1.86	1.85	1.85
	β	2.00		2.00	2.02	2.01	2.02	2.02
17		2.28	dd; 9.1, 7.8	2.28	2.27	2.29	2.27	2.28
18		0.80		0.81	0.81	0.81	0.81	0.81
19		0.83		0.83	0.84	0.83	0.85	0.82
21		1.17		1.17	1.17	1.17	1.17	1.17
22		3.68		3.68	3.68	3.68	3.68	3.68
23	a	1.52		1.52	1.52	1.52	1.52	1.52
	b	1.52		1.52	1.52	1.52	1.52	1.52
24	a	1.48		1.48	1.49	1.48	1.49	1.49
	b	1.73		1.73	1.73	1.73	1.73	1.74
26		1.19		1.19	1.19	1.19	1.19	1.19
27		1.20		1.20	1.20	1.20	1.20	1.20
28Meα		1.31		1.31	1.32	1.31	1.32	1.32
28Meβ		1.47		1.47	1.50	1.47	1.49	1.49
29Meα		1.39		1.39	1.39	1.39	1.39	1.39
29Meβ		1.32		1.32	1.32	1.32	1.32	1.32
1′		3.82		4.07	4.10	4.53	4.55	–
2′				1.25	1.26	5.98	5.99	1.28
3′	*Z*					5.18	5.19	
	E					5.26	5.28	

[a] Because the stereo-structure of the steroid frame is nearly identical within this set of compounds, the *J* coupling constants are given only once.

connected to P-gp inhibitors [26,27].

Considering structure-activity relationships, the several highly active compounds obtained in this work led us to follow our previously applied "best ratio" principle [17]. This means that we aimed to compare the compounds' chemo-sensitizing activities at their strongest, regardless of the compound vs. doxorubicin ratio where this activity was observed.

The length or nature of the alkyl function had no apparent effect on the compounds potency in sensitizing the MDR cells to doxorubicin, all compounds showed similarly high activity in this regard. A slight tendency may be observed for the $\Delta^{14,15}$ compounds (**2**–**4**, **11**–**15**) acting stronger in this regard than their corresponding analogs where the 14-OH group was retained (**5**–**10**), but the differences are so small that it is hard to make a sound judgment on the relevance of this phenomenon.

On the other hand, larger differences were observed between the compounds' activities on the non-MDR L5178 cells. On this cell line, the strongest synergism with doxorubicin was observed for the lactam (**4**) and compound **11**, a methyl substituted $\Delta^{14,15}$ *(Z)*-oxime ether. The oxime formation together with the elimination of the 14-OH group (**2** and **3**) decreased the strength of synergism with doxorubicin as compared to the case of compound **1**. In case of the oxime ethers, the 14,15-anhydro derivatives typically exerted stronger sensitizing activity to doxorubicin than their analogs with intact 14-OH groups, except for compounds **10** vs. **15**. Since oxime ethers substituted with bulky *t*-buthyl groups seem to show a tendency for decreased activity as compared to the corresponding analogs with ethyl groups (**6** vs **10** and **12** vs. **14**), one could hypothesize that the effect of the *t*-butyl group in the oxime ether function may overwrite that of the $\Delta^{14,15}$ moiety in compound **15**.

3. Conclusions

The present study reports the preparation and *in vitro* pharmacological investigation of 14 ecdysteroid diacetonide oximes, oxime ethers and a lactam, with 13 novel derivatives obtained in pure form for the first time. The synthetic procedure was utilized in a way to obtain product mixtures in order to increase chemical diversity, and subsequent use of high-performance separation techniques allowed us to obtain the compounds in high purity. All compounds are reported with a complete NMR signal assignment.

Evaluation of the antiproliferative and cytotoxic activity of the compounds on several cancer cell lines revealed several structure-activity relationships (SAR). A new, *t*-butyl substituted ecdysteroid oxime ether (**10**) was found to exert stronger antiproliferative effect on HeLa and MDA-MB-231 cells than cisplatin. The $\Delta^{14,15}$ *E*-oxime derivative (**2**) exerted a substantially increased cytotoxic and P-gp inhibitory activities in the L5178/L5178$_{MDR}$ cell line pair, as compared to its parental compound.

Clear SAR was observed for the compounds' activity as functional P-gp inhibitors, and many of them were identified as highly potent MDR-selective chemo-sensitizers. In particularly, a novel $\Delta^{14,15}$ δ-lactam ecdysteroid derivative (**4**) was revealed as a most promising new lead compound with low intrinsic cytotoxicity, and strong ability to sensitize MDR and also non-MDR cancer cells towards doxorubicin without interfering with the efflux function of P-gp. Accordingly, it can be expected that a combined treatment of cancer with this compound as a chemo-sensitizer and a chemotherapeutic agent would 1) be effective on the initial, susceptible state of the tumor, and 2) have a strong chance to prevent the acquisition of P-gp mediated resistance through an increased killing effect on the cell population becoming adapted to the chemotherapy.

4. Experimental section

4.1. Chemistry

All applied reagents were purchased from Sigma (Sigma-Aldrich Co., USA). Solvents were obtained from Macron Fine Chemicals (Avantor Performance Materials, USA).

^{1}H (500.1 MHz) and ^{13}C (125.6 MHz) NMR spectra were recorded at room temperature on a Bruker Avance-II spectrometer and on Avance-III spectrometer equipped with a cryo probehead. Regarding the compounds, amounts of approximately 1–10 mg were dissolved in 0.1 ml of methanol-d_4 and transferred to 2.5 mm Bruker MATCH NMR sample tube. Chemical shifts are given on the δ-scale and are referenced to the solvent (MeOH-d_4: $\delta_C = 49.1$ and $\delta_H = 3.31$ ppm). Pulse programs of all experiments (^{1}H, ^{13}C, DEPTQ, DEPT-135, one-dimensional sel-ROE (mixing time: 300 ms), edited gs-HSQC and gs-HMBC) were taken from the Bruker software library. The NMR signals of the product were assigned by comprehensive one- and two-dimensional NMR methods using widely accepted strategies [28,29,30]. Most ^{1}H assignments were accomplished using general knowledge of chemical shift dispersion with the aid of the proton-proton coupling pattern (^{1}H NMR spectra). Mass spectra were obtained on a Waters Acquity iClass UPLC coupled with Thermo Q Exactive Plus with HESI source (Waters Co., USA).

Reaction progress was monitored by thin layer chromatography (TLC) on Kieselgel 60F$_{254}$ silica plates obtained from Merck (Merck, Germany), and examined under UV illumination at 254 nm.

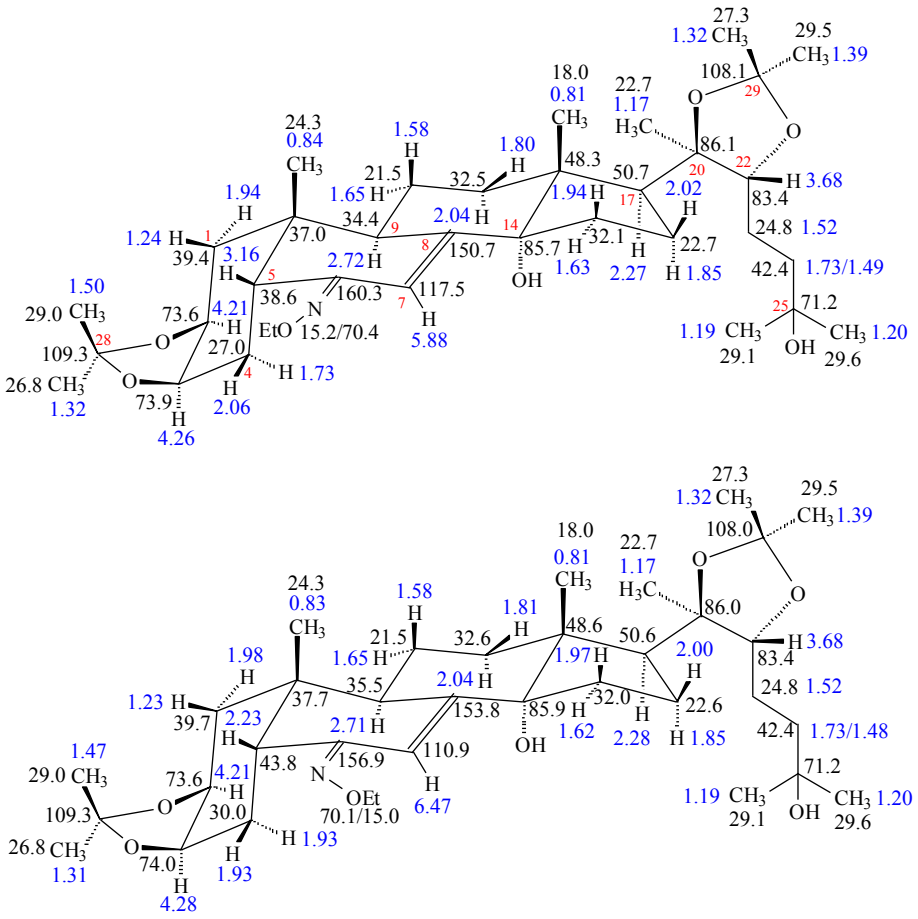

Fig. 2. Characteristic NMR spectra on differentiation and NMR assignments of the isomeric **6** and **7** ecdysteroid 6-oxime ethers are given in the supporting information.

Table 4
Antiproliferative properties of compounds **4**–**15** against four human gynecological cancer cell lines. Inhibition concentration at 50% growth (IC_{50}) values of each compound and the 95% confidence intervals are given for each cell line.

Compound	IC_{50} (μM)			
	HeLa	SiHa	MDA-MB-231	MCF7
4	>30	>30	>30	>30
5	>30	>30	>30	>30
6	>30	>30	>30	22.55 [17.24–29.50]
7	29.12 [24.00–32.94]	>30	25.12 [17.74–35.57]	13.10 [10.89–15.77]
8	15.55 [13.69–17.66]	25.52 [21.95–29.68]	21.36 [18.86–24.19]	13.63 [11.91–15.60]
9	17.55 [14.77–20.84]	>30	26.90 [23.34–31.00]	17.22 [15.21–19.50]
10	8.43 [4.66–9.29]	16.13 [13.02–19.99]	12.36 [11.00–13.89]	11.06 [9.96–12.29]
11	15.43 [12.87–18.50]	>30	25.99 [21.67–29.50]	18.03 [15.86–20.50]
12	29.96 [27.03–33.20]	>30	26.00 [23.44–28.85]	19.59 [17.09–22.46]
13	>30	>30	29.37 [26.11–33.03]	24.16 [20.36–28.68]
14	20.71 [18.63–23.02]	8.14 [5.62–11.79]	15.70 [13.50–18.25]	17.29 [15.33–19.52]
15	26.06 [22.45–30.25]	14.17 [10.60–18.94]	16.93 [14.71–19.49]	19.34 [16.51–22.66]
Cisplatin	14.02 [12.65–15.56]	7.87 [5.83–10.63]	18.65 [16.67–20.85]	6.01 [5.33–6.79]

Compounds were purified by flash chromatography with adequately chosen eluents of *n*-hexane – dichloromethane – methanol on 12 g RediSep NP-silica flash columns (TELEDYNE Isco, USA).

For the RP-HPLC separation of isomeric oxime derivatives a Kinetex XB-C18 250 × 21.4 mm 5 μm preparative (Phenomenex Inc., USA) or an Agilent Eclipse XDB-C8 250 × 9.4 mm 5 μm semi-preparative column (Agilent Technologies Inc., USA) was applied with the use of isocratic grade eluents of acetonitrile and water. Purity of obtained compounds was determined by RP-HPLC with the use of a Kinetex XB-C18 250 × 4.6 mm 5 μm analytical column (Phenomenex Inc., USA). For data collection a Jasco HPLC instrument equipped with an MD-2010 Plus PDA detector (Jasco Analytical Instruments, Japan) was applied in a detection range of 210–400 nm.

Ecdysteroid substrate **1** was synthesized from 20-hydroxyecdysone (20E) obtained from Shaanxi KingsSci Biotechnology Co., Ltd. (Shanghai, People's Republic of China) at 90% purity and recrystallized (EtOAc:MeOH – 2:1) to a RP-HPLC purity of 97.8%. During the synthetic procedure, 20E (10 g) was dissolved in

Table 5
Cytotoxicity of compounds **1**–**15** on L5178 and L5178$_{MDR}$ cells, and functional inhibition of the ABCB1 transporter. Dox = doxorubicin; for the ABCB1 inhibition, positive control: 100 nM of tariquidar (112.4% inhibition), negative control: 2% DMSO (−0.07% inhibition).

Compound	Change in the	14-OH or	IC_{50} (μM) [95% confidence intervals][b]		ABCB1 inhibition (%)	
	B-ring of 1 [a]	$\Delta^{14,15}$	L5178	L5178$_{MDR}$	2 μM	20 μM
1	–	14-OH	110.3 [77.50–157.1]	97.69 [71.07–134.3]	2.54	20.91
2	(*E*)-oxime	$\Delta^{14,15}$	20.91 [17.68–24.74]	24.63 [19.82–30.63]	10.57	82.95
3	(*Z*)-oxime	$\Delta^{14,15}$	34.22 [28.21–41.51]	28.35 [21.97–36.58]	7.15	81.09
4	δ-lactam	$\Delta^{14,15}$	63.42 [47.51–84.65]	72.35 [64.39–81.29]	1.16	4.27
5	(*E*); R = Me	14-OH	40.92 [35.66–46.97]	55.05 [41.53–72.98]	2.25	25.05
6	(*E*); R = Et	14-OH	35.02 [25.35–48.38]	47.00 [31.14–70.93]	17.54	78.79
7	(*Z*); R = Et	14-OH	37.26 [25.65–54.11]	42.16 [41.24–43.10]	18.96	75.03
8	(*E*); R = Allyl	14-OH	31.48 [23.71–41.80]	51.91 [42.69–63.13]	20.98	89.39
9	(*Z*); R = Allyl	14-OH	36.66 [28.32–47.44]	49.29 [43.07–56.40]	24.17	81.80
10	(*E*); R = *t*-But	14-OH	28.06 [21.30–36.98]	29.12 [25.12–33.76]	38.75	112.4
11	(*Z*); R = Me	$\Delta^{14,15}$	45.95 [36.97–57.11]	53.14 [43.54–64.86]	33.36	106.2
12	(*Z*); R = Et	$\Delta^{14,15}$	53.20 [38.64–73.26]	58.94 [45.86–75.74]	56.41	107.7
13	(*Z*); R = Allyl	$\Delta^{14,15}$	55.28 [46.21–66.13]	52.72 [39.97–65.53]	61.13	102.7
14	(*Z*); R = *t*-But	$\Delta^{14,15}$	63.23 [58.57–68.26]	51.22 [39.13–67.04]	58.99	78.76
15	(*E*); R = *t*-But	$\Delta^{14,15}$	63.84 [45.70–89.19]	65.44 [55.66–76.94]	67.46	93.95
Dox	–	–	0.080 [0.053–0.12]	4.49 [3.43–5.89]	–	–

[a] R groups refer to the alkyl substituents of the oxime ethers as in Scheme 1.
[b] IC_{50} values were calculated by the CompuSyn software as the median cytotoxic activities (Dm) from the control lanes on the checkerboard plates of the combination studies, n = 2.

Table 6
Chemo-sensitizing activity of compounds **1**–**15** on the L5178 and L5178$_{MDR}$ cell lines towards doxorubicin at 50, 75 and 90% of growth inhibition (ED_{50}, ED_{75} and ED_{90}, respectively). CI: combination index; CI_{avg}: weighted average CI value; $CI_{avg} = (CI_{50} + 2CI_{75} + 3CI_{90})/6$. CI < 1, CI = 1, and CI > 1 represent synergism, additivity, and antagonism, respectively. Dm, m, and r represent antilog of the x-intercept, slope, and linear correlation coefficient of the median-effect plot, respectively.

Compound	Cell line	Drug ratio	CI at			Dm	m	r	CI_{avg}
			ED_{50}	ED_{75}	ED_{90}				
1 [21]	L5178$_{MDR}$	20.4: 1	0.27	0.14	0.07	11.678	3.246	0.964	0.13
	L5178	163: 1	0.67	0.55	0.46	11.236	2.103	0.942	0.53
2	L5178$_{MDR}$	15: 1	0.26	0.16	0.12	4.454	6.638	1.000	0.16
	L5178	150: 1	0.80	0.79	0.78	10.748	2.572	0.997	0.78
3	L5178$_{MDR}$	30: 1	0.32	0.25	0.20	7.595	3.981	0.994	0.24
	L5178	150: 1	0.98	0.76	0.61	16.049	3.239	0.986	0.72
4	L5178$_{MDR}$	15: 1	0.20	0.12	0.09	6.419	4.953	0.970	0.12
	L5178	150: 1	0.40	0.42	0.46	10.477	2.033	0.966	0.44
5	L5178$_{MDR}$	15: 1	0.17	0.16	0.16	6.605	3.721	0.978	0.16
	L5178	150: 1	1.06	0.79	0.62	14.306	2.947	0.971	0.75
6	L5178$_{MDR}$	7.5: 1	0.18	0.14	0.12	5.001	5.858	1.000	0.14
	L5178	37.5: 1	0.55	0.58	0.60	8.598	2.495	0.972	0.59
7	L5178$_{MDR}$	3.75: 1	0.27	0.16	0.13	3.030	3.329	0.993	0.16
	L5178	37.5: 1	0.63	0.52	0.45	8.078	3.858	0.952	0.50
8	L5178$_{MDR}$	15: 1	0.17	0.13	0.13	4.939	3.193	0.955	0.14
	L5178	150:1	1.03	0.81	0.69	8.970	2.178	0.991	0.79
9	L5178$_{MDR}$	15: 1	0.17	0.16	0.17	7.338	3.771	0.947	0.17
	L5178	75: 1	0.70	0.83	1.03	8.202	1.722	0.956	0.91
10	L5178$_{MDR}$	7.5: 1	0.30	0.20	0.17	3.928	4.610	1.000	0.20
	L5178	37.5: 1	0.58	0.63	0.70	7.606	2.502	0.966	0.66
11	L5178$_{MDR}$	7.5: 1	0.17	0.16	0.15	5.224	3.722	0.971	0.16
	L5178	37.5: 1	0.77	0.47	0.31	8.165	3.044	0.982	0.44
12	L5178$_{MDR}$	7.5: 1	0.21	0.14	0.11	6.133	4.890	0.992	0.14
	L5178	75: 1	0.49	0.50	0.52	7.864	2.094	0.961	0.51
13	L5178$_{MDR}$	3.75: 1	0.25	0.15	0.11	5.614	5.805	1.000	0.15
	L5178	37.5: 1	0.46	0.47	0.47	8.295	2.882	0.981	0.47
14	L5178$_{MDR}$	7.5: 1	0.34	0.26	0.23	8.365	3.378	0.939	0.26
	L5178	37.5: 1	0.53	0.59	0.66	9.652	2.400	0.961	0.62
15	L5178$_{MDR}$	7.5: 1	0.27	0.24	0.23	8.739	3.813	0.960	0.24
	L5178	37.5: 1	1.16	0.85	0.64	7.199	3.273	0.977	0.80

acetone in the concentration of g/100 cm^3 and phosphomolybdic acid was added (10 g) under stirring. After 5 min of stirring at RT, the reaction mixture was neutralized with 10% aqueous $NaHCO_3$. Acetone was evaporated under reduced pressure and the mixture was extracted with EtOAc (3 × 50 ml) followed by drying with Na_2SO_4. After filtration, the solvent was evaporated under reduced pressure and the crude mixture was purified by flash chromatography with isocratic grade eluents of dichloromethane:methanol – 99:1. (Yield: 51%).

Synthesis of ecdysteroid 6-oximes (2–3). 1 g of compound **1** (1,78 mmol) was dissolved in pyridine (10 ml) and 1 g of hydroxylamine hydrochloride (14.39 mmol) was added to the solution under stirring. After 3 days of stirring at 70 °C the reaction was complete and the solvent was evaporated under reduced pressure. Following water addition (50 ml), the mixture was extracted with EtOAc (3 × 50 ml) and the combined organic phase was dried with

Na_2SO_4. A filtration was made to remove drying agent and the solvent was evaporated under reduced pressure. Purification of the crude mixture was carried out by preparative RP-HPLC to obtain (*E*/*Z*)-isomeric oximes **2**–**3**, respectively.

Synthesis of ecdysteroid lactam derivative (4). 0.138 g of oxime **2** (0,25 mmol) was dissolved in anhydrous acetone (10 ml), then 0.027 g of Na_2CO_3 (0.25 mmol) and 0.096 g of *p*-toluenesulfonyl chloride (0,5 mmol) was added to the solution under stirring. After 6 h of stirring at RT, the reaction was stopped and the mixture was cooled to 0 °C. Under stirring, water (10 ml) was added and the mixture was extracted into ethyl acetate (3 × 50 ml). After evaporation under reduced pressure, the mixture was purified with semi-preparative RP-HPLC to obtain lactam derivative **4**.

General Procedure for the synthesis of ecdysteroid 6-oxime ethers (5–15). 200 mg of **1** (0,35 mmol) was dissolved in pyridine (8 ml), and, depending on the oxime ether to be obtained, 200 mg of the appropriate alkoxyamine-hydrochloride was added to the solution under stirring. After stirring at 70 °C for 24 h, the mixture was cooled down to 0 °C, neutralized with KOH dissolved in anhydrous methanol, and evaporated under reduced pressure. Water (50 ml) was then added, and the mixture was extracted with EtOAc (3 × 50 ml). The combined organic layers were dried with Na_2SO_4, and, after filtration, the solvent was evaporated under reduced pressure. Purification of the crude material was carried out by flash chromatography on silica gel to obtain compounds **5**–**15**, respectively. In cases of oxime pairs **2**–**3, 6**–**7, 8**–**9, 14**–**15** preparative RP-HPLC was applied to separate the isomeric oxime and oxime ether derivatives.

Compound 4: White solid; yield: 8% (11.04 mg); RP-HPLC purity: 98.1%; for ^1H and ^{13}C NMR data, see Tables 2 and 3, respectively; HR-HESI-MS: $C_{33}H_{52}O_6N$, calcd. 558.3789, found: 558.3737.

Compound 5: White solid; yield: 28.3% (59.53 mg); RP-HPLC purity: 99.8%; for ^1H and ^{13}C NMR data, see Tables 1 and 3, respectively; HR-HESI-MS: $C_{34}H_{56}O_7N$, calcd. 590.4051, found: 590.4045.

Compound 6: White solid; yield: 15.2% (32.75 mg); RP-HPLC purity: 99.6%; for ^1H and ^{13}C NMR data, see Tables 1 and 3, respectively; HR-HESI-MS: $C_{35}H_{58}O_7N$, calcd. 604.4208, found: 604.4198.

Compound 7: White solid; yield: 2.8% (6.06 mg); RP-HPLC purity: 98.7%; for ^1H and ^{13}C NMR data, see Tables 1 and 3, respectively; HR-HESI-MS: $C_{35}H_{58}O_7N$, calcd. 604.4208, found: 604.4199.

Compound 8: White solid; yield: 15.5% (34.05 mg); RP-HPLC purity: 98.3%; for ^1H and ^{13}C NMR data, see Tables 1 and 3, respectively; HR-HESI-MS: $C_{36}H_{58}O_7N$, calcd. 616.4208, found: 616.4201.

Compound 9: White solid; yield: 1.6% (3.5 mg); RP-HPLC purity: 99.6%; for ^1H and ^{13}C NMR data, see Tables 1 and 3, respectively; HR-HESI-MS: $C_{36}H_{58}O_7N$, calcd. 616.4208, found: 616.4200.

Compound 10: White solid; yield: 38.9% (87.67 mg); RP-HPLC purity: 98.5%; for ^1H and ^{13}C NMR data, see Tables 1 and 3, respectively; HR-HESI-MS: $C_{37}H_{62}O_7N$, calcd. 632.4521, found: 632.4515.

Compound 11: White solid; yield: 43.3% (88.32 mg); RP-HPLC purity: 97.7%; for ^1H and ^{13}C NMR data, see Tables 2 and 3, respectively; HR-HESI-MS: $C_{34}H_{54}O_6N$, calcd. 572.3946, found: 572.3937.

Compound 12: White solid; yield: 33.3% (69.59 mg); RP-HPLC purity: 97.5%; for ^1H and ^{13}C NMR data, see Tables 2 and 3, respectively; HR-HESI-MS: $C_{35}H_{56}O_6N$, calcd. 586.4102, found: 586.4099.

Compound 13: White solid; yield: 2% (4.25 mg); RP-HPLC purity: 98.3%; for ^1H and ^{13}C NMR data, see Tables 2 and 3, respectively; HR-HESI-MS: $C_{36}H_{56}O_6N$, calcd. 598.4102, found: 598.4094.

Compound 14: White solid; yield: 8.3% (18.17 mg); RP-HPLC purity: 98.7%; for ^1H and ^{13}C NMR data, see Tables 2 and 3, respectively; HR-HESI-MS: $C_{37}H_{60}O_6N$, calcd. 614.4415, found: 614.4411.

Compound 15: White solid; yield: 2.5% (5.48 mg); RP-HPLC purity: 95.8%; for ^1H and ^{13}C NMR data, see Tables 2 and 3, respectively; HR-HESI-MS: $C_{37}H_{60}O_6N$, calcd. 614.4415, found: 614.4407.

4.2. Biology

Cell cultures. The human gynecological cancer cell lines MDA-MB-231 and MCF7 (breast cancers), and HeLa (cervical adenocarcinoma) were purchased from ECACC (European Collection of Cell Cultures, Salisbury, UK), while SiHa (cervical carcinoma) was purchased from ATCC (American Tissue Culture Collection, Manassas, Virginia, USA). The cells were grown in Minimum Essential Medium (MEM) supplemented with 10% fetal calf serum (FCS), 1% non-essential aminoacids, and 1% penicillin-streptomycin. All media and supplements for these experiments were obtained from Lonza Group Ltd. (Basel, Switzerland). The cells were maintained at 37 °C in humidified atmosphere containing 5% CO_2. Two mouse lymphoma cell lines were also used: a drug susceptible cell line, L5178 mouse T-cell lymphoma (ECACC catalog number 87111908, U.S. FDA, Silver Spring,MD, U.S.), and its multidrug resistant counterpart ($L5178_{MDR}$) obtained by transfection with pHa MDR1/A retrovirus [31]. Cells were cultured in McCoy's 5A media supplemented with nystatin, L-glutamine, penicillin, streptomycin, and inactivated horse serum, at 37 ◦C and 5% CO_2. The MDR cell line was selected by culturing the infected cells with 60 g/L colchicine (Sigma). Media, fetal bovine serum, horse serum, and antibiotics were purchased from Sigma.

Antiproliferative assay on human gynecological cancer cell lines. The growth-inhibitory activities of the prepared ecdysteroid analogs were determined by the MTT (3-(4,5-dimethylthiazol-2-yl)-2,5-diphenyltetrazolium bromide) method on four human adherent cancer cell lines of gynecological origin [32]. Briefly, cells were seeded into 96 well plates (5000 cells/well) and incubated with increasing concentrations of the tested compounds (0.1–30.0 μM) under cell-culturing conditions. After incubation for 72 h, 5 mg/ml MTT solution was added and the samples were incubated for another 4 h. The precipitated formazan crystals than were dissolved in dimethyl sulfoxide and the absorbance was measured at 545 nm with a microplate reader. Cisplatin, a clinically used anticancer agent was used as a positive control. In order to calculate fifty percent inhibitory concentrations (IC_{50}), sigmoidal dose–response curves were fitted to the measured points by using the non-linear regression model log (inhibitor) vs. normalized response and variable slope with a least squares (ordinary) fit of GraphPad Prism 5.01 software (GraphPad Software Inc., San Diego, CA, USA).

Cytotoxicity assay on murine lymphoma cell lines. Cytotoxic activities on the L5178 and $L5178_{MDR}$ cell lines were performed as described before [18]. Briefly, 5×10^4 cells/well were incubated with serial dilutions of each compound (n = 3) in McCoy's 5 A medium (Sigma-Aldrich) for 48 h at 37 °C, 5% CO_2. Then, 3-(4,5-dimethylthiazol-2-yl)-2,5-diphenyltetrazolium bromide (MTT, Sigma) was added to each well at a final concentration of 0.5 mg/mL per well and after 4 h of incubation, 100 μL of sodium dodecyl sulfate (SDS) 10% (Sigma-Aldrich) in 0.01 M HCl was added to each well. Plates were further incubated overnight, the optical densities were read at 540 and 630 nm using an ELISA reader (Multiskan EX, Thermo Labsystem, Milford, MA, USA), and IC_{50} values were calculated as described above.

Rhodamine 123 accumulation assay. ABCB1 inhibitory activities of the compounds were studied through their effect on the

accumulation of rhodamine 123, a fluorescent dye that is an ABCB1 substrate. Flow cytometry was used as described before [15]. Briefly, 2×10^6 cells/mL were treated with 2 or 20 μM of each compound. After 10 min incubation, rhodamine 123 (Sigma-Aldrich) was added to a final concentration of 5.2 μM and the samples were incubated at 37 °C in a water bath for 20 min. Samples were centrifuged (Heraeus Labofuge 400, Thermo Fisher Scientific, Waltham, MA, USA) (2000 rpm, 2 min) and washed twice with phosphate buffer saline (PBS, Sigma). The final samples were re-suspended in 0.5 mL PBS and its fluorescence measured with a Partec CyFlow flow cytometer (Partec, Münster, Germany). 100 nM of tariquidar was used as positive control, which was kindly provided by Dr. Milica Pesic from the Institute for Biological Research Sinisa Stankovic, Belgrade, Serbia.

Cytotoxicity assay in combination with doxorubicin. The checkerboard microplate method was utilized to test the combined activity of doxorubicin (Teva, Budapest, Hungary) and the ecdysteroid derivatives on the L5178 and $L5178_{MDR}$ cell lines, as described before [17]. Briefly, 5×10^4 cells/well were incubated with doxorubicin and the compound to be tested in McCoy's 5 A medium (Sigma-Aldrich) for 48 h at 37 °C, 5% CO_2. Then, 3-(4,5-dimethylthiazol-2-yl)-2,5-diphenyltetrazolium bromide (MTT, Sigma) was added to each well at a final concentration of 0.5 mg/mL per well, and after 4 h of incubation, 100 μL of sodium dodecyl sulfate (SDS) 10% (Sigma-Aldrich) in 0.01 M HCl was added to each well. The plates were further incubated overnight, and the optical densities were read at 540 and 630 nm using an ELISA reader (Multiskan EX, Thermo Labsystem, Milford, MA, USA). The interaction was evaluated using the CompuSyn software (CompuSyn Inc., Paramus, NJ, USA) at each constant ratio of compound *vs.* doxorubicin (M/M), and combination index (CI) values were obtained for 50%, 75%, and 90% of growth inhibition. Single-drug data obtained from the duplicate control lanes of each plate were utilized to determine cytotoxic activities for each compound.

Acknowledgements

This work was performed in collaboration within the framework of COST Action CM1407 (Challenging organic syntheses inspired by nature—from natural products chemistry to drug discovery), and it was supported by the National Research, Development and Innovation Office, Hungary (NKFIH; K119770 and K109293). A.H. acknowledges the János Bolyai fellowship of the Hungarian Academy of Sciences and the Kálmán Szász Prize.

Appendix A. Supplementary data

Supplementary data related to this article can be found at https://doi.org/10.1016/j.ejmech.2017.12.032.

References

[1] I.H. Lone, K.Z. Khan, B.I. Fozdar, F. Hussain, Steroids 78 (2013) 945–950.
[2] D.P. Jindal, R. Chattopadhaya, S. Guleira, R. Gupta, Eur. J. Med. Chem. 38 (2003) 1025–1034.
[3] D.B. Garcia, R.G. Brown, J.N. Delgado, J. Pharmaceut. Sci. 69 (1980) 995–999.
[4] N.M. Krstić, M.S. Bjelaković, Z. Zizak, M.D. Pavlović, Z.D. Juranić, V.D. Pavlović, Steroids 72 (2007) 406–414.
[5] J. Cui, L. Fan, L. Huang, H. Liu, A. Zhou, Steroids 74 (2009) 62–72.
[6] J. Cui, L. Fan, Y. Huang, Y. Xin, A. Zhou, Steroids 74 (2009) 989–995.
[7] Á. Berényi, R. Minorics, Z. Iványi, I. Ocsovszki, E. Ducza, H. Thole, J. Messinger, J. Wölfling, G. Mótyán, E. Mernyák, É. Frank, G. Schneider, Steroids 78 (2013) 69–78.
[8] R.M. Pascual, S.M. Reyes, J.L. Vega-Baez, S.M. Smith, Steroids 122 (2017) 24–33.
[9] H.L. Qin, J. Leng, C.P. Zhang, I. Jantan, M.W. Amjab, M. Sher, M.N. Hassan, M.A. Hussain, S.N.A. Bukhari, J. Med. Chem. 59 (2016) 3549–3561.
[10] G.F. Zha, H.L. Qin, B.G.M. Youssif, M.W. Amjad, M.A.G. Raja, A.H. Abdelazeem, S.N.A. Bukharim, Eur. J. Med. Chem. 135 (2017) 34–48.
[11] L. Dinan, Phytochemistry 57 (2001) 325–339.
[12] L. Dinan, Arch. Insect Biochem. Physiol. 72 (2009) 126–141.
[13] L. Dinan, R. Lafont, J. Endocrinol. 191 (2006) 1–8.
[14] M. Báthori, N. Tóth, A. Hunyadi, Á. Márki, E. Zádor, Curr. Med. Chem. 15 (2008) 75–79.
[15] M.K. Parr, F. Bortré, A. Naß, J. Hengevoss, P. Diel, G. Wolber, Biol. Sport 32 (2015) 169–173.
[16] R. Lafont, L. Dinan, J. Insect Sci. 3 (7) (2003) 1–30.
[17] A. Martins, N. Tóth, A. Ványolós, Z. Béni, I. Zupkó, J. Molnár, M. Báthori, A. Hunyadi, J. Med. Chem. 55 (2012) 5034–5043.
[18] A. Martins, P. Sipos, K. Dér, J. Csábi, W. Miklós, W. Berger, A. Zalatnai, L. Amaral, J. Molnár, P. Szabó-Révész, A. Hunyadi, BioMed Res. Int. (2015), 895360.
[19] A. Martins, J. Csábi, A. Balázs, D. Kitka, L. Amaral, J. Molnár, A. Simon, G. Tóth, A. Hunyadi, Molecules 55 (2013) 15255–15275.
[20] A. Hunyadi, J. Csábi, A. Martins, J. Molnár, A. Balázs, G. Tóth, Molecules 22 (2017) 199.
[21] J. Csábi, A. Martins, I. Sinka, A. Csorba, J. Molnár, I. Zupkó, G. Tóth, L.M.V. Tillekeratne, A. Hunyadi, Med. Chem. Commun. 7 (2016) 2282–2289.
[22] I.V. Galyautdinov, N.A. Ves'kina, S.R. Afon'kina, L.M. Khalilov, V.N. Odinokov, Russ. J. Org. Chem. 42 (2006) 1352–1357.
[23] R.V. Shafikov, Ya. R. Urazaeva, S.R. Afon'kina, R.G. Savchenko, L.M. Khalilov, V.N. Odinokov, Russ. J. Org. Chem. 45 (2009) 1456–1463.
[24] A. Balázs, A. Hunyadi, J. Csábi, N. Jedlinszki, A. Martins, A. Simon, G. Tóth, Magn. Reson. Chem. 51 (2013) 830–836.
[25] T.C. Chou, Pharmacol. Rev. 58 (2006) 621–681.
[26] S. Marchetti, R. Mazzanti, J.H. Beijnen, J.H.M. Schellens, Oncologist 12 (2007) 927–941.
[27] R. Callaghan, F. Luk, M. Bebawy, Drug Metabol. Dispos. 42 (2014) 623–631.
[28] E. Pretsch, T. Clerc, J. Seibl, W. Simon, Structuraufklaerung Organischer Verbindungen, Springer-Verlag, Berlin, Germany, 1976. C10, C175, C195.
[29] H. Duddeck, W. Dietrich, G. Tóth, Structure Elucidation by Modern NMR, Springer-Steinkopff, Darmstadt, Germany, 1998.
[30] E. Pretsch, G. Tóth, M.E. Munk, M. Badertscher, Computer-aided Structure Elucidation. Spectra Interpretation and Structure Generation, Wiley-VCH, Weinheim, Germany, 2002.
[31] I. Pastan, M.M. Gottesman, K. Ueda, E. Lovelace, A.V. Rutherford, M.C. Willingham, Proc. Nat. Acad. Sci. U. S. Am. 85 (1988) 4486–4490.
[32] T. Mosmann, J. Immunol. Meth. 65 (1983) 55–63.

II.

[4]Ediburgh Cancer Research UK Centre MBC Institute of Genetics and Molecular Medicine, University of Edinburgh, Crewe Road South, Edinburgh EH4, 2XR, UK
[5]Avenida de la Ilustración 114, Parque Tecnológico de Ciencias de la Salud, Centro Pfizer-Universidad de Granada-Junta de Andalucía de Genómica e Investigación Oncológica (GENYO), 18016 Granada, Spain

Correspondence
Juan José Díaz-Mochón, Departamento de Química Farmacéutica y Orgánica, Facultad de Farmacia, Campus de Cartuja, Universidad de Granada, Granada, Spain.
Email: juandiaz@ugr.es

María José Pineda de las Infantas Villatoro, Departamento de Química Farmacéutica y Orgánica, Facultad de Farmacia, Campus de Cartuja, Universidad de Granada, Granada, Spain.
Email: mjpineda@ugr.es

REFERENCES

[1] Z. O'Brien, M. Moghaddam, *Expert Opin. Drug Metab. Toxicol.* **2013**, *9*, 1597.
[2] L. Meijer, E. Raymond, *Acc. Chem. Res.* **2003**, *36*, 417.
[3] P. G. Baraldi, A. Unciti-Broceta, M. J. Pineda de las Infantas, J. J. Díaz-Mochón, A. Espinosa, R. Romagnoli, *Tetrahedron* **2002**, *58*, 7607.
[4] M. J. Pineda de las Infantas, J. D. Unciti-Broceta, R. Contreras, J. A. García, M. A. Gallo, A. Unciti-Broceta, J. J. Díaz-Mochón, *Sci. Rep.* **2015**, *5*, 9139.
[5] M. J. Pineda de las Infantas, S. Torres-Rusillo, J. D. Unciti-Broceta, P. Fernández-Rubio, M. A. Luque-González, M. A. Gallo, A. Unciti-Broceta, I. J. Molina, J. J. Díaz-Mochón, *Org. Biomol. Chem.* **2015**, *13*, 5234.
[6] L. Harmse, R. van Zyl, N. Gray, P. Schultz, S. Leclerc, L. Meijer, C. Doerig, I. Havlik, *Biochem. Pharmacol.* **2001**, *62*, 341.
[7] D. M. Doddrell, D. T. Pegg, M. R. Bendall, *J. Magn. Reson.* **1969**, 1982.
[8] R. Boyer, R. Johnson, K. Krishnamurthy, *J. Magn .Reson.* **2003**, *2*, 165.

Received: 26 February 2018 | Revised: 23 April 2018 | Accepted: 5 May 2018

DOI: 10.1002/mrc.4750

Stereochemistry and complete ^{1}H and ^{13}C NMR signal assignment of C-20-oxime derivatives of posterone 2,3-acetonide in solution state

1 | INTRODUCTION

Less polar derivatives of ecdysteroids, and particularly their acetonides and other dioxolane analogs, were previously shown by our group to exert a strong chemo-sensitizing activity on cancer cells to common chemo-therapeutics, including doxorubicin, vincristine, and paclitaxel.[1,2] While this sensitizing activity could also be observed on drug-susceptible cancer cells, a high selectivity was found towards multidrug resistant (MDR) cancer cell lines transfected to overexpress the ABCB1 multidrug transporter.[2,3] Interestingly, the chemo-sensitizing activity was independent of a functional efflux inhibition: even though some of the tested compounds showed a mild to moderate ABCB1 inhibitory activity; structure–activity relationships for efflux inhibition were significantly different to those describing chemo-sensitizing activity.[1] In particular, several poststerone derivatives, containing a substituted dioxolane (e.g., acetonide) moiety connected to their A-ring, were found to be free from the efflux pump inhibitory activity, while acting as strong chemo-sensitizers in combination with doxorubicin.[3] In addition to this, ecdysteroid 6-oximes and oxime ethers demonstrated markedly increased ABCB1 inhibitory activity, while acting as similarly potent chemo-sensitizers as their corresponding 6-oxo analogs.[4]

Self-assembling nanoparticles provide a promising novel approach against cancer.[5] These can be prepared by functionalizing a potential antitumor agent with a long lipophilic side-chain through functional group(s) hydrolysable in a biological environment (e.g., ester), which will make them working as prodrugs once released. The role of the side-chain in such a conjugate is to induce the self-assembly to nanoparticles in aqueous

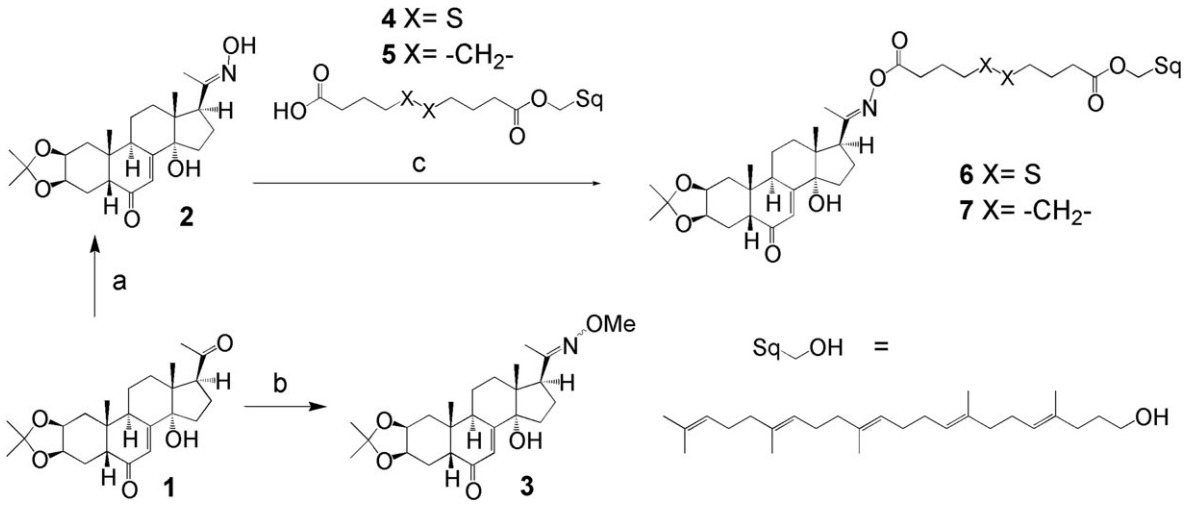

FIGURE 1 Chemical structures and preparation of ecdysteroid derivatives **2–3** and **6–7**. Reagents and conditions: (a; 1) $NH_2OH{\cdot}HCl$ (1.5 eq.), Py, RT, 25 min (2) KOH in anhydrous EtOH; (b; 1) $NH_2OMe{\cdot}HCl$ (3 eq.), Py, 70 °C, 5.5 hr (2) KOH/EtOH; (c) **4** or **5** (1.5 eq.), DCM, DMAP (2 eq.), EDC·HCl (2.5 eq.), Ar

environment due to secondary interactions.[6–8] In our previous work, we applied two different types of linkers: one only with CH_2 units and another with S—S disulfide bridge in the middle of this unit. This last one was found rather advantageous to release the drug molecules from a prodrug form mainly in the inner environment of cancer cells.[9] As part of a research program aiming to prepare and study such compounds from certain ecdysteroids, we turned our attention towards the 20-oxime of poststerone 2,3-acetonide, a potentially strong antitumor ecdysteroid derivative, and its conjugates with long lipophilic side-chains. Due to the abundancy of overlapping signals in the aliphatic region, a complete NMR signal assignment of such compounds bears a significant challenge. Accordingly, to the best of our knowledge, no previous studies are available on the full NMR characterization of such self-assembling drug conjugates.

Most recently, Savchenko and coworkers reported the regioselective preparation of this ecdysteroid oxime, along with its X-ray single crystal investigation and NMR data limited to the nonoverlapping ^1H signals.[10] In the present study, our aim was to perform an in-depth, high-resolution NMR investigation on this compound, two of its oxime ether derivatives, and two of its conjugates with long lipophilic side-chains, potentially able to self-assemble. Publication of the antitumor activity and nanoparticle forming properties of the latter two compounds is just accepted elsewhere.[11]

2 | EXPERIMENTAL

2.1 | Substances

Chemical structures and synthesis of compounds **2–7** are shown in Figure 1.

2.1.1 | Synthesis and purification of compound 2

Poststerone 2,3-acetonide (**1**) was prepared according to previously published procedures.[3] Oximation of derivative **1** was performed at RT, by dissolving 42.2 mg (0.104 mmol) of the substrate in a round-bottom flask in freshly distilled pyridine. A 10.9 mg (0.157 mmol; 1.5 equivalents) of hydroxylamine hydrochloride was added, and the solution was left stirring for 25 min. Following this, the reaction mixture was cooled to 0 °C, and potassium hydroxide (8.8 mg; 0,157 mmol), dissolved in 1 ml of anhydrous ethanol, was added under stirring. The obtained mixture was evaporated under reduced pressure using a rotary evaporator, and water (30 ml) was added to the crude solid followed by extraction with ethyl acetate (4 × 30 ml). The combined organic fractions were dried over Na_2SO_4 and filtered, and the solution was evaporated under reduced pressure to obtain 40.17 mg of crude mixture. RP-HPLC purification was performed using an Agilent Eclipse XDB-C8 250 × 9.4 mm 5 μm semipreparative column (Agilent Technologies Inc., USA) by using isocratic elution with 35% acetonitrile and 65% water at a flow rate of 3 ml/min to obtain poststerone 2,3-acetonide 20-oxime (**2**) in a yield of 69.7% (30.69 mg) and a RP-HPLC purity of 99.1%.

2.1.2 | Synthesis and purification of compound mixture 3

Three hundred milligrams (0.745 mmol) of ecdysteroid substrate **1** was dissolved in 6 ml of freshly distilled pyridine in a round-bottom flask. A 186.7 mg (2.235 mmol, three equivalents) of methoxyamine hydrochloride was

added, and the mixture was left stirring at 70 °C for 5.5 hr. Following this, the reaction mixture was cooled to 0 °C, and neutralization was performed with potassium hydroxide (125.4 mg; 2.235 mmol) dissolved in 5 ml of anhydrous ethanol. The obtained mixture was evaporated using a rotary evaporator, and 40 ml of water was added, followed by extraction with ethyl acetate (4 × 40 ml). The combined organic fractions were dried over Na_2SO_4 and filtered, and the solution was evaporated under reduced pressure to obtain a crude mixture of isomeric *O*-methylated 20-oximes and 6,20-dioximes. Flash chromatographic purification was performed using a 30 g RP-C18 column with gradient elution of acetonitrile increasing from 40% to 55% in 45 min (flow rate: 35 ml/min; UV detection: 254 nm). The fractions collected between 17 and 30 min were combined and evaporated under reduced pressure to obtain a mixture of (*E/Z*)-isomeric 20-*O*-methyl oxime ethers (**3**) in a combined yield of 12% (38.58 mg, combined RP-HPLC purity: 98.3%).

2.1.3 | Synthesis and purification of ecdysteroid conjugates 6 and 7

Functionalization of self-assembly inducer squalene and the preparation of its coupled derivatives **4** and **5** attached to a linker moiety were prepared following previously published procedures.[12] A 34.2 mg (0.0819 mmol) of ecdysteroid substrate **2** was dissolved in 6 ml of anhydrous dichloromethane in a two-neck round-bottom flask. The 1.5 equivalents of the disulfide bridge containing compound **4** (74.6 mg, 0.1229 mmol) or Substrate **5** (70.2 mg, 0.1229 mmol) were added dropwise under stirring. Following this, 13.1 mg (0.1638 mmol, two equivalents) of dimethylaminopyridine and 39.3 mg (0.205 mmol, 2.5 equivalents) of (3-dimethylaminopropyl)-*N*′-ethylcarbodiimide hydrochloride were added, and the mixture was left stirring at room temperature under argon atmosphere for 2 hr. After completion, the mixture was neutralized with 10% aqueous $NaHCO_3$, brine (30 ml) was added, and extraction was performed with dichloromethane (4 × 30 ml). Following this, the combined organic fractions were dried over Na_sSO_4 and filtered, and the solution was evaporated under reduced pressure. Flash chromatographic purification was carried out on 4-g silica columns using isocratic grade eluents of 65% *n*-hexane and 35% ethyl acetate in case of product **6** and 75% *n*-hexane and 25% ethyl acetate in case of product **7** to obtain the compounds as colorless oils.

2.2 | Further experimental details

Solvents and reagents were purchased from Sigma (Sigma-Aldrich Co., USA). All HPLC analysis, including purification, were carried out on a Jasco HPLC instrument (Jasco Analytical Instruments, Japan) coupled with an MD-2010 Plus PDA detector, applied in a detection range of 210–400 nm. Flash chromatographic purification was performed on a Combiflash Rf+ instrument (TELEDYNE Isco, USA) equipped with diode array detection - evaporative light scattering detection (DAD-ELSD) using commercially available prefilled RediSep columns (TELEDYNE Isco, USA). High-resolution mass spectroscopy (HR-MS) spectra were obtained on a Waters Acquity iClass UPLC coupled with Thermo Q Exactive Plus with HESI source (Waters Co., USA), used in positive mode.

2.2.1 | 20-Hydroxyecdysone 2,3-acetonide 20-O-methyl-oxime ether isomers 3

White solid; HR-HESI-MS: $C_{25}H_{38}O_5N$, $[M + H]^+$ Calcd. 432.2750, found: 432.2749.

2.2.2 | Squalenoylated ecdysteroid conjugate 6

Colorless oil; HR-HESI-MS: $C_{59}H_{91}O_8NS_2Na$, $[M + Na]^+$ Calcd. 1028.60838, found: 1028.60949.

2.2.3 | Squalenoylated ecdysteroid conjugate 7

Colorless oil; HR-HESI-MS: $C_{61}H_{96}O_8N$, $[M + H]^+$ Calcd. 970.70912, found: 970.71546.

2.3 | NMR spectroscopy

^1H (950 or 500 MHz) and ^{13}C (239 or 125 MHz) NMR spectra were recorded at room temperature on Bruker Avance III spectrometers equipped with cryo probeheads. All of the NMR experiments on compound **6** were taken at 950/239 MHz, the other compounds **2**, **3**, and **7** were measured at 500/125 MHz. Amounts of approximately 1–5 mg of compounds **2**, **3**, **6**, and **7** were dissolved in 0.6 ml of chloroform-*d* and transferred to 5 mm NMR sample tubes. Chemical shifts are given on the δ-scale and are referenced to the solvent chloroform-*d*: $\delta_C = 77.00$ and $\delta_H = 7.27$ ppm. Pulse programs of all experiments (^1H, ^{13}C, DEPTQ, 1D sel-ROESY [τ_{mix}: 300 ms], 1D sel-TOCSY, gs-HSQC, and gs-HMBC [optimized for 8 and 10 Hz, respectively]), and band-selective-HMBC were taken from the Bruker software library. For 1D measurement, 64 K data points were used to yield the FID. Spectral widths for the 500 MHz ^1H spectra were set to 6,500 Hz, whereas in case of 950 MHz to 7,600 Hz. For 2D measurements, on the 500 MHz spectrometer in case of the HSQC spectrum, the sweep width in F_2 was

TABLE 1 ^{1}H and ^{13}C chemical shifts, multiplicities, and characteristic coupling constants of the steroid part of compounds **2**, **3**, **6**, and **7** in chloroform-*d*

Atom	2	3 (3Z)			6			7	
no.	H	C	H	C	H	*J* (Hz)[a]	C	H	C
1β	1.26	37.58	1.25	37.59	1.27 m		37.61	1.26	37.58
α	1.98		1.97		1.98 m			1.97	
2	4.25	72.10	4.25	72.10	4.25ddd	10.0;6.0;4.7	72.10	4.25	72.08
3	4.29	71.55	4.29	71.56	4.29ddd	4.7;4.7;2.3	71.55	4.29	71.54
4β	2.11	26.64	2.11	26.65	2.13 m		26.66	2.11	26.63
α	1.83		1.83		1.83ddd	15.3;12.5;4.7		1.83	
5	2.37	50.81	2.37	50.83	2.38dd	12.5;4.7	50.82	2.37	50.81
6	-	202.65	-	202.72	-		202.42	-	202.55
7	5.85	121.49	5.84	121.37	5.86d	2.6	121.69	5.84	121.63
8	-	162.15	-	162.45	-		161.73	-	161.91
9	2.86	34.60	2.85	34.61	2.86ddd	11.7;7.0;2.6	34.60	2.86	34.54
10	-	37.83	-	37.84	-		37.84	-	37.83
11β	1.61	20.59	1.61	20.61	1.61 m		20.60	1.61	20.57
α	1.80		1.78		1.80 m			1.79	
12β	1.66	29.85	1.66	29.89	1.70 m		29.90	1.69	29.87
α	2.17		2.14		2.19ddd	13.0;13.0;4.9		2.19	
13	-	48.05	-	47.71	-		48.08	-	48.06
14	-	84.38	-	84.47	-		84.39	-	84.33
15β	2.10	32.04	2.08	32.00	2.13 m		32.08	2.08	32.01
α	1.60		1.57		1.61 m			1.57	
16β	2.30	21.24	2.35	21.17	2.44 m		21.35	2.44	21.30
α	1.94		1.89		2.00 m			1.99	
17	3.11	51.33	3.04	51.35	3.21dd	9.0;9.0	51.95	3.21	51.94
18	0.63	17.20	0.63 (0.69)	17.18 (18.26)	0.70 s		17.36	0.69	17.33
19	0.99	23.60	0.99 (0.86)	23.60 (23.60)	1.00 s		23.60	0.99	23.58
20	-	158.53	-	156.40	-		166.08	-	165.94
21	1.92	15.53	1.83 (1.92)	16.02 (20.26)	1.98 s		17.48	1.83	17.44
22	-	108.32	-	108.29	-		108.33	-	108.33
Meβ-22	1.50	28.53	1.50	28.52	1.51 s		28.53	1.50	28.52
Meα-22	1.34	26.44	1.34	26.44	1.35 s		26.44	1.34	26.43
MeO	-	-	3.85 (3.87)	61.32 (61.53)	-		-	-	-

[a]Because the stereostructure of the steroid frame is identical within compounds of this table, we described the *J* coupling constants only for **6** detected at 950 MHz. s = singlet, d = doublet, m = unresolved multiplet.

7,000 Hz; data points ($t_2 \times t_1$) were acquired with 2 K × 128, in case of the HMBC spectrum, the sweep width in F_2 was 4,000 Hz; data points ($t_2 \times t_1$) were acquired with 2 K × 256, respectively. In the band-selective HMBC experiment applied for compound **7**, the used digital resolution was 1.95/1.71 Hz per point. For 2D measurements, on the 950 MHz spectrometer in case of the HSQC spectrum, the sweep width in F_2 was 7,600 Hz; data points ($t_2 \times t_1$) were acquired with 2 K × 4 K, in case of the HMBC spectrum, the sweep width in F_2 was 7,600 Hz; data points ($t_2 \times t_1$) were acquired with 16 K × 8 K, respectively. For F_1, linear prediction was applied to enhance the resolution. To achieve an appropriate separation of signals, we utilized 1.86/3.61 and 0.93/2.91 Hz per point digital resolution for the HSQC and HMBC experiments, respectively. Most ^{1}H assignments were accomplished using general knowledge of chemical shift dispersion

TABLE 2 ^{1}H and ^{13}C chemical shifts of the R group in compounds **6** and **7** in chloroform-*d*

Atom no.	6		7	
	H	C	H	C
1′	-	170.73	-	171.43
2′	2.59	31.19	2.43	33.0
3′	2.11	23.96	1.68	24.81
4′	2.78	37.62	1.41–1.27	29.08
5′	-	-		29.08
6′	-	-		29.08
7′	2.73	37.78		29.08
8′	2.03	24.22	1.61	24.94
9′	2.44	32.62	2.29	34.32
10′	-	172.95	-	173.91
11′	-	-	-	-
12′	4.05	64.27	4.04	63.99
13′	1.73	26.86	1.72	26.86
14′	2.03	35.78	2.03	35.77
15′	-	133.61	-	133.67
16′	5.14	125.13	5.13	125.03
17′	2.08	26.66	2.08	26.63
18′	1.99	39.67	1.98	39.65
19′	-	135.13	-	135.11
20′	5.15	124.38	5.14	124.35
21′	2.02	28.26[a]	2.01	28.24
22′	2.02	28.27[a]	2.01	28.24
23′	5.155	124.27	5.14	124.25
24′	-	134.97	-	134.96
25′	1.99	39.75	1.98	39.73
26′	2.08	26.66	2.08	26.63
27′	5.13	124.25	5.12	124.23
28′	-	134.91	-	134.89
29′	1.98	39.72	1.98	39.71
30′	2.07	26.76	2.06	26.74
31′	5.11	124.40	5.10	124.37
32′	-	131.26	-	131.25
33′	1.69	25.70	1.68	25.69
34′	1.61	17.68	1.60	17.67
35′	1.61	16.00	1.60	15.99
36′	1.61	16.05	1.60	16.03
37′	1.61	16.04	1.60	16.02
38′	1.61	15.87	1.60	15.86

[a]Tentative assignment.

with the aid of the proton–proton coupling pattern (^{1}H NMR spectra). The NMR signals of the products were assigned by comprehensive one- and two-dimensional NMR methods using widely accepted strategies.[13,14] The ^{1}H and ^{13}C NMR data for the steroid moiety of compounds **2–3** and **6–7** are compiled in Table 1, whereas the signals of the R-groups in compounds **6** and **7** are summarized in Table 2. The characteristic NMR and HRMS spectra of compounds **2–3** and **6–7** are presented as Supporting Information.

3 | RESULTS AND DISCUSSION

Savchenko and coworkers most recently reported the ^{1}H and ^{13}C NMR data of 20-oxime derivative of posterone 2,3-acetonide (**2**), and on the basis of its X-ray single crystal investigation, they proved the (*E*)-configuration of the oxime moiety.[10] As in the ^{1}H and ^{13}C NMR spectra of this compound only one set of signals appeared, the measured diamagnetic change of δC-20 (Δδ 51 ppm) supported the C═O → C═NOH conversion, but in the absence of exact data of Δδ *syn-anti* parameters for the C-21 signal, the unambiguous identification of the *E*/*Z* isomerism was not possible. We have also taken the NMR spectra of compound **2** (see Figures S1–S5), and the NMR data are included in Table 1.

Our HMBC measurement (see Figure S5, cross-peaks H-9/C-11 and H-17/C-16) revealed that the assignment of the CH_2 signals in positions 11 and 16 is in fact the opposite as compared to that published.[10] Furthermore, based on the edited-HSQC spectrum (Figure S4), we achieved full assignment of the diastereotopic methylene hydrogen atoms as well. It should be mentioned that no remarkable NOE sterical interaction could be observed between the broad OH and the H_3-21 (1.92 s) hydrogen atoms, not even when dmso-d_6 was used as solvent. To overcome this problem, we synthetized and investigated also the corresponding —OCH_3 20-oxime-methylether derivate (**3**). Two sets of signals were observed in the NMR spectra in ratio of 95/5, and for the major component, complete ^{1}H and ^{13}C assignment was achieved. In order to differentiate the β or α position of the hydrogen atoms, we utilized a series of selective ROESY experiments (Figure S8). Irradiation of the OCH_3 signal resulted in steric response on the H_3-21 signal (1.83 ppm), and thereby, we now have an unequivocal proof of the *E* configuration of the oxime group. Even though the signal at 1.83 ppm consists of the overlapping H_3-21 and H_α-4 signals, this experiment marked out not only the OCH_3 but also H-2, H-3, H_β-4, H-9, H_β-16, H-17, and H_3-18. In addition to this, the experiments on H_3-18 and H_3-19 resulted in the stereostructure and complete ^{1}H assignments (see Figure 2).

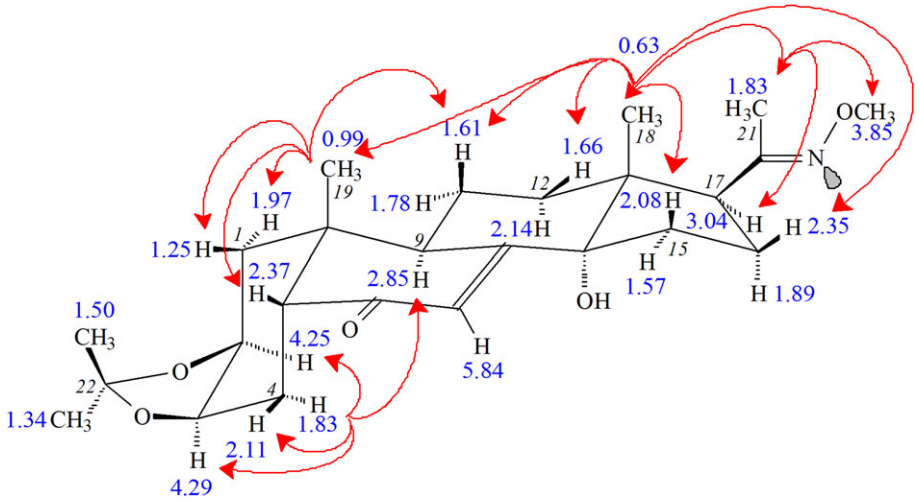

FIGURE 2 Stereostructure of compound **3** and one-dimensional selective rotating frame Overhauser enhancement spectroscopy (ROESY) responses. The red arrows indicate characteristic steric proximities detected by irradiation at MeO, H_3-21+ H_α-4, H_3-18, and H_3-19 signals, blue numbers refer to ^{1}H chemical shifts, and black cursive numbers denote atomic numbering

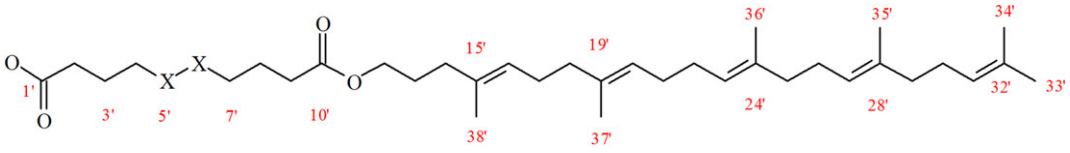

FIGURE 3 Atomic numbering of the long lipophilic side-chain. X = S (compound **6**) or CH_2 (compound **7**)

In the edited HSQC spectrum of compound **3** (Figure S12), we have clearly identified the CH_3-18 (0.69/18.26 ppm) and CH_3-21 (1.92/20.26 ppm) signals also for the minor isomer.

It should be mentioned that in case of the oxime derivative compound **2**, the C-21 signal appeared at 15.53 ppm nearly at the same chemical shift as in the main component of compound **3** (16.02 ppm). This value unequivocally proofs the *E* configuration of the oxime group. That means that compound **2** appears in solution in the same configuration as in solid phase.[10]

The detected $\Delta\delta = 4.2$ ppm *syn-anti* parameter on the C-21 signal in compound **3** is in good agreement with our results on C-6 oxime derivatives of ecdysteroids[4] and unambiguously confirmed the NMR differentiation of the *E*/*Z* isomers. Considering the detected δC-21 (17 ppm) in compounds **6** and **7**, we can conclude that these compounds are also 20(*E*)-oxime derivatives. The appearance of five =CH signals of the R-groups in the ^{1}H (δ5.20–5.00 ppm) and ^{13}C (δ 125.2–124.2 ppm) NMR spectra of compounds **6** and **7** justifies the connection of the long lipophilic side-chain (OR). The atomic numbering for the OR group is shown in Figure 3, and corresponding NMR data are summarized in Table 2.

In the ^{1}H spectrum of compound **6** (Figure S13), the identification of the two O=C—$CH_2CH_2CH_2$—S moieties was achieved by sel-TOCSY experiments (see Figure S14), and irradiation on the H_2-12′ signal (δ4.05 ppm) led to the assignment of the O=C—O—$CH_2CH_2CH_2$—C= moiety (see Figure S14). Considering the H_2-12′/C-10′ cross-peaks (4.05/172.95-ppm) in the HMBC spectrum (Figure S21), the differentiation between the C-10′ and C′-1 ester carbon atoms is straightforward. The H_2-13′ and H_2-14′ hydrogens clearly give HMBC correlation to C-15′ (δ133.61 ppm; Figure S23), and this way the complete NMR assignment of C-1′–C-15′ fragment is revealed. In addition to this, the third cross-peak to C-15′ in this spectrum marked out δH_2-17′ at 2.08 ppm. The H_2-14′/C-16′ (2.03/125.13 ppm) HMBC response (see Figure S22) assigned δC-16′, while the cross-peak at 1.99/125.13 revealed the δH_2-18′ chemical shift. At the same time, the H_2-17′ and H_2-18′ hydrogens show HMBC correlations to C-19′, and this way the signal at δ135.13 can be assigned to this carbon atom. While C-19′ displays a further HMBC cross-peak to a methylene group, this signal at δ2.02 ppm should be H_2-21. In the ^{1}H spectrum, the intensity of this signal is 4H, and in the edHSQC, we detected two methylene signals at 28.26 and 28.27 ppm (controlled also with volume integration); we concluded that the latter should belong to the CH_2 group in position C-22′. This way the H_2-22′/C-24′ HMBC correlation established the δC-24′ = 134.97 ppm assignment. This

carbon atom shows long-range correlation also with the H_2-25′ (δ1.99 ppm) hydrogens.

To continue the signal assignment of the side chain R, we examined the CH_3 signals. Five methyl groups resonate in the ^{1}H NMR at 1.61 ppm, but the sixth CH_3 appears separately as a quartet (J ~ 1 Hz) at 1.69 ppm, and in the edited HSQC spectrum (Figures S17–S18), the corresponding cross-peak is at 1.69/25.70 ppm. In the HMBC experiment (Figure S20), the 1.69/17.68 correlation identified a geminal dimethyl group, that is, two that are situated on the end of the side-chain. Considering the well-known γ-steric effect that necessarily takes place with the methylene in position 31′, their assignment is δC-34′ = 17.68 and δC-33′ = 25.70 ppm. Utilizing a sel-TOCSY experiment irradiating at 1.69 ppm (Figure S15), we managed to identify the H_3-34′, H-31′, H_2-30′ and H_2-29′ signals (because this irradiation affected also the H_β-12 atom of the steroid frame, the H_α-12, H_α-11, H-9 and H-7 signals also appeared). The remaining, so far not assigned quaternary sp^2 = C signal at 134.91 ppm, can only be C-28′, which is strongly supported by the H_2-30′, H_2-29′ and H_2-26′ (δ2.08) HMBC correlations (Figure S23).

In case of compound **7,** we used the same methodology as in case of **6**, but the applied NMR frequency was only 500/125 MHz. To achieve the appropriate resolution also in the HSQC and HMBC measurements, we preferred here their band selective versions. The obtained ^{1}H and ^{13}C chemical shifts of **7** correlated perfectly with the data of **6**, with exception of the methylene groups of the side chain between positions 2′ and 9′. The method of choice for studying this structure fragment was again the one-dimensional sel-TOCSY experiment (Figure S25). Irradiation of the H_2-9′ signal at 2.29 ppm identified not only the hydrogens till H_2-6′, but, through raising the mixing time to 200 ms, we could reach till H_2-2′. Due to the extremely similar ^{1}H chemical shifts of the methylenes in 4′–7′ positions, it was possible to enter for them region 1.47–1.27 ppm. The experiment on H_2-12′ supplied H_2-13′ and H_2-14′ data. Joint irradiation of the five =CH hydrogens in the 5.17–5.17 ppm area revealed all signals of their spin systems.

In conclusion, we obtained for the first time the complete ^{1}H and ^{13}C NMR signal assignment of ecdysteroid C-20-oxime derivatives, including two new, promising potential antitumor agent with a long lipophilic side-chain. The preparation of self-assembling nanoparticles from these latter two compounds, as well as their bioactivity testing, will be reported in the near future.

ACKNOWLEDGEMENTS

This work was supported by the National Research, Development and Innovation Office, Hungary (NKFIH; K119770). Support from the EU-funded Hungarian grant EFOP-3.6.1-16-2016-00008, and GINOP-2.3.2-15-2016-00012 is acknowledged. M. V. and D. B. were supported by the New National Excellence Program of the Ministry of Human Capacities, Hungary (M. V.: ÚNKP-17-3-I-SZTE-66; D. B.:ÚNKP-17-3-III-SE-15). M.V. acknowledges an STSM grant from COST Action CM1407, challenging organic syntheses inspired by nature—from natural products chemistry to drug discovery. The authors are grateful to Mr Norbert Kúsz for his kind assistance in studying compound **2** and to Mr. Attila Csorba for the HRMS measurements.

ORCID

Gábor Tóth http://orcid.org/0000-0001-8436-8256

Dóra Bogdán[1,2]
Rainer Haessner[3]
Máté Vágvölgyi[4]
Daniele Passarella[5]
Attila Hunyadi[4,6]
Tamás Gáti[7]
Gábor Tóth[4,8]

[1]*Department of Organic Chemistry, Semmelweis University, Hőgyes Endre u. 7, Budapest H-1092, Hungary*
[2]*Institute of Materials and Environmental Chemistry, Research Centre for Natural Sciences, Hungarian Academy of Sciences, Magyar tudósok körútja 2, Budapest H-1117, Hungary*
[3]*Institute of Organic Chemistry and Biochemistry, Technical University of Munich, Lichtenbergstr. 4, Garching D-85747, Germany*
[4]*Institute of Pharmacognosy, University of Szeged, Eötvös u. 6, Szeged H-6720, Hungary*
[5]*Dipartimento di Chimica, Università degli Studi di Milano, Via Camillo Golgi, 19, Milan 20133, Italy*
[6]*Interdisciplinary Centre for Natural Products, University of Szeged, Eötvös u. 6, Szeged H-6720, Hungary*
[7]*Servier Research Institute of Medicinal Chemistry (SRIMC), Záhony utca 7, Budapest H-1031, Hungary*
[8]*Department of Inorganic and Analytical Chemistry, NMR Group, Budapest University of Technology and Economics, St. Gellért tér 4, Budapest H-1111, Hungary*

Correspondence
Gábor Tóth, Department of Inorganic and Analytical Chemistry, NMR Group, Budapest University of Technology and Economics, St. Gellért tér 4, Budapest H-1111, Hungary.
Email: drtothgabor@t-online.hu

REFERENCES

[1] A. Martins, N. Tóth, A. Ványolós, Z. Béni, I. Zupkó, J. Molnár, M. Báthori, A. Hunyadi, *J. Med. Chem.* **2012**, *55*, 5034. https://doi.org/10.1021/jm300424n

[2] A. Martins, P. Sipos, K. Dér, J. Csábi, W. Miklos, W. Berger, A. Zalatnai, L. Amaral, J. Molnár, P. Szabó-Révész, A. Hunyadi, *Biomed. Res. Int.* **2015**, *2015*, 895360. https://doi.org/10.1155/2015/895360

[3] A. Hunyadi, J. Csábi, A. Martins, J. Molnár, A. Balázs, G. Tóth, *Molecules* **2017**, *22*, 199. https://doi.org/10.3390/molecules22020199

[4] M. Vágvölgyi, A. Martins, Á. Kulmány, I. Zupkó, T. Gáti, A. Simon, G. Tóth, A. Hunyadi, *Eur. J. Med. Chem.* **2018**, *144*, 730. https://doi.org/10.1016/j.ejmech.2017.12.032

[5] G. Fumagalli, M. Marucci, M. S. Christodoulou, B. Stella, F. Dosio, D. Passarella, *Drug Discov. Today* **2016**, *21*, 1321. https://doi.org/10.1016/j.drudis.2016.06.018

[6] A. Maksimenko, F. Dosio, J. Mougin, A. Ferrero, S. Wack, L. H. Reddy, A.-A. Weyn, E. Lepeltier, C. Bourgaux, B. Stella, L. Cattel, P. A. Couvreur, *Proc. Natl. Acad. Sci. U. S. A.* **2014**, *111*, E217. https://doi.org/10.1073/pnas.1313459110

[7] S. Borrelli, D. Cartelli, F. Secundo, G. Fumagalli, M. S. Christodoulou, A. Borroni, D. Perdicchia, F. Dosio, P. Milla, G. Cappelletti, D. Passarella, *ChemPlusChem* **2015**, *80*, 47. https://doi.org/10.1002/cplu.201402239

[8] G. Fumagalli, B. Stella, I. Pastushenko, F. Ricci, M. S. Christodoulou, G. Damia, D. Mazza, S. Arpicco, C. Giannini, L. Morosi, F. Dosio, P. A. Sotiropoulou, D. Passarella, *ACS Med. Chem. Lett.* **2017**, *8*, 953. https://doi.org/10.1021/acsmedchemlett.7b00262

[9] D. Passarella, D. Comi, A. Vanossi, G. Paganini, F. Colombo, L. Ferrante, V. Zuco, B. Danieli, F. Zunino, *Bioorg. Med. Chem. Lett.* **2009**, *19*, 6358. https://doi.org/10.1016/j.bmcl.2009.09.075

[10] R. G. Savchenko, S. A. Kostyleva, E. S. Meshcheryakova, L. M. Khalilov, L. V. Parfenova, V. N. Odinokov, *Can. J. Chem.* **2017**, *95*, 130. https://doi.org/10.1139/cjc-2016-0413

[11] G. Fumagalli, G. Giorgi, M. Vágvölgyi, E. Colombo, M. S. Christodoulou, V. Collico, D. Prosperi, F. Dosio, A. Hunyadi, M. Montopoli, M. Hyraci, A. Silvani, G. Lesma, L. Dalla Via, D. Passarella, *ACS Med. Chem. Lett. 9*, 468. https://doi.org/10.1021/acsmedchemlett.8b00078

[12] S. Borrelli, M. S. Christodoulou, I. Ficarra, A. Silvani, G. Cappelletti, D. Cartelli, G. Damia, F. Ricci, M. Zucchetti, F. Dosio, D. Passarella, *Eur. J. Med. Chem.* **2014**, *85*, 179. https://doi.org/10.1016/j.ejmech.2014.07.035

[13] H. Duddeck, W. Dietrich, G. Tóth, *Structure elucidation by modern NMR*, Springer-Steinkopff, Darmstadt **1998**.

[14] E. Pretsch, G. Tóth, M. E. Munk, M. Badertscher, *Computer-aided Structure Elucidation. Spectra Interpretation and Structure Generation*, Wiley-VCH, Weinheim **2002**.

SUPPORTING INFORMATION

Additional supporting information may be found online in the Supporting Information section at the end of the article.

[Correction added on 17 July 2018, after first online publication: New Supporting Information materials have been added.]

III.

ACS Medicinal Chemistry Letters

Letter

Cite This: ACS Med. Chem. Lett. 2018, 9, 468−471

Heteronanoparticles by Self-Assembly of Ecdysteroid and Doxorubicin Conjugates To Overcome Cancer Resistance

Gaia Fumagalli,[†] Giulia Giorgi,[†] Máté Vágvölgyi,[‡] Eleonora Colombo,[†] Michael S. Christodoulou,[§] Veronica Collico,[∥] Davide Prosperi,[∥] Franco Dosio,[#] Attila Hunyadi,[‡] Monica Montopoli,[⊥] Mariafrancesca Hyeraci,[⊥] Alessandra Silvani,[†] Giordano Lesma,[†] Lisa Dalla Via,*[,⊥,▽] and Daniele Passarella*[,†,▽]

[†]Dipartimento di Chimica, Università degli Studi di Milano, Milano 20133, Italy

[‡]Szegedi Tudomanyegyetem (SZTE), Institute of Pharmacognosy, University of Szeged, 6720 Szeged, Hungary

[§]DISFARM, Sezione "A. Marchesini", Università degli Studi di Milano, Via Venezian 21, 20133 Milano, Italy

[∥]Dipartimento di Biotecnologie e Bioscienze, Università Milano Bicocca, P.zza della Scienza 2, 20126 Milano, Italy

[⊥]Dipartimento di Scienze del Farmaco, Università degli Studi di Padova, Via F. Marzolo 5, 35131 Padova, Italy

[#]Dipartimento di Scienza e Tecnologia del Farmaco, Università degli Studi di Torino, Torino 10125, Italy

Supporting Information

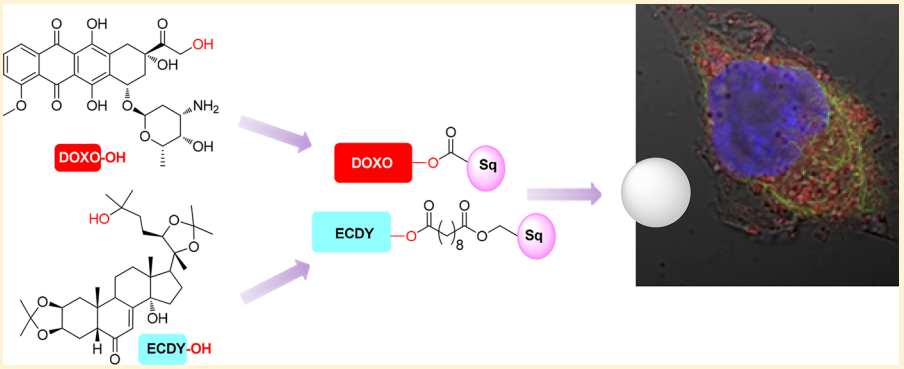

ABSTRACT: Heteronanoparticles (H-NPs) consisting of conjugates characterized by a squalene tail linked to doxorubicin and ecdysteroid derivatives are presented. Biological evaluation on A2780ADR cell line confirms not only the maintenance of the activity of the parental drug but also the ability to overcome cancer resistance. The *in vitro* cell uptake was demonstrated, and the involvement of an endosomal-mediated pathway was suggested.

KEYWORDS: *Self-assembled-nanoparticles, ecdysteroids, doxorubicin, drug toxicity, cancer*

The formation of self-assembled nanoparticles (NPs) using anticancer drug conjugates could be a useful and smart approach to face cancer.[1−3] In the past few years, we developed a step-by-step project that moved from the preparation of a novel class of squalene conjugates with paclitaxel, podophyllotoxin, camptothecin, and epothilone A[4] and reached, as highest evidence of efficacy, the preparation of heteronanoparticles with doxorubicin and cyclopamine conjugates that were able to reduce *in vivo* the tumor growth and toxicity due to the use of the single drugs.[5−8] The conjugates were characterized by a squalene tail that makes them able to self-assemble in water and by a drug unit connected via a disulfide-containing linker to secure the release inside the cell.

Our interest in facing the resistance of different kinds of tumor cells[9] drove us to consider the formation of self-assembled heteronanoparticles as a promising approach. Martins et al. recently reported the chemo-sensitizing effect of apolar ecdysteroids on MDR cancer cells.[10] The antiproliferative activity of these compounds was very low, and they exerted a mild activity in modulating the ABCB1-mediated efflux of rhodamine 123. Further studies revealed that the chemo-sensitizing activity can be independent of efflux inhibition, in particular, ketals of poststerone, a known *in vivo* metabolite of 20-hydroxyecdysone that sensitized ABCB1-transfected cancer cells to doxorubicin in a highly MDR selective manner without significantly interfering with the efflux function.

In this scenario, we planned the preparation of some ecdysone conjugates containing the squalene tail to be combined with the known squalenoylated doxorubicin[11]

Received: February 15, 2018
Accepted: April 17, 2018
Published: April 17, 2018

DOI: 10.1021/acsmedchemlett.8b00078
ACS Med. Chem. Lett. 2018, 9, 468−471

(Chart 1) and investigate their ability to form heteronanoparticles (H-NPs) toward the treatment of doxorubicin

Chart 1. Schematic Representation of the Building Blocks and Obtained Conjugates

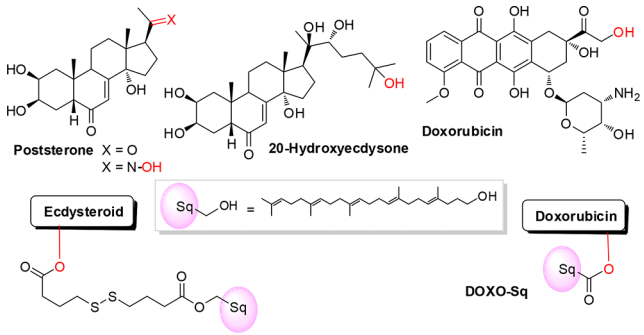

resistant cell lines. In the light of the synergistic effect of ecdysteroid acetonides with doxorubicin,[10] we focused our attention on diketals of 20-hydroxyecdysone and related derivatives of poststerone.

Five different conjugates were prepared according to Schemes 1 and 2 (see Table 1 and also the Supporting Information). 20-Hydroxyecdysone derivatives **3a–c** were synthesized following a three-step procedure (Scheme 1): (a) condensation reaction between the protected 20-hydroxyecdysone **1** and the proper acid **2**, (b) deprotection of the carboxylic group, and (c) final condensation with 1′,2-tris-norsqualene alcohol. Compounds **6a** and **6b** were prepared by a condensation reaction between compounds **5**[4] and **4**.[12]

Scheme 1. Synthesis of the Conjugates 3a–c

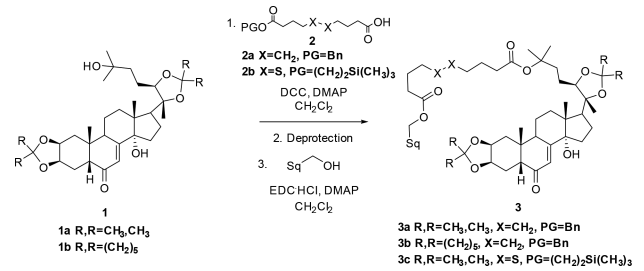

Scheme 2. Synthesis of the Conjugates 6a,b

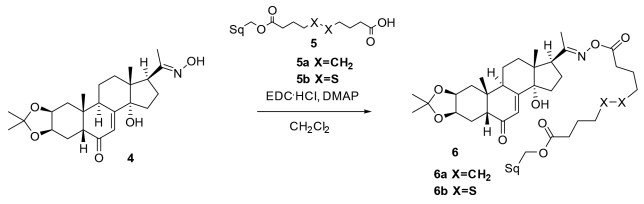

Table 1. Ecdysteroid Conjugates and Corresponding Starting Material

starting material	X	PG	deprotection	product
1a + 2a	CH_2	Bn	H_2, $Pd(OH)_2$	**3a**
1b + 2a	CH_2	Bn	H_2, $Pd(OH)_2$	**3b**
1a + 2b	S	$(CH_2)_2SiMe_3$	TBAF	**3c**
4 + 5a	CH_2			**6a**
4 + 5b	S			**6b**

Next, the ability of the conjugates to self-assemble in nanoparticles was investigated. Briefly, compound solution in THF was added dropwise into ultrapure water. The spontaneous self-assembly into NPs is a consequence of local interactions between the hydrophobic molecules, mainly guided by squalene chains interactions. Subsequently, the organic solvent was removed under reduced pressure (see Supporting Information). The nanosuspensions were characterized by dynamic light scattering (DLS) and transmission electron microscopy (TEM). DLS analysis confirmed the formation of nanoassemblies in aqueous medium. The assemblies were monodisperse (PdI < 0.2) with sizes around 200 nm, except for the **6a** NPs that exhibited a 2-fold larger hydrodynamic diameter (366.3 ± 20.17 nm) (Table 2). The highly negative ζ-potential values (<−20.0 mV) suggested that the electrostatic repulsion between NPs contributed to the stability of the nanoassemblies in aqueous medium.

Table 2. NPs Characterization by Dynamic Light Scattering (ZetaSizer, Malvern)[a]

NPs	h.d. ± SD (nm)	P.I.	ζ-pot. ± SD (mV)
3a	198.1 ± 0.9	0.106 ± 0.041	−49.8 ± 0.9
3b	205.1 ± 0.6	0.050 ± 0.026	−43.0 ± 0.9
3c	214 ± 3.4	0.086 ± 0.046	−30.0 ± 4.6
6a	366.3 ± 20.17	0.161 ± 0.032	−21.5 ± 4.55
6b	221.8 ± 4.879	0.081 ± 0.088	−21.7 ± 1.50

[a]h.d., hydrodynamic diameter; P.I., polydispersity index; ζ-pot., ζ-potential.

Compounds **3a–c** and **6a,b** were further mixed with squalene-conjugated doxorubicine (**DOXO-Sq**) that is well-known to have a better therapeutic index than doxorubicin[11] and to form heteronanoparticles (H-NPs) according to our recent paper.[7] H-NPs were prepared by mixing the compound solutions (125 μL, 250 μg, 2 mg mL^{-1}) with DOXO-Sq solution (2 mg mL^{-1}) in THF with a molar ratio compound/DOXO-Sq of 50 and by dropping the organic solution into 250 μL of ultrapure water as previously described.[11] The mixture became opalescent suggesting the possible formation of particles. H-NPs filtered with a 0.45 μm filter were characterized by DLS and TEM. DLS analysis (Table 3) confirmed the formation of H-NPs in aqueous medium. The assemblies were monodisperse (PdI < 0.2) but larger compared to the homogeneous NPs, except for the **6a,b** NPs where **DOXO-Sq** resulted in a decrease of (or did not alter) the particle dimension, respectively. Also, the ζ-potential values decreased.

Table 3. H-NPs Characterization by Dynamic Light Scattering (ZetaSizer, Malvern)[a]

X:DOXO-Sq 50:1			
X	h.d. ± SD (nm)	P.I.	ζ-pot. ± SD (mV)
3a	533.1 ± 26.60	0.160 ± 0.104	−9.73 ± 0.95
3b	538.2 ± 33.41	n.d.	−9.39 ± 2.91
3c	579.2 ± 104.4	0.226 ± 0.276	−20.3 ± 2.52
6a	187.7 ± 14.48	0.223 ± 0.069	−13.5 ± 9.65
6b	298.7 ± 11.43	0.264 ± 0.014	−11.1 ± 3.48

[a]h.d., hydrodinamic diameter; P.I., polydispersity index; ζ-pot., ζ-potential.

DOI: 10.1021/acsmedchemlett.8b00078
ACS Med. Chem. Lett. 2018, 9, 468–471

Figure 1 reports TEM analysis for NPs obtained by self-assembly of compound **6b** and the H-NPs **6b/DOXO-Sq**

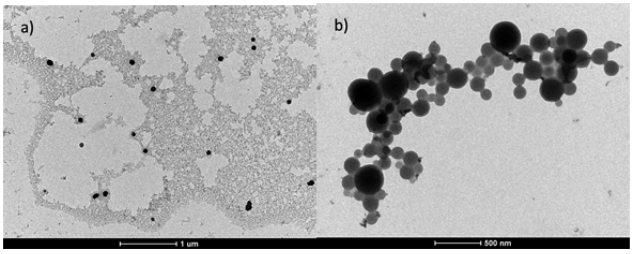

Figure 1. TEM analysis for NPs-**6b** (a, scale reported 1 μm) and H-NPs **6b/DOXO-Sq** (b, scale reported 500 nm).

(50:1). The images show compact nanoparticles whose diameter is smaller if compared with the data obtained by DLS but similar in the case of H-NPs.

The ability of both NPs and H-NPs to inhibit cell growth was assayed on A2780ADR cells, a human ovarian carcinoma doxorubicin-resistant cell line. The obtained results are shown in Table 4 and are expressed as GI_{50} values, i.e., the concentration of the test agent inducing 50% reduction in cell number compared with control cultures.

Table 4. Inhibition of A2780ADR Cell Growth

	A2780-ADR cells (GI_{50}, μM)[a]	
	NPs	X:DOXO-Sq 50:1
3a	>50	0.50 ± 0.02
3b	>50	0.78 ± 0.02
3c	>50	0.69 ± 0.15
6a	19 ± 3	0.34 ± 0.08
6b	39 ± 4	0.26 ± 0.03
DOXO-Sq	1.17 ± 0.06	----

[a]Values are the mean ± SD of at least four independent experiments.

Considering the NPs, it can be noted that **DOXO-Sq** exerts an interesting inhibitory effect on A2780ADR proliferation, showing a GI_{50} value of about 1 μM. This capacity, notwithstanding about ten times lower with respect to that of doxorubicin (GI_{50}= 0.16 ± 0.01 μM), confirms, in accordance with previous studies,[11] the ability of the drug to induce an antiproliferative effect even following squalenoylation. Otherwise, the NPs obtained by squalene-conjugated ecdysteroids provoke in the same experimental conditions a negligible effect on cells, and indeed, only for the nanoassemblies **6a** and **6b** a detectable and quite low cytotoxicity on A2780ADR cells was demonstrated. Notably, the H-NPs obtained by mixing **3a−c** and **6a**,**b** with **DOXO-Sq** induce a significant antiproliferative effect, with GI_{50} values from 1.5 to more than 4 times lower with respect to that obtained for **DOXO-Sq**. These data suggest the ability of the H-NPs to overcome, at least partially, the resistance phenomenon. In this connection, it was of interest to investigate the effect of tamoxifen, a well-known inhibitor of the P-glycoprotein[13] on the intracellular uptake of the H-NPs **3a**/**DOXO-Sq**, taken as an example, and of doxorubicin, used as reference. The cell internalization in A2780ADR was monitored by flow cytometry. As expected, the presence of tamoxifen significantly increased the drug accumulation in these cells. In detail, the intracellular mean fluorescence intensity of doxorubicin rose by 27% after exposure to the P-glycoprotein inhibitor. Otherwise, no difference in fluorescence was observed between the cells treated and those not treated with tamoxifen. This result further supports the hypothesis that these new H-NPs can play a crucial role in drug resistance mechanism, suggesting the inability or at least the reduction of P-glycoprotein to mediate their efflux from resistant cells. The *in vitro* cell internalization was then further investigated by fluorescence microscopy to verify any change in the uptake pathway. For this purpose, A2780ADR cells were incubated for 2 h in the presence of doxorubicin and the H-NPs **3a**/**DOXO-Sq**. The results are shown in Figure 2a,b, respectively.

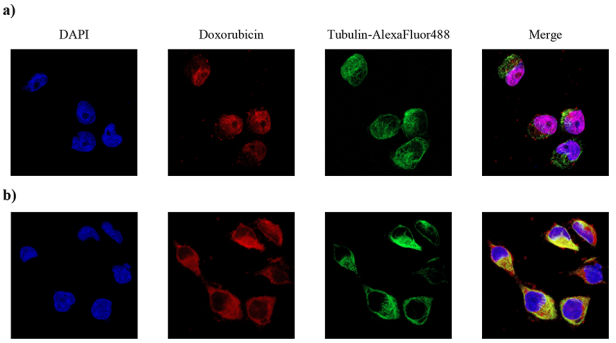

Figure 2. Fluorescence microscopy of A2780ADR cells incubated for 2 h in the presence of doxorubicin (a) or H-NPs **3a**/**DOXO-Sq** (b) at 5 μM. The nucleus and cytoplasm were stained with DAPI and antibody antitubulin conjugated with AlexaFluor488, respectively.

The cell penetration of both agents is rapid; nevertheless, the intracellular localization differs: for the drug, a major localization in the nuclei is observed (a), while for the H-NPs, a staining almost exclusive in the cytoplasm appears (b).

A more in depth microscopy analysis (Figure 3) highlights in the cytoplasm of A2780ADR cells treated with the H-NPs **3a**/**DOXO-Sq** the occurrence of vesicles characterized by a mean diameter of about 0.9 μm, a value significantly higher with respect to the hydrodynamic diameter of the corresponding H-NP (533.1 ± 26.60, Table 3). The more complex membrane trafficking pathway of NPs[14] with respect to free doxorubicin[15] could be responsible for the delay in nucleus accumulation of the H-NPs **3a**/**DOXO-Sq**.

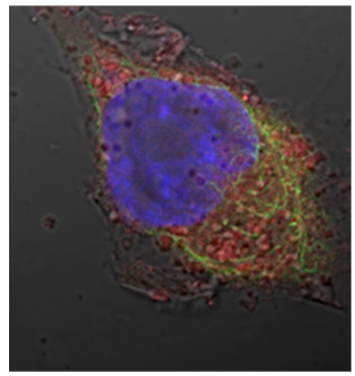

Figure 3. Fluorescence microscopy of A2780ADR cell treated for 2 h with H-NPs **3a**/**DOXO-Sq**.

The obtained results highlight the effectiveness of self-assembled H-NPs to face cancer resistance and show a general

DOI: 10.1021/acsmedchemlett.8b00078
ACS Med. Chem. Lett. 2018, 9, 468−471

strategy that could be applied in various pathologies where combined therapy could be beneficial.

■ ASSOCIATED CONTENT

Supporting Information

The Supporting Information is available free of charge on the ACS Publications website at DOI: 10.1021/acsmedchemlett.8b00078.

Experimental details regarding preparation of compounds **3a−c** and **6a,b**, nanoparticles preparation and characterization, and biological evaluation (cell cultures, inhibition growth assay, cytofluorimetric analysis, and confocal microscopy analysis) (PDF)

■ AUTHOR INFORMATION

Corresponding Authors

*E-mail: daniele.passarella@unimi.it.
*E-mail: lisa.dallavia@unipd.it.

ORCID

Michael S. Christodoulou: 0000-0002-5098-3143
Davide Prosperi: 0000-0003-4577-9575
Alessandra Silvani: 0000-0002-0397-2636
Daniele Passarella: 0000-0001-6180-9581

Author Contributions

[▽]These authors contributed equally. The manuscript was written through contributions of all authors. All authors have given approval to the final version of the manuscript.

Notes

The authors declare no competing financial interest.

■ ACKNOWLEDGMENTS

D.P., G.L., and A.S. express their gratitude to the family of Prof. Bruno Danieli (who passed away in 2014) for a research grant to financially support a fellowship for G.G. L.D.V. is grateful for the financial support provided by Dipartimento di Scienze del Farmaco, Università di Padova−Progetti di Ricerca di Dipartimento PRID 2017. A.H. acknowledges the National Research, Development and Innovation Office, Hungary (NKFIH; K119770). M.V. was supported by the New National Excellence Program of the Ministry of Human Capacities, Hungary (ÚNKP-17-3), and by an STSM grant from COST Action CM1407, Challenging organic syntheses inspired by nature−from natural products chemistry to drug discovery.

■ REFERENCES

(1) Xing, P.; Zhao, Y. Multifunctional Nanoparticles Self-Assembled from Small Organic Building Blocks for Biomedicine. *Adv. Mater.* **2016**, *28*, 7304−7339.

(2) Arias, J. L.; Reddy, L. H.; Othman, M.; Gillet, B.; Desmaele, D.; Zouhiri, F.; Dosio, F.; Gref, R.; Couvreur, P. Squalene Based Nanocomposites: A New Platform for the Design of Multifunctional Pharmaceutical Theragnostics. *ACS Nano* **2011**, *5*, 1513−1521.

(3) Fumagalli, G.; Marucci, M.; Christodoulou, M. S.; Stella, B.; Dosio, F.; Passarella, D. Self Assembly Drug Conjugates for Anticancer Treatment. *Drug Discovery Today* **2016**, *21*, 1321−1329.

(4) Borrelli, S.; Christodoulou, M. S.; Ficarra, I.; Silvani, A.; Cappelletti, G.; Cartelli, D.; Damia, G.; Ricci, F.; Zucchetti, M.; Dosio, F.; Passarella, D. New Class of Squalene-Based Releasable Nanoassemblies of Paclitaxel, Podophyllotoxin, Camptothecin and Epothilone A. *Eur. J. Med. Chem.* **2014**, *85*, 179−190.

(5) Borrelli, S.; Cartelli, D.; Secundo, F.; Fumagalli, G.; Christodoulou, M. S.; Borroni, A.; Perdicchia, D.; Dosio, F.; Milla, P.; Cappelletti, G.; Passarella, D. Self-Assembled Squalene-based Fluorescent Heteronanoparticles. *ChemPlusChem* **2015**, *80*, 47−49.

(6) Fumagalli, G.; Mazza, D.; Christodoulou, M. S.; Damia, G.; Ricci, F.; Perdicchia, D.; Stella, B.; Dosio, F.; Sotiropoulou, P. A.; Passarella, D. Cyclopamine−Paclitaxel-Containing Nanoparticles: Internalization in Cells Detected by Confocal and Super Resolution Microscopy. *ChemPlusChem* **2015**, *80*, 1380−1383.

(7) Fumagalli, G.; Stella, B.; Pastushenko, I.; Ricci, F.; Christodoulou, M. S.; Damia, G.; Mazza, D.; Arpicco, S.; Giannini, C.; Morosi, L.; Dosio, F.; Sotiropoulou, P. A.; Passarella, D. Heteronanoparticles by self-Assembly of Doxorubicin and Cyclopamine Conjugates. *ACS Med. Chem. Lett.* **2017**, *8*, 953−957.

(8) Fumagalli, G.; Christodoulou, M. S.; Riva, B.; Revuelta, I.; Marucci, C.; Collico, V.; Prosperi, D.; Riva, S.; Perdicchia, D.; Bassanini, I.; García-Argáez, A.; Dalla Via, L.; Passarella, D. Self-assembled 4-(1,2-diphenylbut-1-en-1-yl)aniline Based Nanoparticles: Podophyllotoxin and Aloin as Building Blocks. *Org. Biomol. Chem.* **2017**, *15*, 1106−1109.

(9) (a) Sotiropoulou, P. A.; Christodoulou, M. S.; Silvani, A.; Herold-Mende, C.; Passarella, D. Chemical Approaches to Targeting Drug Resistance in Cancer Stem Cells. *Drug Discovery Today* **2014**, *19*, 1547−1562. (b) Marucci, C.; Fumagalli, G.; Calogero, F.; Silvani, A.; Christodoulou, M. S.; Martinet, N.; Passarella, D. Natural Products and Cancer Stem Cells. *Curr. Pharm. Des.* **2015**, *21*, 5547−5557.

(10) Martins, A.; Tóth, N.; Ványolós, A.; Béni, Z.; Zupkó, I.; Molnár, J.; Báthori, M.; Hunyadi, A. Significant Activity of Ecdysteroids on the Resistance to Doxorubicin in Mammalian Cancer Cells Expressing the Human ABCB1 Transporter. *J. Med. Chem.* **2012**, *55*, 5034−5043.

(11) Maksimenko, A.; Dosio, F.; Mougin, J.; Ferrero, A.; Wack, S.; Reddy, L. H.; Weyn, A.-A.; Lepeltier, E.; Bourgaux, C.; Stella, B.; Cattel, L.; Couvreur, P. A Unique Squalenoylated and Nonpegylated Doxorubicin Nanomedicine with Systemic Long-Circulating Properties and Anticancer Activity. *Proc. Natl. Acad. Sci. U. S. A.* **2014**, *111*, E217−E226.

(12) Savchenko, R. G.; Kostyleva, S. A.; Meshcheryakova, E. S.; Khalilov, L. M.; Parfenova, L. V.; Odinokov, V. N. Synthesis of Novel α-Aminoecdysteroids via Regio- and Stereoselective Oxymation/Hydrogenation of 20-Hydroxyecdysone Derivatives. *Can. J. Chem.* **2017**, *95*, 130−133.

(13) Callaghan, R.; Higgins, C. F. Interaction of Tamoxifen with the Multidrug Resistance P-Glycoprotein. *Br. J. Cancer* **1995**, *71*, 294−299.

(14) Hinde, E.; Thammasiraphop, K.; Duong, H. T. T.; Yeow, J.; Karagoz, B.; Boyer, C.; Gooding, J. J.; Gaus, K. Pair Correlation Microscopy Reveals the Role of Nanoparticle Shape in Intracellular Transport and Site of Drug Release. *Nat. Nanotechnol.* **2016**, *12*, 81−89.

(15) Regev, R.; Yeheskely-Hayon, D.; Katzir, H.; Eytan, G. D. Transport of Anthracyclines and Mitoxantrone Across Membranes by a Flip-flop Mechanism. *Biochem. Pharmacol.* **2005**, *70*, 161−169.

DOI: 10.1021/acsmedchemlett.8b00078
ACS Med. Chem. Lett. 2018, 9, 468−471

IV.

A GENUINELY MULTIDISCIPLINARY JOURNAL

CHEMPLUSCHEM

CENTERING ON CHEMISTRY

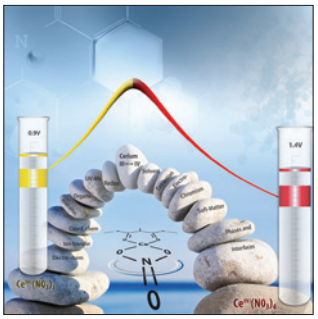

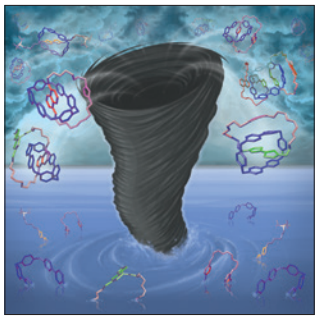

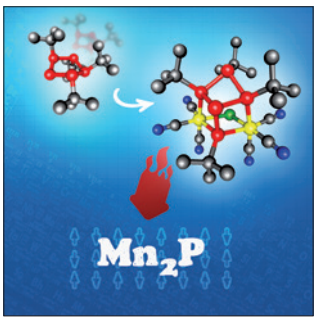

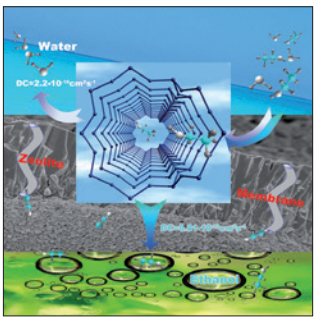

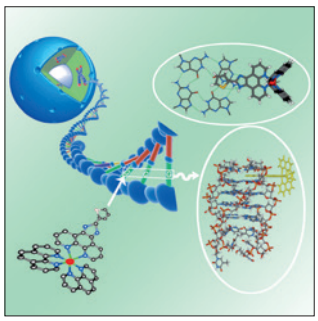


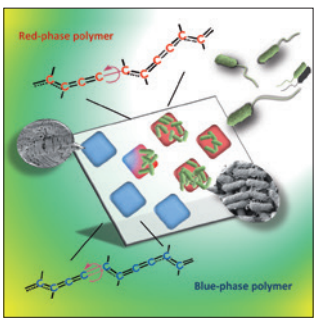

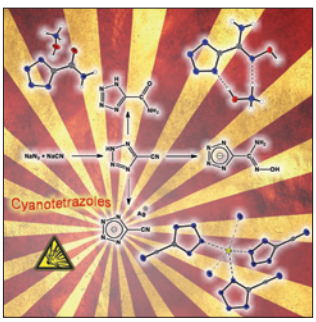

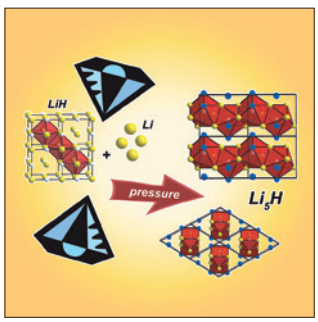

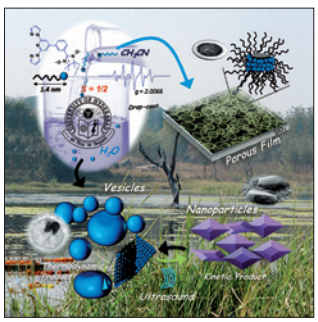

Reprint

A Journal of

ChemPubSoc Europe

WILEY-VCH

www.chempluschem.org

ChemPubSoc Europe

DOI: 10.1002/cplu.201700463

CHEMPLUSCHEM Full Papers

Synthesis of Nontoxic Protoflavone Derivatives through Selective Continuous-Flow Hydrogenation of the Flavonoid B-Ring

Sándor B. Ötvös,*[a, b] Máté Vágvölgyi,[c] Gábor Girst,[a, c] Ching-Ying Kuo,[d] Hui-Chun Wang,[d] Ferenc Fülöp,*[a, b] and Attila Hunyadi*[c, e]

Protoflavones are unique natural flavonoids with a non-aromatic B-ring, known for their potent antitumor properties. However, their cytotoxicity represents a strong limitation in the further exploration of their pharmacological potential. In the current study, we sought to selectively saturate the *p*-quinol B-ring of protoapigenone and that of its 1′-*O*-butyl ether, in order to obtain non-toxic protoflavone analogues expressing the dihydro- or tetrahydroprotoflavone structure also occurring in nature. The benefits of a strictly controlled continuous-flow environment in combination with on-demand electrolytic H_2 gas generation were exploited to suppress undesired side reactions and to safely and selectively yield the desired substances. The obtained tetrahydroprotoflavones were free of the cytotoxicity of their parent compounds, and, even though tetrahydroprotoapigenone 1-*O*-butyl ether showed a weak inhibition of DNA damage response through Chk1, neither compounds influenced the cytotoxicity of doxorubicin either.

Introduction

Protoflavones represent a relatively rare, special class of natural flavonoids most typically occurring in fern species.[1] These compounds express a non-aromatic B-ring, that is, a *p*-quinol-derived moiety that can be either a dienone or its partially or fully saturated analogue. Figure 1 shows the structures of a few selected examples of protoflavonoids isolated from plants: protoapigenone from *Thelypteris torresiana*, 5′,6′-dihydroprotogenkwanone from *Phegopteris decursive-pinnata*, and tetrahydroprotogenkwanone from *Pseudophegopteris subaurita*.[1]

[a] *Dr. S. B. Ötvös, G. Girst, Prof. F. Fülöp*
Institute of Pharmaceutical Chemistry
University of Szeged
Eötvös u. 6, 6720 Szeged (Hungary)
E-mail: otvossandor@pharm.u-szeged.hu
fulop@pharm.u-szeged.hu

[b] *Dr. S. B. Ötvös, Prof. F. Fülöp*
MTA-SZTE Stereochemistry Research Group
Hungarian Academy of Sciences
Eötvös u. 6, 6720 Szeged (Hungary)

[c] *M. Vágvölgyi, G. Girst, Dr. A. Hunyadi*
Institute of Pharmacognosy
University of Szeged
Eötvös u. 6, 6720 Szeged (Hungary)
E-mail: hunyadi.a@pharm.u-szeged.hu

[d] *Dr. C.-Y. Kuo, Dr. H.-C. Wang*
Graduate Institute of Natural Products, College of Pharmacy
Kaohsiung Medical University
Shih-Chuan 1st Rd. 100, 807 Kaohsiung (Taiwan, R.O.C.)

[e] *Dr. A. Hunyadi*
Interdisciplinary Centre of Natural Products
University of Szeged
Eötvös u. 6, 6720 Szeged (Hungary)

Supporting information and the ORCID identification number(s) for the author(s) of this article can be found under https://doi.org/10.1002/cplu.201700463.

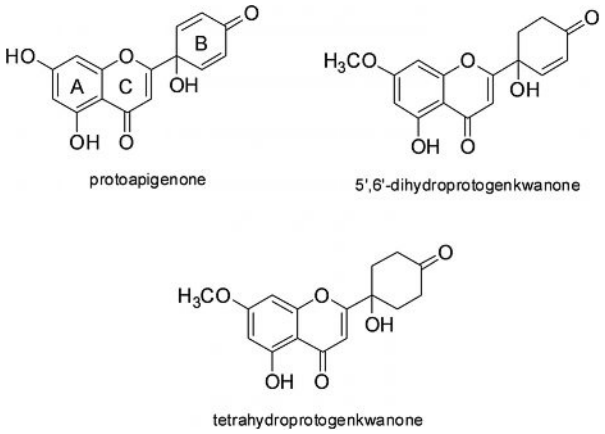

Figure 1. Selected examples of natural protoflavones containing B-rings with different saturation levels.

Protoapigenone was identified as a potent anticancer agent in various in vitro and in vivo bioassays. Moreover, most protoflavones can efficiently bypass multidrug resistance conferred by the efflux transporters ABCB1 and ABCG2, and several of these compounds can selectively kill certain resistant cancer cells that have evolved through adaptation to chemotherapeutics.[2] It may be of particular interest that protoapigenone, together with its synthetic analogue WYC0209, can interfere with crucial DNA damage response mechanisms through the ATR/ATM signaling, which confers these compounds a chemo-sensitizing activity towards DNA damaging chemotherapeutics such as, for example, cisplatin and doxorubicin.[3] Protoapigenone can also inhibit GST-π,[4] a detoxifying enzyme that plays an important role in the chemoresistance of cancer.[5] As for the structure–activity relationships, it appears that the presence of a symmetric dienone *p*-quinol moiety in the B-ring is crucial for the strong cytotoxic activity of protoflavones, and that B-

ring substituents typically decrease this activity.[6] On the other hand, a nonbranching aliphatic side chain three or four carbon atoms in length can be favorable at C-1′: introducing a 1′-*O*-butyl ether moiety to the structure of protoapigenone, for example, can significantly increase the cytotoxic activity while it also greatly improves chemical stability.[7]

On the other hand, protoflavones can also exert bioactivities other than those related to their antitumor effects. Protoapigenone can inhibit the lytic cycle of Epstein Barr virus by inhibiting the expression of lytic proteins, hence preventing the proliferation of the virus.[8] In a recent study, protoapigenone 1′-*O*-propargyl ether was identified as the first nonplanar flavonoid with a strong xanthine oxidase inhibitory activity; this compound is about twice as effective as allopurinol.[9] These examples indicate that protoflavones might likely have a versatile and complex pharmacology, and that a valuable chemical–pharmacological space is potentially hidden behind the cytotoxicity of these compounds.

In this context, the aim of the current study was 1) to investigate whether it is possible to selectively saturate the protoflavone B-ring in order to obtain structural element(s) that are naturally occurring in the dihydro- and/or tetrahydroprotoflavones, and 2) to initiate studies on related pharmacological changes, first focusing on the cytotoxicity and the effect on DNA damage response.

Results and Discussion

Synthesis of tetrahydroprotoflavones

Our synthetic strategy toward the anticipated tetrahydroprotoflavone derivatives involved the oxidative dearomatization of apigenin (a commercially available 4′,5,7-trihydroxyflavone), and the catalytic hydrogenation of the B-ring of the resulting protoflavones. The dearomatization was performed according to our previously published procedure using a common hypervalent iodine reagent, [bis(trifluoroacetoxy)iodo]benzene (PIFA) in acetonitrile in the presence of water or *n*-butanol (Scheme 1).[7] The mixtures were stirred for 1 h at 80 °C to yield protoapigenone (**2**) or protoapigenone 1′-*O*-butyl ether (**3**) after a simple chromatographic purification (see the Experimental Section).

The selective hydrogenation of the B-ring of protoflavones **2** and **3** constitutes a significant synthetic challenge in view of the large number of possible side reactions, including the unwanted reduction of the carbonyl group(s),[10] the (partial)hydrogenation of the C- or even the A-ring, and also the competitive rearomatization of the dienone core (ring B).[11] Moreover,

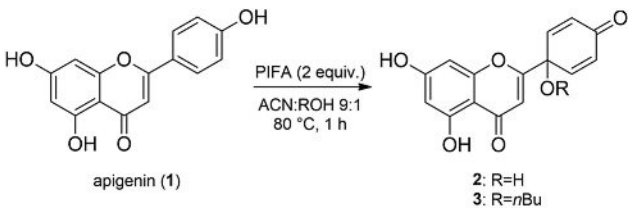

Scheme 1. Synthesis of protoflavones **2** and **3** from apigenin.

in traditional batch-based methodologies, such triphasic catalytic reactions pose a challenge because of the hazardous and highly explosive nature of the gaseous reactant. Since heterogeneous catalytic hydrogenations can offer significant benefits through the advantageous features of continuous processing, we set out to exploit the benefits of a strictly controlled continuous-flow reactor environment.[12]

The heterogeneous catalytic hydrogenations were performed in a high-pressure/high-temperature flow hydrogenation mesoreactor (H-Cube).[13] The H_2 gas necessary for the reactions was generated in situ by electrolytic decomposition of deionized water. The hydrogenation catalyst was placed in a stainless steel cartridge, where the triphasic reaction took place. These features ensured improved operational safety and simplicity over traditional hydrogenation techniques.[14] Importantly, the flow system furnished an excellent level of control over the most important reaction parameters that determine the product selectivity.[15] A representation of the flow reactor is shown in Figure 2.

Based on our previous results on selective C–C double-bond reductions of various aromatic enones,[10a] we initially chose the Lindlar catalyst (5% palladium on $CaCO_3$, poisoned with lead) for a rapid optimization study. In the ambient-temperature (25 °C) hydrogenation of protoapigenone 1′-*O*-butyl ether (**3**) in ethyl acetate (EtOAc) as solvent (at a flow rate of 1 mL min^{-1}), the total conversion steeply rose as a function of the reaction pressure. At 20 and 40 bar, conversions of merely 19 and 43% occurred, respectively (Table 1, entries 1 and 2), but at 80 bar, almost all the starting material was consumed, giving a conversion of 99% (Table 1, entry 3). In these cases, however, the selectivity of the hydrogenation of the dienone core was decreased by the rearomatization of the B-ring, leading to the formation of about 10% apigenin (**1**). As the undesired rearomatization occurs via palladium-mediated hydrogenolysis at C-1′,[11] we attempted to reduce the residence time on the catalyst bed (by improving the flow rate) in order to sup-

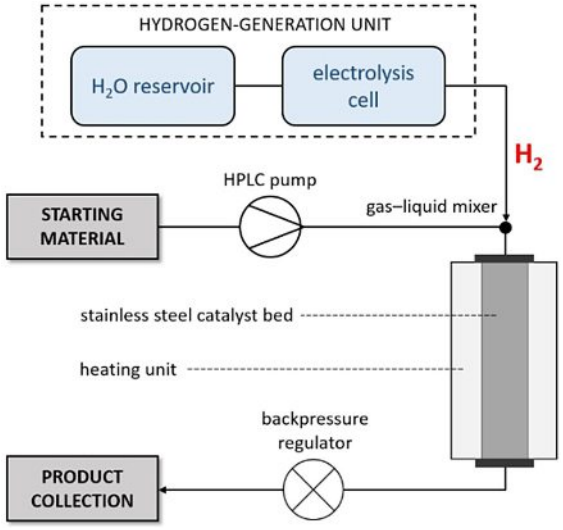

Figure 2. Schematic representation of the continuous-flow hydrogenation reactor.

Table 1. Selective continuous-flow hydrogenation of protoflavones **2** and **3**.

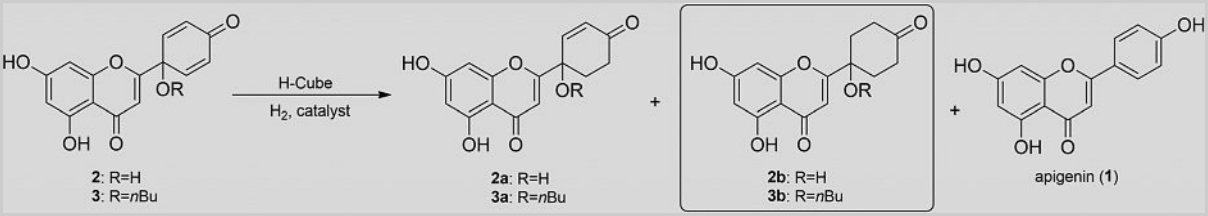

Entry	Substrate[a]	Catalyst	Solvent	*p* [bar]	*T* [°C]	Flow [mL min^{-1}]	Conversion [%][b]	Selectivity [%][b]		
								3a or **2a**	**3b** or **2b**	**1**
1	**3**	Lindlar	EtOAc	20	25	1	19	n.d.	n.d.	n.d.
2	**3**	Lindlar	EtOAc	40	25	1	43	0	88	12
3	**3**	Lindlar	EtOAc	80	25	1	99	0	92	8
4	**3**	Lindlar	EtOAc	80	25	1.5	38	n.d.	n.d.	n.d.
5	**3**	Lindlar	EtOAc	40	50	1	78	0	66	34
6	**3**	Lindlar	MeOH	80	25	1	97	0	81	19
7	**3**	5% Pd/C	EtOAc	20	25	1	71	0	82	18
8	**3**	5% Pd/C	EtOAc	40	25	1	100	0	84	16
9	**2**	5% Pd/C	EtOAc	40	25	1	99	traces	77	23
10	**2**	5% Pd/C	MeOH	40	25	1	99	traces	80	20

[a] $c_{substrate} = 1$ mg mL^{-1}. [b] Determined by ^{1}H NMR spectroscopic analysis of the crude material.

press apigenin (**1**) formation. Unfortunately, when we increased the flow rate, the total conversion fell significantly below optimal (Table 1, entry 4). Furthermore, the extent of unwanted rearomatization was found to be strongly dependent on the temperature applied: heating the reactor zone from 25 to 50 °C at 40 bar resulted in a significant increase in apigenin (**1**) formation at the expense of the amount of the desired tetrahydro derivative **3b** (Table 1, entry 2 vs. entry 5). It should be emphasized that (partial) reduction of the 4*H*-chromen-4-one core was not detected under any of the reaction conditions applied.

Although, by using Lindlar catalyst, we managed to find suitable reaction conditions for the highly selective formation of tetrahydroprotoflavone **3b** (Table 1, entry 3), unfortunately, rapid deactivation of the catalyst prevented successful preparative-scale continuous-flow synthesis (6 h run under the optimized reaction conditions without changing the catalyst column, see the Experimental Section). We therefore repeated the reaction at 25 °C and 80 bar with MeOH as the solvent (Table 1, entry 6). In a small-scale model reaction, the conversion and product ratio were similar to those recorded when EtOAc was used as the solvent, but scale-up proved again impractical because of fast catalyst deactivation. We speculated that the irreversible nature of the substrate adsorption on the catalyst support may account for the rapid catalyst deactivation. We then turned our attention to 5% palladium on charcoal (Pd/C) as a heterogeneous hydrogenation catalyst. After a couple of small-scale test reactions (entries 7 and 8), we achieved complete conversion and an excellent chemoselectivity toward the formation of the desired tetrahydroprotoflavone **3b** (**3b**/**1** ratio was 84:16, entry 8). In this case, no catalyst deactivation occurred, and successful preparative-scale synthesis could be achieved.

The previously optimized reaction conditions with 5% Pd/C as catalyst could simply be transferred to the hydrogenation of protoapigenone (**2**); however, the solvent was switched to MeOH due to solubility issues (Table 1, entries 9 and 10). Interestingly, traces of the corresponding dihydroprotoflavone byproduct **2a** with a partially hydrogenated B-ring could be detected in this case, but the desired tetrahydro derivative **2b** could be obtained with high chemoselectivity as the main product (Table 1, entry 10). Upon scaling up, no catalyst deactivation occurred.

Bioactivity testing

In accordance with our overall aim to explore the pharmacology of B-ring-saturated protoflavones, compounds **2b** and **3b** were tested for their in vitro cytotoxicity on MCF-7 (breast), HeLa (cervix), and SiHa (cervix) cancer cell lines. As expected, the compounds did not show relevant cytotoxicity; an IC_{50} value could be calculated only for compound **3b** on HeLa cells (55.12 ± 1.11 μM); all other results corresponded to less than 50% inhibition at protoflavone concentrations as high as 100 μM. This confirmed our previous assumption that a great decrease in cytotoxicity should be observed upon saturation of the B-rings of compounds **2** and **3**, which were previously found to kill, for example, MCF-7 cells at IC_{50} values of 1.70 and 1.38 μM, respectively.[7]

The compounds were also tested for their potential to interfere with the ATR/ATM signaling pathways, whose inhibition would confer them chemosensitizing activity towards DNA-damaging chemotherapeutics. After MCF-7 cells were pretreated with or without 5, 10, or 20 μM of compound **2b** or **3b** for 30 min, DNA damage was induced by exposing the cells to 1 μM of doxorubicin for 6 h; the results are shown in Figure 3. In contrast with the parental protoapigenone (**2**), compound **2b** was found to be inactive on checkpoint kinase 1 and 2 (Chk1 and Chk2, respectively). Compound **3b** was able to exert significant inhibitory activity on the phosphorylation (i.e., activation) of Chk1, but only at the highest tested dose,

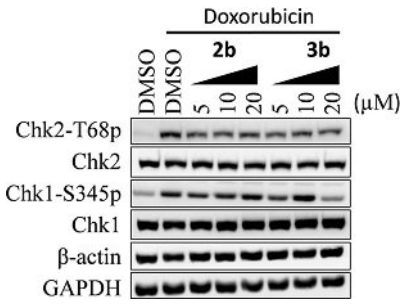

Figure 3. Inhibition of doxorubicin-induced DNA damage response by compounds **2b** and **3b**. Chk1 and Chk2: Checkpoint kinase 1 and 2, respectively.

20 μM. This would imply that this compound, at least at a higher dose, might have potential as a chemosensitizing agent for use as an adjuvant in chemotherapy. In order to test this hypothesis, a series of combination studies were performed with compound **2b** or **3b** together with doxorubicin. The checkerboard microplate method was utilized, and three biological replicates (each in triplicate) were performed in order to assure the highest possible accuracy and reveal any mild interaction. In this experiment, neither compound was found to interfere with the cytotoxicity of doxorubicin.

Conclusion

By developing a highly selective and efficient continuous-flow method, we successfully saturated the B-ring of two cytotoxic protoflavones, protoapigenone and its 1′-*O*-butyl ether. This allowed us to obtain, for the first time, compounds containing the rare, natural tetrahydroprotoflavone moiety. Our study on the compounds' cytotoxicity and their effect on the DNA damage response through the ATR/ATM signaling pathway revealed that related bioactivities, including the inhibition of Chk1 and Chk2 phosphorylation, require the presence of a symmetric dienone moiety in the flavonoid B-ring as in protoapigenone. Even though a higher dose of the 1′-*O*-butyl ether derivative **3b** was able to inhibit Chk1 phosphorylation, none of the compounds demonstrated any interaction with the in vitro cytotoxicity of doxorubicin. Accordingly, our synthetic method can conveniently knock out all those bioactivities of protoflavonoids that could potentially confer them toxic side effects. This opens up new possibilities to explore the pharmacology of this unique group of natural products.

Experimental Section

Product analysis

The identity of protoflavone substrates **2** and **3** was confirmed by HPLC-PDA in comparison with authentic reference compounds whose full characterization has been reported previously.[7] Protoflavones **2b** and **3b** were characterized by means of NMR, MS, and HPLC methods. ^{1}H, ^{13}C, ^{13}C HSQC, and ^{13}C HMBC NMR spectra were recorded in [D_6]DMSO on a Bruker Avance DRX 400 instrument with TMS as the internal standard, at 400.1 and 100.6 MHz, respectively. Copies of the NMR spectra can be found in the Supporting Information. High-resolution mass spectrometry (HRMS) was performed on a Q-Exactive Plus Orbitrap spectrometer (Thermo Fisher Scientific, USA) in positive-ion mode by using flow injection analysis. Samples were dissolved in methanol at 100 μg mL^{-1} concentration, and 10 μL portions were injected at a flow rate of 200 μL min^{-1} eluting with a water/acetonitrile mixture (50:50) containing 0.1 % formic acid. HRMS spectra are available in the Supporting Information. Each derivative was analyzed by RP-HPLC on a Jasco HPLC instrument equipped with a MD-2010 Plus PDA detector (Jasco Analytical Instruments, Japan) in a detection range of 210–400 nm. Chromatographic identification of substrate **2** and its derivatives **1**, **2a**, and **2b** was carried out by using a Kinetex XB-C18 100A 5μ 250×4.6 mm RP-HPLC column (Phenomenex Inc., USA) with isocratic grade elution with MeOH/water (60:40) applied for a run time of 20 minutes with a flow rate of 0.9 mL min^{-1}. In the case of protoflavone substrate **3** and products **1**, **3a**, and **3b**, a Kinetex Biphenyl 100A 5μ 250×4.6 mm RP-HPLC column was chosen (Phenomenex Inc., USA) for qualitative chromatographic analysis, and a gradient elution (acetonitrile/water 35:65 v/v continuously increasing to 70:30 in 25 minutes) was applied at a constant flow rate of 1 mL min^{-1}. Following chromatographic purification, all obtained derivatives were tested for their purity by RP-HPLC utilizing the abovementioned methods.

Synthesis of protoflavones 2 and 3

Apigenin was dissolved at a concentration of 1 mg mL^{-1} in a 9:1 v/v mixture of acetonitrile (ACN) and water or *n*-butanol. PIFA (2 equiv) was added to the mixture. After the mixture had been stirred at 80 °C for 1 hour, it was was cooled down, evaporated under reduced pressure, and purified by flash chromatography using mixtures of CH_2Cl_2/MeOH (97:3) or *n*-hexane/EtOAc/acetone (80:15:5) as eluent to obtain compound **2** or **3**, respectively. Characteristic properties of these compounds has been reported previously; yields of all synthetic attempts were in perfect agreement with the available data.[7]

General procedure for the continuous-flow hydrogenations

The hydrogenation reactions were carried out in an H-Cube system (ThalesNano Inc.) The catalyst cartridge (internal dimensions: 30 mm×4 mm) contained approximately 100 mg of the appropriate hydrogenation catalyst. The continuous stream of the reaction solution was provided by a conventional HPLC pump (KnauerWellChrom K-120). For each reaction, a 1-mg mL^{-1} solution of the corresponding protoflavone was prepared in EtOAc or MeOH (HPLC grade). The mixture was homogenized by sonication and then pumped through the reactor under the selected conditions. For small-scale test reactions (screening purposes), 15 mL solutions were prepared. For preparative-scale syntheses, the concentration of the starting material was not varied, but 360 mL solutions were prepared and pumped through the instrument without changing the catalyst cartridge. Between two reactions, the catalyst bed was washed for 15 min with EtOAc or MeOH at 1 mL min^{-1}.
The conversion and the product ratio were determined by ^{1}H NMR analysis of the crude materials, from the relative intensities of the signals of the dienone B-ring of the starting material, the aromatic B-ring signals of apigenin, and the A- or C-ring signals of the hydrogenated product.

Product purification

Chromatographic purification of products **2b** and **3b** was carried out using a CombiFlash R_f+ Lumen flash chromatographic instru-

ment (TELEDYNE Isco, USA) with integrated UV/Vis, PDA, and ELS detection applied with commercially available prefilled columns (TELEDYNE Isco, USA) for normal-phase separations in a detection range of 210–366 nm. Protoflavone derivative **2b** was purified using a poliamide column for gradient-grade separation applying mixtures of CH_2Cl_2/MeOH where the ratio of MeOH was set to constantly increase from 2% to 5% in 50 minutes. Product **3b** was purified utilizing a silica column and gradient-grade elution with *n*-hexane (solvent A) and ethyl acetate/acetone 3:1 (solvent B). In this case, the ratio of solvent B was set to continuously increase from 5% to 20% in 70 minutes.

Analytical data

Tetrahydroprotoapigenone (2b): Yield: 69.3%; RP-HPLC purity: 97.0%; pale-brown solid; ^{1}H NMR (400.1 MHz, [D$_6$]DMSO) δ_H: 1.99–2.10 (m, 2H, CH_2), 2.16–2.25 (m, 2H, CH_2), 2.26–2.37 (m, 2H, CH_2), 2.64–2.78 (m, 2H, CH_2),6.19 (s, 1H, Ar-H), 6.38 (s, 1H, Ar-H), 6.41 (s, 1H, Ar-H); ^{13}C NMR (100.6 MHz, [D$_6$]DMSO) δ_C: 35.1, 37.0, 71.2, 94.9, 99.9, 104.4, 105.6, 158.5, 162.3, 165.5, 175.0, 182.9, 210.2. HRMS $C_{15}H_{15}O_6$, calculated: 291.08631, found: 291.08604.

Tetrahydroprotoapigenone 1′-*O*-butyl ether (3b): Yield: 57.5%; RP-HPLC purity: 99.8%; pale-yellow solid; ^{1}H NMR (400.1 MHz, [D$_6$]DMSO) δ_H: 0.85 (t, 3H, CH_3, J=7.00 Hz), 1.29–1.42 (m, 2H, CH_2), 1.47–1.58 (m, 2H, CH_2), 2.13–2.27 (m, 4H, 2CH_2), 2.32–2.42 (m, 2H, CH_2), 2.52–2.62 (m, 2H, CH_2), 3.35 (t, 2H, CH_2, J=6.61 Hz), 6.20 (s, 1H, Ar-H), 6.32 (s, 1H, Ar-H), 6.38 (s, 1H, Ar-H); ^{13}C NMR (100.6 MHz, [D$_6$]DMSO) δ_C: 14.6, 19.7, 32.0, 32.5, 36.7, 63.5, 76.1, 94.9, 100.0, 104.7, 108.2, 158.6, 162.3, 165.7, 170.2, 182.5, 209.8. HRMS $C_{19}H_{23}O_6$, calculated: 347.14891, found: 347.14833.

Bioactivity testing

Detection of DNA damage response was achieved by Western blot assay as previously described.[4] Primary phospho-specific antibodies, which recognize the phosphorylated Chk1 serine 345 or Chk2 threonine 68 residues, respectively, were used to detect DNA damage induced by doxorubicin treatment. The antibodies recognize full-length Chk1, Chk2, actin, and gapdh, showing that treatment with the compounds did not affect gene expression of these proteins, which served as protein loading controls. The binding of primary antibodies was detected with horseradish peroxidase coupled secondary antibodies followed by an enhanced chemiluminescent reaction. The chemiluminescent signals on the blots were captured using a luminescent image analyzer. For testing the interaction between the new compounds and doxorubicin, the cultured MCF-7 breast cancer cells were treated by using the checkerboard microplate method, and a serial dilution (0–80 μM concentration range) of **2b** or **3b** was combined with a serial dilution of doxorubicin (0–2 μM concentration range) for 48 hours. The surviving cells were detected by the MTT assay. In the case of compound **2b** which did not exert measurable cytotoxicity at the applied concentration range when employed alone, IC_{50} values of doxorubicin were calculated by the GraphPad Prism 5.03 software (GraphPad Software Inc., San Diego, CA, USA), and datasets obtained for the single treatment were compared with those of the combinations. In the case of compound **3b**, the corresponding wells of the replicate plates were averaged into one dataset, which was then utilized to calculate combination index values for the constant ratios of compound vs. doxorubicin by using the CompuSyn software (CompuSyn Inc., Paramus, NJ, USA).

Acknowledgements

This study was funded by the National Research, Development and Innovation Office, Hungary (NKFIH; K119770). We acknowledge support from the EU-funded Hungarian grant EFOP-3.6.1–16–2016-00008, and from the Project-Based Personnel exchange Program (PPP) of the Hungarian Academy of Sciences and the Ministry of Science and Technology, Taiwan, R.O.C. H.C.W. acknowledges the grant 103-2320-B-037-007-MY3 from the Ministry of Science and Technology, Taiwan (R.O.C). S.B.Ö. acknowledges the Premium Post-Doctoral Research Program of the Hungarian Academy of Sciences; A.H. acknowledges the János Bolyai fellowship of the Hungarian Academy of Sciences and the Kálmán Szász Prize. We are grateful to Attila Csorba for the HRMS measurements.

Conflict of interest

The authors declare no conflict of interest.

Keywords: cancer · DNA damage · flavonoids · flow chemistry · hydrogenation

[1] A. Hunyadi, A. Martins, B. Danko, F. R. Chang, Y. C. Wu, *Phytochem. Rev.* **2014**, *13*, 69–77.
[2] B. Dankó, S. Toth, A. Martins, M. Vagvolgyi, N. Kusz, J. Molnar, F. R. Chang, Y. C. Wu, G. Szakacs, A. Hunyadi, *ChemMedChem* **2017**, *12*, 850–859.
[3] H.-C. Wang, A. Y.-L. Lee, W.-C. Chou, C.-C. Wu, C.-N. Tseng, K. Y.-T. Liu, W.-L. Lin, F.-R. Chang, D.-W. Chuang, A. Hunyadi, Y.-C. Wu, *Mol. Cancer Ther.* **2012**, *11*, 1443–1453.
[4] W. Y. Chen, Y. A. Hsieh, C. I. Tsai, Y. F. Kang, F. R. Chang, Y. C. Wu, C. C. Wu, *Invest. New Drugs* **2011**, *29*, 1347–1359.
[5] D. M. Townsend, K. D. Tew, *Oncogene* **2003**, *22*, 7369–7375.
[6] A. S. Lin, F. R. Chang, C. C. Wu, C. C. Liaw, Y. C. Wu, *Planta Med.* **2005**, *71*, 867–870.
[7] A. Hunyadi, D. W. Chuang, B. Danko, M. Y. Chiang, C. L. Lee, H. C. Wang, C. C. Wu, F. R. Chang, Y. C. Wu, *PloS One* **2011**, *6*, e23922.
[8] C. P. Tung, F. R. Chang, Y. C. Wu, D. W. Chuang, A. Hunyadi, S. T. Liu, *J. Gen. Virol.* **2011**, *92*, 1760–1768.
[9] A. Hunyadi, A. Martins, B. Danko, D.-W. Chuang, P. Trouillas, F.-R. Chang, Y.-C. Wu, G. Falkay, *Tetrahedron Lett.* **2013**, *54*, 6529–6532.
[10] a) C.-T. Hsieh, S. B. Ötvös, Y.-C. Wu, I. M. Mándity, F.-R. Chang, F. Fülöp, *ChemPlusChem* **2015**, *80*, 859–864; b) S. B. Ötvös, C.-T. Hsieh, Y.-C. Wu, J.-H. Li, F.-R. Chang, F. Fülöp, *Molecules* **2016**, *21*, 318.
[11] a) K. Endo, K. Seya, H. Hikino, *Tetrahedron* **1989**, *45*, 3673–3682; b) F. Busqué, M. Cantó, P. de March, M. Figueredo, J. Font, S. Rodríguez, *Tetrahedron: Asymmetry* **2003**, *14*, 2021–2032.
[12] a) M. Irfan, T. N. Glasnov, C. O. Kappe, *ChemSusChem* **2011**, *4*, 300–316; b) I. M. Mándity, S. B. Ötvös, F. Fülöp, *ChemistryOpen* **2015**, *4*, 212–223; c) V. Hessel, D. Kralisch, N. Kockmann, T. Noël, Q. Wang, *ChemSusChem* **2013**, *6*, 746–789; d) J. Wegner, S. Ceylan, A. Kirschning, *Chem. Commun.* **2011**, *47*, 4583–4592.
[13] R. V. Jones, L. Godorhazy, N. Varga, D. Szalay, L. Urge, F. Darvas, *J. Comb. Chem.* **2006**, *8*, 110–116.
[14] I. M. Mándity, S. B. Ötvös, G. Szőllősi, F. Fülöp, *Chem. Rec.* **2016**, *16*, 1018–1033.
[15] Z. Szakonyi, T. Gonda, S. B. Ötvös, F. Fülöp, *Tetrahedron: Asymmetry* **2014**, *25*, 1138–1145.

Manuscript received: November 2, 2017
Revised manuscript received: November 17, 2017
Accepted manuscript online: November 18, 2017
Version of record online: December 7, 2017

V.

International Journal of
Molecular Sciences

MDPI

Article

Less Cytotoxic Protoflavones as Antiviral Agents: Protoapigenone 1′-*O*-isopropyl ether Shows Improved Selectivity Against the Epstein–Barr Virus Lytic Cycle

Máté Vágvölgyi [1], Gábor Girst [1,2], Norbert Kúsz [1], Sándor B. Ötvös [2,3], Ferenc Fülöp [2,3], Judit Hohmann [1,4], Jean-Yves Servais [5], Carole Seguin-Devaux [5], Fang-Rong Chang [6], Michael S. Chen [7], Li-Kwan Chang [7] and Attila Hunyadi [1,4,*]

1 Institute of Pharmacognosy, Interdisciplinary Excellence Centre, University of Szeged, 6720 Szeged, Hungary; vagvolgyi.mate@pharm.u-szeged.hu (M.V.); girst.gabor@pharmacognosy.hu (G.G.); kusz.norbert@pharm.u-szeged.hu (N.K.); hohmann@pharm.u-szeged.hu (J.H.)
2 Institute of Pharmaceutical Chemistry, University of Szeged, 6720 Szeged, Hungary; otvossandor@pharm.u-szeged.hu (S.B.Ö.); fulop@pharm.u-szeged.hu (F.F.)
3 MTA-SZTE Stereochemistry Research Group, Hungarian Academy of Sciences, 6720 Szeged, Hungary
4 Interdisciplinary Centre for Natural Products, University of Szeged, 6720 Szeged, Hungary
5 Department of Infection and Immunity, Luxembourg Institute of Health, L-4354 Esch-sur-Alzette, Luxemburg; Jean-Yves.Servais@lih.lu (J.-Y.S.); Carole.Devaux@lih.lu (C.S.-D.)
6 Graduate Institute of Natural Products, Kaohsiung Medical University, Kaohsiung 807, Taiwan; aaronfrc@kmu.edu.tw
7 Department of Biochemical Science and Technology, College of Life Science, National Taiwan University, Taipei City 10617, Taiwan; b05b02041@ntu.edu.tw (M.S.C.); changlk@ntu.edu.tw (L.-K.C.)
* Correspondence: hunyadi.a@pharm.u-szeged.hu; Tel.: +36-62-546-456

Received: 17 October 2019; Accepted: 9 December 2019; Published: 12 December 2019

Abstract: Protoflavones, a rare group of natural flavonoids with a non-aromatic B-ring, are best known for their antitumor properties. The protoflavone B-ring is a versatile moiety that might be explored for various pharmacological purposes, but the common cytotoxicity of these compounds is a limitation to such efforts. Protoapigenone was previously found to be active against the lytic cycle of Epstein–Barr virus (EBV). Further, the 5-hydroxyflavone moiety is a known pharmacophore against HIV-integrase. The aim of this work was to prepare a series of less cytotoxic protoflavone analogs and study their antiviral activity against HIV and EBV. Twenty-seven compounds, including 18 new derivatives, were prepared from apigenin through oxidative de-aromatization and subsequent continuous-flow hydrogenation, deuteration, and/or 4′-oxime formation. One compound was active against HIV at the micromolar range, and three compounds showed significant activity against the EBV lytic cycle at the medium-low nanomolar range. Among these derivatives, protoapigenone 1′-*O*-isopropyl ether (**6**) was identified as a promising lead that had a 73-times selectivity of antiviral over cytotoxic activity, which exceeds the selectivity of protoapigenone by 2.4-times. Our results open new opportunities for designing novel potent and safe anti-EBV agents that are based on the natural protoflavone moiety.

Keywords: natural product; drug discovery; protoflavonoid; continuous-flow chemistry; oxime; antitumor; antiviral; Epstein–Barr virus; lytic cycle

1. Introduction

Protoflavonoids represent a relatively rare, naturally occurring group of flavonoids, which possess a non-aromatic B-ring and a hydroxyl function at C-1′. This unique structural moiety can appear in various forms, it is most typically a symmetric dienone *p*-quinol that may be partially or fully saturated, as shown by the examples of some natural protoflavones illustrated in Figure 1 [1].

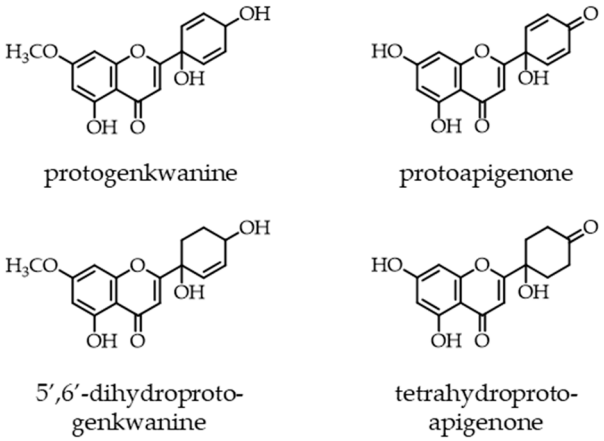

Figure 1. Examples of natural protoflavones with different moieties in their B-ring. A symmetric dienone structure, as in protoapigenone, is prerequisite of a strong cytotoxic activity.

Many protoflavones are known for their potent anticancer activity and, until now, this is the bioactivity that is by far the most deeply investigated for this compound family. Protoflavones are known to be cytotoxic on a wide range of cancer cell lines in vitro, and some can selectively kill multi-drug resistant cancer cell lines that are adapted to chemotherapeutics [2,3]. Some protoflavones, e.g., protoapigenone, were also tested in vivo and found active against a variety of tumor xenograft models [1]. A particularly interesting pharmacodynamic property of protoapigenone is that it is a potent inhibitor of the ATR-mediated activation of checkpoint kinase 1 (Chk1) [4], a DNA damage response mechanism that is an emerging antitumor target in the focus of several currently ongoing clinical trials [5].

From the available structure-activity relationships that were obtained from synthetic [6] and semi-synthetic [7] analogs, it is known that (a) presence of a symmetric dienone with a non-substituted *p*-quinol B-ring is essential for a strong cytotoxic effect [8], (b) the presence of a longer non-branching (e.g., butyl) alkyl substituent at the 1′-OH can further enhance cytotoxicity against some cell lines, and (c) a branching 1′-*O*-alkyl substituent (e.g., isopropyl) strongly decreases cytotoxicity. It is also worth noting that a 1′-*O*-alkyl substitution results in a chemically much more stable B-ring when compared to the non-substituted *p*-quinol [7].

However, the possible use of protoflavonoids might exceed their antitumor potential. The non-aromatic B-ring containing an sp^3 carbon at C-1′ makes the three-dimensional (3D) structure of these compounds very unique among flavonoids. This might lead to a versatile pharmacology that is hardly explored. Previously, we identified protoapigenone 1′-*O*-propargyl ether as the first non-planar flavonoid that can exert a potent inhibitory effect on xanthine oxidase, a pro-oxidant enzyme that is involved in many chronic diseases [9]. In addition to this, we found that protoapigenone exerts an antiviral effect against the Epstein–Barr Virus (EBV) in vitro through inhibiting the expression of EBV lytic proteins [10]. These results suggest that the chemical space of protoflavones has still much to offer in bioactivities other than antitumor effect, while cytotoxicity itself certainly represents a limitation for exploring these.

We recently reported a method for the highly selective saturation of the protoflavone B-ring by means of continuous flow hydrogenation under mild reaction conditions to overcome this limitation.

This allowed for us to obtain the rare, naturally occurring tetrahydroprotoflavone moiety, while also providing an effective tool to eliminate the cytotoxicity of the derivatives [11].

The aim of our current work was to further explore the antiviral potential of protoflavonoids by preparing a series of less cytotoxic derivatives, and then test them against EBV and, while considering the antiretroviral activity of various other types of flavonoids [12–14], also against HIV.

2. Results and Discussion

2.1. Synthesis of B-Ring Modified Protoapigenone Analogs

First, we prepared the 1′-*O*-alkyl substituted protoapigenone derivatives from apigenin (**1**), following our previously described procedure [7]. Oxidative dearomatization of the B-ring of apigenin was achieved by a hypervalent iodine reagent, [bis(trifluoroacetoxy)iodo]benzene, and the solvent was 10% *v*/*v* of water or alcohol in acetonitrile depending on the substituent to be coupled at C-1′. This allowed for us to obtain compounds **2**–**8** as potential intermediates for further transformations, among which **6** was already a compound of interest for this study due to its very weak cytotoxicity when compared to the others.

As detailed above, the function that is dominantly responsible for the cytotoxicity of protoflavones is the symmetric dienone moiety on the B-ring, conferring pro-oxidant and Micheal-acceptor properties to the compound. While considering this, we employed two different targeted synthetic strategies for eliminating cytotoxicity: (i) Saturation of the double bonds through hydrogenation or deuteration and (ii) substituting the 4′-oxo group with an oxime function. Scheme 1 shows synthetic routes.

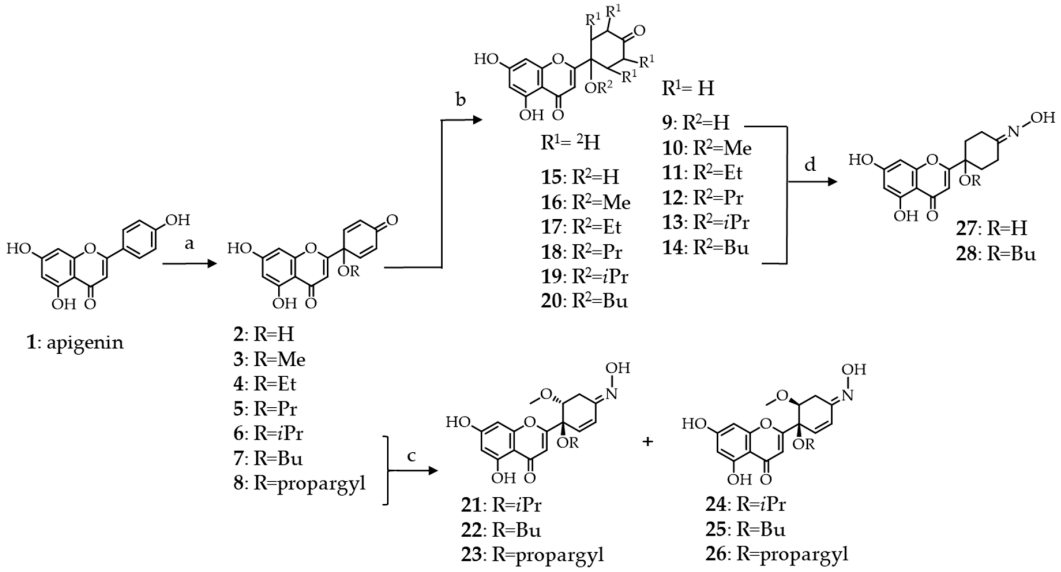

Scheme 1. Semi-synthetic routes employed for the preparation of tetrahydro-, tetradeutero- or 4′-oxime analogs of protoapigenone and its 1′-*O*-alkyl ether derivatives. Oxime derivatives **21**–**28** were obtained as racemates, however, for simplicity only one enantiomer is shown. *Reaction conditions:* (**a**) CH_3CN/ROH—9:1, PIFA (2 equiv.), 80°C, 1 h; (**b**) H-Cube®, **9**–**14**: H_2, 5% Pd/C or **15**–**20**: D_2, 5% Pd/$BaSO_4$; (**c**) NH_2OH·HCl (3 equiv.), MeOH, reflux, 24 h; and, (**d**) NH_2OH·HCl (4 equiv.), MeOH, reflux, 3 h.

The hydrogenation of protoflavonoids' dienone moiety might result various products. Following our previously published procedure, the saturation of the protoflavone B-ring was achieved with high selectivity under mild reaction conditions while utilizing a modified H-cube® continuous flow hydrogenation reactor [11]. Employing this device has several advantages when compared to traditional batch hydrogenation, i.e., the ease of handling of the explosive gas, precise control over the reaction conditions, instrumentally controlled gas pressure, sustainability, and safe applicability.

During this process, hydrogen gas was in situ generated by an electrolytic cell fueled with high purity water, and forwarded to interact with the substrate's solution. The mixture was then passed through a stainless-steel tube that was filled with the catalyst, where the triphasic reaction took place. During each transformation, the catalyst bed was placed in a thermostat to assure temperature control. Products of the reactions were collected into glass vials and subsequently purified by RP-HPLC to obtain tetrahydroprotoapigenone analogs **9**–**14** in high purity (Scheme 1).

Deuterium is applied in organic chemistry for several purposes. It is employed as a tracer in studies that aim to follow the reaction routes or as a reference for determining the influence of isotope effects on the development of a reaction during kinetic studies. Isotope labeling is a versatile technique that can be used many ways, including e.g., metabolomic studies, and the importance of deuterium in isotope labeling is increasing as new applications emerge [15,16].

Deuterium can also be of potential interest for discovery, since it can significantly influence bioactivity of a compound due to the so-called isotope effect [17,18]. Several methods are available for the synthetic preparation of deuterium containing compounds. The conventional batch synthesis of deuterated molecules suffers from similar drawbacks as hydrogenation, such as the lack of sustainability and the low purity and high price of D_2 gas. Therefore, we used a previously established continuous-flow method in this current work [19–21], during which the required deuterium gas was in situ generated from high-purity D_2O with H-Cube®. The reaction was performed in an aprotic solvent, ethyl acetate, to ensure that no hydrogen-deuterium exchange occurs during the transformation. For the same reason, we chose barium sulfate as the catalyst carrier, since activated charcoal might contain protic contaminations on its surface. In all other aspects of the synthesis, we followed the same procedure as in the case of hydrogenation, to obtain tetradeuteroprotoapigenone derivatives **15**–**20** (Scheme 1).

Several studies underline that the preparation of flavonoid oxime derivatives can be a simple yet effective synthetic option for enhancing certain biological effects of the parent compound, e.g., antimicrobial [22], antioxidant [23], and antitumor [24] properties. Compounds with different B-ring saturation and/or 1′-*O*-substituents (**6**–**9** and **14**) were selected for the preparation of 4′-oximes to further increase chemical and consequential pharmacological diversity (Scheme 1).

Our preliminary small-scale test reactions indicated that oxime formation of protoflavones is regioselective at the 4′-keto group, and under the synthetic conditions applied, we did not observe the formation of 4-oxime nor 4,4′-dioxime side products. On the other hand, the solvent appeared to play a crucial role in the possible outcome of the transformation. Pyridine, ethanol, and acetonitrile are probably among the most commonly used solvents in oxime synthesis. However, none of these worked in our case and, finally, we found methanol to be the best solvent for reacting protoflavones with hydroxylamine. The yields appeared to vary greatly, depending on the substrate's concentration in the reaction solution, and we obtained the best yields with ca. 2–2.5 mg/mL concentrations; both lower and higher concentrations could significantly decrease the efficiency of the transformation.

Regioselective transformation of the tetrahydroprotoflavone analogs **9** and **14** to their corresponding 4′-oximes **27** and **28** was straightforward. However, in the case of protoflavones **6**–**8**, each transformation was accompanied by a regioselective Michael addition of methanol at C-2′, forming a methoxy group and saturating one of the double bonds to yield 2′-methoxy-2′3′-dihydroprotoapigenone 4′-oxime derivatives **21**–**26**. The orientation of the methoxy group was apparently random, since the 1′,2′-*cis* and *trans* derivatives were formed in a ca. 1:1 ratio. When assigning the relative configuration of the 1′,2′-carbon atoms, we could not observe diagnostic NOESY cross-peaks between the 2′-methoxy and the 1′-*O*-alkyl substituents for any of these compounds. Therefore, *cis*-*trans* isomers were assigned based on the characteristic coupling constant patterns that were observed between H-2′ and H-3′a or H-3′b. To achieve this, structures were optimized by the MMFF94x force field in CCG-MOE, the H2′-C2′-C3′-H3′a, and H2′-C2′-C3′-H3′b dihedral angles were measured, and theoretical ^{1}H-^{1}H ^{3}J coupling constants were calculated by means of the Bothner-By equation. The experimental coupling constants showed good agreement with the calculated values, unambiguously assigning compounds **21**–**23** as the 1′,2′-*trans*, and **24**–**26** as the 1′,2′-*cis* isomers. Nevertheless, while each compound was

obtained as racemate, the newly formed oxime took a defined orientation in all of them. This suggests that the solvent addition took place to an intermediate of the reaction in a way that it determined the final orientation of the oxime. We considered compounds **27** and **28** as internal references, since the exact data of the Δδ syn-anti parameters were not available this way, which provided us with the chemical shifts for both neighbouring methylenes of the oxime. In these compounds, C-3′ (syn) and C-5′ (anti) gave ^{13}C NMR chemical shifts at ca. 18.8 and 26.2 ppm, respectively. The ^{13}C NMR signals of the 3′-CH_2 moieties of compounds **21**–**26** appeared within the range of 22.7–23.7 ppm, which strongly suggests that the oxime is present in *E*-orientation in each of these compounds while also taking the effect of the electron-rich neighbouring OCH_3 group into account.

2.2. Biological Activities

2.2.1. Antiretroviral Activity

Compounds **2**, **6**–**14**, and **21**–**28** were tested against HIV-1 while using a pseudotype virus assay allowing only one cycle of viral replication and being more sensitive for compounds targeting the early steps of HIV replication, such as reverse transcription and integration [25]. Tetrahydroprotoapigenone (**9**) was found to inhibit viral infection by ca. 50% at the non-cytotoxic concentration of 100 μM (see Supplementary Materials, Table S1). While this represents a rather weak activity, it might still be of interest, since this compound was not cytotoxic on the host cells at as high as 500 μM concentration.

2.2.2. Antiviral Activity against EBV

Compounds **2** and **6**–**28** were tested for their activity on the EBV lytic cycle. To assess this, the P3HR1 cells were treated with sodium butyrate and TPA for 24 h. As expected, lytic protein Rta was expressed after lytic induction. As a first screening, the cells were treated with protoapigenone (**2**), used as a positive control, or compounds **6**–**28** at the induction of lytic cycle for 24 h. The concentration selected for screening was 0.25 μM, where protoapigenone (**2**) was previously found to exert a strong activity [10]. The results indicated that three of the analogs, **6**, **7**, and **8** can inhibit EBV lytic cycle at this concentration. These compounds were then tested for the dose dependency of their effect on the expression of Rta; Figure 2 shows the results.

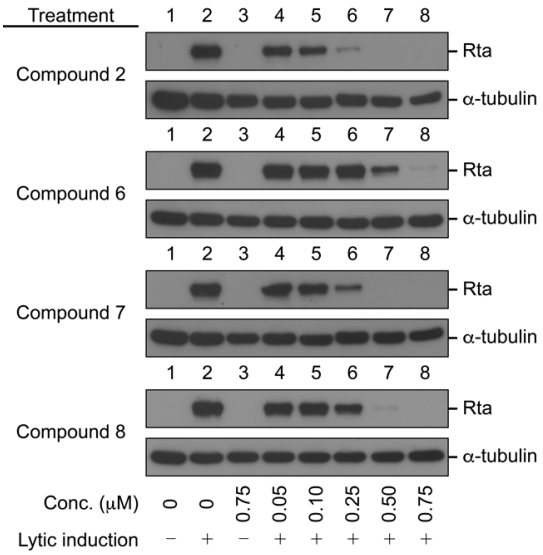

Figure 2. Inhibition of the expression of Epstein–Barr Virus (EBV) Rta by protoapigenone (**2**) and its analogs **6**–**8**. The cells were treated with the compounds at the time of lytic induction with SB and TPA. Cell lysates were harvested at 24 h after lytic induction. Proteins in the lysate were detected by immunoblotting using anti-Rta and anti-α-tubulin antibodies. Calculated IC_{50} values for **2**, **6**, **7,** and **8** were 0.127, 0.467, 0.208, and 0.285 μM, respectively.

We found that, similarly to protoapigenone (**2**), compounds **6**, **7,** and **8** also caused a marked reduction in the Rta levels at 0.50, 0.25, and 0.50 μM, respectively, and the IC_{50} values were calculated as 0.467, 0.208, and 0.285 μM, respectively. The positive control protoapigenone (**2**) acted with an IC_{50} value of 0.127 μM, which was in good agreement with our previous findings [10]. Subsequently, we conducted MTT assay to evaluate the cytotoxicity of these compounds to P3HR1 cells; Figure 3 shows the results.

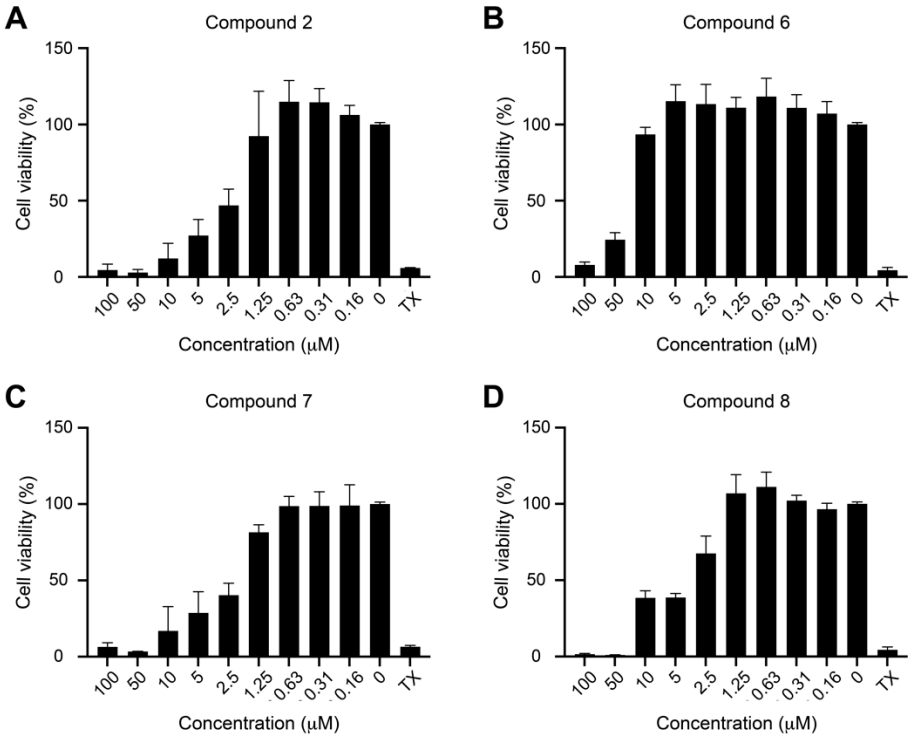

Figure 3. Cytotoxicity of protoapigenone (**A**) and its analogs (**B**–**D**) to P3HR1 cells. Cells were cultured for 24 h in a medium containing protoapigenone (**2**) or compounds **6**–**8**. Cell viability was evaluated by using MTT assay. Cells treated with 1% Triton X-100 (TX) were used as a positive control. The experiment was performed twice, and each sample involved in the experiment was prepared in duplicate. Error bars represent SD. Calculated IC_{50} values for compounds **2**, **6**, **7**, and **8** were 3.86, 34.12, 2.04, and 4.93 μM, respectively.

Compounds **7** and **8** were similarly active as protoapigenone, as expected from our previously published structure-activity relationship (SAR) study on the effect of 1′-*O*-alkyl substituents on the cytotoxic activity of protoflavones [7] (**2**), and the isopropyl-ether derivative **6** was much weaker in this regard. Selectivity of the anti-EBV vs. cytotoxic effect of these compounds, expressed as a ratio of the corresponding IC_{50} values, could therefore be calculated, as follows: **2** (30.1), **6** (73.0), **7** (9.80), and **8** (17.3). This means that compound **6** demonstrated a relevant, ca. 2.6-times increase in selectivity when compared to protoapigenone. It needs to be stressed that this selectivity increase is due to the much weaker cytotoxic activity of compound **6** as compared to protoapigenone, and it does not refer to a stronger anti-EBV activity. While this successfully fulfills our objectives that were set for this study, it might be worthy to further explore SAR regarding the role of the 1′-*O*-alkyl chain in the future. For example, when considering that the 1′-*O*-butyl derivative compound **7** exerted an over two-fold stronger anti-EBV activity than the 1′-*O*-isopropyl compound **6**, it might be a relevant strategy to study further analogs with a longer branching side-chain coupled at C-1′, such as *i*-butyl, *i*-pentyl, etc.

It is also worth noting that it was also found to be possible to shift the bioactivity profile of protoflavones to the other direction, i.e., increasing cytotoxicity and decreasing anti-EBV activity, by appropriate modifications of the B-ring. As compared with protoapigenone (**2**), compound **7** was less

effective against EBV and more cytotoxic, i.e., ca. three-times less selective in this regard. Therefore, the SAR of protoflavonoids might be explored towards various therapeutic targets, and this is certainly a need to evaluate their real value concerning drug discovery.

3. Materials and Methods

3.1. Synthesis and Chromatographic Purification

Reagents were purchased from Sigma (Merck KGaA, Darmstadt, Germany) and the solvents were obtained from Macron Fine Chemicals (Avantor Performance Materials, Center Valley, Pennsylvania, USA). The reactions were monitored by TLC on Kieselgel $60F_{254}$ silica plates purchased from Merck (Merck KGaA, Darmstadt, Germany), and characteristic spots of compounds were examined under UV illumination at 254 and 366 nm. Chromatographic purification of components was carried out in one or two steps, depending on the complexity of protoflavone product mixtures. For flash chromatography, a CombiFlash® Rf+ Lumen apparatus (TELEDYNE Isco, Lincoln, NE, USA) was utilized that was equipped with ELS and diode array detectors. Components were separated on commercially available RediSep NP-silica flash columns (TELEDYNE Isco, Lincoln, NE, USA) or manually filled polyamide columns. The mobile phase eluents consisted of mixtures of *n*-hexane—ethyl acetate or dichloromethane—methanol, modified according to the polarity of the analytes. To determine the composition of sample mixtures or to evaluate the purity of compounds, RP-HPLC analysis was performed on a Kinetex XB-C18 250 × 4.6 mm, 5 μm or a Kinetex Biphenyl 250 × 4.6 mm, 5 μm column (Phenomenex Inc., Torrance, CA, USA) at 1 mL/min. flow rate, while using a dual pump (PU-2080) Jasco HPLC instrument (Jasco International Co. Ltd., Hachioji, Tokyo, Japan) that was equipped with an MD-2010 Plus PDA detector to collect data in a detection range of 210–400 nm. For preparative purposes, an Armen Spot Prep II integrated HPLC purification system (Gilson, Middleton, WI, USA) with dual-wavelength detection was applied, operating at 230 and 300 nm. Preparative separations were performed on the corresponding Kinetex XB-C18 or Biphenyl 250 × 21.2 mm, 5 μm columns with adequately chosen eluents of acetonitrile–water, and the flow rates were 15 mL/min.

3.1.1. Preparation of Protoapigenone Derivatives **2–8**

Protoapigenone and its 1′-*O*-alkyl ether analogs were synthesized while following our previously described procedures [7]. Briefly, apigenin (1 mg/mL) was dissolved in a 9:1 *v/v* ratio mixture of acetonitrile and H_2O or the alcohol to be coupled at C-1′. Under stirring, two equivalents of [bis(trifluoroacetoxy)iodo]benzene was added slowly to the solution and the reaction was left to develop for 1 h at 80 °C. After completion, the solvent was evaporated on a rotary evaporator and the residue was purified by flash chromatography, allowing for obtaining the corresponding protoflavones in pure form.

3.1.2. Preparation of Tetrahydroprotoapigenone Derivatives **9–14**

Selective hydrogenation of protoflavones was carried out based on our previous strategy [11] that relied on the application of an H-Cube® continuous flow hydrogenation system (ThalesNano Inc., Budapest, Hungary). The applied catalyst cartridge was a stainless-steel column (internal dimensions: 50 mm × 4.6 mm) containing approximately 200 mg of 5% Pd/C catalyst. The cartridge was inserted into an external thermostat (Jetstream 2 plus, Jasco International Co. Ltd., Hachioji, Tokyo, Japan) set to 25 °C. A standard HPLC pump (Well-Chrom K-120, Knauer GmbH, Berlin, Germany) was used to provide continuous stream. In each case, the flow rate was set to 1 mL/min., and 40 bar pressure was applied in the system.

For each reaction, 20 mg of the corresponding protoflavone was dissolved/suspended in 20 mL of HPLC grade ethyl acetate and homogenized by sonication. The catalyst bed was washed with the solvent for 15 min. to ensure reproducibility between each reaction. Following transformations, preparative RP-HPLC was utilized for chromatographic purification.

3.1.3. Preparation of Tetradeuteroprotoapigenone Derivatives **15**–**20**

The selective deuteration of the protoflavone B ring was performed similarly to that described for hydrogenation with only slight modifications. In this case, approximately 400 mg of 5% Pd/$BaSO_4$ was used as a catalyst, and the reservoir of the instrument was filled up with high purity heavy water (D_2O). The obtained compounds **15**–**20** were purified by preparative RP-HPLC.

3.1.4. Preparation of Protoflavone 4′-oxime Derivatives **21**–**26**

An aliquot of 150 mg of compound **6**, **7**, or **8** was dissolved in methanol in a concentration of 2.5 mg/mL (50 mL). Following this, three equivalents of hydroxylamine hydrochloride were added to the solution, and the mixture was refluxed for 24 h at 70 °C. Silica gel (3–5 g) was added to the solution and the solvent was evaporated to prepare for dry loading separation. The dried residue was applied to flash chromatography, and products were pre-purified by a gradient separation program starting with *n*-hexane, and the ratio of ethyl acetate was gradually increasing 90%, *v/v*, in 15 min. Following this, cis- and trans-isomeric racemate pairs (**21** and **24**, **22** and **25**, **23**, and **26**, respectively) were separated by means of preparative RP-HPLC to obtain racemates **21**–**26**.

3.1.5. Preparation of Tetrahydroprotoflavone 4′-oxime Derivatives **27**–**28**

An aliquot of 60 mg of tetrahydroprotoflavone **9** or **14** was dissolved in methanol in a concentration of 2.5 mg/mL (25 mL). Four equivalents of hydroxylamine hydrochloride were added to the mixture and the solution was stirred at 70 °C for 3 h. Following this, solvent was evaporated on a rotary evaporator and brine (40 mL) was added to the residue. Extraction was performed with EtOAc (3 × 40 mL), and the organic fractions were then combined and dried over Na_2SO_4. The drying agent was removed through filtration, and the solution was evaporated under reduced pressure. Eventually, preparative RP-HPLC was applied to obtain oxime derivatives **27** and **28**.

3.2. Structure Elucidation

NMR and MS techniques characterized the compounds. NMR spectra were recorded at 25 °C on a Bruker Avance DRX 400 MHz (Bruker Co., Billerica, MA, USA) or on a Bruker Avance NEO 500 MHz spectrometer that was equipped with a Prodigy BBO 5 mm CryoProbe with the use of TMS as an internal standard. Typically, 5–10 mg of the corresponding protoflavone was dissolved in DMSO-d_6 and transferred to NMR tubes for recording spectra. The data report and spectra analysis were carried out with MestReNova v6.0.2-5475 software (Mestrelab Research S.L., Santiago de Compostela, Spain). ^{1}H and ^{13}C NMR chemical shifts are listed below; residual hydrogen signals of the B-rings of deuterated compounds **15**–**20** are marked with an asterisk. Mass spectra were recorded on an API 2000 triple quadrupole tandem mass spectrometer (AB SCIEX, Foster City, CA, USA) that was equipped with ESI ion source that was used in the negative ionization mode. ^{1}H and ^{13}C (JMOD) spectra of the new compounds are provided as Supplementary Materials, Figures S1–S36, and their mass spectra as Figures S37–S54.

Compound **10**: Pale yellow solid, Isolated yield: 25.2% (5.1 mg); RP-HPLC purity: 97%. ^{1}H NMR (500 MHz, DMSO-d_6): 12.65 (1H, s), 10.93 (1H, br s), 6.39 (1H, d, J = 1.9 Hz), 6.34 (1H, s), 6.20 (1H, d, J = 1.9 Hz), 3.22 (3H, s), 2.56 (2H, m), 2.35 (2H, m), 2.18–2.22 (4H, m). ^{13}C NMR (125 MHz, DMSO-d_6): 208.9, 181.7, 168.9, 164.5, 161.4, 157.8, 107.5, 103.9, 99.0, 94.1, 75.7, 51.0, 2 × 35.8, 2 × 30.8. ESI-MS (*m/z*): 303.4 $[M\text{-}H]^-$.

Compound **11**: Pale yellow solid, Isolated yield: 70.5% (15.5 mg); RP-HPLC purity: 98%. ^{1}H NMR (500 MHz, DMSO-d_6): 12.66 (1H, s), 10.94 (1H, br s), 6.39 (1H, d, J = 1.9 Hz), 6.32 (1H, s), 6.20 (1H, d, J = 1.9 Hz), 3.40 (2H, q, J = 6.9 Hz), 2.55 (2H, m), 2.34 (2H, m), 2.16–2.22 (4H, m), 1.16 (3H, t, J = 6.9 Hz). ^{13}C NMR (125 MHz, DMSO-d_6): 209.0, 181.7, 169.6, 164.5, 161.4, 157.7, 107.1, 103.8, 99.0, 94.0, 75.5, 58.6, 2 × 35.9, 2 × 31.3, 15.5. ESI-MS (*m/z*): 317.7 $[M\text{-}H]^-$.

Compound **12**: Pale brown solid, Isolated yield: 30.1% (6.1 mg); RP-HPLC purity: 99%. ^{1}H NMR (500 MHz, DMSO-d_6): 12.65 (1H, s), 10.97 (1H, br s), 6.38 (1H, d, J = 1.9 Hz), 6.32 (1H, s), 6.20 (1H, d, J = 1.9 Hz), 3.30 (2H, t, J = 6.4 Hz), 2.56 (2H, m), 2.36 (2H, m), 2.16–2.22 (4H, m), 1.55 (2H, m), 0.89 (3H, t, J = 7.4 Hz). ^{13}C NMR (125 MHz, DMSO-d_6): 209.0, 181.7, 169.3, 164.6, 161.4, 157.7, 107.3, 103.8, 99.0, 94.0, 75.2, 64.5, 2 × 35.9, 2 × 31.2, 22.8, 10.7. ESI-MS (*m*/*z*): 331.3 [M-H]$^{-}$.

Compound **13**: Pale yellow solid, Isolated yield: 44% (8.9 mg); RP-HPLC purity: 99%. ^{1}H NMR (500 MHz, DMSO-d_6): 12.62 (1H, s), 10.99 (1H, br s), 6.42 (1H, s), 6.39 (1H, d, J = 1.9 Hz), 6.20 (1H, d, J = 1.9 Hz), 3.82 (1H, septet, J = 6.1 Hz), 2.55 (2H, m), 2.42 (2H, m), 2.13–2.21 (4H, m), 1.02 (6H, d, J = 6.1 Hz). ^{13}C NMR (125 MHz, DMSO-d_6): 209.2, 181.7, 169.0, 164.8, 161.4, 157.5, 108.0, 103.9, 99.1, 93.9, 75.0, 66.1, 2 × 36.1, 2 × 31.6, 2 × 24.0. ESI-MS (*m*/*z*): 331.4 [M-H]$^{-}$.

Compound **15**: Pale yellow solid, Isolated yield: 63.1% (12.6 mg); RP-HPLC purity: 98.9%. ^{1}H NMR (500 MHz, DMSO-d_6): 12.73 (1H, s), 6.41 (1H, s), 6.38 (1H, d, J = 1.9 Hz), 6.18 (1H, d, J = 1.9 Hz), 6.08 (1H, br s), 2 × 2.26 * (d, J = 4.7 Hz), 2 × 2.17* (d, J = 4.7 Hz). ^{13}C NMR (125 MHz, DMSO-d_6): 209.6, 182.0, 174.3, 164.5, 161.4, 157.6, 104.7, 103.6, 98.9, 94.0, 70.2, 2 × 35.7, 2 × 33.7. ESI-MS (*m*/*z*): 293.5 [M-H]$^{-}$.

Compound **16**: White solid, Isolated yield: 40.5% (8.2 mg); RP-HPLC purity: 95%. ^{1}H NMR (500 MHz, DMSO-d_6): 12.65 (1H, s), 10.96 (1H, br s), 6.39 (1H, d, J = 1.9 Hz), 6.34 (1H, s), 6.20 (1H, d, J = 1.9 Hz), 3.21 (3H, s), 2.52* (br d, J = 6.1 Hz) 2.33* (br d, J = 6.1 Hz), 2 × 2.18* (m). ^{13}C NMR (125 MHz, DMSO-d_6): 209.1, 181.7, 168.9, 164.6, 161.4, 157.8, 107.6, 103.8, 99.0, 94.1, 75.7, 51.0, 2 × 35.4, 2 × 30.4. ESI-MS (*m*/*z*): 307.4 [M-H]$^{-}$.

Compound **17**: Pale pink solid, Isolated yield: 60.6% (12.1 mg); RP-HPLC purity: 96%. ^{1}H NMR (500 MHz, DMSO-d_6): 12.66 (1H, s), 10.94 (1H, br s), 6.39 (1H, d, J = 1.9 Hz), 6.32 (1H, s), 6.21 (1H, d, J = 1.9 Hz), 3.40 (2H, q, J = 6.9 Hz), 2.54* (br d, J = 6.0 Hz), 2.32* (br d, J = 6.0 Hz), 2 × 2.17* (m), 1.16 (3H, t, J = 6.9 Hz). ^{13}C NMR (125 MHz, DMSO-d_6): 209.1, 181.7, 169.5, 164.6, 161.4, 157.7, 107.1, 103.8, 99.0, 94.0, 75.4, 58.6, 2 × 35.5, 2 × 30.9, 15.5. ESI-MS (*m*/*z*): 321.3 [M-H]$^{-}$.

Compound **18**: White solid, Isolated yield: 51.4% (10.4 mg); RP-HPLC purity: 98%. ^{1}H NMR (500 MHz, DMSO-d_6): 12.64 (1H, s), 10.97 (1H, br s), 6.38 (1H, d, J = 1.9 Hz), 6.32 (1H, s), 6.20 (1H, d, J = 1.9 Hz), 3.30 (2H, t, J = 6.3 Hz), 2.53* (br d, J = 6.1 Hz), 2.34* (br d, J = 6.1 Hz), 2 × 2.17* (m), 1.55 (2H, m), 0.88 (3H, t, J = 7.3 Hz). ^{13}C NMR (125 MHz, DMSO-d_6): 209.6, 182.1, 169.7, 165.1, 161.9, 158.2, 107.8, 104.3, 99.5, 94.5, 75.5, 64.9, 2 × 35.9, 2 × 31.3, 23.2, 11.1. ESI-MS (*m*/*z*): 335.5 [M-H]$^{-}$.

Compound **19**: White solid, Isolated yield: 55.8% (11.3 mg); RP-HPLC purity: 99%. ^{1}H NMR (500 MHz, DMSO-d_6): 12.62 (1H, s), 11.01 (1H, br s), 6.42 (1H, s), 6.39 (1H, d, J = 1.9 Hz), 6.21 (1H, d, J = 1.9 Hz), 3.81 (1H, septet, J = 6.1 Hz), 2.53* (br d, J = 5.9 Hz), 2.39* (br d, J = 5.9 Hz), 2.17* (m), 2.13* (m), 1.01 (6H, d, J = 6.1 Hz). ^{13}C NMR (125 MHz, DMSO-d_6): 209.4, 181.7, 169.0, 164.8, 161.4, 157.5, 108.0, 103.8, 99.1, 93.9, 75.0, 66.0, 2 × 35.7, 2 × 31.2, 2 × 24.0. ESI-MS (*m*/*z*): 335.5 [M-H]$^{-}$.

Compound **20**: White solid, Isolated yield: 73.5% (14.7 mg); RP-HPLC purity: 99%. ^{1}H NMR (500 MHz, DMSO-d_6): 12.64 (1H, s), 10.98 (1H, br s), 6.37 (1H, d, J = 1.7 Hz), 6.32 (1H, s), 6.19 (1H, d, J = 1.7 Hz), 3.33 (2H, overlap with H_2O signal, J = 5.7 Hz), 2.53* (br d, J = 6.1 Hz), 2.34* (br d, J = 6.1 Hz), 2 × 2.17 * (m), 1.52 (2H, m), 1.36 (2H, m), 0.85 (3H, t, J = 7.4 Hz). ^{13}C NMR (125 MHz, DMSO-d_6): 209.2, 181.6, 169.3, 164.7, 161.4, 157.7, 107.4, 103.8, 99.1, 94.0, 75.1, 62.5, 2 × 35.5, 31.6, 2 × 30.8, 18.9, 13.8. ESI-MS (*m*/*z*): 349.8 [M-H]$^{-}$.

Racemate **21**: Pale brown solid; Isolated yield: 24.3% (41.67 mg); RP-HPLC purity at 241 nm: 99.5%. ^{1}H NMR (500 MHz, DMSO-d_6): 12.69 (1H, s), 11.45 (1H, s), 6.50 (1H, d, J = 10.1 Hz), 6.35 (1H, s), 6.34 (1H, d, J = 1.8 Hz), 6.32 (1H, d, J = 10.1 Hz), 6.20 (1H, d, J = 1.8 Hz), 3.91 (1H, septet, J = 6.1 Hz), 3.71 (1H, dd, J = 10.0 and 4.4 Hz), 3.18 (3H, s), 3.01 (1H, dd, J = 16.7 and 4.4 Hz), 2.43 (1H, dd, J = 16.7 and 10.0 Hz), 1.11 (3H, d, J = 6.1 Hz), 1.07 (3H, d, J = 6.1 Hz). ^{13}C NMR (125 MHz, DMSO-d_6): 181.5, 169.9, 164.6, 161.5, 157.6, 152.3, 130.1, 129.9, 108.4, 103.9, 99.1, 94.0, 79.0, 77.9, 67.6, 57.3, 24.03, 24.02, 23.6. ESI-MS (*m*/*z*): 374.7 [M-H]$^{-}$.

Racemate **22**: Pale brown solid; Isolated yield: 27.8% (47.43 mg); RP-HPLC purity at 247 nm: 99.9%. ^{1}H NMR (500 MHz, DMSO-d_6): 12.68 (1H, s), 11.43 (1H, br s), 6.48 (1H, d, J = 10.0 Hz), 6.33 (1H,

d, *J* = 2.0 Hz), 6.29 (1H, d, *J* = 10.0 Hz), 6.25 (1H, s), 6.21 (1H, d, *J* = 2.0 Hz), 3.76 (1H, dd, *J* = 10.1 and 4.7 Hz), 3.43 (2H, m), 3.18 (3H, s), 3.03 (1H, dd, *J* = 16.8 and 4.7 Hz), 2.45 (1H, dd, *J* = 16.8 and 10.2 Hz), 1.50 (2H, m), 1.32 (2H, m), 0.85 (3H, t, *J* = 7.4 Hz). ^{13}C NMR (125 MHz, DMSO-d_6): 181.4, 168.5, 164.5, 161.5, 157.8, 152.2, 130.1, 129.7, 108.2, 103.9, 99.1, 94.0, 78.6, 77.7, 64.1, 57.5, 31.8, 23.7, 18.8, 13.7. ESI-MS (*m*/*z*): 388.0 $[M-H]^-$.

Racemate **23**: Pale brown solid; Isolated yield: 25.1% (43.11 mg); RP-HPLC purity at 248 nm: 99.8%. ^{1}H NMR (500 MHz, DMSO-d_6): 12.67 (1H, s), 11.52 (1H, s), 6.52 (1H, d, *J* = 10.0 Hz), 6.33 (1H, d, *J* = 1.9 Hz), 6.32 (1H, s), 6.29 (1H, d, *J* = 10.0 Hz), 6.21 (1H, d, *J* = 1.9 Hz), 4.27 (1H, dd, *J* = 15.7 and 2.3 Hz), 4.18 (1H, dd, *J* = 15.7 and 2.3 Hz), 3.80 (1H, dd, *J* = 10.2 and 4.7 Hz), 3.46 (1H, t, *J* = 2.3 Hz), 3.18 (3H, s), 3.07 (1H, dd, *J* = 16.7 and 4.7 Hz), 2.43 (1H, dd, *J* = 16.7 and 10.2 Hz). ^{13}C NMR (125 MHz, DMSO-d_6): 181.5, 167.8, 164.5, 161.5, 157.7, 152.1, 130.8, 128.7, 108.4, 104.0, 99.1, 94.1, 80.5, 78.33, 78.31, 77.5, 57.4, 53.3, 23.7. ESI-MS (*m*/*z*): 370.3 $[M-H]^-$.

Racemate **24**: Pale brown solid; Isolated yield: 29.6% (50.76 mg); RP-HPLC purity at 246 nm: 97.3%. ^{1}H NMR (500 MHz, DMSO-d_6): 12.66 (1H, s), 11.38 (1H, s), 6.47 (3H, m, overlapping signals), 6.36 (1H, d, *J* = 1.9 Hz), 6.21 (1H, d, *J* = 1.9 Hz), 3.84–3.92 (2H, m, overlapping signals), 3.12 (1H, dd, *J* = 12.3 and 4.2 Hz), 3.10 (3H, s), 2.52 (1H, dd, *J* = 3.4 Hz; partially overlapped with DMSO signal), 1.04 (3H, d, *J* = 6.1 Hz), 0.97 (3H, d, *J* = 6.1 Hz). ^{13}C NMR (125 MHz, DMSO-d_6): 181.5, 168.7, 164.7, 161.5, 157.4, 151.1, 130.1, 127.3, 108.9, 103.9, 99.1, 93.8, 78.2, 76.6, 66.6, 56.9, 24.4, 23.8, 22.7. ESI-MS (*m*/*z*): 374.7 $[M-H]^-$.

Racemate **25**: Pale brown solid; Isolated yield: 33.2% (56.64 mg); RP-HPLC purity at 247 nm: 99.7%. ^{1}H NMR (500 MHz, DMSO-d_6): 12.65 (1H, br s), 11.39 (1H, s), 10.92 (1H, br s), 6.48 (1H, d, *J* = 10.3 Hz), 6.42 (1H, s), 6.36 (1H, d, *J* = 10.3 Hz), 6.32 (1H, d, *J* = 2.1 Hz), 6.21 (1H, d, *J* = 2.1 Hz), 3.90 (1H, br t, *J* = 4.3 Hz), 3.45 (1H, m), 3.28 (1H, m), 3.15 (3H, s), 3.02 (1H, dd, *J* = 17.4 and 5.1 Hz), 2.61 (1H, dd, *J* = 17.4 and 3.9 Hz), 1.45 (2H, m), 1.30 (2H, m), 0.82 (3H, t, *J* = 7.4 Hz). ^{13}C NMR (125 MHz, DMSO-d_6): 181.5, 168.0, 164.5, 161.5, 157.5, 151.1, 130.1, 127.6, 108.7, 103.9, 99.1, 93.8, 78.0, 77.3, 62.8, 57.2, 31.6, 23.3, 18.7, 13.6. ESI-MS (*m*/*z*): 388.2 $[M-H]^-$.

Racemate **26**: Pale brown solid; Isolated yield: 31.8% (54.62 mg); RP-HPLC purity at 248 nm: 97.3%. ^{1}H NMR (500 MHz, DMSO-d_6): 12.65 (1H, s), 11.48 (1H, s), 6.53 (1H, d, *J* = 10.3 Hz), 6.44 (1H, s), 6.40 (1H, d, *J* = 10.3 Hz), 6.34 (1H, d, *J* = 1.9 Hz), 6.20 (1H, d, *J* = 1.9 Hz), 4.21 (1H, dd, *J* = 15.8 and 2.3 Hz), 4.15 (1H, dd, *J* = 15.8 and 2.3 Hz), 3.93 (1H, dd, *J* = 4.6 and 3.6 Hz), 3.39 (1H, t, *J* = 2.3 Hz), 3.14 (3H, s), 3.04 (1H, dd, *J* = 17.4 and 4.6 Hz), 2.57 (1H, dd, *J* = 17.4 and 3.6 Hz). ^{13}C NMR (125 MHz, DMSO-d_6): 181.5, 167.1, 164.6, 161.5, 157.5, 151.0, 131.1, 126.0, 109.0, 104.0, 99.1, 93.9, 80.3, 77.9, 77.6, 77.4, 57.2, 52.1, 23.1. ESI-MS (*m*/*z*): 370.2 $[M-H]^-$.

Racemate **27**: Pale white solid; Isolated yield: 48.3% (30.5 mg); RP-HPLC purity at 247 nm: 96.1%. ^{1}H NMR (500 MHz, DMSO-d_6): 12.75 (1H, s), 10.34 (1H, s), 6.37 (1H, d, *J* = 1.9 Hz), 6.36 (1H, s), 6.18 (1H, d, *J* = 1.9 Hz), 5.84 (1H, br s), 3.08 (1H, br d, *J* = 14.2 Hz), 2.45 (1H, td, *J* = 13.4 and 4.9 Hz), 2.21 (1H, m), 2.06 (1H, m), 1.98 (1H, td, *J* = 12.9 and 4.6 Hz), 1.80–1.89 (3H, m, overlapping signals). ^{13}C NMR (125 MHz, DMSO-d_6): 182.1, 174.9, 164.4, 161.4, 157.6, 155.4, 104.5, 103.6, 98.9, 94.0, 71.2, 34.6, 33.3, 26.3, 18.8. ESI-MS (*m*/*z*): 304.4 $[M-H]^-$.

Racemate **28**: Pale white solid; Isolated yield: 42.1% (26.4 mg); RP-HPLC purity at 250 nm: 96.6%. ^{1}H NMR (500 MHz, DMSO-d_6): 12.66 (1H, s), 10.36 (1H, s), 6.38 (1H, d, *J* = 1.9 Hz), 6.27 (1H, s), 6.19 (1H, d, *J* = 1.9 Hz), 3.28 (2H, t, *J* = 6.1 Hz), 3.05 (1H, br d, *J* = 14.4 Hz), 2.33 (1H, td, *J* = 13.9 and 5.4 Hz), 2.16–2.23 (3H, m, overlapping signals), 1.98 (1H, td, *J* = 13.6 and 5.1 Hz), 1.87 (1H, td, *J* = 14.2 and 4.3 Hz), 1.78 (1H, td, *J* = 13.3 and 4.6 Hz), 1.49 (2H, m), 1.35 (2H, m), 0.84 (3H, t, *J* = 7.4 Hz). ^{13}C NMR (125 MHz, DMSO-d_6): 181.7, 170.0, 164.5, 161.4, 157.7, 155.0, 107.1, 103.8, 99.0, 94.0, 76.0, 62.2, 31.8, 31.6, 30.6, 26.2, 18.9, 18.8, 13.8. ESI-MS (*m*/*z*): 360.5 [M-H]-.

3.3. Cell Lines and Viruses

The U373-CD4-CCR5 cell line was obtained from the AIDS Research and Reagent Program, NIAID. Cells were cultured according to the protocol of the provider with 10% heat-inactivated fetal bovine

serum (Lonza, Maastricht, The Netherlands) supplemented with 2 mM L-glutamine, 100 units/mL of penicillin, and 100 µg/mL streptomycin (Invitrogen, Merelbeke, Belgium). Pseudotyped viral particules bearing the ADA HIV Env were produced, as described previously [25].

EBV-positive BL cell line P3HR1 cells were cultured in RPMI 1640 medium [26,27]. Culture media were supplemented with 10% fetal calf serum. P3HR1 cells were treated with 3 mM sodium butyrate and 30 nM 12-*O*-tetradecanoylphobol-13-actetae (TPA) to induce the EBV lytic cycle [26,27].

3.4. Anti-HIV Testing

Antiviral activity was assessed while using a Pseudotype Virus Assay, allowing for one cycle of viral replication [25]. The U373-CD4-CCR5 cells were infected by pseudotyped virus pNL4.3ΔenvLuc-ADA 8 using spinoculation at 1200 g during 2 h in the presence of compounds and cultured for two consecutive days in the presence of the compounds. After 48 h, luciferase activity expressed as Relative Light Units was measured (Luciferase System kit, Promega, The Netherlands). Drug cytotoxicity was evaluated while using MTT (3-(4,5-dimethylthiazol-2-yl)-2,5-diphenyltetrazolium bromide, Sigma, Belgium) 48 h after incubation with the compounds by measuring A540 and A690 using a POLARstar Omega Plate Reader (BMG Lab Technologies, Belgium) after 48 h of incubation with the compounds. The value of OD540–OD690 was calculated.

3.5. Immunoblot Analysis of EBV Rta Protein

P3HR1 cells were lysed in mRIPA buffer (50 mM Tris-HCl, pH 7.8, 150 mM NaCl, 5 mM EDTA, 0.5% Triton X-100, 0.5% NP-40) [26,27]. Approximately 5% of the lysate was loaded to a gel and then separated by electrophoresis in 10% SDS-PAGE. The proteins in the gel were electroblotted onto a polyvinylidene difluoride (PVDF) blotting membrane while using a Hoefer transfer system. Rta was detected while using mouse anti-Rta monoclonal antibody (Argene, Verniolle, France). α-Tubulin was detected using mouse anti-α-tubulin monoclonal antibody (Abcam, Cambridge, UK). Primary antibodies were detected using horseradish peroxidase-conjugated secondary antibodies (Cell Signaling Technology, Danvers, MA, USA) and then visualized using SuperSignal West Pico Chemiluminescent substrate (Thermo Fisher Scientific, Waltham, MA, USA).

3.6. Cytotoxicity Assay

P3HR1 cells (5×10^4) were seeded in wells of a 96-well plate and then cultured for 24 h in 100 µL of RPMI 1640 medium containing protoapigenone or its analogs. Subsequently, 1% Triton X-100 was added as a negative control. Cytotoxicity was determined by Cell Proliferation Kit I (Roche, Basel, Switzerland). An aliquot of 10 µL of the MTT labeling reagent was added to each well and the plate was incubated for 4 h at 37°C. Afterwards, 100 µL solubilization solution was added to each well to dissolve insoluble formazan and was incubated overnight. Optical density was measured at 595 nm and 650 nm.

4. Conclusions

As a result of this work, the chemical space of non-cytotoxic protoflavonoids was significantly extended through the preparation of derivatives without the symmetric dienone moiety, such as saturated (hydrogenated or deuterated) B-ring and/or 4′-oxime containing protoflavones. Compound **9** was found to exert a weak antiretroviral activity that, due to the extremely low cytotoxicity of this compound, might still be of interest. Further, three compounds, the isopropyl-, butyl-, and propargyl-ether derivatives of protoapigenone were identified to act as potent anti-EBV agents at similar, medium-low nanomolar concentration range as their parent compound **2**. Importantly, protoapigenone 1′-*O*-isopropyl ether demonstrated an order of magnitude lower cytotoxic effect when compared to protoapigenone, which makes compound **6** ca. 2.6-times more selective anti-EBV agent. Therefore, this compound can serve as a possible new lead for the development of safe and effective protoflavone derivatives against the lytic cycle of EBV.

Altogether, as a result of this work, it might also be concluded that targeted chemical modifications of the protoflavone B-ring to decrease cytotoxicity represent a valid strategy towards the discovery of new bioactive compounds against pathologies other than cancer.

Supplementary Materials: Supplementary materials can be found at http://www.mdpi.com/1422-0067/20/24/6269/s1.

Author Contributions: Conceptualization, A.H.; investigation, M.V., G.G., N.K., J.-Y.S., M.S.C.; resources, F.F., F.-R.C., A.H.; data curation, M.V., N.K.; writing—original draft preparation, M.V., G.G.; writing—review and editing, M.V., N.K., A.H.; supervision, S.B.Ö., C.S.-D., L.-K.C., A.H.; funding acquisition, J.H., A.H.

Funding: This work was funded by the National Research, Development and Innovation Office, Hungary (NKFIH; K119770), the PN-II-PT-PCCA-2013-4-0930, European Cooperation ERA-NET HIVERA contract 11/2016 and NKFIH NN 118176, the Ministry of Human Capacities, Hungary grant 20391-3/2018/FEKUSTRAT, and the EU-funded Hungarian grant EFOP-3.6.1-16-2016-00008.

Conflicts of Interest: The authors declare no conflict of interest. The funders had no role in the design of the study; in the collection, analyses, or interpretation of data; in the writing of the manuscript, or in the decision to publish the results.

References

1. Hunyadi, A.; Martins, A.; Danko, B.; Chang, F.R.; Wu, Y.C. Protoflavones: A class of unusual flavonoids as promising novel anticancer agents. *Phytochem. Rev.* **2014**, *13*, 69–77. [CrossRef]
2. Danko, B.; Toth, S.; Martins, A.; Vagvolgyi, M.; Kusz, N.; Molnar, J.; Chang, F.R.; Wu, Y.C.; Szakacs, G.; Hunyadi, A. Synthesis and SAR Study of Anticancer Protoflavone Derivatives: Investigation of Cytotoxicity and Interaction with ABCB1 and ABCG2 Multidrug Efflux Transporters. *ChemMedChem* **2017**, *12*, 850–859. [CrossRef] [PubMed]
3. Stanković, T.; Dankó, B.; Martins, A.; Dragoj, M.; Stojković, S.; Isaković, A.; Wang, H.-C.; Wu, Y.-C.; Hunyadi, A.; Pešić, M. Lower antioxidative capacity of multidrug-resistant cancer cells confers collateral sensitivity to protoflavone derivatives. *Cancer Chemother. Pharmacol.* **2015**, *76*, 555–565. [CrossRef] [PubMed]
4. Wang, H.C.; Lee, A.Y.; Chou, W.C.; Wu, C.C.; Tseng, C.N.; Liu, K.Y.; Lin, W.L.; Chang, F.R.; Chuang, D.W.; Hunyadi, A.; et al. Inhibition of ATR-dependent signaling by protoapigenone and its derivative sensitizes cancer cells to interstrand cross-link-generating agents in vitro and in vivo. *Mol. Cancer Ther.* **2012**, *11*, 1443–1453. [CrossRef] [PubMed]
5. Lecona, E.; Fernandez-Capetillo, O. Targeting ATR in cancer. *Nat. Rev. Cancer* **2018**, *18*, 586–595. [CrossRef] [PubMed]
6. Lin, A.S.; Nakagawa-Goto, K.; Chang, F.R.; Yu, D.; Morris-Natschke, S.L.; Wu, C.C.; Chen, S.L.; Wu, Y.C.; Lee, K.H. First total synthesis of protoapigenone and its analogues as potent cytotoxic agents. *J. Med. Chem.* **2007**, *50*, 3921–3927. [CrossRef]
7. Hunyadi, A.; Chuang, D.W.; Danko, B.; Chiang, M.Y.; Lee, C.L.; Wang, H.C.; Wu, C.C.; Chang, F.R.; Wu, Y.C. Direct semi-synthesis of the anticancer lead-drug protoapigenone from apigenin, and synthesis of further new cytotoxic protoflavone derivatives. *PLoS ONE* **2011**, *6*, e23922. [CrossRef]
8. Lin, A.S.; Chang, F.R.; Wu, C.C.; Liaw, C.C.; Wu, Y.C. New cytotoxic flavonoids from Thelypteris torresiana. *Planta Med.* **2005**, *71*, 867–870. [CrossRef]
9. Hunyadi, A.; Martins, A.; Danko, B.; Chuang, D.-W.; Trouillas, P.; Chang, F.-R.; Wu, Y.-C.; Falkay, G. Discovery of the first non-planar flavonoid that can strongly inhibit xanthine oxidase: Protoapigenone 1′-O-propargyl ether. *Tetrahedron. Lett.* **2013**, *54*, 6529–6532. [CrossRef]
10. Tung, C.P.; Chang, F.R.; Wu, Y.C.; Chuang, D.W.; Hunyadi, A.; Liu, S.T. Inhibition of the Epstein-Barr virus lytic cycle by protoapigenone. *J. Gen. Virol.* **2011**, *92*, 1760–1768. [CrossRef]
11. Ötvös, S.B.; Vágvölgyi, M.; Girst, G.; Kuo, C.-Y.; Wang, H.-C.; Fülöp, F.; Hunyadi, A. Synthesis of Nontoxic Protoflavone Derivatives through Selective Continuous-Flow Hydrogenation of the Flavonoid B-Ring. *ChemPlusChem* **2018**, *83*, 72–76. [CrossRef]
12. Ko, Y.-J.; Oh, H.-J.; Ahn, H.-M.; Kang, H.-J.; Kim, J.-H.; Ko, Y.H. Flavonoids as potential inhibitors of retroviral enzymes. *J. Korean Soc. Appl. Biol. Chem.* **2009**, *52*, 321–326. [CrossRef]

13. Kurapati, K.R.V.; Atluri, V.S.; Samikkannu, T.; Garcia, G.; Nair, M.P.N. Natural Products as Anti-HIV Agents and Role in HIV-Associated Neurocognitive Disorders (HAND): A Brief Overview. *Front. Microbiol.* **2016**, *6*, 1444. [CrossRef] [PubMed]
14. Áy, É.; Hunyadi, A.; Mezei, M.; Minárovits, J.; Hohmann, J. Flavonol 7-O-Glucoside Herbacitrin Inhibits HIV-1 Replication through Simultaneous Integrase and Reverse Transcriptase Inhibition. *Evid. Based Complement. Altern. Med.* **2019**, *2019*, 6. [CrossRef]
15. Iglesias, J.; Sleno, L.; Volmer, D.A. Isotopic labeling of metabolites in drug discovery applications. *Curr. Drug Metab.* **2012**, *13*, 1213–1225. [CrossRef]
16. Robins, R.J.; Billault, I.; Duan, J.-R.; Guiet, S.; Pionnier, S.; Zhang, B.-L. Measurement of 2H distribution in natural products by quantitative 2H NMR: An approach to understanding metabolism and enzyme mechanism? *Phytochem. Rev.* **2003**, *2*, 87–102. [CrossRef]
17. Krumbiegel, P. Large deuterium isotope effects and their use: A historical review. *Isot. Environ. Health Stud.* **2011**, *47*, 1–17. [CrossRef]
18. Gant, T.G. Using deuterium in drug discovery: Leaving the label in the drug. *J. Med. Chem.* **2014**, *57*, 3595–3611. [CrossRef]
19. Ötvös, S.B.; Hsieh, C.-T.; Wu, Y.-C.; Li, J.-H.; Chang, F.-R.; Fülöp, F. Continuous-Flow Synthesis of Deuterium-Labeled Antidiabetic Chalcones: Studies towards the Selective Deuteration of the Alkynone Core. *Molecular* **2016**, *21*, 318. [CrossRef]
20. Otvos, S.B.; Mandity, I.M.; Fulop, F. Highly selective deuteration of pharmaceutically relevant nitrogen-containing heterocycles: A flow chemistry approach. *Mol. Divers.* **2011**, *15*, 605–611. [CrossRef]
21. Hsieh, C.-T.; Ötvös, S.B.; Wu, Y.-C.; Mándity, I.M.; Chang, F.-R.; Fülöp, F. Highly Selective Continuous-Flow Synthesis of Potentially Bioactive Deuterated Chalcone Derivatives. *ChemPlusChem* **2015**, *80*, 859–864. [CrossRef]
22. Kozłowska, J.; Grela, E.; Baczyńska, D.; Grabowiecka, A.; Anioł, M. Novel O-alkyl Derivatives of Naringenin and Their Oximes with Antimicrobial and Anticancer Activity. *Molecules* **2019**, *24*, 679. [CrossRef]
23. Türkkan, B.; Özyürek, M.; Bener, M.; Güçlü, K.; Apak, R. Synthesis, characterization and antioxidant capacity of naringenin-oxime. *Spectrochim. Acta Part A Mol. Biomol. Spectrosc.* **2012**, *85*, 235–240. [CrossRef]
24. Latif, A.D.; Gonda, T.; Vágvölgyi, M.; Kúsz, N.; Kulmány, Á.; Ocsovszki, I.; Zomborszki, Z.P.; Zupkó, I.; Hunyadi, A. Synthesis and In Vitro Antitumor Activity of Naringenin Oxime and Oxime Ether Derivatives. *Int. J. Mol. Sci.* **2019**, *20*, 2184. [CrossRef]
25. Arendt, V.; Amand, M.; Iserentant, G.; Lemaire, M.; Masquelier, C.; Ndayisaba, G.F.; Verhofstede, C.; Karita, E.; Allen, S.; Chevigné, A.; et al. Predominance of the heterozygous CCR5 delta-24 deletion in African individuals resistant to HIV infection might be related to a defect in CCR5 addressing at the cell surface. *J. Int. AIDS Soc.* **2019**, *22*, e25384. [CrossRef]
26. Chang, L.K.; Lee, Y.H.; Cheng, T.S.; Hong, Y.R.; Lu, P.J.; Wang, J.J.; Wang, W.H.; Kuo, C.W.; Li, S.S.; Liu, S.T. Post-translational modification of Rta of Epstein-Barr virus by SUMO-1. *J. Biol. Chem.* **2004**, *279*, 38803–38812. [CrossRef]
27. Yang, Y.C.; Yoshikai, Y.; Hsu, S.W.; Saitoh, H.; Chang, L.K. Role of RNF4 in the ubiquitination of Rta of Epstein-Barr virus. *J. Biol. Chem.* **2013**, *288*, 12866–12879. [CrossRef]